Dissecting Human Haematopoietic Progenitors

Marina Samitsch

St Hilda's College

University of Oxford

Thesis submitted for the degree of Doctor of Philosophy, University of Oxford

Molecular Haematology Unit

Weatherall Institute of Molecular Medicine

Trinity Term 2013

Acknowledgements

I would like to thank Prof. Vyas for providing me with the opportunity to work on this project and the time I could spend in his lab.

A huge thank you goes out to my mum and dad, my brother and everyone else in my family who have been there with moral support throughout all this time.

Nicolas, thank you for your guidance, supervision and help, as well as the frequent trips to the White Hart, and teaching me what this is really all about, and how science works. Terri, thank you for being my desk-neighbour and partner in crime and always putting me back on my feet and for all the friendship! Lynn, thank you for your kind words and precise scientific advice over the years. Batchimeg, thank you for all the wisdom and help. And thank you Jess, for lighting up the lab with your good mood! I am grateful for the advice I had from Ludo, Gaetan, Gemma, Joey, Kate, Hedia, Sarah, Dimitris, all the laughs and good times I have shared with Elisa, Inn Inn, Ana, Helen, Vivien, Chrissy, Bente, I-Jun, John, Marta, Ross, Jon and everyone else in the WIMM! A big thanks to Kelly for putting the perspective right and I will obviously miss her and thanks to Joey for keeping up the fun and listening to my whining! Also, I'd like to thank Angela, Andrew, Julia and Terri for showing me that a PhD can be completed and for always telling me to hang in there.

To Dimple and all the others who are not finished yet – good luck and I know you can do this! And thanks to everyone else in the Vyas and Porcher labs past and present, who I might have forgotten!

I'd like to thank my friends and housemates Kate, Claire and Charlotte for their support after long and trying days in the lab. A very special thank you goes out to Chloe, who was always there with tea, laughs and greatness, and Aletheia, who inspired me on this journey. Also, THANKS to the crew from Jack Straws Lane 2010/11 for being there in my first year. Kate, for being a great friend and someone to share Austrian memories with!

A warm thanks to Shay, Steve, Emma and Jess for shenanigans and escapism from science to return refreshed to the bench. Another for the MMA class at OMAA led by Mark to let me vent frustration in trying times.

Importantly, I would like to thank everyone in the WIMM administration and core facilities for making everything run smoothly! Huge thanks to Paul, Kevin and Craig for offering FACS advice and fiddling with the Aria when I failed.

I would like to thank my college supervisor, Dr. Mary Board, and St.Hilda's college, as well as Celgene, who funded my studentship for these amazing three years.

Another very important person especially during the latter half was Dr. Marella De Bruijn who always had an open ear for my problems – many, many thanks. Also thank you to Liz Cloke and Stella Keeble for listening and good advice in troubling times.

This DPhil was a great journey which taught me a lot about science, life and helped me grow up. A thank you for everyone who was part of it and supported me throughout.

Abstract

Human haematopoiesis resembles a complex hierarchy, however most intermediate stages are only poorly defined. Efforts to characterise human progenitors have been inconsistent and failed to integrate previous knowledge. Furthermore, characterisation of normal progenitors has important implications in acute myeloid leukaemia (AML) biology. We previously established that leukaemic stem cells (LSCs) resemble the immunophenotypic progenitor compartments more closely than the stem cell fraction. Therefore, I set out to characterise human stem and progenitor cells (HSCPs) on phenotypic, molecular and functional level to complete the picture of human haematopoiesis.

I purified HSPCs based on their immunophenotype from adult bone marrow (BM) and umbilical cord blood (CB) to investigate steady state and neonatal haematopoiesis. To define differentiation potentials, HSPCs were subjected to functional in vitro assays on bulk and clonal level. Limit dilution assays were used to determine the frequency of cells with multiple differentiation potentials. RNA sequencing revealed underlying lineage priming and specific gene expression signatures.

I successfully characterized the incompletely defined $Lin^-CD34^+CD38^-CD45RA^+$ fraction in BM and CB, containing a $CD10^{lo}$ lymphoid-primed multipotent progenitor (LMPP) with T cell, B cell, NK cell, granulocytic and monocytic differentiation potential, and succeeded in placing it in the haematopoietic hierarchy with relation to similar lympho-myeloid progenitors defined by other groups.

This research lays the foundation to characterise early human progenitors with a comprehensive toolkit on a phenotypic, molecular and functional level. Findings from this thesis might provide knowledge about potential targets in LSCs.

Abbreviations

AML	acute myeloid leukaemia
APC	Allophycocyanin
ATRA	all trans retinoic acid
BM	bone marrow
CB	cord blood
CD	Cluster Of Differentiation
CLP	common lymphoid progenitor
CMP	common myeloid progenitor
DC	dendritic cell
DL1	delta-ligand 1
DNA	deoxyribonucleic acid
FACS	fluorescence activated cell sorting
FCS	fetal calf serum
FITC	fluorescine iso-thiocyanate
FLT3L	FLT-3 Ligand
FMO	fluorescence minus one
FSC	forward scatter
FTOC	fetal thymic organ culture
G-CSF	granulocyte-stimulating factor
GMP	Granulocyte-macrophage progenitor
HSC	haematopoietic stem cell
HSPCs	haematopoietic stem and progenitor cells
IL-	interleukin
IL-7	interleukin-7
IMDM	Iscove's Modified Dulbecco's Medium
LIC	leukaemia initiating cell
lin-	lineage negative
LMPP	lymphoid-primed multipotent progenitor
LSC	leukaemic stem cell
lt-HSC	long-term haematopoietic stem cell
M-CSF	macrophage stimulating colony factor
MEM	minimum essential medium
MEP	Megakaryocyte-erythrocyte progenitor
MGG stain	May–Grünwald–Giemsa Stain
MLP	multilymphoid progenitor
MNC	mononuclear cells
MPP	multipotent progenitor
MS5	Murine stromal cell cline 5
NK cell	natural killer cell
NOD/SCID	non obese diabetic/severe compromised immune deficiency

OP9	osteopetrosis 9
PB	peripheral blood
PBS	phosphate buffered saline
PCA	principal component analysis
PCR	polymerase chain reaction
PE	Phycoerythrin
PreAmp	Preamplification
QDOT	Quantum Dot
RNA	ribonucleic acid
RT	reverse transcription
SCF	stem cell factor
SD	standard deviation
SEM	standard error of the mean
SL-ICs	SCID-leukaemia initiating cells
SS	single stain
SSC	side scatter
st-HSC	short-term haematopoietic stem cell
TPO	thrombopoetin
UCB	umbilical cord blood

List of All Figures

Chapter 4

Chapter 5

Chapter 6

Chapter 7

Chapter 8

List of All Tables

Chapter 2

Chapter 4

Chapter 5

Chapter 6

Chapter 7

1 Introduction

1.1 Hierarchies and Models of Haematopoiesis

The human haematopoietic system has served as a paradigm to understand differentiation and the characteristics of stem cells over the last decades.

All blood cells are derived from pluripotent haematopoietic stem cells (HSCs) that can self-renew and give rise to multi-lineage progeny. Haematopoiesis is often depicted as a hierarchy with the HSC at the apex. It gradually loses pluripotency and self-renewal ability as it differentiates through series of gradually more committed progenitors and lineage-restricted precursors down to mature blood cells. Many different models of haematopoiesis have been proposed, in model organisms as well as in the human system.

The method of choice to purify and subsequently characterise haematopoietic stem and progenitor cells (HSPCs) is flow cytometry. Due to considerable technical progress, researchers today are capable of isolating functionally distinct HSPC populations on basis of their immunophenotype. Subsequent in vitro and in vivo assay paired with molecular techniques allow characterisation of HSPCs from fetal, neonatal and adult tissues.

Many fundamental findings in haematopoiesis are derived from research performed in model organisms. Studies in specific mutants and transplantation experiments have been performed in the mouse model due to ethical, logistical and technical reasons. Ease of manipulation of genes, the usage of highly inbred strains to eliminate variability and the short lifespan of mice facilitate experiments greatly[1].

It has to be considered that discoveries from the murine haematopoietic system cannot be translated fully into the human. However, the immunophenotype differs significantly between human and murine haematopoietic cells. For example, CD34, which is expressed on human HSCs[2], is not found on murine HSCs[3]. Furthermore, long-term reconstitution potential, which is one of the hallmarks of HSCs, is assayed through transplantation into a host organism. Therefore, human HSCs are transplanted into sublethally irradiated immunocompromised recipient mice[4], which will not provide the optimum physiological microenvironment for human HSCs. Among other species-related differences between human and murine biology, care has to be taken if findings from one system are translated into the other[1]. Nevertheless, the mouse model has been essential for haematopoietic research.

Considerable efforts have focussed on delineating the haematopoietic pathways of differentiation, which will be introduced in this section.

1.1.1 The Classical Model

The most prominent model of haematopoiesis is known as the classical or dichotomic model. Over the last decades, it has been regarded as the prime example of how blood stem cells differentiate. Until recently, it stood unchallenged.

This model is characterised by a divide in differentiation potentials, between all lymphoid lineages and the erythro-myeloid lineages. This classification most likely arose from histological examination of bone marrow (BM) cells. All blood cells are generated in the BM, apart from T cells, which develop in the thymus. Therefore,

when BM cells were observed for their morphological features, myeloid cells, red cells and platelets could be easily distinguished at different stages of development due to their morphology. B cells and their precursors on the other hand are very hard to separate only on basis of their morphological features. In addition, the purpose and function of B and T cells still remained to be identified. These are the reasons which led to the notion that lymphoid cells and MkE/myeloid cells arose from two separate forks of the haematopoietic hierarchy[5].

More evidence to this model was added when a common lymphoid progenitor (CLP) was identified in murine BM in the IL-7Ra+c-kit^{low} fraction[6]. This population could give rise to B, T and NK cells in sublethally irradiated recipients, but not to Mac-1+ myeloid cells. In vitro, single IL-7Ra+ CLPs never generated erythroid or myeloid cells[6] in this study.

Also, a common myeloid progenitor was found to reside in the murine adult BM by Weissman's group, and could be identified on basis of its CD34 and FcgRII/III expression in the Sca-1- fraction. It possessed MkE, Mk, E, GM, M, G and mixed GEMM clonogenic potential when plated in methylcellulose (MeC) limit dilution assays[7].

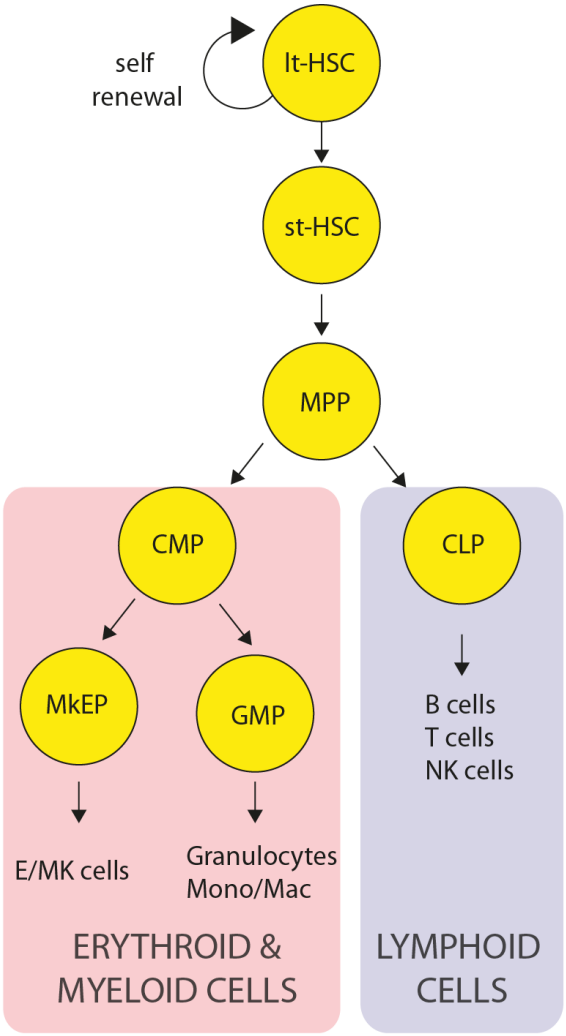

Figure 1.1. The Classical, Dichotomic Model Of Haematopoiesis.
In the classical model, the self-renewing lt-HSC gives rise to to a st-HSC with short-term reconstitution ability, which then gives rise to the MPP. Downstream of the MPP, the split into an erythroid/megakaryocytic/myeloid branch and a lymphoid branch occurs. The MkE-myeloid branch is initiated by the CMP, whereas the lymphoid cells are thought to arise from a CLP.
lt-HSC, long-term haematopoietic stem cell; st, short-term; MPP, multipotent progenitor; CMP, common myeloid progenitor; CLP, common lymphoid progenitor; MkEP, megakaryocyte-erythroid progenitor; GMP, granulocyte-macrophage progenitor; Mono, monocytes; Mac, macrophages; E, erythroid; Mk, megakaryocytic; NK, natural killer cells.

Another report also identified lymphoid biased progenitors in the thymus, which had lost in vivo myeloid reconstitution ability but could still give rise to B and T cells. These “low CD4” cells also had less proliferative potential than total Lin-BM cells. However, when injected directly into the thymus, no B cells were generated[8]; therefore suggesting that myeloid differentiation potential in a CLP is lost before B cell potential.

Another reason which lends credibility to the dichotomic hierarchy is the similarity of the mechanisms which rearrange TCR and IgG genes in B and T cells. A close developmental relationship among these cell types is suggested by this fact.

However, there are also reports which dispute the existence of CMPs and CLPs.

Nutt and colleagues could divide the murine CMP into 3 different subpopulations with respect to Flt3 and PU.1-driven GFP expression. Flt3-PU.1^{lo} CMPs mainly generated MkE colonies in vitro and expressed GATA-1, whereas the Flt3+PU.1^{hi} CMP and Flt3-PU.1^{hi} CMP both gave rise to macrophages and granulocytes and expressed transcripts for M-CSFR and G-CSFR[9].

Moreover, Pronk et al dissected the MkE-myeloid progenitor compartment in great detail in the murine bone marrow. They detected a variety of differentially primed progenitors at different stages of maturity. With the help of lineage exclusion and the markers c-kit, Sca-1, CD41, CD150, FcgRII/III, Ter119 and Endoglin, Mk-progenitors, Pre-MegEs, Pre-CFU-Es, Pro-Erythrocytes, CFU-E, GMPs and Pre-GMs were identified. Multi-lineage primed CMPs were the exception and rarely detected. Gene expression analysis then suggested that most progenitors were primed for one or two lineages, and rarely for all MkE/myeloid potentials[10]. These results tie in with work performed by Arinobu et al, who also utilized *Gata1* and

PU.1 expression to pinpoint MegE-primed (*Gata1*) and GM-lymphoid primed MPPs[11].

Studies have been published which contradict the original CLP research and show that it mainly gives rise to B cells in vivo and also V(D)J Recombinase is already active at the CLP stage[12]. In further in vitro assays on supportive stromal cells, the murine CLP has also been found to generate significant numbers of myeloid cells on a clonal level[13,14].

In human, the evidence for a dichotomic hierarchy is not as strong. Even though a CMP was identified by Manz et al., its existence remains debated. In vitro assays showed that only roughly 28% of the Lin-CD34+CD38-CD45RA-CD123+ immunophenotypic CMPs indeed generated G/M as well as MkE colonies on single cell level.

The human CLP still remains to be identified. Pang et al published a progenitor in the Lin-CD34+CD38+CD127+ fraction which was claimed to retain all lymphoid potentials, and it was termed CLP. However, there was no comprehensive in vitro and/or in vivo data to confirm this hypothesis in their report[15].

This classical model provided an excellent working model for many years, however, it is also an oversimplification, like most models.

Increasing evidence from other studies proposes a different, alternative model to the dichotomic hierarchy.

1.1.2 The Alternative Model

With the identification of a lymphoid-primed multipotent progenitor (LMPP) in murine BM in 2005, a cell type had been found which retained all lymphoid, monocytic and granulocytic differentiation potential but had lost erythroid and

megakaryocytic differentiation capacity[16]. This population could not be placed into the classical, dichotomic haematopoietic hierarchy.

Adolfsson and colleagues[16,17] therefore proposed a different hierarchical organization of haematopoiesis, which is illustrated in Figure 1.2. This alternative tree featured the segregation of MkE potential from the short-term-HSC (st-HSC), which differentiates through a potential CMP intermediate into erythroid and megakaryocytic cells. On the other hand, the st-HSC also gives rise to an LMPP population, downstream of which a GMP and potential CLP population can be found. The LMPP population has already down regulated critical regulators of erythro- and megakaryopoiesis, such as GATA-1, SCL/TAL1, EPOR and TPOR, which suggests that the LMPP might have undergone an irreversible lineage commitment step with the loss of MkE-potential.

Both CMP and LMPP are hypothesized to be able to generate a GMP.

This model remains challenged until this day, however, increasing evidence supports the segregation of the MkE branch, as more progenitors are identified which retain myeloid and lymphoid differentiation potential[18].

In human haematopoiesis, reports which publish similar cell populations are accumulating. The human LMPP was first identified by Goardon et al[19]. In human adult bone marrow, it resides in the Lin-CD34+CD38-CD45RA+ compartment. It retains full lymphoid differentiation capacity and also can give rise to monocytic

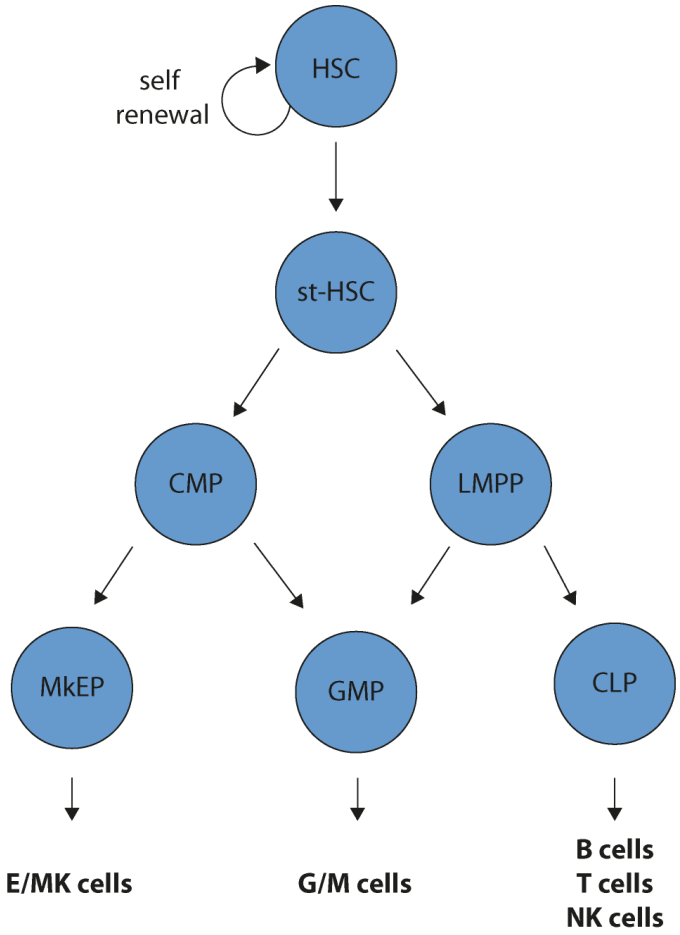

Figure 1.2. The Alternative Model Of Haematopoiesis.
The lt-HSC gives rise to a st-HSC with intermediate reconstitution potential, and downstream of this population, the MkE lineage branches off. It is unclear if this passes through a CMP. On the other side of the hierarchy, an LMPP population is generated, which possesses all lymphoid and granulocyte/macrophage potentials. The CMP and LMPP are hypothesized to give rise to a GMP population. The LMPP then generates all lymphoid cells, through a potential CLP intermediate progenitor.
lt-HSC, long-term haematopoietic stem cell; st, short-term; LMPP, lymphoid-primed multipotent progenitor; CMP, common myeloid progenitor; CLP, common lymphoid progenitor; MkEP, megakaryocyte-erythroid progenitor; GMP, granulocyte-macrophage progenitor; Mono, monocytes; Mac, macrophages; E, erythroid; Mk, megakaryocytic; NK, natural killer cells.

and granulocytic progeny. In terms of gene expression, LMPPs express lymphoid priming genes (Runx3, Notch-1, Flt3), but also myeloid genes such as CEBPa, SPI1(PU.1) and down regulate expression of MkE genes, such as GATA-1, EPOR or SCL/TAL1[19].

Another population retaining combined lympho-myeloid differentiation potential has been identified in CB and BM by Doulatov et al. Their CD10+ MLP can give rise to B cells, NK cells, T cells, DCs and monocytes[20].

Kohn et al also published a population with LMPP-like characteristics in human BM, however it was unclear whether granulocytic and monocytic cells could be detected among its progeny[21]. This population is characterised by high expression of CD62L (L-Selectin) and CD45RA.

These reports, in addition to other findings of CD10+ postnatal progenitors with lympho-myeloid differentiation capacity[22], for example, reinforce the alternative model in human haematopoiesis.

1.1.3 The Myeloid Based Model

Pioneered by Kawamoto et al, the myeloid-based model follows the hypothesis that all haematopoietic cells are by default programmed to differentiate into a myeloid cell. In clonal multilineage assays permissive for B, T and myeloid (M) cells with progenitors from murine foetal liver and adult murine BM, only bi-lineage colonies were found. These colonies were either of a B/M or a T/M nature, and no B/T clones were detected. Later on, the assay was modified to permit detection of erythroid development, which resulted in similar findings. These collective results were summarized in the myeloid-based model in which a multipotent cell (i.e. HSC or MPP), with myeloid (M), erythroid-megakaryocytic (E), T cell (T) and B cell (B)

differentiation potential gives rise to a ME branch, and a lympho-myeloid branch (MTB). The ME progenitor can generate E and M cells. The MTB in turn differentiates into a MB and MT progenitor. It is characteristic for the myeloid-based model, in which each progenitor retains myeloid differentiation capacity by default. Kawamoto et al suggested that this is due to the fact that phagocytosis is the most primitive way of host defence. If every progenitor retains myeloid differentiation capacity, it could result in an advantage in infection[23-26].

Additional evidence supporting this model was found when B-macrophage bipotential progenitors were identified in murine BM. These CD19-CD45R+ cells could give rise to macrophages and B cells on a clonal level, however at very low frequencies (3.3%)[27].

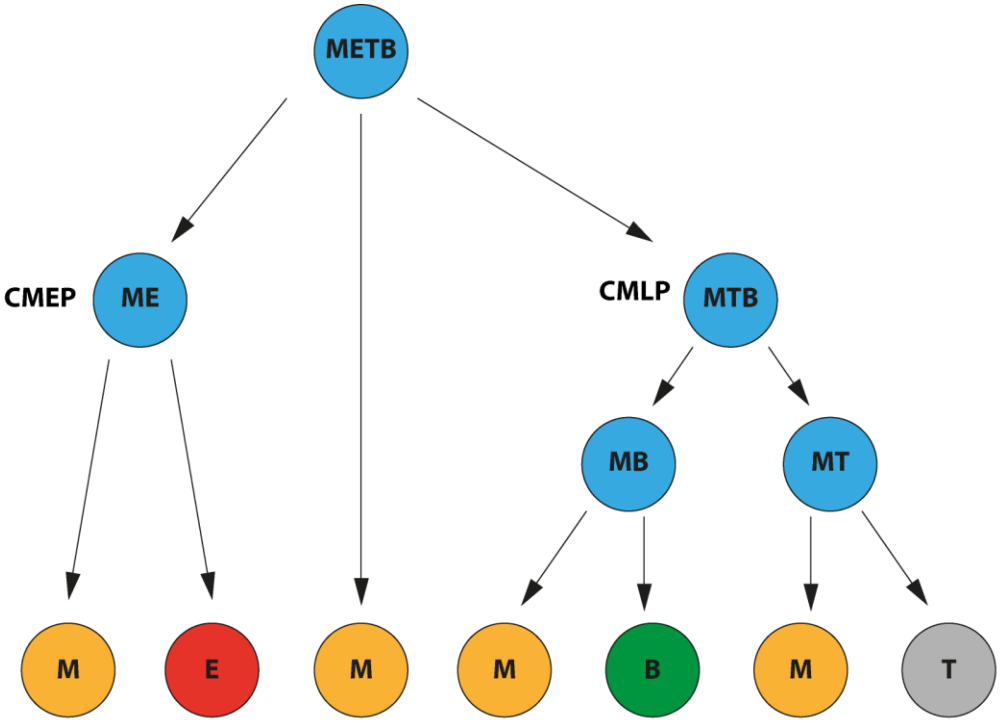

Figure 1.3. The Myeloid-Based Model Of Haematopoiesis.
A multipotent cell, with myeloid (M), erythroid-megakaryocytic (E), T cell (T) and B cell (B) differentiation potential gives rise to a ME branch, and a lympho-myeloid branch (MTB). The ME progenitor can generate E and M cells. The MTB in turn differentiates into a MB and MT progenitor. This concept is characteristic for the myeloid-based model, in which each progenitor retains myeloid differentiation capacity by default.

1.1.4 The Stochastic Model

Till et al first investigated spleen colony forming cells (CGU-S) in 1964[28]. They reasoned that the CFU-S cells had one of two potential fates they could undergo. Those were either self-renewal and giving rise to a daughter CFU-S cell (birth), or differentiation (death). This decision is governed by a probabilistic rule, which is based on the frequency of CFU-S derived from the experiment. With the help of Monte Carlo calculations, cell fate decisions could be modelled and illustrated. This is reflected in the early cell fate decisions of HSPCs, which are seemingly stochastic. Ogawa et al refined these findings and adapted them to fit with a model of human haematopoiesis. This is illustrated in Figure 1.4 A. A cell with all potentials (i.e. a HSC or MPP) gives rise to all combinations of tri- and bi-potential progenitors, which in turn generate the fully differentiated cells.

1.1.5 The Sequential Model

Studies from murine foetal liver CFU-S differentiation in liquid culture prompted Nicola and Johnson[29] to propose a sequential model of haematopoiesis. In this hierarchy a CFU-S cell passes through a progenitor stage which generates a CFC-M. The progenitor then passes through a CFC-GM stage, until it finally reaches the CFC-E stage, which is the last remaining differentiation potential[29].

The sequence of the differentiation potentials lost has been changed and Brown et al pioneered a hierarchy which is shown in Figure 1.4 B. Here, a multipotent cell passes through a sequence of progenitors which gives rise to precursors for different cells at defined points. This model was first based on studies with the acute pro-myelocytic leukaemia cell line HL-60[30]. Later on the model was modified

to lie in accordance with phylogeny and the order in which differentiation potentials are lost is MkE, granulocyte, monocyte, B and T cell potentials[31]. Interestingly, the definition of the LMPP[16,19] would fit into such a model, as would the MLP, which retains lymphoid and monocytic capacity, but has lost granulocytic differentiation ability.

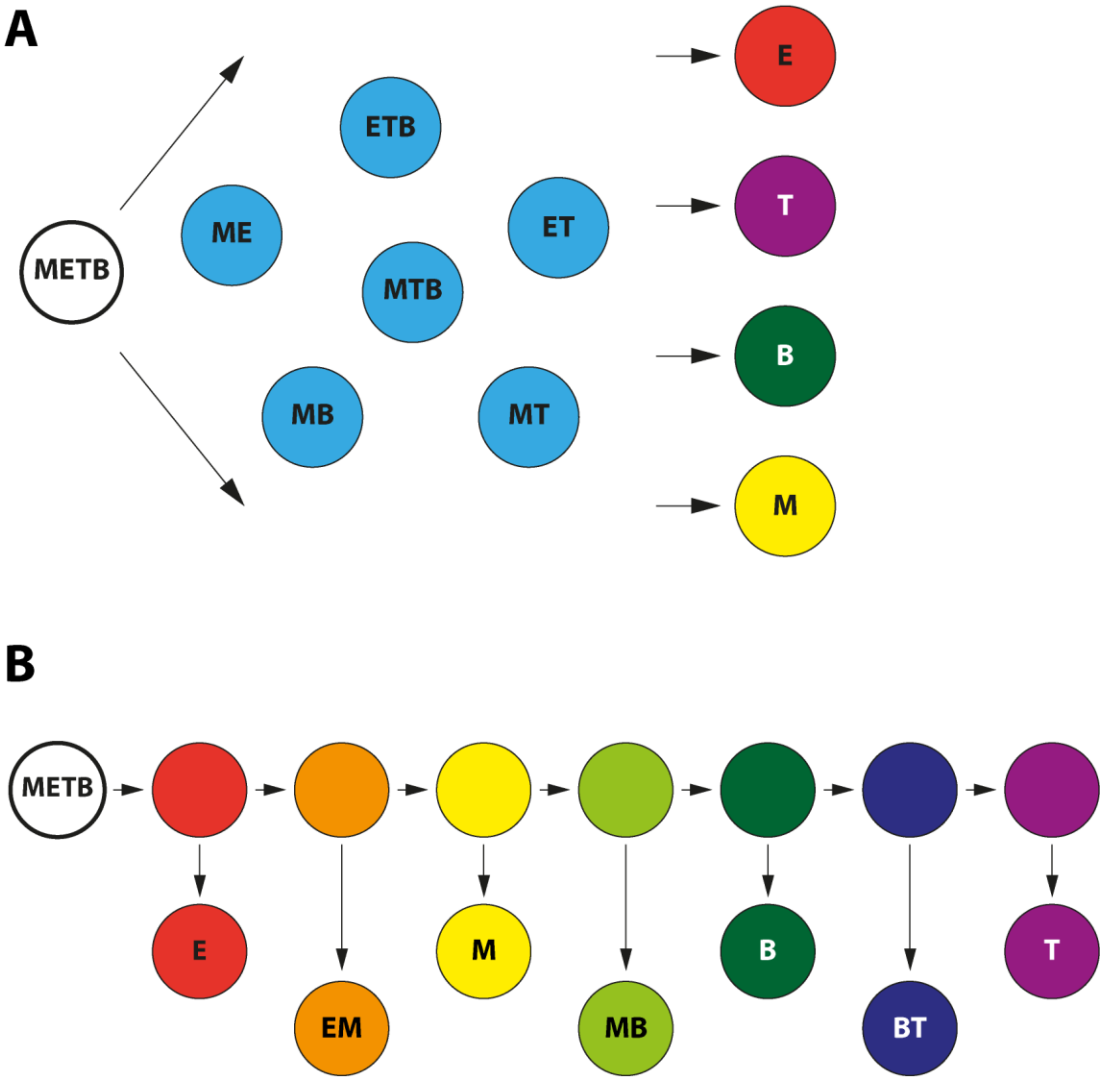

Figure 1.4. Other Models Of Haematopoiesis.
A) The Stochastic Model proposes that the cell fate decision of stem and progenitor cells is governed by a probabilistic rule, which stochastically determines the decision the cells take. So the multipotent cell (i.e. HSC or MPP) with METB potentials can give rise to all combinations of tri- and bi-potential progenitors (shown in blue) which then in turn give rise to fully differentiated cells (E, T, B, M).
B) The Sequential Model suggests that a multipotent cell (i.e. HSC or MPP) passes through a sequence of progenitors, which gradually lose cell fate potentials and generate differentiated progeny "along the way".
E, erythroid-megakaryocytic; M, myeloid; B, B cell; T, T cell.

1.2 Human Stem And Progenitor Cell Biology

1.2.1 Human Haematopoietic Stem Cell and Multipotent Progenitor

HSCs are the pluripotent cells which sustain generation of all blood cell lineages throughout life. They have extensive self-renewal potential and are capable of multilineage engraftment in recipients in the long term.

The human HSC was first identified to reside in the CD34+ fraction of human BM[32,33]. CD34 has been one of the most important markers since to enrich for HSPCs. Exclusion of lineage positive (mature) cells is also a popular means to enrich for immature cells. By further identification of the marker Thy-1 (CD90)[34] the frequency of HSCs could be increased in the CD34+ fraction in foetal BM. This population also only takes up low levels of the dye Rhodamine123 and was shown to contain human pluripotent progenitors[35]. Finally, expression of CD38, a marker of proliferation, was shown to segregate more committed progenitors from CD38- immature cells[36]. It was established that HSCs could be identified to high purity with the immunophenotype of Lin-CD34+CD38-CD90+.

Lt-multilineage reconstitution potential of the HSC was established in xenograft assays[35,37].

Majeti et al also first identified the human multipotent progenitor (MPP) in CB, to reside in the Lin-CD34+CD38-CD90-CD45RA- fraction. It was shown to have intermediate replating potential between the HSC (CD90+CD45RA-) and a yet unidentified CD90-CD45RA+ population. In xenograft assays, it gave rise to transient multilineage engraftment[37].

1.2.2 Human Lympho-Myeloid Progenitors

A lymphoid-primed multipotent progenitor (LMPP) was identified in murine BM[16], which challenged the dichotomic concept of the classical model of haematopoiesis.

In human, the Lin-CD34+CD38-CD90-CD45RA+ compartment was first investigated in CB by Majeti et al. They classified it as a population with low replating potential and no long-term reconstitution ability[37]. Its characteristics and lineage potentials were not defined until Goardon et al found this population also in BM and subjected it to in vitro and in vivo assays. LMPP-like characteristics were attributed to the Lin-CD34+CD38-CD90-CD45RA+ fraction (1.4% of Lin-CD34+); it could give rise to B, monocytic and granulocytic cells on MS5 stromal cells and T cell progenitors on OP9-DL1 stromal cells. Limit dilution assays were used to determine the frequency of LMPPs in the CD38-CD45RA+ compartment. 1 in 6 immunophenotypic LMPPs gave rise to B and myeloid cells, and 1 in 12 to T cells[19].

Replating experiments showed that the candidate LMPP had a replating potential intermediate between the MPP and the CMP (roughly 20 CFU per 2500 cells plated). If plated in methylcellulose to investigate myeloid and erythroid colony forming ability, the LMPP showed virtually no erythroid potential after 14 days. Its cloning efficiency ranged around 20% and was at a similar level as MPP cloning efficiency. In conditions permissive for megakaryocyte differentiation, the LMPP failed to generate any colonies which stained positive for GPIIB/IIIa[19].

Gene expression analysis of 5 and 10 cells showed that those cells expressed genes of lymphoid priming, but also had started to down regulate HSC- associated genes. Megakaryocyte-erythroid genes were down regulated or could not even be detected. Myeloid genes, such as CSF2R, CSF3R, and interestingly, PU.1 (SPI1) were expressed at intermediate levels in these candidate LMPPs[19].

In murine haematopoiesis, when mice carrying a mutation in the PU.1 locus were generated, they were defective for B, T and myeloid cells; however they gave rise to normal numbers of erythroid and megakaryocytic cells[38]. This data is consistent with studies from GATA-1 and PU.1 reporter mice, in which GATA-1+ MPPs were MkE primed and PU.1+ MPPs gave predominantly rise to myeloid and lymphoid cells[11]. Taken together, these data suggest that PU.1 is very important at the LMPP stage and the specification of the myeloid and lymphoid lineages.

The properties of the CD38-CD45RA+ compartment were also investigated by other groups. Doulatov et al subjected CB and BM samples to analysis and they published the multi-lymphoid progenitor (MLP) in 2010[20]. According to their analysis, the CD45RA+ compartment in CB and BM is exclusively CD10+, and can also co-express CD7. It constituted 2% of the Lin- compartment.

When subjected to in vitro assays, the MLP gave rise to monocytic, dendritic, B, NK and T cells, also on a clonal level. It failed to give rise to granulocytic progeny in liquid culture. In methylcellulose, the MLP only proliferated poorly and differentiated into macrophage colonies. The researchers did not assess megakaryocyte potential in this study, even if it is unlikely that the MLP would show any significant Mk potential.

MLPs are thought to be the main source of DCs, and in vitro they could give rise to functional DCs which could be stimulated with TLR-ligands[20]. In this study, MLPs were also transplanted into non-obese diabetic–severe combined immunodeficiency mice with a null mutation for the common γ -chain (NSG mice) intrafemorally. Engraftment levels were very low (0.03%) and peaked after two weeks[20]. Gene expression analysis of the MLP revealed that it had comparatively high levels of Pax5, a B cell gene, GATA-3 and other lymphoid transcripts[20]. Microarray analysis subsequently showed that the gene expression profile of MLPs clustered between immature populations (HSC and MPP) and mature lymphoid populations (BNK progenitor and pro-B cells); this data suggests that the MLP is a progenitor with predominantly lymphoid differentiation potential[39].

The published data concerning LMPP and MLP suggests that these two populations are two classes of lympho-myeloid progenitors with similar properties. One of the questions which has been a major focus of attention in this thesis is how LMPP and MLP are related.

Recently, another group also identified a population in human BM which was also classified as a human LMPP. Their approach fractionated BM from young donors with the help of CD34, CD45RA, CD10, CD7 and CD62L (L-selectin)[21]. The resulting Lin-CD34+CD45RA+CD62L^{hi}CD10- population (hereafter referred to as CD62L^{hi}) was subjected to in vitro functional assays and in vivo xenograft assays. In MeC assays permissive for E, M and G colony formation, the CD62L^{hi} population did not give rise to any colonies at all.

In liquid culture on supporting stromal cell lines, CD62L^{hi} generated significant numbers of B, NK, DC and myeloid cells from one to three plated cells (not specified if single cell level). The frequency of cells in the CD62L^{hi} fraction with B/NK potential was found to be 1 in 5. Additional data suggests that the myeloid progeny was mainly of monocytic nature; however it is not specified if the CD62L^{hi} lacks granulocytic potential or if it was not looked for.

Assays on OP9-DL1 stroma permitted for the differentiation of CD62L^{hi} into T cells, at a frequency of 1 in 5 in the CD62L^{hi} fraction. Single cell cloning efficiency of the CD62L^{hi} population ranged around 10%.

Kohn et al also managed to engraft CD62L^{hi} in NSG recipients after intratibial injection after 2 weeks at a level of 0.03% hCD45+ in the murine BM. The graft consisted of both CD33+ myeloid (~75%) and CD19+ B cells (~15%).

To relate the CD62Lhi population to immature (Lin-CD34+CD38-) and more mature, lymphoid-primed CD10+ population, microarray analysis was performed. It was found that the CD62Lhi population clustered between the immature and mature cells, as expected. Upregulated transcription factors and genes encoding cell surface markers included the Runx family, CEPBA, CD33, CD2, IL2RG amongst others. Kit was found to be significantly up-regulated when compared to the Lin-CD34+CD38- and CD10+ populations[21].

Taken together, these data suggest that Kohn et al identified another cell progenitor with lympho-myeloid differentiation potential and detectable lineage priming for the lymphoid lineages.

Research from our and other groups has shown that with the aid of different cell surface markers, a great number of progenitor cells can be identified with all

nuances of lineage potentials. Recently, a study involving the labelling of single murine LMPPs with individual barcodes, subsequent transplantation into recipients and massive parallel sequencing of the progeny generated by single LMPPs, found considerable heterogeneity in this progenitor compartment. This elegant experimental design permitted the tracking of single LMPPs in a physiological environment. Interestingly, it was shown that the LMPP is a highly heterogeneous population with distinct classes of different lineage imprinting. The highest proportion of LMPPs seemed to give rise to DCs, followed by B and B-DC imprinted classes[40]. This data suggests that there is much more work to be done in order to dissect the LMPP compartment in detail and establish on clonal level which lineages are being generated from the LMPP.

1.2.3 Human Myeloid Progenitors

In contrast to the lymphoid branch of the human haematopoietic hierarchy, myeloid progenitors could be identified with seemingly more ease.

Manz published an approach to purify CMP, GMP and MEP from human BM with the help of CD45RA and CD123 (IL-3Ra) antigen expression. Three distinct populations could be identified and their functional potentials were determined in vitro. The CMP was found to reside in the CD45RA-CD123^{lo} fraction, the GMP was determined to express CD45RA and CD123 and the MEP was found to be negative for both markers[41]. As it turned out to be difficult to separate MEP and CMP on the basis of these two markers, an additional antigen was included – CD110 (TPOR). TPOR+ cells in the CD45RA-CD123$^{lo/-}$ fraction were shown to

retain virtually only erythro-megakaryocytic potential, whereas the TPOR- cells behaved like the multipotential CMP[42].

However, the CD110 antibody was discontinued by the manufacturer, as it could not be validated that it bound to the TPOR. Due to this reason, this antigen could not be included in the research in this thesis.

Doulatov et al proposed a different approach to purify CMP, GMP and MEP, through expression of FLT3 (CD135) and CD45RA. The CMP was hypothesized to reside in the CD135+CD45RA+ population, the GMP in the CD135+CD45RA+ fraction and the MEP was found to lack expression of both markers. However, the characterisation of these immunophenotypic compartments lacks in vitro verification, as no megakaryocytic assays were performed[20].

The GMP, in human[19] as well as in mouse[43], has shown residual lymphoid potential. This issue has not yet been resolved and GMPs remain incompletely purified.

1.3 Haematopoietic Progenitors and Acute Myeloid Leukaemia

The main focus of this research laboratory lies on Acute Myeloid Leukaemia (AML). AML is a very aggressive haematological malignancy and one of the most common adult leukaemias. About a third of every leukaemia diagnosed in the UK is an AML[44] and has the highest prevalence in patients over 65 years of age (accessed on the 22nd of July 2013). According to Cancer Research UK, less than half of the patients survive, and about 2.5% of all cancers are AMLs[45] (accessed on the 22nd of July 2013).

Diseases, in which an accumulation of immature myeloid precursor cells (“blasts”) arises in the bone marrow, are classed as AMLs. They may arise de novo, or as a result of a pre-existing blood disorder, for example, myelodysplastic syndrome (MDS). They can be divided into different subgroups by the French-American-British (FAB) according to their morphology. Clinical features of AML include bone marrow failure (which can result in anaemia, easy bruising and/or infections) and the immature blasts can infiltrate various organs[46].

The etiology of AML is complex; genetic lesions and karyotypic abnormalities may be caused through the exposure to toxins or ionising radiation[47,48]. Karyotypic abnormalities have been used as a framework to determine clinical remission rates, response to leukaemia drugs and the probability of relapse[49-52]. Due to these reasons, AML is one of the main research interests of this group.

1.3.1 Leukaemic Stem Cells

AML, as a disease in which accumulation of incompletely differentiated precursors occurs, has been hypothesized to be driven by a self-renewing population, which is capable of reconstituting the leukaemic phenotype[53-55]. This leukaemic stem cell (LSC) population is thought to be a small subset of the cancer cells which has the potential to differentiate into all bulk cells of the tumour. Furthermore, it can expand the LSC pool by symmetric division and therefore maintain the tumour[56].

LSCs are hypothesized to reside in the bone marrow, in the protective environment of the BM niche. With respect to therapy, LSCs have to be eradicated in course of the treatment, as they are capable of reconstituting the disease, even if there are no bulk cancer cells detected in the peripheral blood.

Leukaemic activity was hypothesized to reside in the stem/early progenitor compartment in AML. Lapidot et al were the first to identify an AML-initiating cell through transplantation into immunocompromised mice[57]. Bonnet and Dick further then transplanted CD34+CD38+ cells into immunocompromised, irradiated mice and could faithfully reconstitute the phenotype of the patient leukaemia, including genetic abnormalities and blast aberrations[54]. This data suggests that the transforming leukaemic event occurs in the early-stem and progenitor fraction, or maybe in the HSC. It is also worth mentioning, that other groups have profound leukaemic activity in the CD34+CD38+ fraction of leukaemic BM[58,59]. It was hypothesized that this was due to the CD38-antibody bound by the sorted cells, which allowed the AML-cells to be cleared by the residual immune function of the host. These conflicting results can be attributed to the large heterogeneity of AML phenotypes and patient-patient variability[58]. More research will help to clarify these questions.

1.3.2 Leukaemic Activity In The Progenitor Compartment

Further research from our research group[19] has identified the immunophenotypic compartment in normal bone marrow which most closely resembles LSCs. Surprisingly, LSC activity was localised in the LMPP-like and GMP-like fractions of AML bone marrow. In in vivo experiments the LMPP-like population could reconstitute the leukaemia, and global mRNA profiles of normal LMPP and LMPP-like populations clustered together. Gene set enrichment analysis also showed that a signature associated with self-renewal was enriched in LMPP-like and GMP-like LSCs. This suggests a hybrid LSC with the self-renewal property of stem

cells and the proliferative potential of progenitors, which may fuel the disease and drive relapse[19].

These findings are consistent with previous reports which suggested that leukaemic activity resides in the CD34+CD38- compartment[54] and more precisely in the CD90- fraction[60]. Figure 1.5 illustrates the model of leukaemogenesis which was established on basis of the experiments performed led by Goardon et al[19]. The HSC gives rise to an MPP population, which in turn is found upstream of the LMPP (CD38-CD45RA+) population. AMLs show a corresponding expansion of LMPP and GMP compartments in AML. These LMPP-like and GMP-like populations can self-renew and give rise to the AML blast population. It could also be established that the LMPP-like population can give rise to the GMP-like population in the xenograft assay.

In a mouse model of mixed-lineage leukaemia, similar observations were made, as the leukaemic activity was found to reside in a GMP-like population with an enrichment for HSC-genes in the LSC population[61].

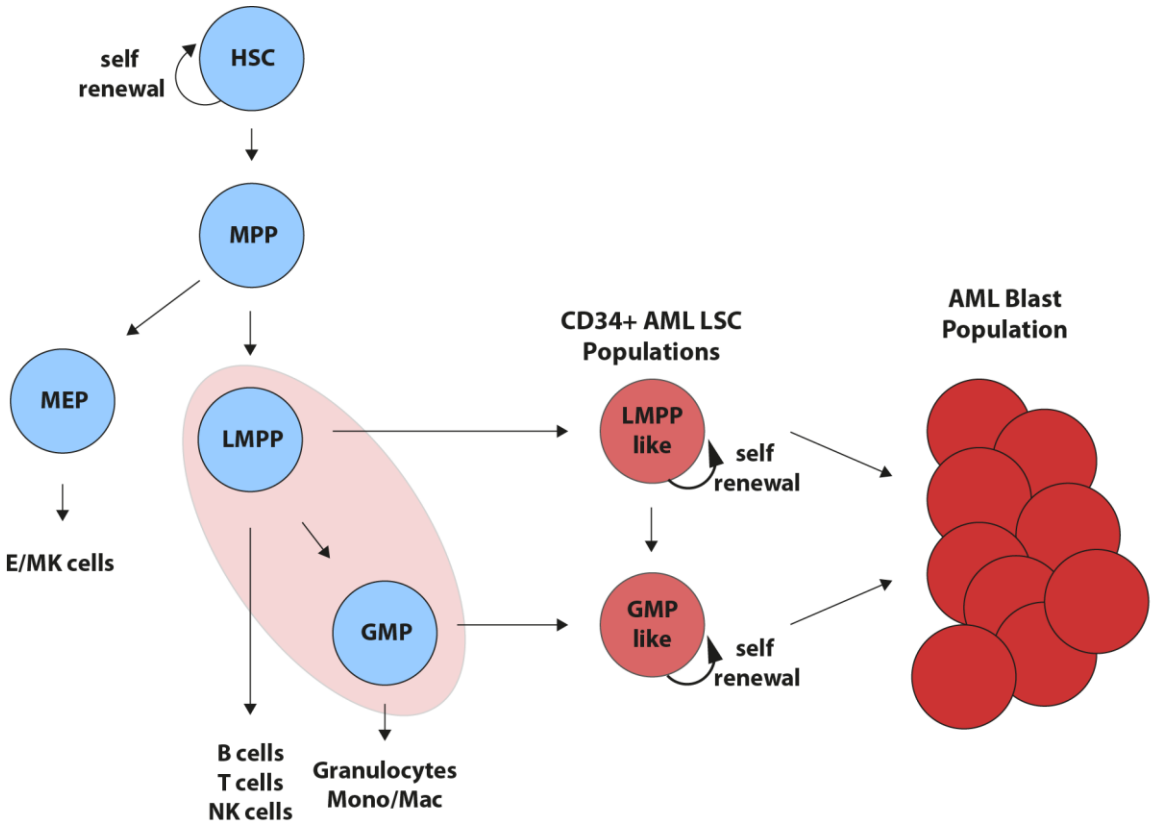

Figure 1.5. Model of Human Haematopoiesis And Acute Myeloid Leukaemia LSCs.
Immunophenotyping, in vitro assays, in vivo transplantation and gene expression profiling were combined to establish a model of AML leukaemogenesis. The HSC gives rise to an MPP population, which in turn is found upstream of the LMPP (CD38-CD45RA+) population. AMLs show a corresponding expansion of LMPP and GMP compartments in AML. These LMPP-like and GMP-like populations can self-renew and give rise to the AML blast population. Principle component analysis showed that the transcriptional profiles of the LMPP- and GMP-like populations most closely resembled their normal immunophenotypic counterparts. One of the differences between the leukaemic and normal populations, however was the enrichment of a stem-like signature in the leukaemic samples. This suggests that the LSC populations are hybrid populations with the self-renewal properties of stem cells and the proliferative potential of progenitors. It could also be established that the LMPP-like population can give rise to the GMP-like population.
HSC, haematopoietic stem cell; LMPP, lymphoid-primed multipotent progenitor; MEP, megakaryocyte-erythroid progenitor; GMP, granulocyte-macrophage progenitor; Mono, monocytes; Mac, macrophages; E, erythroid; Mk, megakaryocytic; NK, natural killer cells.

1.3.3 Relevance Of The Research Performed In This Thesis For AML Biology

In order to identify the LMPP-like LSCs in AML, it is essential to understand the corresponding LMPP in the normal context. As mentioned before, LSCs might not be targeted by leukaemia therapies and could cause relapse. If the LMPP-like LSC population could be purified to a higher degree (the frequency of LSCs in the LMPP-like compartment is only 1 in 10^4) it might be possible to subject it to functional and molecular assays to define its properties. Certain molecular mechanisms could be targeted by specific inhibition, or with antibodies which could result in phagocyte-mediated clearance, as published recently[62].

Therefore it is crucial that the relationship of the LMPP in the human haematopoietic hierarchy is understood, as well as the molecular mechanisms it is governed by and the functional potentials of this particular progenitor population.

If this questions are solved, they will provide a foundation to ask what drives transformation of the LMPP, and if it occurs at the LMPP level or early in haematopoiesis/leukaemogenesis.

1.4 Research Questions

The research performed in this doctorate set out to investigate human haematopoietic progenitors in detail. The main focus lies on the identification and characterisation of human myelo-lymphoid progenitors, especially progenitors residing in the Lin-CD34+CD38-CD45RA+ fraction of human BM and CB. This could be achieved by finding an additional marker to separate LMPP

subpopulations with distinct functional potentials, which can be investigated in vitro, as this information will be essential to target the LMPP-like and GMP-like LSC population in acute myeloid leukaemia.

As described in the introduction, much more work has to be performed in order to define the human haematopoietic hierarchy more clearly. This thesis and the methods optimised in the process lay the foundation for additional experiments to investigate these questions.

Furthermore, many conflicting publications of early human progenitors have not yet been related to each other. I set out to clarify the relationship between the human lymphoid primed multipotent progenitor (LMPP)[19], with the multilymphoid progenitor (MLP)[20] and the CD62Lhi population[21].

In addition, global mRNA expression profiles were acquired by next-generation sequencing to investigate lineage priming on the molecular level.

1.5 Summary Of The Research Questions Asked In This Thesis

- Validation of LMPP T cell and NK in vitro functional potential
- Definition of functional potentials and hierarchical relationship of LMPP and MLP
- Testing of additional markers to purify the LMPP further (CD53, CD84, CD127)
- Testing of CD62L LMPP and GMP subpopulations

2 Materials and Methods

2.1 Samples

2.1.1 Normal Human Umbilical Cord Blood and Bone Marrow

Fresh umbilical cord blood (UCB) was obtained from consenting mothers via the National Blood Service (NBS) from the Oxford NHS Blood and Transplant (Oxford, UK) on the day of birth. Frozen umbilical cord blood buffy coat was obtained from the NBS in Filton (NBS Filton, Bristol, UK) from consenting mothers. Fresh UCB mononuclear cells (MNCs) were diluted with RMPI 1640 (Gibco, Invitrogen, UK) and isolated by Ficoll density centrifugation (Lymphoprep™, Fresenius Kabi Norge AS) 2-4hrs after collection. UCB buffy coat was thawed in a 37°C waterbath, passed through a 70μm cell strainer (BD, US) and washed with RPMI (Gibco, Invitrogen, UK). MNCs were isolated by Ficoll density centrifugation (Lymphoprep™, Fresenius Kabi Norge AS).

Normal human bone marrow was obtained from patients undergoing orthopaedic surgery with informed consent (MDS Bio OXREC C 06/1606/110) with a normal blood count/film. The bone marrow was diluted in RPMI 1600 medium (Gibco, Invitrogen, UK), passed through a 70μm strainer and layered onto Lymphoprep™ (Fresenius Kabi Norge AS). Following a 25min centrifugation step at room temperature at 1,800rpm without braking, the mononuclear cell layer is removed and washed for 10min at room temperature at 1,400rpm with IMDM (Gibco, Invitrogen, UK) 10%FCS with 10ng/mL DNase.

2.1.2 CD34+ Enrichment

Fluorescence activated cell sorting is a time consuming procedure, the duration of which might impact negatively on the viability of HSPCs. Thus we tried to minimise sorting and cell processing time by preselecting CD34+ cells from CB and BM. Magnetic cell separation is a widely used technique to separate cells based on the expression of a desired antigen (positive selection) which is recognized by a mAB which can be bound to a magnetic bead. The labelled cells are retained by magnetic forces in a tube or column while unbound cells are washed off. By removal of the magnetic force, the cells of interest can be eluted with high purity. Different kits which use this principle are available for purchase. The supplier of choice in our group was Miltenyi. CB and BM MNCs derived from frozen buffy coat were enriched with MACS microbead kit (Miltenyi Biotech, Germany) for CD34+ cells as described in the manufacturer's manual. Figure 2.1 shows the variability of the Miltenyi CD34 microbead kit, in which the CD34+ content of BM samples is assessed by simple FACS analysis. The percentage of CD34+ cells is evaluated in the unseparated, depleted and enriched fractions. We could never extract all of the CD34+ cells. There was wide range of CD34+ cells in the enriched fraction (from 46.8% - 98.2%, N=3).

This prompted us to test three kits from different suppliers: the Miltenyi CD34 microbead kit, EasySep Human CD34 Selection Kit by StemCell Technologies and the Dynal CD34 Progenitor Cell Selection System by Life Technologies. Detailed information about the different experimental set ups can be found in Table 2.1. The kits were tested on a range of different samples, from Acute Myeloid Leukaemia (AML) to myelodysplastic syndrome (MDS) cell and normal human BM cells. Every sample was counted and

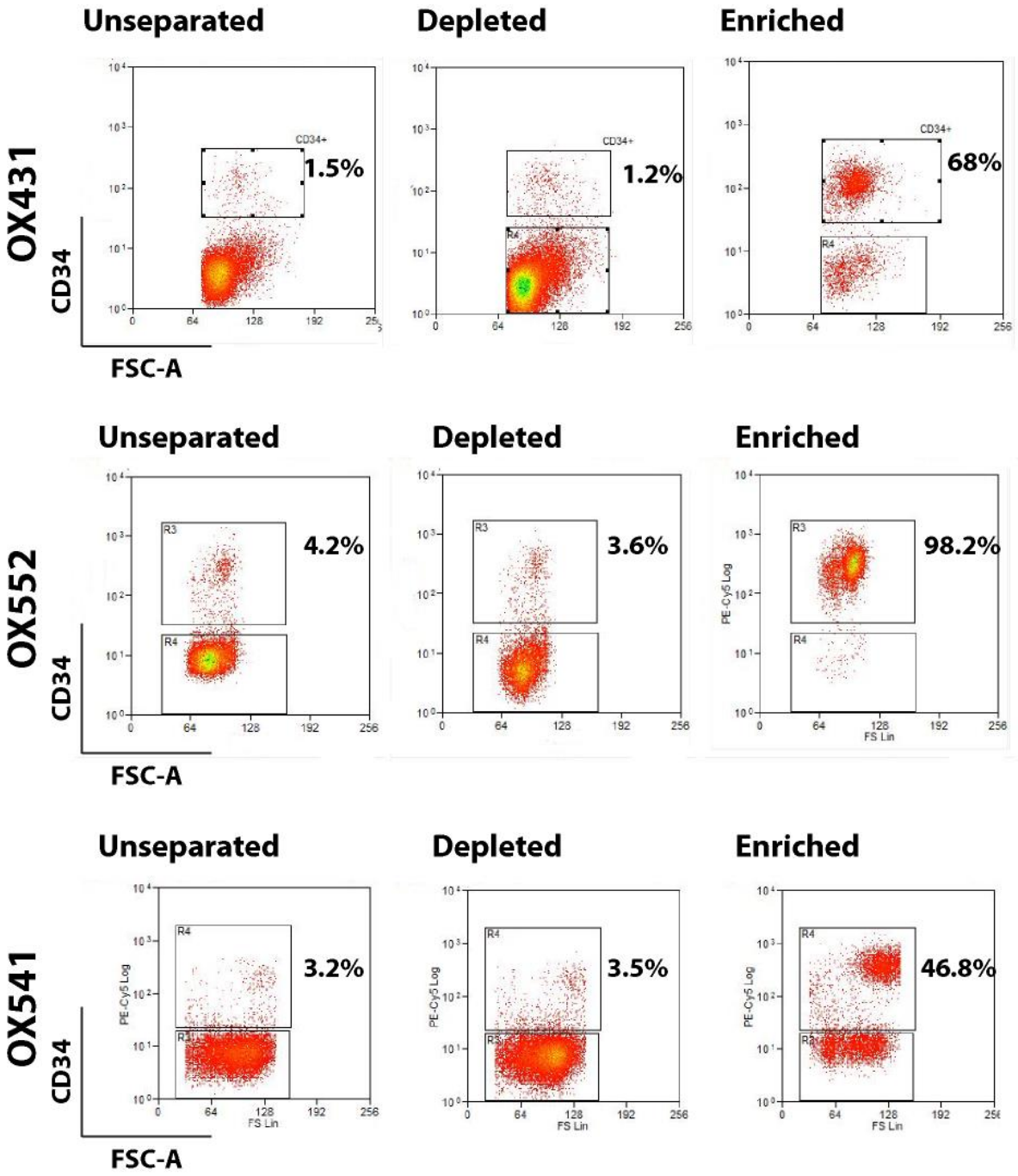

Figure 2.1. CD34+ Enrichment Variability Across Samples.
Three samples human control bone marrow samples from individuals with haemochromatosis and immune cytopenia were subjected to a Miltenyi MACS based CD34+ enrichment procedure Percentages of the CD34+ fractions are shown for the unseparated, depleted and enriched fraction of the three samples.

Name	CD34 MicroBead Kit with MACS© LS Columns	EasySep Human CD34 Selection Kit	Dynal CD34 Progenitor Cell Selection System
Supplier	Miltenyi	Stem Cell Technologies	Life Technologies/Invitrogen
Time	75 mins	70 mins	100 mins
Principle	CD34+ cells are bound to magnetic particles and are retained in the column via magnetic forces; other unbound cells are removed with the flow through.	CD34+ cells are bound to dextran-coated magnetic nanoparticles using a bispecific Tetrameric Antibody Complex. Unbound cells are poured off.	CD34+ cells are bound to magnetic particles using an antibody directed to the desired antigen. Unbound cells are poured off.
Bead Diameter [µm]	0.05, biodegradable	not specified	4.5
CD34 Epitope recognised	QBEND10	QBEND10	461
Max. number of cells	$2x10^9$	$2x10^9$	not specified
FC Receptor Blocking Step	yes	FCR blocking reagent in selection cocktail	not specified
Other notes	no bead removal step	no bead removal step	bead detaching step necessary

Table 2.1: Comparison Of Experimental Procedures and Separation Principles Of CD34 Enrichment Kits.
Three kits for magnetic selection of CD34+ from blood or bone marrow were compared with respect to their principles and specifications.

divided into three equal parts and separated with each kit. Figure 2.2 shows the enriched fractions across all kits from 4 different samples, comparing them to the unseparated samples (top row). CD34+ percentages were evaluated by FACS. Surprisingly, the Stem Cell Technologies kit failed to extract any CD34+ cells at all in disease samples; a problem which could not be resolved even after thorough discussion with the Stem Cell Technologies support team. In the only normal sample tested, the enriched fraction contained a mere 15.6% CD34+ cells. The enriched fraction in the samples separated with the Dynal kit had variable purities (34.1%-95.8% CD34+) and performed relatively poor isolating normal CD34+. The enriched fractions selected by the Miltenyi CD34 microbead kit showed the highest purity in 3 out of 4 cases and extracted normal CD34+ cells most successfully. Figure 2.3 also illustrates the amount of CD34+ cells left in the depleted fractions/flow through, and compares them to the unseparated fraction (top row). None of the tested kits succeeded in extracting all CD34+ cells. However, the Miltenyi kit was very efficient at extracting $CD34^{hi}$-expressing cells. All kits struggled with the extraction of $CD34^{lo/dim}$ cells. These results are summarised in Table 2.2, including CD34+ percentages and cell numbers from unseparated and depleted fractions. Taking the processing time and these results into consideration, we decided that the Miltenyi CD34 microbead kit was the best alternative on the market at the time and it was used for the remainder of this study.

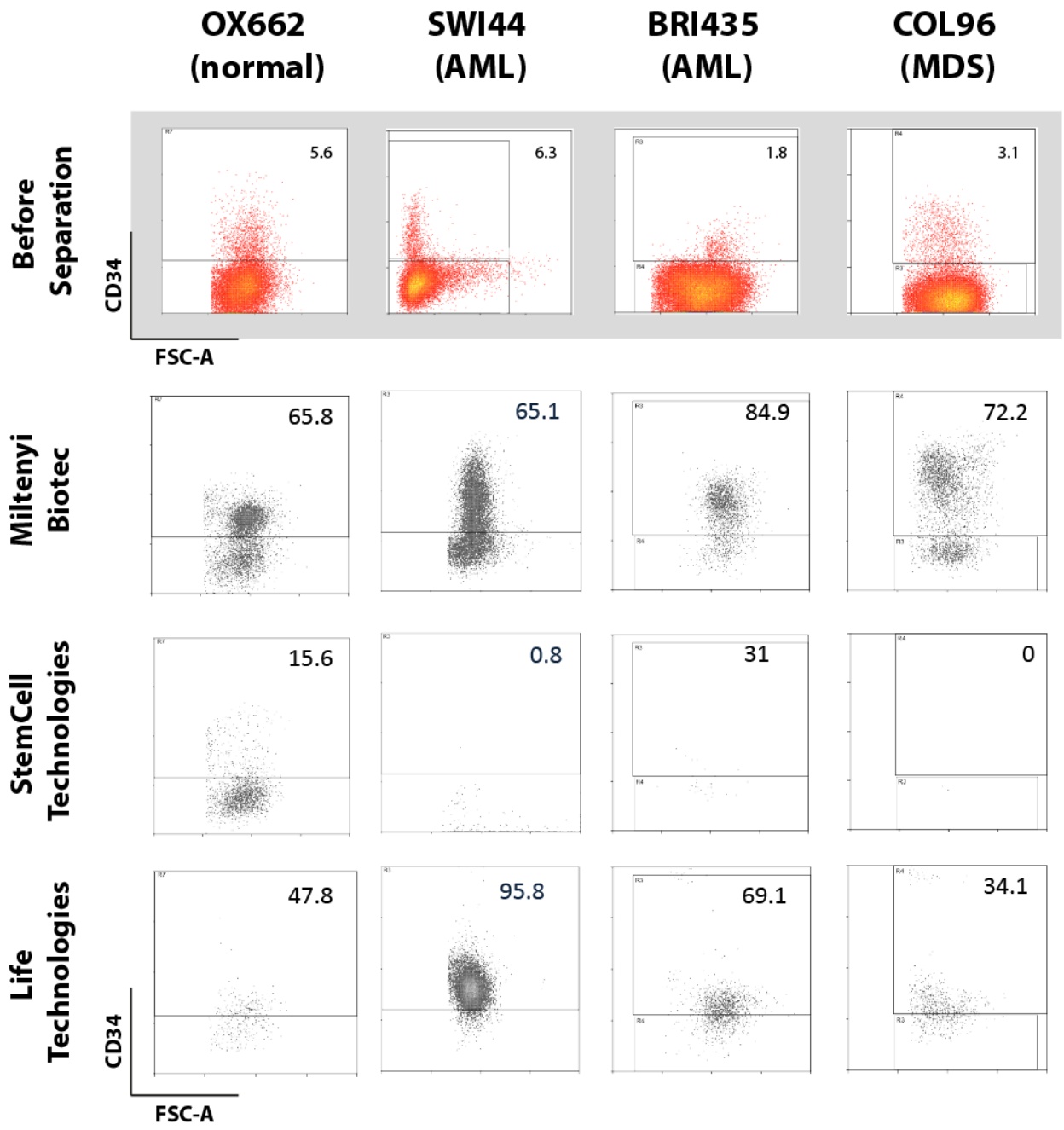

Figure 2.2. Comparison of the Enriched Fraction Using Different Methods of CD34+ Separation.

Four different samples, with varying diagnoses, were split into equal parts and separated with different CD34+ kits as described by the manufacturer's protocol. FACS profiles of the CD34+ enriched fractions are shown. All plots are gated on live and single cells. AML, acute myeloid leukaemia; MDS, myelodysplastic syndrome.

			Miltenyi		StemCell Technologies		Life Technologies	
		Before separation	Depleted	Retained	Depleted	Retained	Depleted	Retained
OX662 (normal)	Cell count	500	400	4.2	386	0.2	448	2
	# CD34+ cells calculated	7.8	17.1	2.8	21.7	0.0	20.5	1.0
	FACS CD34%	5.6%	4.3%	65.7%	5.6%	15.6%	4.6%	47.8%
SWI44 (AML)	Cell count	47	37.5	1.55	36	0	35	0.5
	# CD34+ cells calculated	6.3	1.0	1.0	1.8	N.A.	1.3	0.5
	FACS CD34%	6.3%	2.6%	65.2%	5.0%	0.0%	3.7%	95.8%
BRI435 (AML)	Cell count	13.6	6.6	1.8	11.7	0	10.3	0.004
	# CD34+ cells calculated	0.26	0.11	0.15	0.037	0	0.15	0.03
	FACS CD34%	1.9%	1.6%	84.0%	3.2%	0.0%	1.5%	69.0%
COL96 (MDS)	Cell count	8.2	7.4	0.12	6.16	0	9.75	0.0003
	# CD34+ cells calculated	0.26	0.19	0.09	0.15	0	0.21	0.001
	FACS CD34%	3.1%	2.6%	73.0%	2.5%	0.0%	2.2%	66.0%

Table 2.2: Comparison Of All CD34 Enrichment Experiments Across All 3 Different CD34 Enrichment Kits.
4 bone marrow samples (left) with varying diagnoses were split into equal parts (see cell count before separation) and separated with 3 different kits (top). All different fractions were counted and their CD34+% evaluated by FACS. Depleted refers to the flow through, enriched refers to the fraction which should contain most of the CD34+ cells. "# CD34+ cells calculated" refers to the calculated number of CD34+ cells which hypothetically should be present in the fraction (calculated from % of CD34+ cells and counted cell number). All cell counts are given in x10^6. .

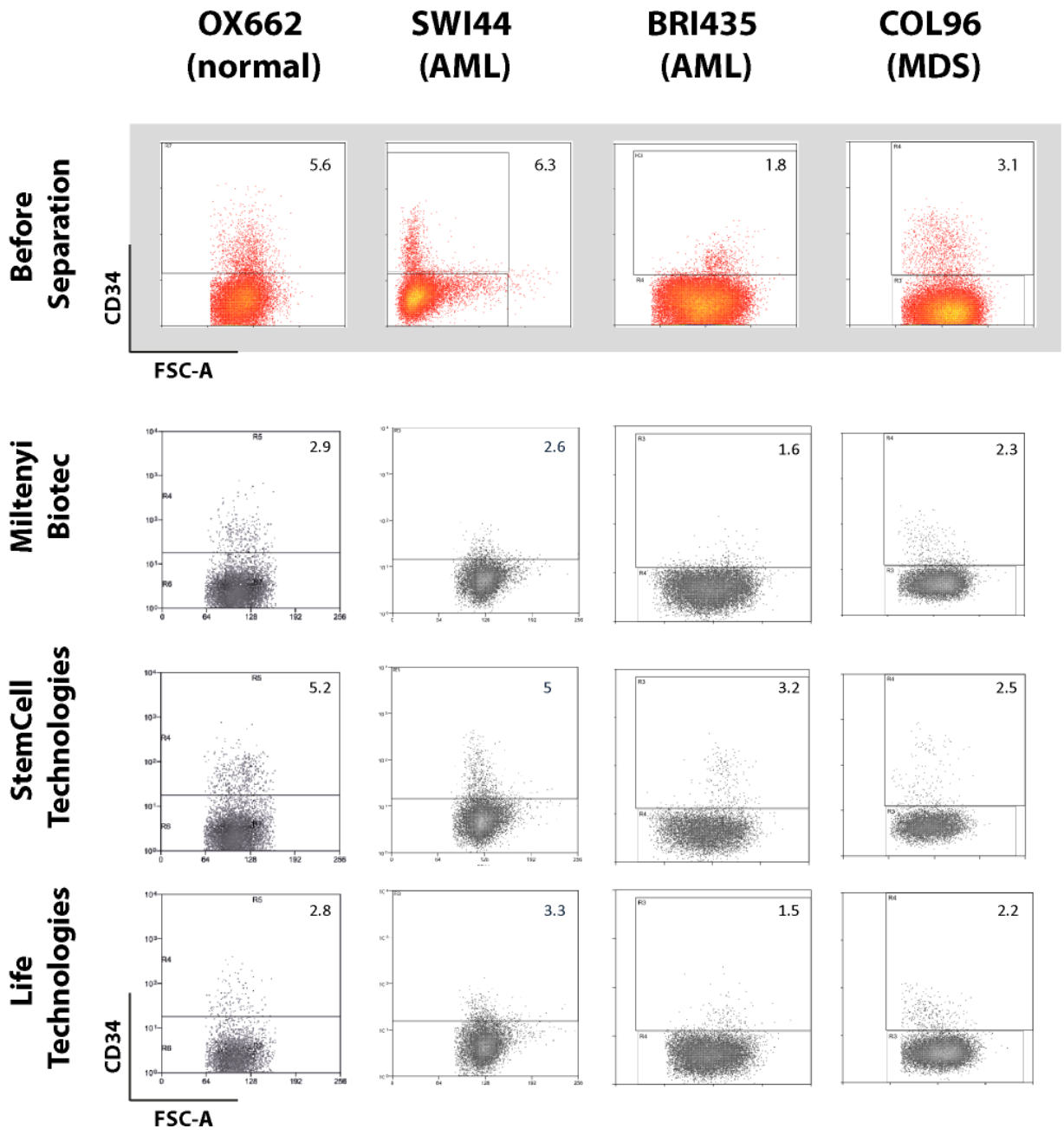

Figure 2.3. Comparison of the Depleted Fraction Using Different Methods of CD34+ Separation.

Four different samples, with varying diagnoses, were split into equal parts and separated with different CD34+ kits as described by the manufacturer's protocol. FACS profiles of the samples before separation (top row) and of the depleted fractions after separation are shown. The numbers indicate the percentage of CD34+ cells in the depleted fractions. All plots are gated on live and single cells. AML, acute myeloid leukaemia; MDS, myelodysplastic syndrome

2.1.3 Overnight Culture

CD34+ cells from CB or BM were cultured overnight in StemSpan SFEM (StemCell Technologies, Canada) with 100ng/mL hSCF, hFLT3L, hTPO (Peprotech, Rocky Hill, NJ, US) before sorting at a maximum density of 1.5 x 10^6 per mL.

2.2 Flow Cytometry

The method of choice to purify HSPCs from single cell suspensions of BM or peripheral blood (PB) is fluorescence activated cell sorting (FACS) and is based on labelling specific cell surface markers expressed on populations with a monoclonal antibody conjugated to a fluorophore or a fluorochrome. With the help of a carrier fluid (typically PBS buffer based), cells are transported through a flow cytometer to the flow cell, where they pass an array of lasers, which is capable of exciting the fluorescent label on the cell. According to the signals emitted by the cells, desired populations can be separated and sorted to obtain highly purified populations. Detectors record and amplify the fluorescent signal emitted from the cell. This is converted by a computer program to a single event defined by its mean fluorescence intensity (MFI) and represented as a dot on a scatter plot. Modern flow cytometers can analyse and sort several thousands of events per second and contain up to 7 lasers. Up to 32 different parameters can be analysed in parallel in theory. In practice, availability of reagents and compensation requirements limit the amount of antigens that can be interrogated in parallel. In our group, at this time, a maximum of 12 fluorochromes is used. As mentioned before, compensation can be an extensive problem.

Fluorochromes can be excited by light of a particular wavelength (typically lasers are used for this task), which causes them to adopt a higher state of energy. When they fall back to their original energy level, they can emit light of a particular wavelength. In flow cytometers, this light is directed via beam splitters and mirrors through band-pass filters which only let specific wavelengths pass, into a photomultiplier tube (PMT) detector.

If emission spectra of two different fluorochromes overlap, the signal emitted will not only be recorded by the designated detector, but also by detectors for other fluorochromes. For example, a signal emitted from the fluorochrome FITC will not only be detectable in the FITC channel, but will also “bleed” into the channel for PE when both are excited with the 488nm laser.

This problem can be solved by using single stained controls to quantify the amount of spectral overlap. The cytometer voltages can then be adjusted to optimise separation. In order to eliminate the bleed through, the spectral overlap has to be compensated. This happens in many modern flow cytometers as an automated process. The instrument only requires the data from single stained controls, which contain a positive and a negative population to calculate the optimum compensation with the help of a matrix. However, in my hands, I prefer to manually check compensation every time I perform an experiment. As mentioned before, the more fluorochromes, or “colours”, are used in parallel, the more care has to be given to the correct controls.

Aside from single stained controls, unstained and fluorescence-minus-one controls (FMOs) are useful tools to ensure properly compensated FACS data. FMOs are, as the name suggests, controls that contain all of the fluorochromes used in one

particular FACS staining panel, but one. An example of such a staining panel for a sample and FMOs can be found in Table 2.3. FMOs not only provide a means to check the automated compensation of the flow cytometer, but also enable the researcher to set a gate with respect to all the other fluorochromes in the staining panel.

Figure 2.4 illustrates how I optimised gating with the aid of FMOs. This is an example of the first four plots of a common HSPC sort. In the first panel, events are plotted with respect to forward scatter, which provides an indication of cell size and the MFI for Hoechst. Hoechst is a dsDNA dye that can penetrate the plasma membrane of dead or dying cells. This figure shows the Hoechst FMO however, therefore indicating the correct position of the gate. Moving on, dead cells are excluded and only the $Hoechst^-$ cells are further considered for analysis and/or sorting. The second panel shows the exclusion of doublets or large fragments of debris etc. In the third panel, cells are analysed for their expression of lineage markers, for example CD2, CD3, CD19 and CD56. In the last panel cells are plotted with respect to their expression of the early haematopoietic and endothelial marker CD34 and CD38, which is a marker associated with proliferation.

The second row focuses on the FMO for QDot605, which sets the gate for $lineage^-$ cells. The third row shows FMO PerCP, which is conjugated to the anti-CD34 monoclonal antibody (mAB), and therefore the gate to sort the desired $CD34^+$ HSPCs can be placed accordingly. FMO FITC is depicted in the bottom row, is a very crucial control to ensure the CD38 gate is set correctly. CD38 is a very important antigen in our study, because it can separate early stem and progenitors (CD38-) from more committed progenitors (CD38+). CD38 expression resembles

a continuum, rather than discrete populations and due to this reason, FMOs are essential to ensure gates are drawn correctly to only sort specifically sorted cells.

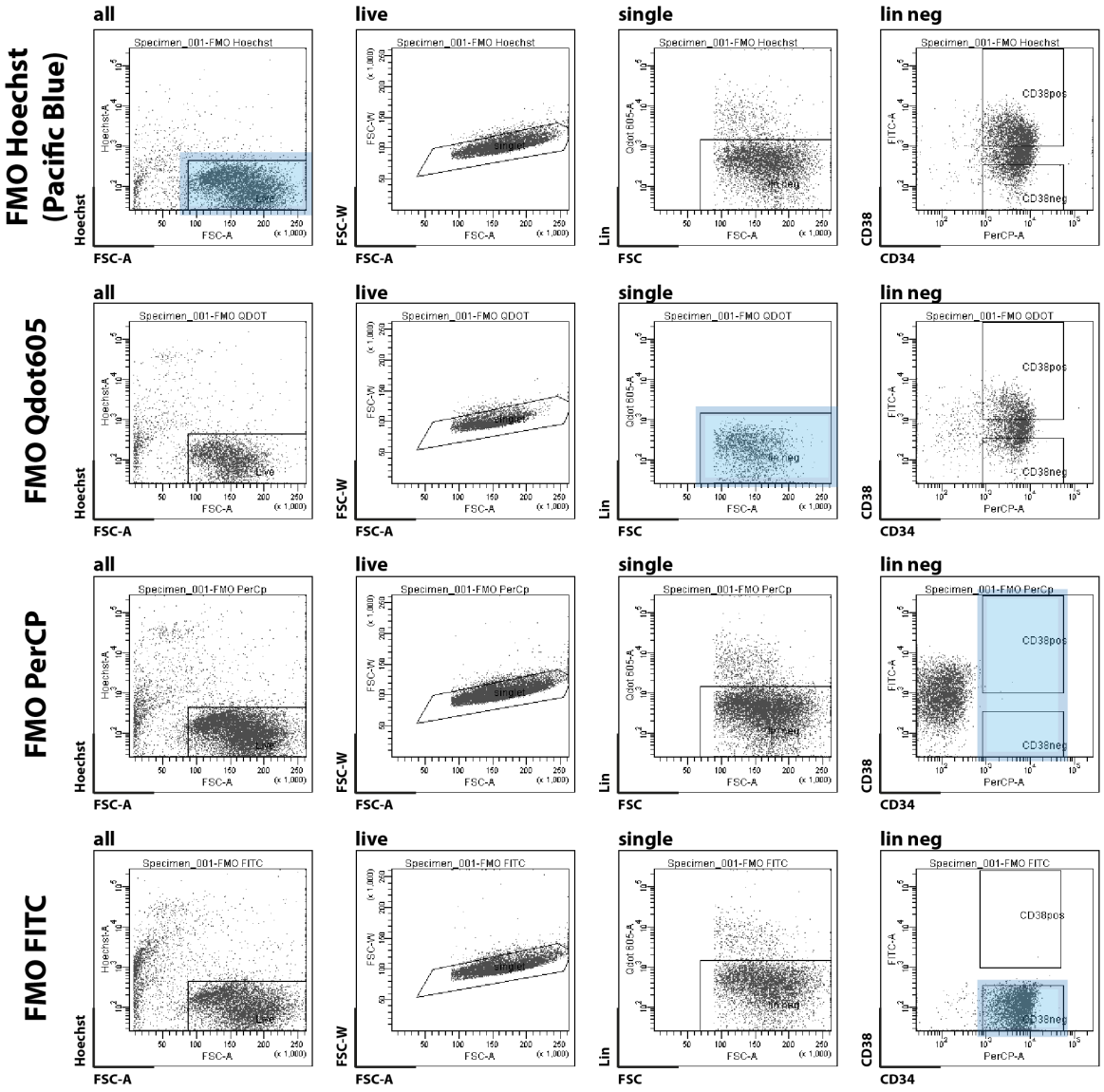

Figure 2.4. Gating with FMOs.
Fluorescence Minus One (FMO) controls are used to determine the position of gates in order to sort certain populations. The examples here illustrate the way gates are placed to ensure only specifically stained cells are sorted/analysed, especially if the expression of the antigen in question resembles a continuum rather than discrete populations. The first panel in each row shows a live gate which excludes Hoechst+ cells. The second panel focusses on doublet exclusion to ensure only single cells are analysed to prevent false positives. The third panel represents an example of a typical lineage exclusion gate, and the fourth panel illustrates how CD34+ cells can be separated on basis of their CD38 expression to select immature (CD38-) and more mature (CD38+) populations.

2.2.1 General Staining Procedure

Cell staining was performed in accordance with published literature[19] CD34+ cells (see CD34+ isolation protocol) were stained with monoclonal antibodies. An example of a typical staining panel is demonstrated in Table 2.3. Cells were incubated with the titrated amount of antibody on ice for 20 minutes in the dark. After the incubation period, cells were washed with 2mL FACS buffer. The cells were then pelleted for 5 min at 1,200 rpm at room temperature. Cells stained with Qdot (Invitrogen) conjugates were washed twice after the incubation period. Cells were incubated with streptavidin APC Efluor780 as a secondary staining step for 10 minutes. They were then washed once and filtered through a 70µm strainer before sorting.

	CD38 FITC	CD34 PerCP	CD45RA PE	CD123 PeCy7	CD10 APC	CD90 Biotin + SA APC eFluor780	Lineage Qdot605	Hoechst Pacific Blue
FMO FITC		5µL	2.5µL	5µL	2.5µL	2µL	2µL	3µL
FMO PerCP	5µL		2.5µL	5µL	2.5µL	2µL	2µL	3µL
FMO PE	5µL	5µL		5µL	2.5µL	2µL	2µL	3µL
FMO PeCy7	5µL	5µL	2.5µL		2.5µL	2µL	2µL	3µL
FMO APC	5µL	5µL	2.5µL	5µL		2µL	2µL	3µL
FMO APC eFluor780	5µL	5µL	2.5µL	5µL	2.5µL		2µL	3µL
FMO Qdot605	5µL	5µL	2.5µL	5µL	2.5µL	2µL		3µL
FMO Pacific Blue	5µL	5µL	2.5µL	5µL	2.5µL	2µL	2µL	
Sample	5µL	5µL	2.5µL	5	2.5	2µL	2µL	3µL

Table 2.3. Example of A Typical FACS Panel Presented As Pipetting Scheme.

2.2.2 Titration of Monoclonal Antibodies

Every newly acquired antibody in use was titrated to guarantee optimum staining properties, titration plots and optimised concentrations can be found in Figure 2.5 A-D. A. MNCs were stained with varying amounts of the antibody to be tested (e.g. 1µL, 2.5µL, 5µL etc) and analysed on a flow cytometer. Mean fluorescence intensity (MFI) values of the positive (stained) and negative (unstained) fraction were used to calculate the signal to noise ratio. The signal to noise ratio provides an indication of the resolution between the stained and unstained populations. Generally, the amount of antibody with the highest signal to noise ratio was selected for future experiments. If a plateau of many similar signal to noise ratios was evaluated, the most cost-effective concentration was selected.

CD45RA FITC HI100

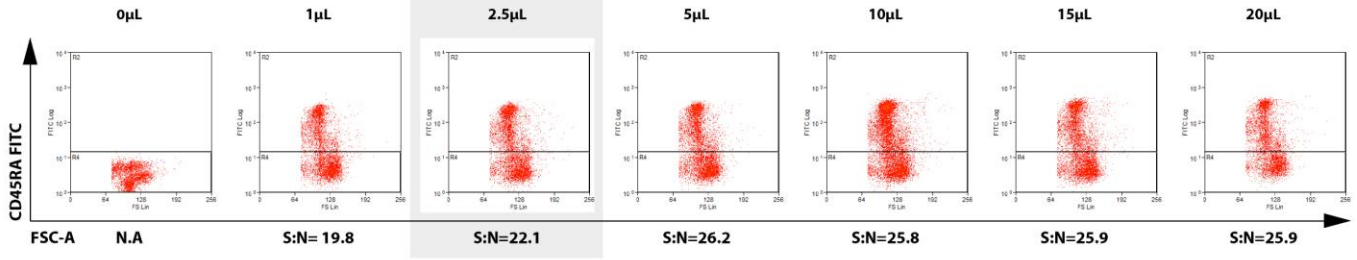

CD38 FITC HIT2

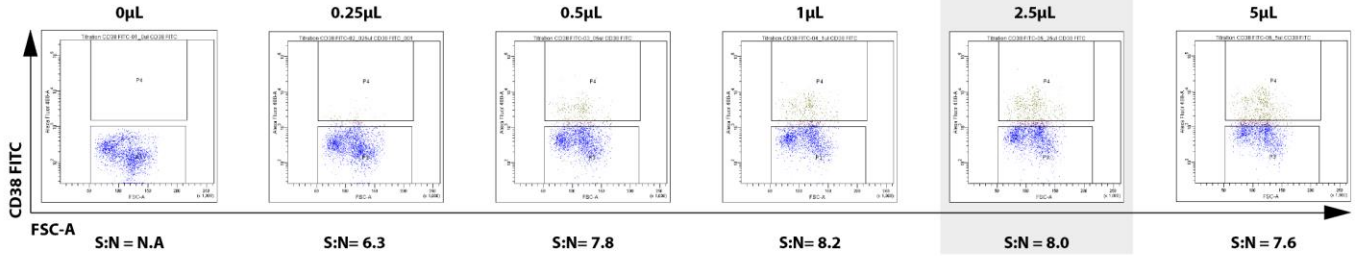

CD38 Alexa Fluor 700 HIT2

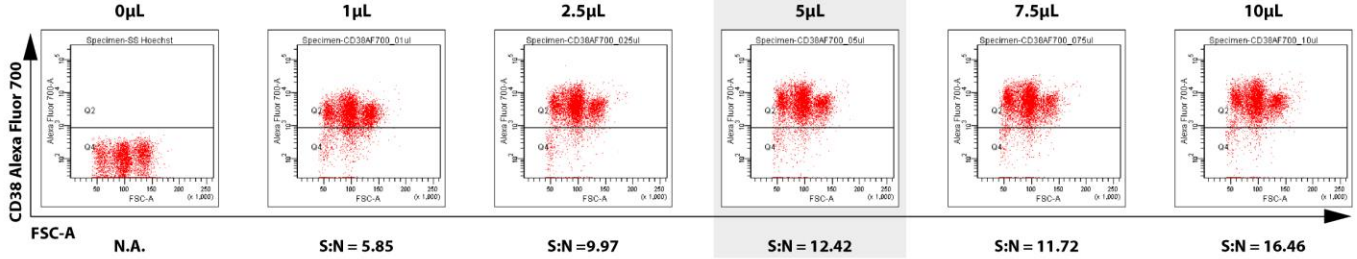

BAH-1 APC

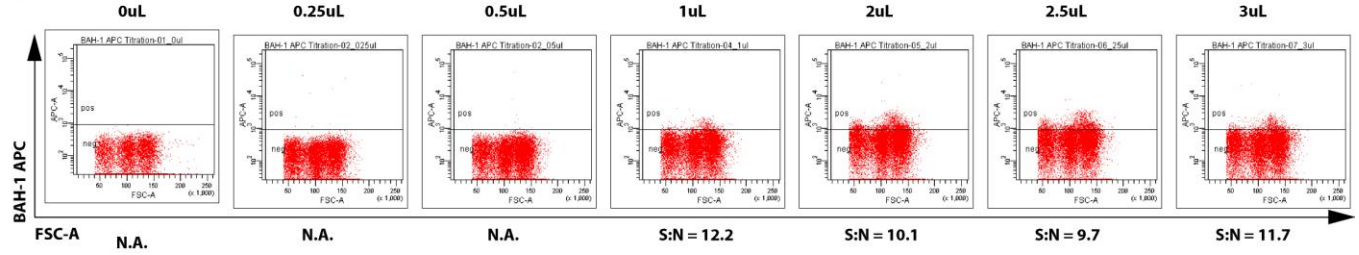

BAH-1 PE on CB MNCs

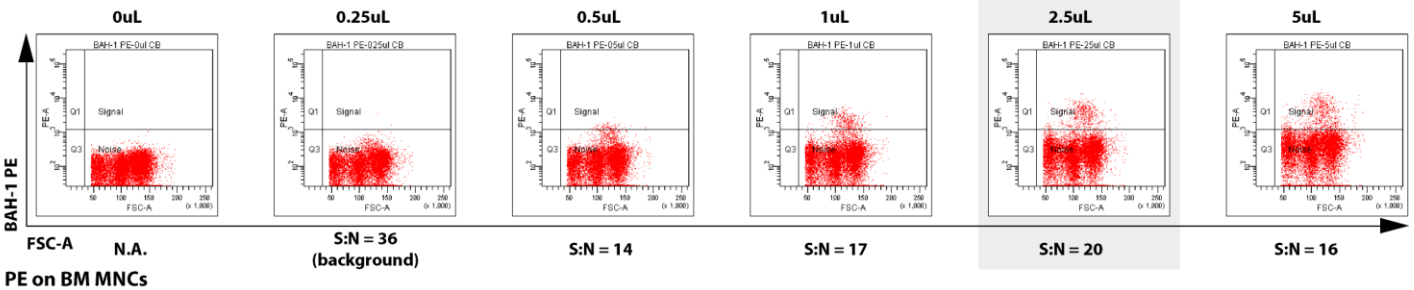

BAH-1 PE on BM MNCs

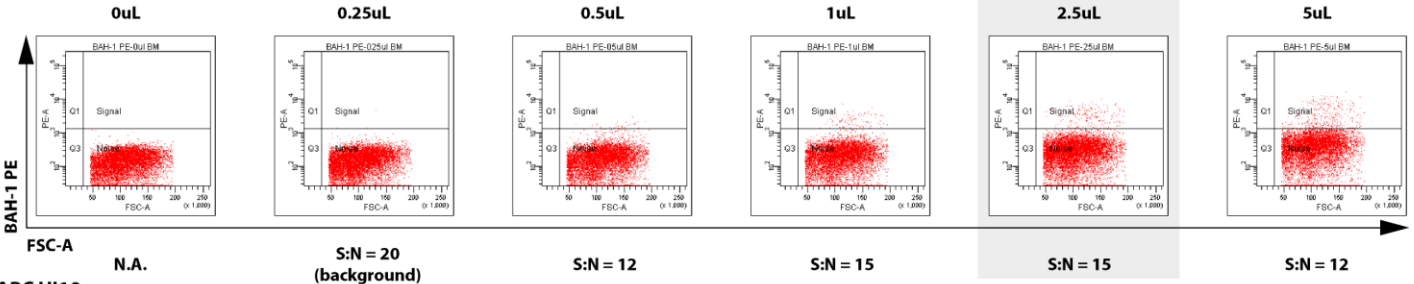

CD10 APC HI10a

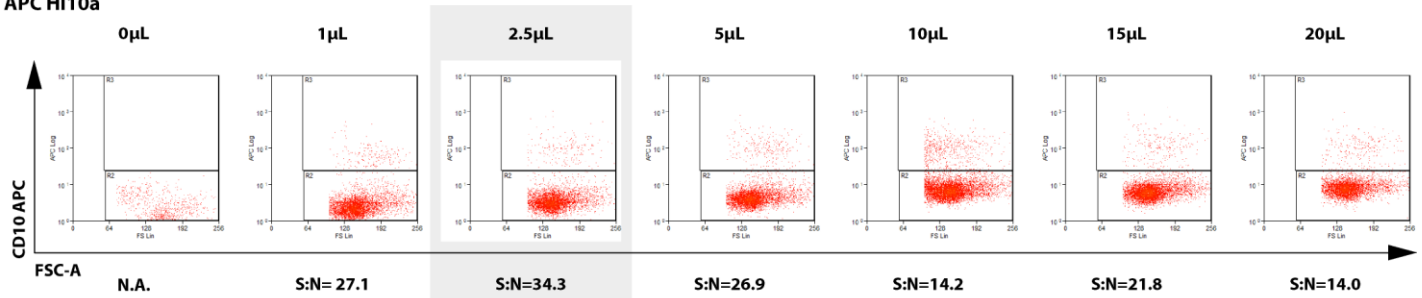

CD38 PECy7 HB7

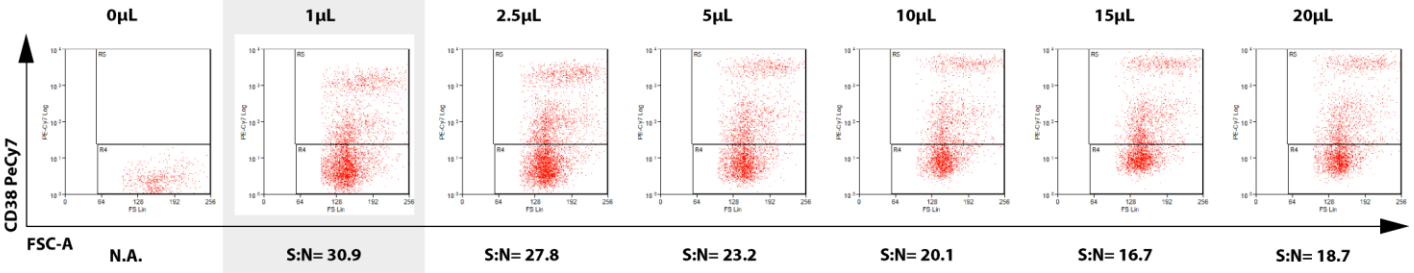

CD38 Alexa Fluor 647 HB7

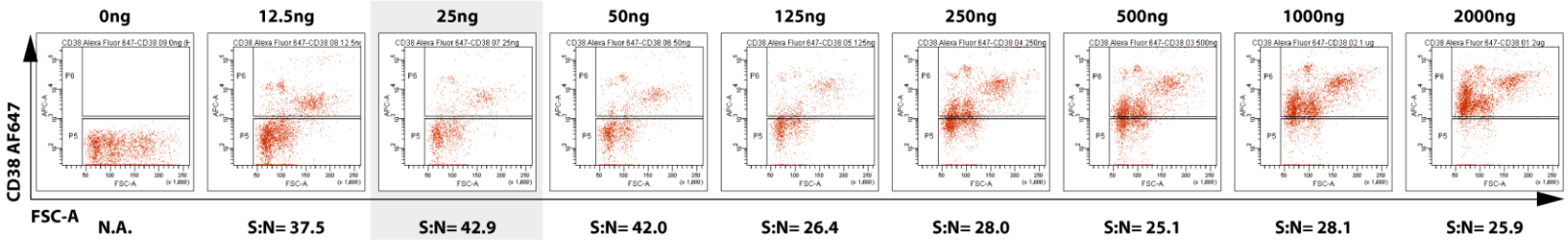

CD45RA Alexa Fluor 488 L481

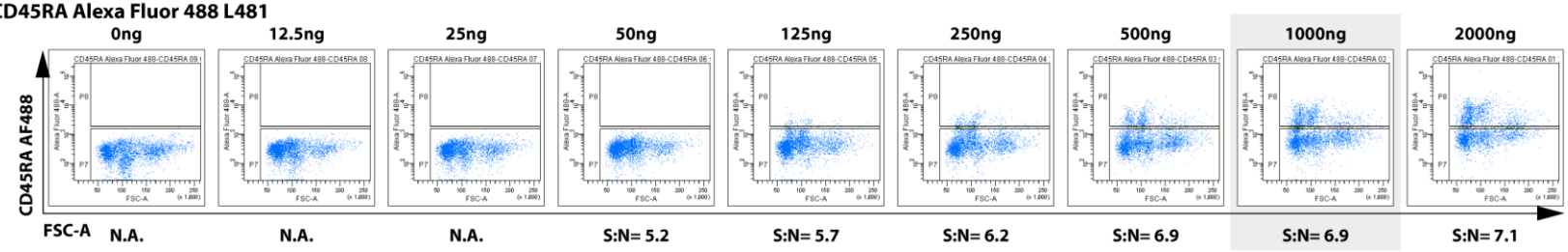

CD10 Alexa Fluor 555 W8E7

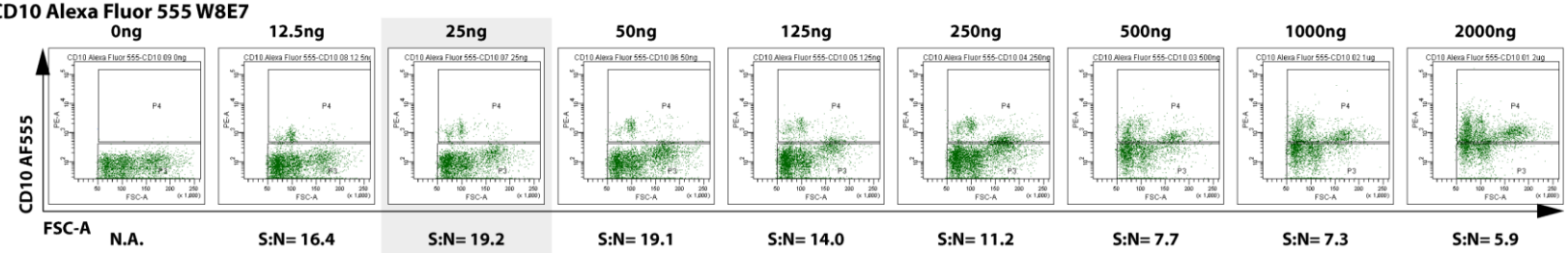

CD10 Alexa Fluor 555 HI10a

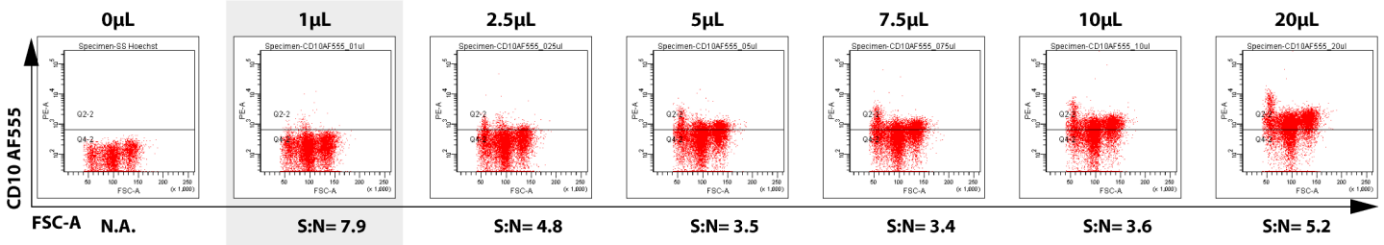

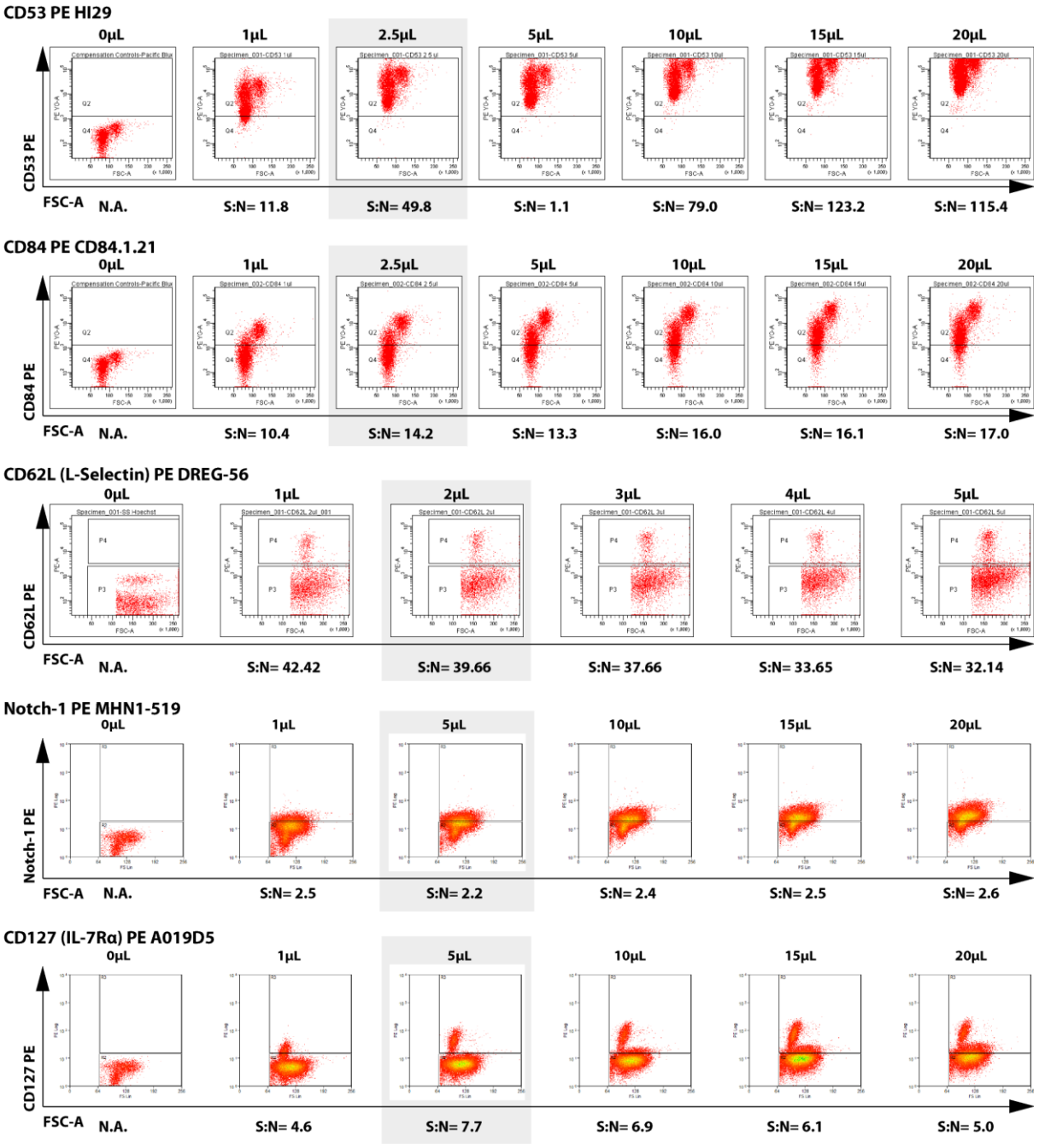

Figure 2.5. Titrations Of Monoclonal Antibodies For FACS Analysis.
17 Titrations of different antibodies and clones performed to evaluate the best concentration for staining. This was evaluated by calculating the signal to noise (S:N) ratio, which can be seen under every FACS plot. Every titration was performed on $1x10^6$ CB MNCs in a total volume of 100µL, unless otherwise stated. Plots highlighted in grey indicate the optimum antibody concentration.

2.2.3 CYAN Procedure

DAKO Cytomation CYAN flow cytometers were set up as dictated by the supporting SUMMIT software package. The start-up and shut down procedures were performed as specified. Photomultiplier tube (PMT) voltages were adjusted with the help of an unstained control. PMT voltages were altered for each fluorescent channel until the unstained cell peak fell into the first quadrant of the histogram. Compensation for spectral overlap of fluorophores was manually adjusted with single stained controls (SS) in the Visicomp mode.

2.2.4 BD Flow Cytometers

BD FACS AriaIIIu and BD LSR Fortessa flow cytometers require a daily performance check – Cytometer Set up and Tracking (CST) – in order to deliver reliable data. Fluorescent beads, supplied by BD, with their composition and conjugated fluorophores a company secret, are used to adjust PMT voltages and generate a summary of the current flow cytometer's parameters. Prior to every experiment, CST was performed with the correct bead lot and appropriate cytometer configuration. In order to compensate for spectral overlap, single stained controls, either prepared with cells or BD CompBeads© were analysed. Compensation was then automatically calculated by an algorithm in the supporting software, DiVa©. Fluorescence Minus One controls (FMOs) were used to correct the automated compensation.

2.2.5 Sorting

I performed my own cell sorts. Cells were sorted on a BD FACSAriaIII, equipped with 4 lasers (375nm violet laser, 488nm blue laser, 561nm yellow-green laser and 635nm red). Fluidic start up and CST was performed prior to every sort.

Compensation was optimised with single stained controls and FMOs. Accudrop Drop Delay, necessary to maximize the purity of the sorted populations, was also adjusted before every sort. The purity setting for 4-way sorts was always set to “4-way purity”, “single cell” for plate sorts and “purity” for sorts into 2 tubes or less. These purity masks are specified by DiVa and compromise yield in order to achieve the purest sorted populations. After every sort, the flow cytometer was cleaned and decontaminated according to core facility guidelines and fluidics shut-down was performed.

A summary of the purities relative to the relevant population can be found in Table 2.4.

Sorted Population	Average Post-Sort Purity (%)	SD	N
HSC	92	1.8	9
MPP	96	0.8	11
CD62L+ LMPP	97	0.9	8
CD62L- LMPP	93	2.4	5
MLP	97	2.0	6
CMP	97	1.0	10
CD62L+ GMP	95	1.6	9
CD62L- GMP	97	0.7	10
MEP	97	0.7	10

Table 2.4. Summary of Post-Sort Purities Across Different Sorted Populations.
HSPC populations were sorted from CB and BM samples and after each sort, the post-sort purity was checked, provided enough cells were acquired. The average purity plus the standard deviation are given with respect of each sorted population. The sorting panel used in this analysis

2.2.6 Sorting Strategy

Sorting strategies were optimised in a way that would allow for maximum recovery of cells. Every consecutive round of sorting halves the amount of a certain population, which has to be kept in mind when optimising a sorting strategy. Only 4 populations can be sorted at the same time on the FACS AriaII or FACS AriaIIIu, which were the two main types of sorters used in this study. Figure 2.6 shows examples of the sorting strategies used in this study.

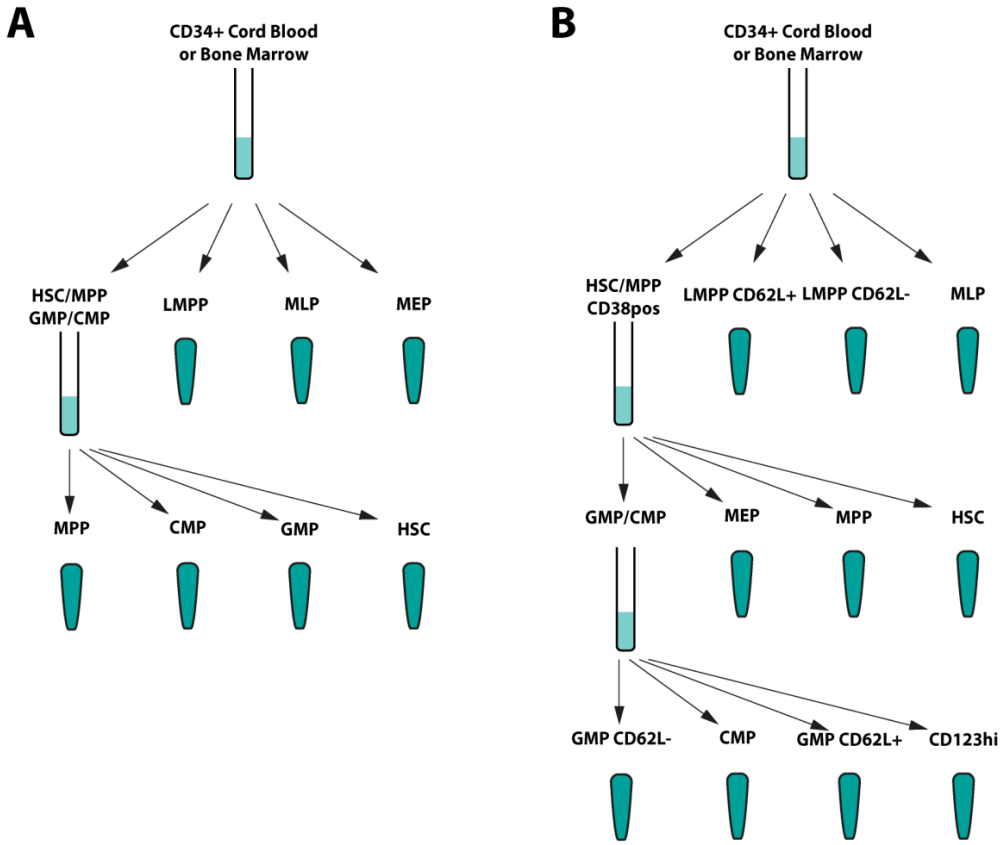

Figure 2.6. Sorting Strategies for Cord Blood and Bone Marrow Sorts of Haematopoietic Stem and Progenitor Cells.
A) This standard sorting strategy is applied to sort all basic populations of the human haematopoietic hierarchy in two consecutive rounds of sorting.
B) CD62L sorting strategy. This sorting strategy maximises the amount of populations that can be sorted on a 4-way sorter. In between sorting stages, cells are spun down and the supernatant is taken off to minimise sorting time.
CMP, common myeloid progenitor; MEP, megakaryocyte-erythroid progenitor; GMP, granulocyte-macrophage progenitor; HSC, haematopoietic stem cell; MPP, multipotent progenitor; LMPP, lymphoid primed multipotent progenitor; MLP, multilymphoid progenitor.

2.2.7 Panels

All sorting and analysis panels, including the fluorochrome conjugated to the antibody, the specific clone and the amount of antibody used per 100µL of staining volume are detailed in Table 2.5 (all panels), Table 2.6 (Lineage used in this study) and Table 2.7 (a list summarising all antibodies used in this study with respect to the supplier).

Standard HSPC Panel			
Antigen	**Colour**	**Clone**	**Amount per test (µL)**
CD34	PerCP	581	5
CD38	FITC	HIT2	5
CD90	Biotin	eBio5E10	2
CD45RA	PE	HI100	2.5
CD123	PE Cy7	6H6	5
Lineage	QDot605	N.A.	2
Hoechst	Pacific Blue	N.A.	2

Standard MLP Panel			
Antigen	**Colour**	**Clone**	**Amount per test (µL)**
CD10	APC	HI10a or CB CALLA	2.5
CD34	PerCP	581	5
CD38	FITC	HIT2	5
CD90	Biotin	eBio5E10	2
CD45RA	PE	HI100	2.5
CD123	PE Cy7	6H6	5
Lineage	QDot605	N.A.	2
Hoechst	Pacific Blue	N.A.	2

Table 2.5.Summary Of All FACS Panels In Use In This Study.
All FACS panels used in this study for sorting or analysis are summarized here with respect to antigen recognized, fluorochrome conjugated to, clone and titrated amount. Light blue – sorting panels; red – short term differentiation assay analysis panels; green, myeloid, B, NK cell differentiation analysis panels; brown, T cell differentiation analysis panels.

Expanded MLP Panel			
Antigen	**Colour**	**Clone**	**Amount per test (µL)**
CD7	FITC	4H9	5
CD10	APC	HI10a or CB CALLA	2.5
CD34	PerCP	581	5
CD38	Alexa Fluor 700	HIT2	5
CD90	Biotin	eBio5E10	2
CD45RA	PE	HI100	2.5
CD123	PE Cy7	6H6	5
Lineage	QDot605	N.A.	2
Hoechst	Pacific Blue	N.A.	2

CD127 & MLP Panel			
Antigen	**Colour**	**Clone**	**Amount per test (µL)**
CD127	PE	A019D5	5
CD10	APC	HI10a or CB CALLA	2.5
CD34	PerCP	581	5
CD38	Alexa Fluor 700	HIT2	5
CD90	Biotin	eBio5E10	2
CD45RA	FITC	HI100	5
CD123	PE Cy7	6H6	5
Lineage	QDot605	N.A.	2
Hoechst	Pacific Blue	N.A.	2

Table 2.5.Summary Of All FACS Panels In Use In This Study.
All FACS panels used in this study for sorting or analysis are summarized here with respect to antigen recognized, fluorochrome conjugated to, clone and titrated amount. Light blue – sorting panels; red – short term differentiation assay analysis panels; green, myeloid, B, NK cell differentiation analysis panels; brown, T cell differentiation analysis panels.

CD62L Panel			
Antigen	**Colour**	**Clone**	**Amount per test (µL)**
CD62L	PE	DREG-56	2.5
CD10	APC	HI10a or CB CALLA	2.5
CD34	PerCP	581	5
CD38	Alexa Fluor 700	HIT2	5
CD90	Biotin	eBio5E10	2
CD45RA	FITC	HI100	5
CD123	PE Cy7	6H6	5
Lineage	QDot605	N.A.	2
Hoechst	Pacific Blue	N.A.	2

CD84 Sorting Panel			
Antigen	**Colour**	**Clone**	**Amount per test (µL)**
CD38	FITC	HIT2	5
CD34	PerCP	581	5
CD90	Biotin	eBio5E10	2
CD123	PE Cy7	6H6	5
CD45RA	APC	HI100	5
CD84	PE	CD84.1.21	2.5
Lineage	QDot605	N.A.	2
Hoechst	Pacific Blue	N.A.	2

CD53 Sorting Panel			
Antigen	**Colour**	**Clone**	**Amount per test (µL)**
CD38	FITC	HIT2	5
CD34	PerCP	581	5
CD90	Biotin	eBio5E10	2
CD123	PE Cy7	6H6	5
CD45RA	APC	HI100	5
CD53	PE	HI29	2.5
Lineage	QDot605	N.A.	2
Hoechst	Pacific Blue	N.A.	2

Table 2.5.Summary Of All FACS Panels In Use In This Study.
All FACS panels used in this study for sorting or analysis are summarized here with respect to antigen recognized, fluorochrome conjugated to, clone and titrated amount. Light blue – sorting panels; red – short term differentiation assay analysis panels; green, myeloid, B, NK cell differentiation analysis panels; brown, T cell differentiation analysis panels.

BD Antibody Panel			
Antigen	**Colour**	**Clone**	**Amount per test (µL)**
CD34	PerCP	581	5
CD90	Biotin	eBio5E10	2
CD123	PE Cy7	6H5	5
CD10	Alexa Fluor 555	W8E7	5
CD38	Alexa Fluor 647	HB7	2.5
CD45RA	Alexa Fluor 488	L481	5
Lineage	QDot605	N.A.	2
Hoechst	Pacific Blue	N.A.	2

Dye Swap MLP Panel			
Antigen	**Colour**	**Clone**	**Amount per test (µL)**
CD10	PE	CD10 CB CALLA	2.5
CD34	PerCP	581	5
CD38	FITC	HIT2	5
CD90	Biotin	eBio5E10	2
CD45RA	APC	HI100	5
CD123	PE Cy7	6H6	5
Lineage	QDot605	N.A.	2
Hoechst	Pacific Blue	N.A.	2

Doulatov Panel[20]			
Antigen	**Colour**	**Clone**	**Amount per test (µL)**
CD7	PE Cy5	8H8.1	2.5
CD10	APC	HI10a	2.5
CD34	APC Cy7	581	2.5
CD38	PE Cy7	HB7	1
CD90	Qdot605	eBio5E10	2
CD45RA	FITC	HI100	5
CD135	PE	4G8	5
Hoechst	Pacific Blue	N.A.	2

Table 2.5.Summary Of All FACS Panels In Use In This Study.
All FACS panels used in this study for sorting or analysis are summarized here with respect to antigen recognized, fluorochrome conjugated to, clone and titrated amount. Light blue – sorting panels; red – short term differentiation assay analysis panels; green, myeloid, B, NK cell differentiation analysis panels; brown, T cell differentiation analysis panels.

Short Term Differentiation Panel - Std			
Antigen	**Colour**	**Clone**	**Amount per test (µL)**
CD45	APC eFluor780	HI30	2.5
CD34	PerCP	581	5
CD38	FITC	HIT2	5
CD45RA	PE	HI100	2.5
CD123	PE Cy7	6H6	5
CD10	APC	HI10a	2.5

Short Term Differentiation Panel - BD			
Antigen	**Colour**	**Clone**	**Amount per test (µL)**
CD45	APC eFluor780	HI30	2.5
CD34	PerCP	581	5
CD38	Alexa Fluor 647	HB7	2.5
CD45RA	Alexa Fluor 488	L481	5
CD123	PE Cy7	6H6	5
CD10	Alexa Fluor 555	W8E7	5

Table 2.5.Summary Of All FACS Panels In Use In This Study.
All FACS panels used in this study for sorting or analysis are summarized here with respect to antigen recognized, fluorochrome conjugated to, clone and titrated amount. Light blue – sorting panels; red – short term differentiation assay analysis panels; green, myeloid, B, NK cell differentiation analysis panels; brown, T cell differentiation analysis panels.

Myeloid B NK cell panel			
Antigen	**Colour**	**Clone**	**Amount per test (µL)**
CD45	APC eFluor 780	HI30	2.5
CD14	PE	61D3	1
CD15	PerCP	W6D3	5
CD19	PE Cy7	HIB19	2.5
CD56	APC	MEM188	5

Simple Myeloid/B Panel			
Antigen	**Colour**	**Clone**	**Amount per test (µL)**
CD45	APC eFluor780	HI30	2.5
CD33	PE	WM53	2.5
CD19	FITC	HIB19	2.5

Expanded Myeloid B NK cell panel			
Antigen	**Colour**	**Clone**	**Amount per test (µL)**
CD45	APC eFluor 780	HI30	2.5
CD14	PE	61D3	1
CD15	PerCP	W6D3	5
CD19	PE Cy7	HIB19	2.5
CD56	PE Cy5	MEM188	5
CD3	Alexa Fluor 700	OKT3	2.5
FCeRI	FITC	AER-37 (CRA1)	2.5
CCR3	APC	eBio5E8-G9-B4	2.5

Table 2.5.Summary Of All FACS Panels In Use In This Study.
All FACS panels used in this study for sorting or analysis are summarized here with respect to antigen recognized, fluorochrome conjugated to, clone and titrated amount. Light blue – sorting panels; red – short term differentiation assay analysis panels; green, myeloid, B, NK cell differentiation analysis panels; brown, T cell differentiation analysis panels.

Alternate T Cell Panel			
Antigen	**Colour**	**Clone**	**Amount per test (µL)**
CD45	APC eFluor780	HI30	2.5
CD1a	APC	HI149	2.5
CD7	FITC	4H9	2.5
CD3	Alexa Fluor700	OKT3	2.5
CD14	PE	61D3	1
CD15	PerCP	W6D3	5

T Cell panel			
Antigen	**Colour**	**Clone**	**Amount per test (µL)**
CD45	APC eFluor 780	HI30	2.5
CD1a	PE	HI149	2.5
CD7	FITC	4H9	2.5
CD4	APC	RPA-T4	2.5
CD8a	PE Cy7	RPA-T8	2.5
CD3	Alexa Fluor 700	OKT3	2.5

Expanded T Cell Panel			
Antigen	**Colour**	**Clone**	**Amount per test (µL)**
CD45	APC eFluor780	HI30	2.5
CD1a	APC	HI149	2.5
CD7	FITC	4H9	2.5
CD3	Alexa Fluor700	OKT3	2.5
CD14	PE	61D3	1
CD15	PerCP	W6D3	5
CD19	PE Cy7	HIB19	2.5
CD56	PE Cy5	MEM188	5

Table 2.5.Summary Of All FACS Panels In Use In This Study.
All FACS panels used in this study for sorting or analysis are summarized here with respect to antigen recognized, fluorochrome conjugated to, clone and titrated amount. Light blue – sorting panels; red – short term differentiation assay analysis panels; green, myeloid, B, NK cell differentiation analysis panels; brown, T cell differentiation analysis panels.

My Lineage			
Antigen	**Clone**	**Antigen**	**Clone**
CD2	RPA-2.10	CD11b	ICRF44
CD3	HIT3a	CD14	61D3
CD4	RPA-T4	CD19	HIB19
CD7	eBio124-1d1	CD20	2H7
CD8a	RPA-T8	CD56	MEM188
CD10	eBio CB CALLA	CD235a	HIR2

Table 2.6.Summary Of "My Lineage" Panel.
All antigens and clones of the lineage exclusion panel used in this study are summarized. These antibodies were not conjugated to any fluorochrome. QDot605 conjugated to goat-anti-mouse fab fragments were used as a secondary reagent.

Antigen recognized	Clone	Format	Supplier
CCR3	eBio5E8-G9-B4	APC	eBioscience
CD10	W8E7	Alexa Fluor 555	BD Biosciences
CD10	HI10a	APC	BD Biosciences
CD10	eBio CB CALLA	APC	eBioscience
CD10	eBio CB CALLA	PE	eBioscience
CD10	eBio CB CALLA	Purified	eBioscience
CD114	LMM741	PE	Biolegend
CD11b	IV M047	PE Cy7	Biolegend
CD11b	ICRF44	Purified	eBioscience
CD123	6H6	PE Cy7	eBioscience
CD127	eBioRDR5	PE	eBioscience
CD127	A019D5	PE	Biolegend
CD135	4G8	PE	BD Biosciences
CD135	BV10A4H2	PE	eBioscience
CD14	M5E2	APC	eBioscience
CD14	61D3	PE	eBioscience
CD14	61D3	Purified	eBioscience
CD15	W6D3	PerCP	Biolegend
CD15	HI98	FITC	eBioscience
CD16	CB16	PeCy7	eBioscience
CD19	HIB19	FITC	eBioscience
CD19	HIB19	PE Cy7	eBioscience
CD19	HIB19	Purified	eBioscience
CD1a	HI149	Alexa Fluor 647	eBioscience
CD1a	HI149	PE	eBioscience
CD2	RPA-2.10	Purified	eBioscience
CD20	2H7	Purified	eBioscience
CD235a	HIR2	Purified	eBioscience
CD3	OKT3	Alexa Fluor 700	eBioscience
CD3	HIT3a	Purified	eBioscience
CD33	WM53	PE	eBioscience
CD34	581	PerCP	Biolegend
CD34	581	APC Cy7	BioLegend/eBiosciences

Continued on next page.

Antigen recognized	Clone	Format	Supplier
CD38	HB7	Alexa Fluor 647	BD Biosciences
CD38	HB7	PE Cy7	BD Biosciences
CD38	HIT2	FITC	eBioscience
CD38	HIT2	Alexa Fluor 700	eBioscience
CD4	RPA-T4	Alexa Fluor 700	Biolegend
CD4	RPA-T4	APC	eBioscience
CD4	RPA-T4	Purified	eBioscience
CD41a	HIP8	PE	eBioscience
CD45	HI30	APC eFluor780	eBioscience
CD45RA	HI100	PE	eBioscience
CD45RA	L481	Alexa Fluor 488	BD Biosciences
CD45RA	HI100	FITC	eBioscience
CD5	UCHT2	PeCy7	Biolegend
CD53	HI29	PE	eBioscience
CD56	MEM188	PE Cy5	Biolegend
CD56	VI NK26	PeCy5	Biolegend
CD56	MEM188	APC	eBioscience
CD56	MEM188	Purified	eBioscience
CD62L	DREG-56	PE	eBioscience
CD7	8H8.1	PeCy5	Beckmann Coulter
CD7	4H9	FITC	eBioscience
CD7	eBio124-1d1	Purified	eBioscience
CD83	HB15e	PeCy7	eBioscience
CD84	CD84.1.21	PE	Biolegend
CD8a	RPA-T8	BV605	eBioscience
CD8a	RPA-T8	PE Cy7	eBioscience
CD8a	RPA-T8	Purified	eBioscience
CD90	eBio5E10	Biotin	eBioscience
FCeR1a	AER-37 (CRA1)	FITC	eBioscience
HLA-DR	LN3	PeCy5	eBioscience
Notch-1	MHN1-519	PE	Biolegend
TCR alpha/beta	IP26	PeCy5	eBioscience

Table 2.7. Comprehensive List of All Flow Cytometry Antibodies Used In This Study.

2.3 Long-term Differentiaton Protocols

2.3.1 MS5 Stromal Cell Line Maintenance

MS5 cells were a generous gift from Dr. Francoise Pflumio. MS5 cells were maintained in αMEM (Gibco, Invitrogen, UK) with 10%FCS (PAA, Austria), 1% Penicillin (100U/ml) –Streptomycin (100µg/mL) (Gibco, Invitrogen, UK), 1% L-Glutamine (Gibco, Invitrogen, UK)[63]. Cells were passaged at 80-90% confluency after detaching with 1X Trypsin-EDTA (Gibco, Invitrogen, UK), which translates to 2-3 times a week. MS5 cells were passaged for up to 10 weeks, before a fresh vial with a low passage number was thawed. Media were prepared freshly every week.

2.3.2 Differentiation of HSPCs on MS5 Stromal Cells

The protocol was adapted from published literature[19]. Co-cultures were initiated in 24-well cell culture plates (Corning Incorporated, NY, US), coated with 0.1% Gelatine from porcine skin (Sigma Aldrich, St.Louis, MO, US) in PBS (Gibco, Invitrogen, UK) on confluent monolayers of MS5 cells in complete medium – αMEM (without MgCl2 and CaCl2) (Gibco, Invitrogen, UK) with 10%FCS (Hyclone, defined), 1% Penicillin (100U/ml), Streptomycin (100µg/mL) (Gibco, Invitrogen, UK), 1% L-Glutamine (Gibco, Invitrogen, UK) and cytokines, 20ng/mL hSCF, 10ng/mL hFlt3L, 10ng/mL hG-CSF (all Peprotech, Rocky Hill, NJ), 10^{-7}M all-trans retinoic acid (ATRA) (Sigma-Aldrich, St.Louis MO, US) and 10^{-7}M Dup697 (Cayman chemicals, US). 100 haematopoietic cells were plated per well of a 24-well plate. Upon seeding, 2x cytokine concentration of the complete medium was used. Half of the medium was changed weekly. Please refer to Table 2.8 for other media compositions in terms of the cytokine combination.

"Our Condition B[19]"		
Concentration		**Additive**
20	ng/mL	SCF
10	ng/mL	Flt3L
10	ng/mL	G-CSF
10	^(-7)M	Dup697
10	^(-7)M	ATRA (opt.)

"JED1 Condition[20]"		
Concentration		**Additive**
100	ng/mL	SCF
50	ng/mL	TPO
20	ng/mL	GM-CSF
20	ng/mL	G-CSF
20	ng/mL	IL-7
10	ng/mL	IL-2
10	ng/mL	M-CSF

"JED2 Condition[20]"		
Concentration		**Additive**
100	ng/mL	SCF
50	ng/mL	TPO
20	ng/mL	IL-7
10	ng/mL	IL-2

"Our Condition"		
Concentration		**Additive**
20	ng/mL	SCF
10	ng/mL	Flt3L
10	ng/mL	G-CSF
10	ng/mL	IL-15
10	ng/mL	IL-2
10	^(-7)M	Dup697
10	^(-7)M	ATRA (opt.)

"Akashi Eosinophil Condition[64]"		
Concentration		**Additive**
50	ng/mL	GM-CSF
20	ng/mL	IL-3
20	ng/mL	IL-5
20	ng/mL	TPO
20	ng/mL	SCF
4	U/mL	EPO

Table 2.8. Culture Conditions To Differentiate HSPCs Into B, NK and Myeloid Cells on MS5 Monolayers

Cultures were disaggregated by vigorous pipetting and passing through a 70µm cell strainer (BD, US) and analysed by FACS (see section XX detailed FACS protocols and Table 2.5 for antibody panels).

2.3.3 Maintenance of OP9, OP9-DL1 and OP9-DL4 cells

The OP9, OP9-DL1 and OP9-DL4 cells were a generous gift from Dr. Juan-Carlos Zúñiga-Pflücker. Cell lines were maintained in αMEM (without $MgCl_2$ and $CaCl_2$)

(Gibco, Invitrogen, UK) reconstituted in 18mOhm MilliQ from powder with heat-inactivated 20%FCS (PAA, Austria) and 1% Penicillin (100U/ml), Streptomycin (100µg/mL) (Gibco, Invitrogen, UK and 1% L-Glutamine (Gibco, Invitrogen, UK). Cells were passaged at 80% confluency and propagated for a period of up to two and a half months. Medium containing serum was always prepared freshly; pure reconstituted αMEM without serum was stable for up to 2 weeks. FCS was thawed at 37°C, left at 37°C for an hour after it was fully thawed, heat-inactivated at 56°C for an hour and then chilled in an ice water-bath for another hour. It was subsequently aliquotted and frozen at -20°C.

2.3.4 Differentiation of HSPCs on OP9-DL1 cells

The protocol was adapted from published literature[19,65,66]. Co-cultures were initiated in 24-well cell culture plates (Corning Incorporated, NY, US), coated with 0.1% Gelatine from porcine skin (Sigma Aldrich, St.Louis, MO, US) in PBS (Gibco, Invitrogen, UK), seeded as to reach near confluency on the next day. 100 haematopoietic cells were seeded per well of a 24-well plate. Haematopoietic cells were cultured in αMEM (without $MgCl_2$ and $CaCl_2$) (Gibco, Invitrogen, UK) supplemented with 20% heat-inactivated FCS (Hyclone, defined, SH Perbio) and 10ng/mL SCF, 5ng/mL Flt3L and 5ng/mL IL-7 (Peprotech). Please refer to Table 2.9 for other media compositions in terms of the cytokine combination. Upon seeding of haematopoietic cells, 2x cytokine concentration of the complete medium was used. The culture was disaggregated every week and the haematopoietic cells were passed onto a fresh monolayer of OP9-DL1 cells in freshly prepared medium. Cultures were disaggregated by vigorous pipetting and passing through a 70µm cell

strainer (BD, US) and analysed by FACS (see Section 2.2.1 for detailed FACS protocols and Table 2.5 for antibody panels).

"5ng Condition"		
Concentration		**Additive**
5	ng/mL	Flt3L
5	ng/mL	IL-7

"1ng Condition"		
Concentration		**Additive**
1	ng/mL	Flt3L
1	ng/mL	IL-7

"T and Myeloid Condition"		
Concentration		**Additive**
20	ng/mL	GM-CSF
10	ng/mL	SCF
5	ng/mL	Flt3L
5	ng/mL	IL-7

"MS5-DL1 Condition"		
Concentration		**Additive**
50	ng/mL	SCF
5	ng/mL	Flt3L
5	ng/mL	IL-7
150	mM	β-Insulin

"Six Condition"[66]		
Concentration		**Additive**
10	ng/mL	SCF
5	ng/mL	Flt3L
5	ng/mL	IL-7

Table 2.9. Culture Conditions To Differentiate HSPCs Into T Cells On Stromal Cells Transduced With Delta-Like 1 or Delta-Like 4

2.3.5 Limit Dilution Assay

The protocol was adapted from published literature[19]. Co-cultures were initiated in 96-well flat bottomed cell culture plates (Corning Incorporated, NY, US), coated with 0.1% Gelatine from porcine skin (Sigma Aldrich, St.Louis, MO, US) in PBS (Gibco, Invitrogen, UK), seeded with 2,500 cells per well (in a total volume of 200µL).

Haematopoietic cells were sorted directly into the wells by the single cell deposition unit of the FACS Aria IIIu. 36 replicates of each concentration (1, 2, 5, 10 cells) were plated. After the designated culture period, cultures were dissociated and transferred to round bottomed 96-well plates (Corning Incorporated, NY, US). Plates were centrifuged at 1,200 rpm for 5 minutes and 100µL supernatant was taken off.

Antibody mixes were prepared in 100µL FACS Buffer per well. Plates were incubated on ice for 20 minutes in the dark, subsequently centrifuged at 1,200rpm and 100µL supernatant was taken off. Immediately before analysis, Hoechst 22358 at the correct dilution (1:10,000) was added in 100µL. Analysis was performed on a Cyan ADP (Dakocytomation, Ely, UK) flow cytometer. Data analysis was performed using L-Calc (available from http://www.stemcell.com/en/Products/All-Products/LCalc-Software.aspx).

2.4 Short-Term Differentiation Assay

Short term differentiation assays were carried out on MS5 stromal layers in 24 or 12 well plates, coated with 0.1% Gelatine from porcine skin (Sigma Aldrich, St.Louis, MO, US). 102 – 103 HSPCs were cultured in aMEM (reconstituted in house from powder, Gibco, Invitrogen, UK) supplemented with 10% (v/v, Hyclone, defined, Fisher),1% Pen/Strep and cytokines. Exact cytokine concentrations can be found in Table 2.9.

HSPCs were cultured for 1,2 and 4 or 4,6 and 8 days. At each designated time point, one well of the culture was harvested and subjected to FACS analysis on the LSRFortessa (BD Biosciences, Erembodegem, Belgium).

"Majeti Conditions[37]"		
Concentration		**Additive**
100	ng/mL	Flt3L
100	ng/mL	SCF
50	ng/mL	TPO
20	ng/mL	IL-3
20	ng/mL	IL-6
40	µg/mL	LDL

"IL-7 Conditions"		
Concentration		**Additive**
100	ng/mL	Flt3L
100	ng/mL	SCF
50	ng/mL	TPO
20	ng/mL	IL-7
40	µg/mL	LDL

Differentiation Medium		
Concentration (v/v)	**Reagent**	**Supplier**
	αMEM	Gibco, Invitrogen, UK
10%	Hyclone	Hyclone, Fisher
1%	L-Glutamine	Gibco, Invitrogen, UK
1%	Pen/Strep	Gibco, Invitrogen, UK

"Basic Condition"		
Concentration		**Additive**
100	ng/mL	Flt3L
100	ng/mL	SCF
50	ng/mL	TPO
40	µg/mL	LDL

Table 2.10. Culture Conditions To Differentiate HSPCs In The Short Term.

2.5 Methylcellulose Colony Assays

2.5.1 Plating of HSPCs in Methylcellulose

Methylcellulose Methocult H4435 Enriched (StemCell Technologies, Canada) was thawed and aliquotted as recommended by the manufacturer. 150 sorted cells/plate were resuspended in IMDM (Gibco, Invitrogen, UK) supplemented with 2% FCS (PAA, Austria) and mixed with MeC to achieve optimum plating viscosity. 1.1mL of methylcellulose was used per dish (35mm, Corning Incorporated, NY, US).

Methylcellulose was dispensed with a 2mL syringe (Terumo Europe, Leuven, Belgium) and a 19 gauge needle (Microlance, BD, US). Plated cells were incubated at 37°C in a humidified atmosphere for 14 days.

2.5.2 Scoring of Colonies

Colonies were enumerated and scored as colony-forming-unit(CFU)-granulocyte, CFU-macrophage, CFU-granulocyte/macrophage, CFU-mixed and burst-forming-unit erythrocyte (BFU-E). A figure to illustrate colonies which were picked according to morphology and stained with Modified Wright's stain, can be found in Figure 2.7. A illustrates colonies which were picked from HSPCs plated in methylcellulose and B shows the same for colonies picked from plated which were seeded with CB cells.

2.5.3 Cytospin And Modified Wright's Stain

Colonies were picked under an inverted microscope (Zeiss, Axiovert 40C) at 10x or 20x magnification and resuspended in 200µL PBS (Gibco, Invitrogen, UK). The cell suspension was transferred to a glass slide (VWR International) and centrifuged at 1000rpm for 10 minutes in a Shandon Cytospin 4 centrifuge (Thermo Electron Corporation). Slides were stained using the Hemathek (Bayer Health Care) automated machine and imaged on an AMG EVOS XL microscope (AMG).

2.5.4 Mounting and Fixing Of Slides

Slides were mounted with Entellan New (Merck, Darmstadt, Germany) and covered with a 22x50mm coverslip (VWR International).

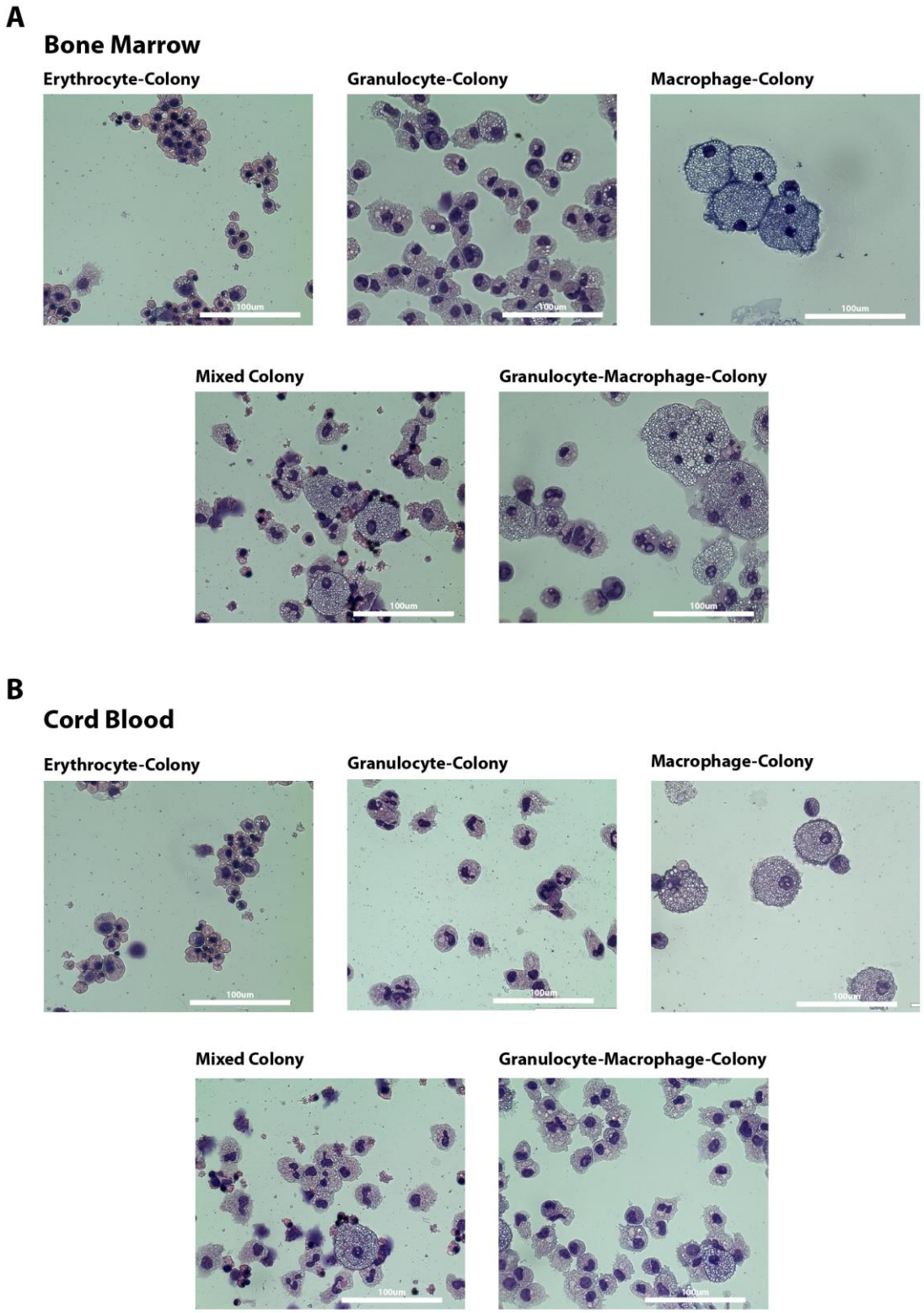

Figure 2.7. Modified Wright's Stain Images of Methylcellulose Colonies From Bone Marrow and Cord Blood.
150 HSPCs were cultured in MeC for 14 days. Colonies were picked and cytospun onto glass slides. Subsequently they were stained with a Modified Wright's stain and images on the Evos AMG microscope were taken.
A) Colonies derived from bone marrow cells.
B) Colonies derived from cord blood HSPCs.
HSPCs, haematopoietic stem and progenitor cells.

2.6 RNA

2.6.1 Sorting Procedure for RNAse-free Sorts

Flow sorted populations of cells from of CB and BM were stained and prepared as described in Sections 2.1 and 2.2.. The working area, gloves and materials were sprayed with RNAse-ZAP (Cat. No. R2020, Sigma-Aldrich, St. Louis, MO, USA), pipettes and racks were UV sterilized in addition. Cells were pre-sort purity checked and sorted directly into an Eppendorf tube containing 75µL of RLT buffer (QIAGEN RNeasy Micro Kit, Cat.No. 74004). Cell numbers sorted per replicate of a certain population ranged from ~500 up to 10,000 cells. After the desired number of sorted cells was reached, the sort was paused and the sorted cells were spun down and flash frozen on dry ice immediately. Frozen samples were stored at -80°C until RNA was extracted.

2.6.2 RNA Extraction with the QIAgen Mini Kit

RNA was extracted from cells sorted into RLT buffer with the QIAGEN RNeasy Micro kit (Cat. No. 74004), as described in the manual (QIAGEN, UK). Frozen whole cell lysates were stored at -80°C and strictly thawed on ice. All equipment used for this procedure was cleaned prior to extraction with RNAse-ZAP (Cat. No. R2020, Sigma-Aldrich, St. Louis, MO, USA). Pipettes and racks were crosslinked in addition to RNAse-ZAP treatment. RNA was eluted in 10µL of nuclease-free water (QIAGEN, UK).

2.6.3 Quality Checking of RNA on the Agilent Bioanalyzer

RNA quality and concentration was determined with the Agilent 2100 Bioanalyzer (Santa Clara, USA) on an Agilent RNA 6000 Pico Chip (Agilent, Santa Clara, US). Procedures were carried out as described in the kit manual, with one exception: the

RNA denaturing step at 70°C for 2 minutes was omitted. RIN (RNA integrity number) scores and traces were used to determine the quality of the extracted RNA. RNA concentration supplied by the Agilent 2100 Bioanalyzer was corrected to account for the amount of RNA calculated from the area of the 18S and 28S peaks.

2.7 C1 Single Cell Capture

Cells were sorted into FACS buffer and diluted with C1 Cell Suspension Reagent (Fluidigm, USA) in a ratio of 6:4. A maximum of 20µL can be loaded onto one C1 Single-Cell Auto Prep Array IFCs (barcode: 1782, Fluidigm, USA), but only 5µL will be captured. Primer pools, lysis final mix, RT final mix and the preamp final mix were prepared according to the protocol supplied by Fluidigm (PN 100-4904 B1).After the capture, each well was inspected and scored for single live cells (“1”), debris (“d”), no cell (“0”) or more than one cell (“2”) on a Life Tech microscope.

3 Flow Cytometry And Sorting Panels

In order to define differentiation potentials of human haematopoietic stem and progenitor cells (HSPCs), the relevant populations have to be isolated and assessed in a suitable in vitro or in vivo assay. To sort not only phenotypic, but also functional HSPCs, the FACS panels used for isolation have to be carefully selected, validated and optimised.

3.1 Selection Of The Standard Backbone Flow Cytometry Panel to Isolate HSPCs

The method of choice to purify HSPCs from single cell suspensions of BM or peripheral blood (PB) is fluorescence activated cell sorting (FACS) and is based on labelling specific cell surface markers expressed on populations with a monoclonal antibody conjugated to a fluorophore or a fluorochrome.

In order to sort and analyse human HSPCs, we had to develop a staining panel that contained the most important antigens to separate different populations[19,20,37,67,68]. To ensure reproducibility, the antibody clones, which are used to isolate HSPCs, have to be kept consistent with the original publications that defined the population functionally. The fluorochromes are also crucial. Depending on the nature of the expression of a marker (e.g. a continuum, or one or more clearly defined populations), the necessary brightness of a fluorochrome has to be considered. For clearly defined populations, a weak colour (i.e. Pacific Blue, APC Cy7 etc.) might be sufficient. If the expression of an unknown antigen is investigated, a brighter fluorochrome might be the best choice (i.e. PE, APC, PECy7 etc.). With regard to these considerations, I adapted the panel used in Goardon et al[19] for the isolation of

basic HSPCs (haematopoietic stem cells (HSC), multipotent progenitors (MPP), lymphoid primed multipotent progenitors (LMPP), common myeloid progenitors (CMP), granulocyte-macrophage progenitors (GMP) and megakaryocyte-erythroid progenitors (MEP)). The details can be found in Table 2.5 “Standard HSPC Panel”. The backbone panel that was used in this study contained mABs directed against CD34, CD38, CD123 (IL-3Ra), CD90 (Thy 1.1), CD45RA and a “lineage cocktail” to exclude mature cells from the final analysis. The lineage cocktail contained antibodies directed against CD2, CD3, CD4 and CD8 to exclude T cells, CD7 and CD10 to exclude lymphoid progenitors, CD11b and CD14 to exclude mature myeloid cells, CD19 and CD20 to exclude B cells, CD56 to exclude NK cells and CD235a (Glycophorin A) to exclude erythroid cells. The lineage exclusion panel can be found in Table 2.6 with all antibodies and their respective clones.

To sort these HSPCs, a gating strategy as in Figure 3.1A is used to separate all the HSPCs. The scheme in A is a simple representation of how HSCs, MPPs, LMPPs, CMPs, GMPs, and MEPs in BM or CB are separated. Dead cells are excluded as Hoechst+, subsequently only single and lineage- cells are considered for analysis. The CD34+CD38- population contains the CD45RA-CD90+ HSC, the CD45RA-CD90- MPP and the CD45RA+CD90- LMPP[19,37]. On the other hand, the CD34+CD38+ fraction of CB and BM contains more committed progenitors, which can be separated according to their expression of the markers CD45RA and CD123. The CMP is CD45RA-CD123+, the MEP lacks expression of both CD45RA and CD123 and the GMP is CD45RA+CD123+. B and C show a representative example of such a staining in normal BM (B), and in normal CB (C).

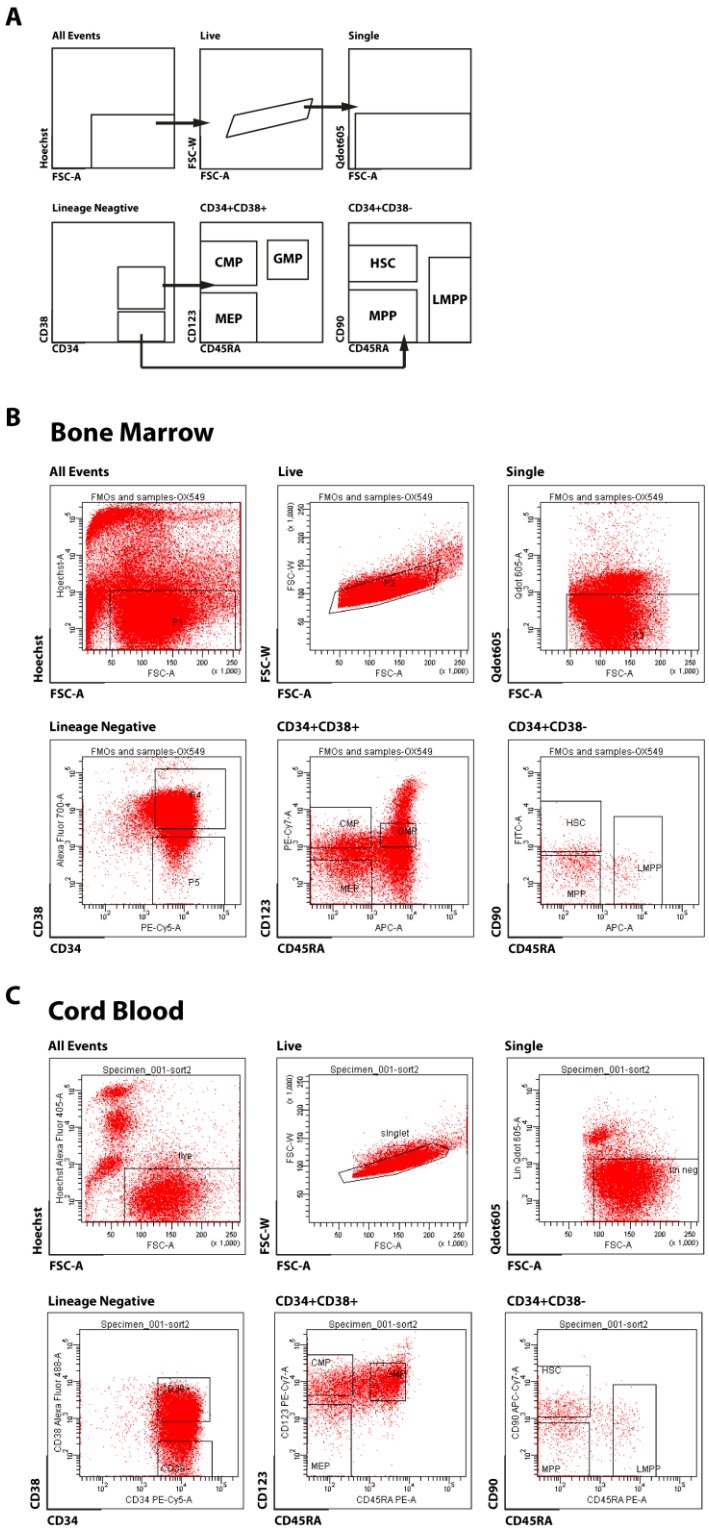

Figure 3.1. FACS Gating Strategy and Profiles Of Stem And Progenitor Cells.
A Scheme summarising the basic gating strategy used in this thesis.
B Example of a bone marrow sample analysed with the gating strategy as described in A.
C Example of a cord blood sample gated with the strategy detailed in A.
CMP, common myeloid progenitor; MEP, megakaryocyte-erythroid progenitor; GMP, granulocyte-macrophage progenitor; HSC, haematopoietic stem cell; MPP, multipotent progenitor; LMPP, lymphoid primed multipotent progenitor.

Basic sorting of these HSPCs from CB and subsequent colony assays confirmed the differentiation potentials. Figure 3.2 illustrates this experiment (N=1). 150 cells from HSC, MPP, LMPP, CMP, GMP and MEP were tested. HSC and MPP have similarly high cloning efficiencies (~45%) and could give rise to all types of colonies, and both showed prominent erythroid output. The CMP had the highest cloning efficiency of all investigated populations (60%) and 3 out of 4 colonies generated by CMPs was scored as erythroid. The MEP mainly gave rise to erythroid colonies to (90% of colonies generated were red) and its cloning efficiency was around 40%. The LMPP and GMP did not produce any erythroid colonies, as expected and showed cloning efficiencies around 30%[19].

This backbone panel was extended and modified in order to enable sorting of subpopulations and other, newly identified progenitors. One of the most important FACS panels used in this study is the “MLP Panel” see Table 2.5 (“Standard MLP Panel”). It includes CD10 conjugated to APC, which is a relatively bright fluorochrome, which permits isolation of the CD10+ MLP.

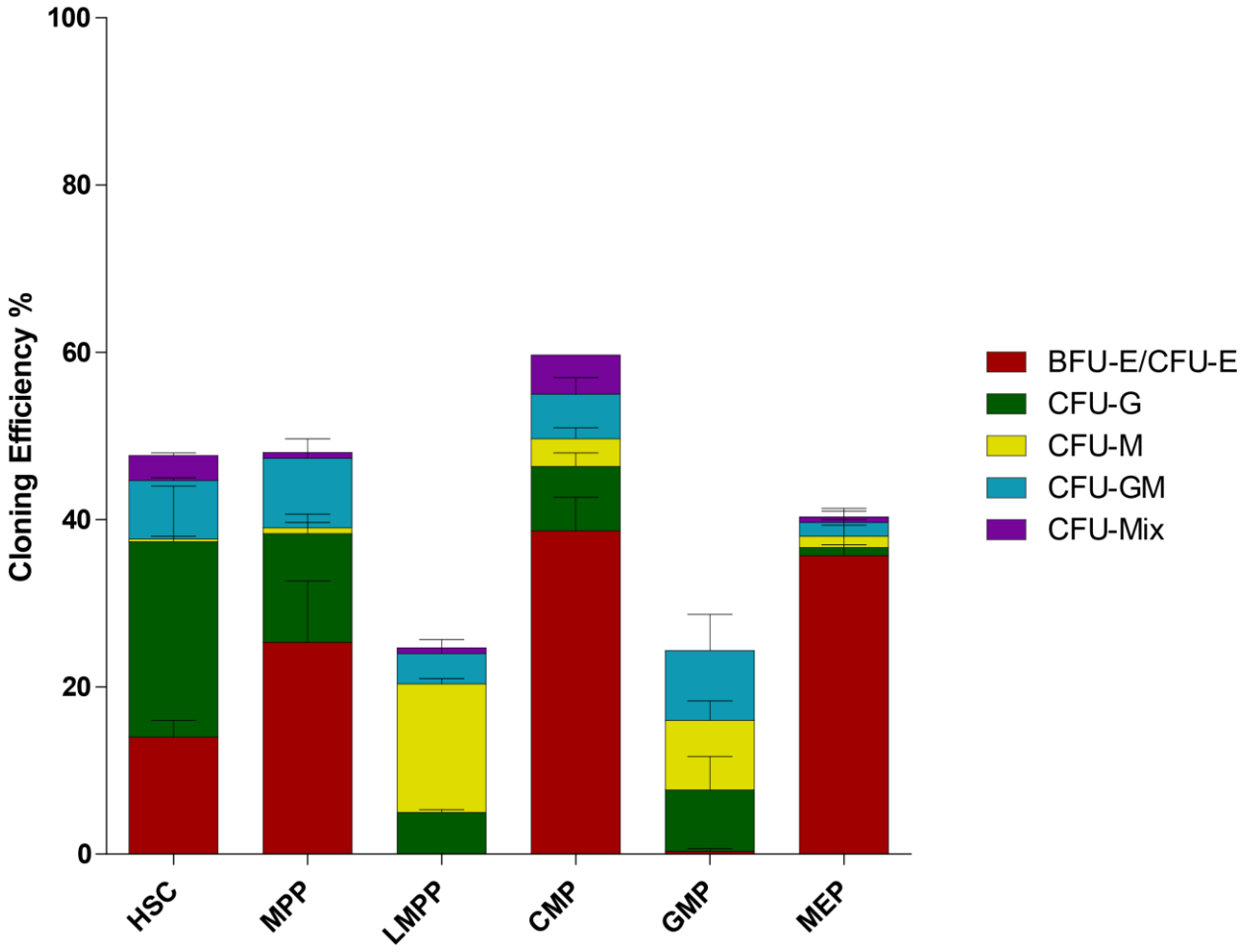

Figure 3.2.Stem and Progenitor Cell Colony-Forming Assay To Validate Sorted Populations From CB.

Sorted HSPCs from CB were cultured in MeC at 150 cells/plate for 14 days. Cloning efficiencies were calculated after scoring. Bars represent mean plus standard deviation of 2 technical replicates. CMP, common myeloid progenitor; MEP, megakaryocyte-erythroid progenitor; GMP, granulocyte-macrophage progenitor; HSC, haematopoietic stem cell; MPP, multipotent progenitor; LMPP, lymphoid primed multipotent progenitor.

3.2 Sorting Strategy And Post-Sort Purity

The sorting strategies to isolate HSPCs were optimised to allow for maximum recovery of cells. Every consecutive round of sorting halves the amount of cells in the sample. This is due to the efficiency of the sorter, which analyses more cells than it is able to sort. Furthermore, the purity mask setting on the instrument also influences whether a cell will be sorted. The more stringently the purity mask is set to guarantee high purities, the fewer cells will be sorted. All of these factors have to be kept in mind when a sorting strategy is developed. On the FACS AriaII or FACS AriaIIIu, which were the two main types of sorters used in this study, only 4 populations can be sorted at the same time. If more than 4 populations of the same sample are to be isolated, certain populations will have to be re-sorted. Sorting strategies as they were used in this study can be found in Figure 3.3.

Figure 3.3A shows a two-tiered strategy for the isolation of 7 different HSPC populations. In the first round of sorting, the smallest populations are collected (LMPP, MLP, MEP) and everything else (CD38+ fraction plus MPP and HSC) is sorted into a separate tube. After a quick spin to reduce the volume, which will minimize sorting time, this last tube is re-sorted and HSC, MPP, CMP and GMP are collected.

Figure 3.3B illustrates a three-tiered strategy to isolate 10 separate HSPC populations. As mentioned before, every pass through the flow cytometer roughly divides the cell numbers per sample by two. Therefore, cell losses can be very extensive after multiple rounds of sorting.

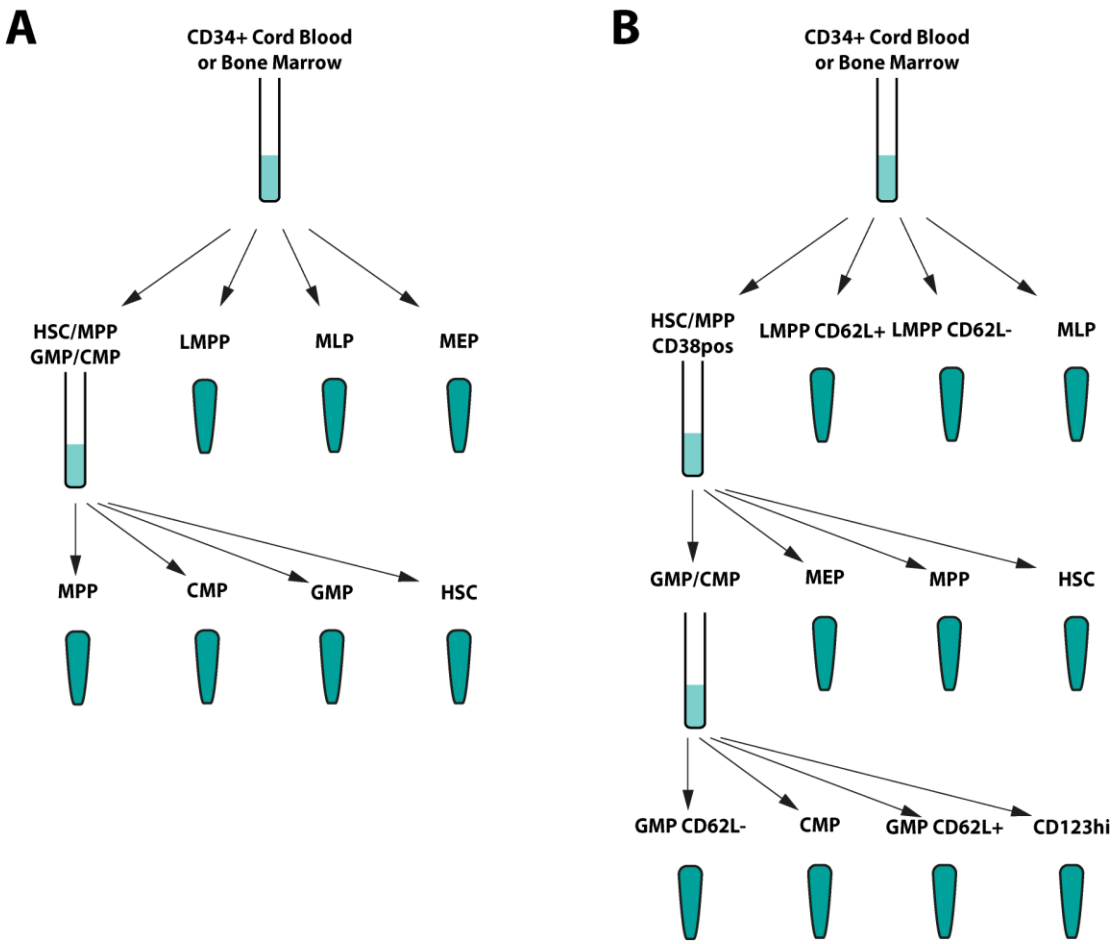

Figure 3.3. Sorting Strategies for Cord Blood and Bone Marrow Sorts of Haematopoietic Stem and Progenitor Cells.

A) This standard sorting strategy is applied to sort all basic populations of the human haematopoietic hierarchy in two consecutive rounds of sorting.

B) CD62L sorting strategy. This sorting strategy maximises the amount of populations that can be sorted on a 4-way sorter. In between sorting stages, cells are spun down and the supernatant is taken off to minimise sorting time.

CMP, common myeloid progenitor; MEP, megakaryocyte-erythroid progenitor; GMP, granulocyte-macrophage progenitor; HSC, haematopoietic stem cell; MPP, multipotent progenitor; LMPP, lymphoid primed multipotent progenitor; MLP, multilymphoid progenitor.

In order to monitor the purity of sorted samples, a purity check is performed. This can either happen pre-sort or post-sort. If cells are sorted into a lysing agent, I perform a pre-sort purity check, because otherwise it will be impossible to assess purity. To perform these checks, a low number of cells of the sorted population is analysed by the flow cytometer again to assess whether they fall into the correct gate. Figure 3.4 illustrates this procedure. CB cells were stained with monoclonal antibodies and three different populations (GMP, MLP and LMPP) were isolated (A). After the initial sort, the populations were analysed again. The results of this analysis can be seen in Figure 3.4B. The gates are slightly widened compared to the original sorting gates. This is done because sorting gates are very tight and enclose the desired population without any room to spare to achieve high sorting purity. Analysis gates are usually less strict to allow for the natural spread of a population. In the re-analysis, it can be seen that all LMPPs fall into the LMPP-gate, and most GMPs can be detected in the GMP gate. This confirms sorting purities of 100% and 98%, respectively. In cases where the purity is not sufficient, populations may be double sorted, and the settings on the flow cytometer can be changed to improve the purity. For example the purity mask can be adjusted to compromise yield, but to favour purity. Another parameter that affects purity is the Accudrop drop delay. This programme specifies when the charge is transferred by flow cytometer to the cell, which is to be sorted. If it is not adjusted correctly, impurities can be detected.

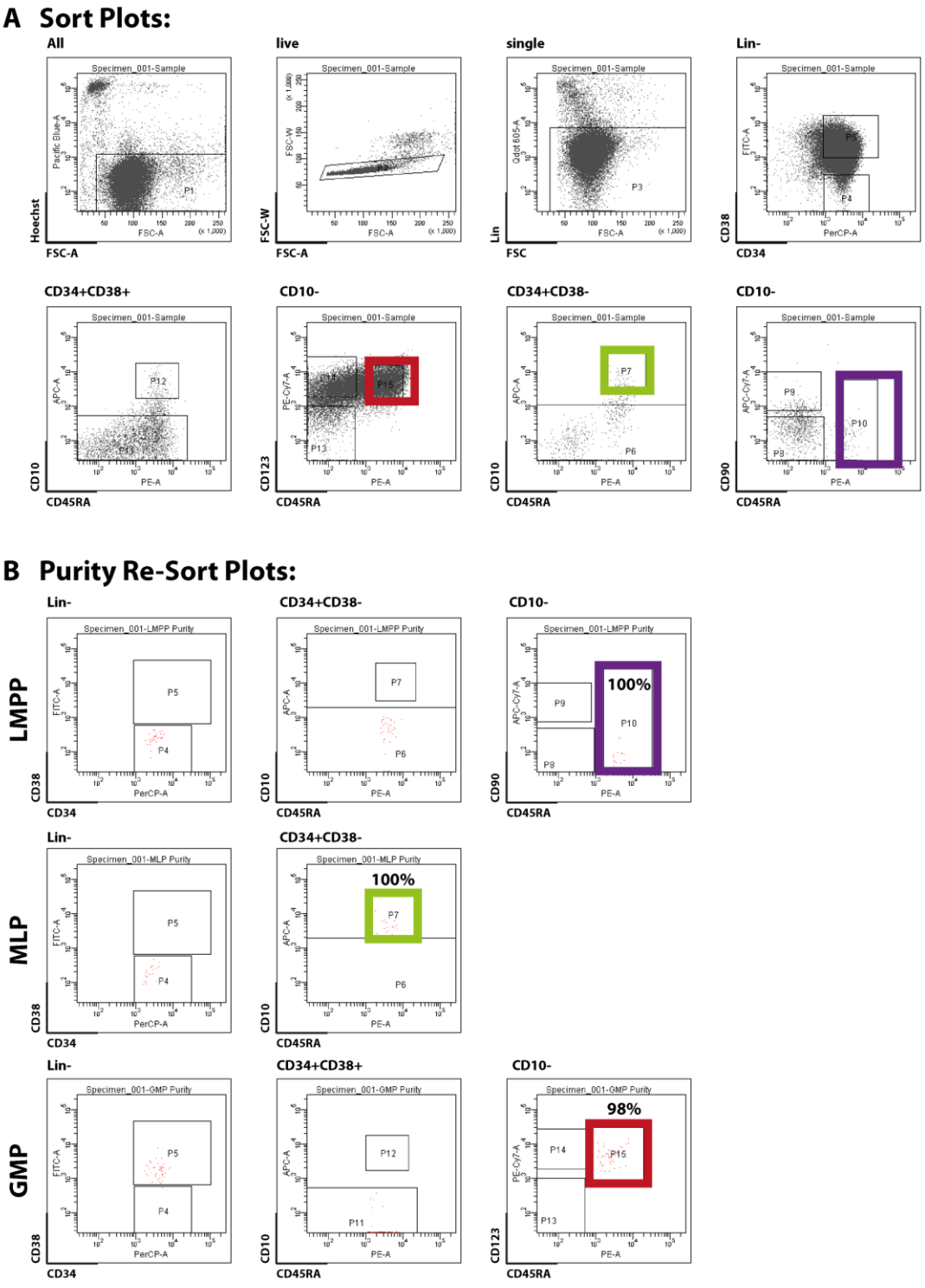

Figure 3.4. Post-Sort Purity.

A Cells isolated from CB were stained with mABs and sorted on a FACS AriaIIIu flow cytometer to isolate GMP (red), MLP (green) and LMPP (purple). Populations were collected and they post-sort purity was checked.

B Illustrates the post sort purity check. Cells from the sorted populations are analsyed with the same cytometer settings on the sorter post-sort. The sorting gates are widended to analysis gates and it is calculated how many of the events fall into their original gate. LMPPs acquired in this experiment showed a post-sort purity of 100%, as did MLPs. GMPs could be sorted to 98% purity.

GMP, granulocyte-macrophage progenitor; MLP, multilymphoid progenitor; LMPP, lymphoid-primed multipotent progenitor; Lin, lineage.

3.3 MLP Panel Troubleshooting

One of the questions I asked in my thesis prompted us to include CD10 into the standard staining panel to assess the difference between the LMPP and the multilymphoid progenitor (MLP). FACS analysis revealed that the staining profiles differed from a test staining and the sort for the experiment a few months later, (Figure 3.5). The top row represents the test staining, and in the bottom row, the experiment is shown. The panels for the exclusion of lin+ cells and CD34/CD38 analysis look very similar; variation can be attributed to the forward scatter settings of the FACS machines, which change slightly over time. The CD45RA/CD10 plots however, (highlighted in grey), which are gated on Lin-CD34+CD38-, differ with respect to the CD10 expression. To validate that this pattern was real, we sought to investigate if this was due to a compensation artefact. Another reason might be the improved laser power of the flow cytometer in the second experiment, after it had been upgraded. To address the compensation artefact question, a dye swap experiment between CD10 and CD45RA was performed, which features exchanging the PE and APC fluorochromes on CD10 and CD45RA. If the diagonal pattern persisted, it can be concluded that it is a biological phenomenon and not due to a compensation problem. Should the pattern disappear however, this would hint that there is an issue with compensation. If this characteristic diagonal pattern was detectable when the fluorochromes conjugated to CD45RA and CD10 were swapped, CD10 expression in the CD45RA+ compartment was higher than previously expected. If the pattern disappeared or appeared vice-versa, a compensation-related artefact had occurred. Importantly, the same cord

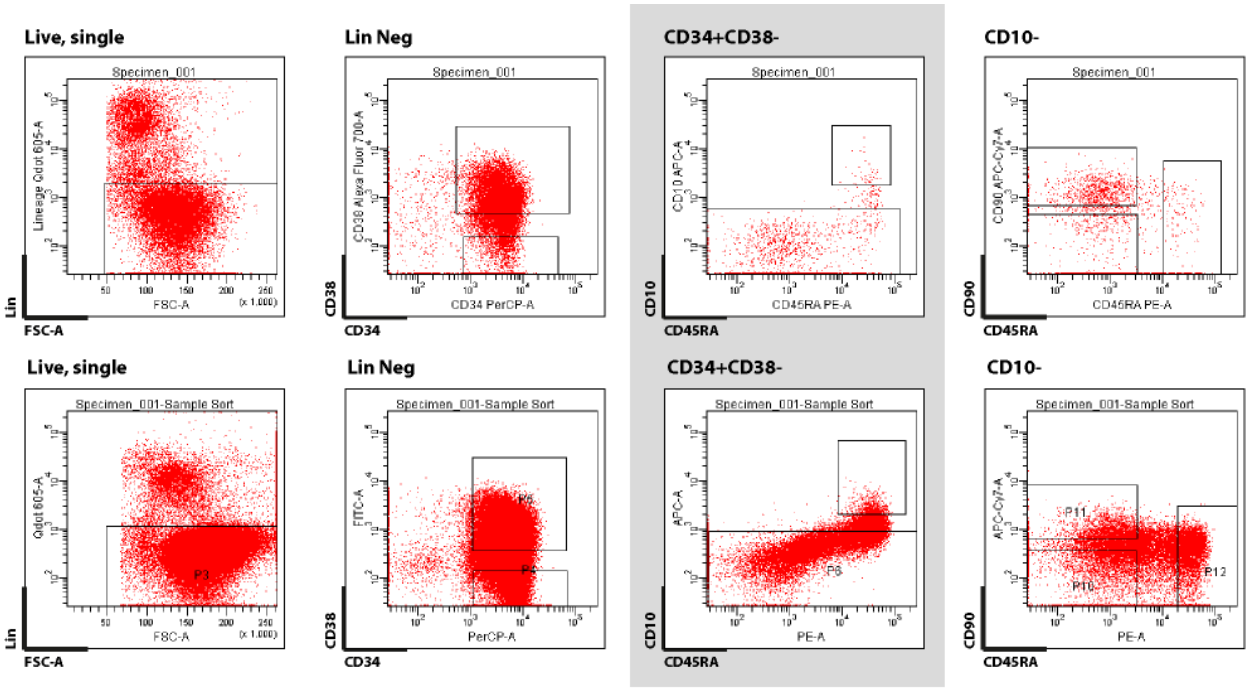

Figure 3.5. CD10 Staining - Shifting Patterns.
Cord blood was stained with fluorochrome conjugated monoclonal antibodies to separate human stem and progenitor cells. The top row shows a typical example of a normal cord blood profile. In the bottom row, the CD10 signal seems to shift the entire population resulting in a characteristic diagonal pattern (see 3rd panel, bottom row).

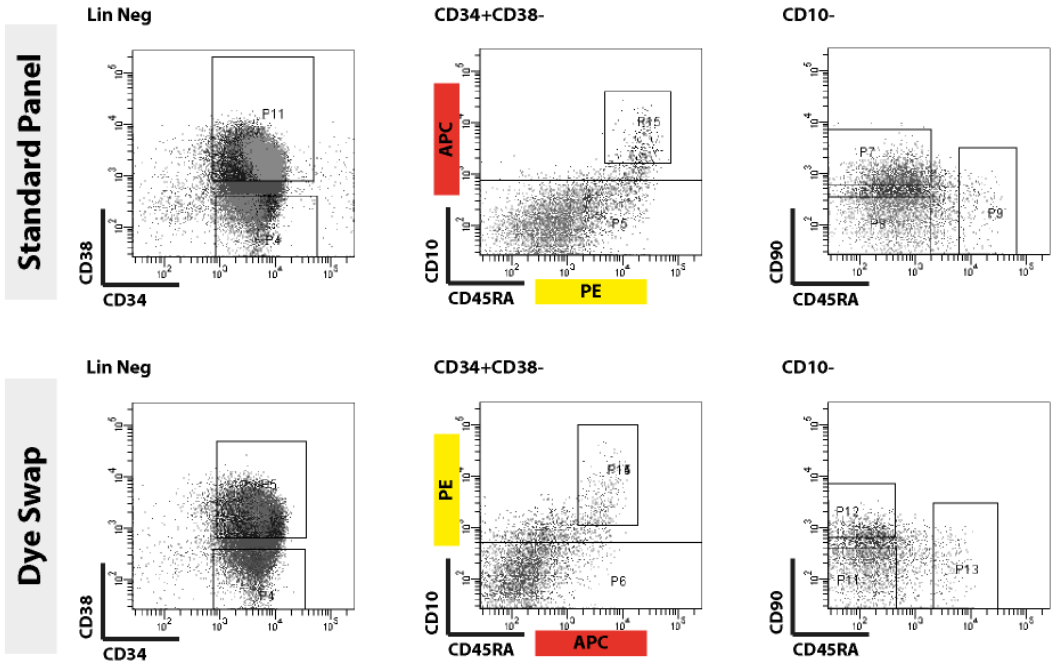

Figure 3.6: CD10 Staining - Dye Swap.
Cord blood was stained with fluorochrome conjugated monoclonal antibodies to separate human stem and progenitor cells, with two slightly different panels. The top row shows our standard staining approach, and the bottom row illustrates how the profile changes if the fluorochromes conjugated to CD10 and CD45RA are swapped.

blood sample was stained with both panels. As it can be seen in Figure 3.6, the diagonal pattern is present in both the standard as well as the dye swapped panel. This experiment confirmed the standard FACS panel which was in current use. The in vitro functional assays to verify the differentiation potentials of the populations sorted with the MLP panel can be found in Chapter 4.

3.4 Discussion

As mentioned before, flow sorting procedures have to be impeccable in order to process the cells as quickly as possible. FACS is an amazing technique which has advanced greatly in recent years. It is essential for us to purify stem and progenitor cells which we seek to characterise. However, there are also limitations. Cell sorting is a very time consuming technique and can harm fragile cell types in the process of passing through the fluidics system of the flow cytometer. There is also the potential danger of contamination to consider, because most sorters are not in a contained system. It might be considered to add antibiotics to the media in the collection tubes for sorting if cells are to be cultured subsequently. I also took special care to ensure that the FACS panel is optimised in terms of compensation requirements. Otherwise, one might risk false positive results or data which is difficult to interpret. To prevent this from happening, compensation controls, including single stains and FMOs, have to be included in every single sorting experiment. Thus it can be established that each experiment has been performed in a reproducible manner with daily adjustments to balance out changes in cytometer performance.

The choice of cells or beads used as controls is also very important. They should be from the same organism, of similar size and exhibit comparative levels of auto-

fluorescence. In this study, MNCs have been routinely used as the basis for FMO controls, whereas commercially available compensation beads were used for single stains.

Another very crucial point that we had to bear in mind when working with fluorescently labelled mABs, is the question of fluorophore, clone and manufacturing batch. The stability of certain fluorescent labels can be affected by improper handling or exposure to light. There is also evidence that particular fluorochromes might be harmful and harbour cytotoxic effects in culture, especially the so called Quantum Dots (Qdot)[69-71]. In this study, Qdot605 was used to select lineage positive cells, which were never sorted or cultured. Also, every Qdot staining was followed by stringent washes to minimise exposure of non-Qdot stained cells to the potentially harmful reagent. Moreover the correct amount of fluorescently labelled mAB for a particular application has to be titrated. Ideally, cells which harbour similar properties to the cells of interest should be used to test a range of concentrations of mAB. The signal to noise (S:N) ratio can easily be evaluated and the mAB concentration which yields in the highest S:N will provide the optimum amount of mAB used for staining.

As mentioned previously, cells isolated from CB or BM can express the F_c receptor (FcR), i.e. macrophages. FcRs are important in the immune response, because they can bind the F_c region of antibodies which might be bound to a pathogen. To prevent FcRs from binding the Fc portion of mABs used for analysis, an FcR blocking reagent can be used. Furthermore, the FACS staining buffer should contain 10% of FCS, which will not only contribute to saturating the FcRs, but also provide a protective coating for the cells. Live-dead cell discrimination is a further step to reduce the background in FACS experiments. Plasma membranes of dead or dying cells are permeable, which can permit fluorescent antibodies to concentrate in the

interior. This might result in a false positive read out on the flow cytometer. Therefore, dead cells need to be labelled in order to be excluded from the final analysis or sort. Hoechst 33258 is a dye which can pass the damaged plasma membrane of dying/dead cells and it will exhibit fluorescence if bound to DNA.

Doublet exclusion is another way to ensure the flow cytometry procedure is reliable and reproducible. Doublets can be eliminated by plotting cells on a plot showing FSC-Area and FSC-Volume. Single cells should show a linear relationship of these parameters, whereas doublets or large debris will be easily discernible of falling out of the diagonal.

There are a few more points to stress concerning the actual sorting procedure to purify HSPCs. The purity of the isolated populations has to be monitored. Pre- and post-sort purity checks can be performed. If the population of interest is sorted directly into lysing reagents (RLT buffer, for example), pre-sort purities were acquired. Post-sorting purities were checked for every sorted population, provided enough events were acquired.

Bearing all these precautions in mind, paired with swift processing and the presence of appropriate controls, FACS can be a very effective tool to purify and isolate small populations to a great extent.

4 Optimisation of In Vitro Functional Assays

4.1 MS5 Stromal Co-Culture – Differentiation of HSPCs into B cells, NK Cells and Myeloid Cells

In vitro assays are an important way to assess differentiation potentials of short lived progenitor cells, as a substitute for an in vivo model. Although it is possible to engraft single HSCs into immunodeficient mice[72], it is much more difficult to transplant even large numbers of transient progenitors and assess (multilineage) engraftment.

In vitro models which feature culture of HSPCs on monolayers of human or murine stromal cells are a widely accepted substitute. Murine stromal-5 (MS5) cells have been used over the last 15 years for this purpose[73,74].

The MS5 cell line which was in use in our group was evaluated for its capacity to differentiate primary human CD34+ into B cells (CD19+) and myeloid cells (CD33+). CD34+ cells from BM samples were cultured on MS5 monolayers in the presence of defined serum, cytokines (SCF, Flt3L, G-CSF, Dup697 and ATRA) for 5 weeks with weekly media changes. SCF and Flt3L are cytokines important to stimulate differentiation and proliferation of stem and progenitor cells; Dup697 is a cyclooxygenase inhibitor which promotes B cell differentiation in culture and all trans retinoic acid (ATRA) can push neutrophils towards maturation and supports B cell differentiation. For composition of media and precise cytokine concentrations, please see Table 2.8, “Our Condition B”. After the designated culture period, monolayers were dissociated and the cell suspension of human and murine cells stained with fluorescently labelled mABs. The mABs in this study were hCD45, to discern the human cells from the murine stromal cells; CD33, to stain myeloid cells and CD19 to

mark B cells. CD19+ B cell output was not very robust, even after 5 weeks, and CD33+ myeloid cells also showed variability (Figure 4.1).

The old MS5 stromal cell line was replaced with MS5 cells of a low passage number kindly provided by Professor Francoise Pflumio. The same culture conditions were tested with sorted CD34+ cells and FACS purified HSPCs from CB (Figure 4.2). After 5 weeks, CD34+ cells gave rise to 74% CD33+ cells and 9% CD19+ cells, and expanded about 10-fold. HSC, MPP and LMPP gave rise to both B and myeloid cells, and expanded their cell numbers from 10- up to 15-fold. CMP, GMP and MEP mainly gave rise to myeloid cells. GMP and MEP expanded 2- to 5 fold; the CMP up to 20-fold. A possible explanation for the CD19+ cells which were detected in the CMP [explained] could be the relatively low sorting purity of 94%, and it is widely known that the GMP retains residual lymphoid potential[19].

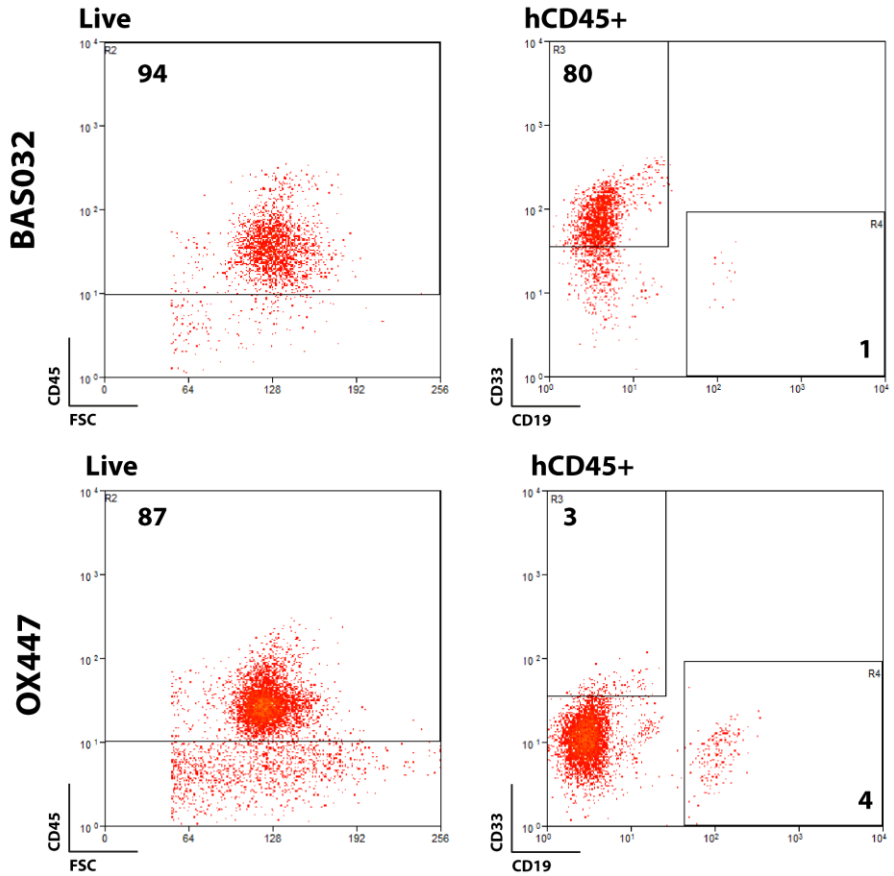

Figure 4.1. Inefficient MS5 Stromal Cell Line to Differentiate CD34+ Cells Into B and Myeloid Cells.

CD34+ cells from patients diagnosed with idiopathic thrombocytopenia (BAS032) and neutropenia (OX447) were plated on MS5 stromal monolayers at a concentration of 200 cells/mL. Wells were harvested after 5 weeks by vigorous pipetting and stained with monoclonal antibodies directed against human CD45, CD19 and CD33. CD19+ B cells and CD33+ myeloid cells could be detected by FACS analysis.

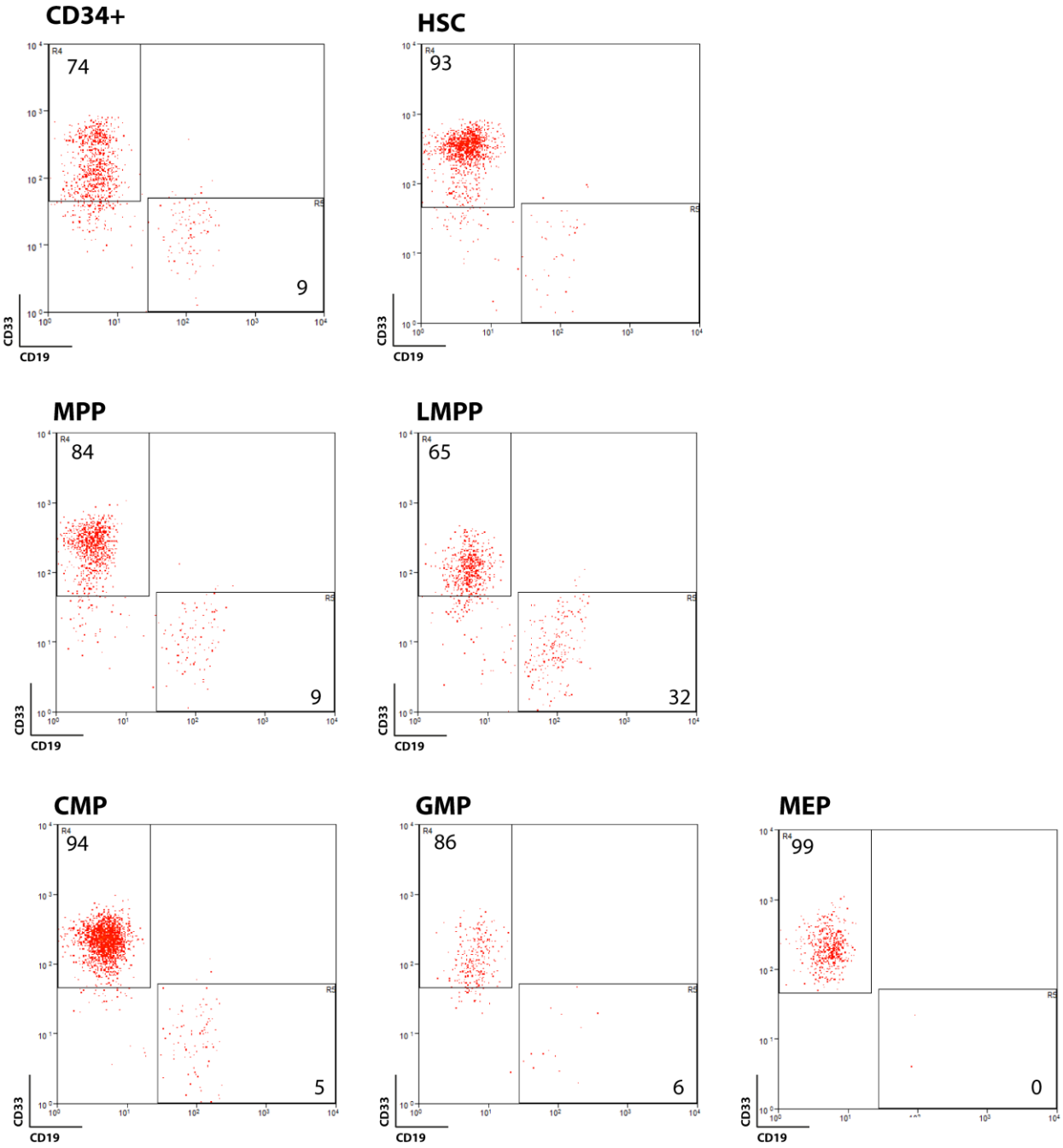

Figure 4.2. Efficient Generation of B and Myeloid Cells from Sorted HSPCs and Sorted CD34+ Cells.

Sorted human stem and progenitor cells were plated on newly obtained MS5 stromal monolayers at a concentration of 200 cells/mL (100 cells in 500µL of medium). Medium was changed weekly and supplemented with 20ng/mL SCF, 10ng/mL Flt3L, G-CSF and IL-15, as well as 10^{-7}mM Dup697 and ATRA. Wells were harvested after 5 weeks by vigorous pipetting and stained with monoclonal antibodies directed against human CD45, CD19 and CD33. CD19+ B cells and CD33+ myeloid cells could be detected by FACS analysis. Every plot is gated on live, single and human CD45+ cells.

CMP, common myeloid progenitor; MEP, megakaryocyte-erythroid progenitor; GMP, granulocyte-macrophage progenitor; HSC, haematopoietic stem cell; MPP, multipotent progenitor; LMPP, lymphoid primed multipotent progenitor.

Limit Dilution Analysis (LDA) was performed to derive frequencies of cells with certain potentials in a population. For example, how many immunophenotypic LMPPs can give rise to B cells? In order to perform limit dilution assays single LMPPs from CB were expanded over a period of 3 weeks in liquid culture. Instead of using CD33 to identify pan-myeloid differentiation, mABs against CD14 to label monocytes and CD15 to mark granulocytic/neutrophilic cells were used in addition to CD45 and CD33. Multi- and bi-lineage progeny could be detected in wells seeded with single LMPPs, as is shown in Figure 4.3. The reason for the 3-week culture period as opposed to the five-week culture period used in Figure 3.8 is that LMPPs are progenitors and give rise to terminally differentiated cells quicker than purified HSCs or a heterogeneous population of bulk CD34+ cells.

Trial limit dilution experiments were performed with sorted CD34+ cells from CB. Single, 5, 10 and 100 cells were sorted into individual wells and maintained in culture for 5 weeks. Only wells that contained at least 30 hCD45+ cells were scored for B, M or mixed (BM) progeny. Figure 4.4 A demonstrates how the frequency of cells with B and myeloid potential can be calculated with the help of L-Calc [75]. This programme, utilizes the Poisson distribution to predict a probability for a cell to perform a defined task (i.e. being responsive or non-responsive to a drug). If cells are plated at increasing concentrations, an inverse linear relationship between cell dose and non-responsive wells will be detectable. According to the Poisson distribution, the cell concentration at which 37% of wells are empty will indicate the frequency of responsive cells. In this experiment, 1 in 8 CD34+ cells could give rise to both B and myeloid cells in culture. The standard deviation and 95% confidence interval were also calculated in L-Calc. Figure 4.4 B represents an example of how a 96 well plate is scored for B, myeloid and mixed wells.

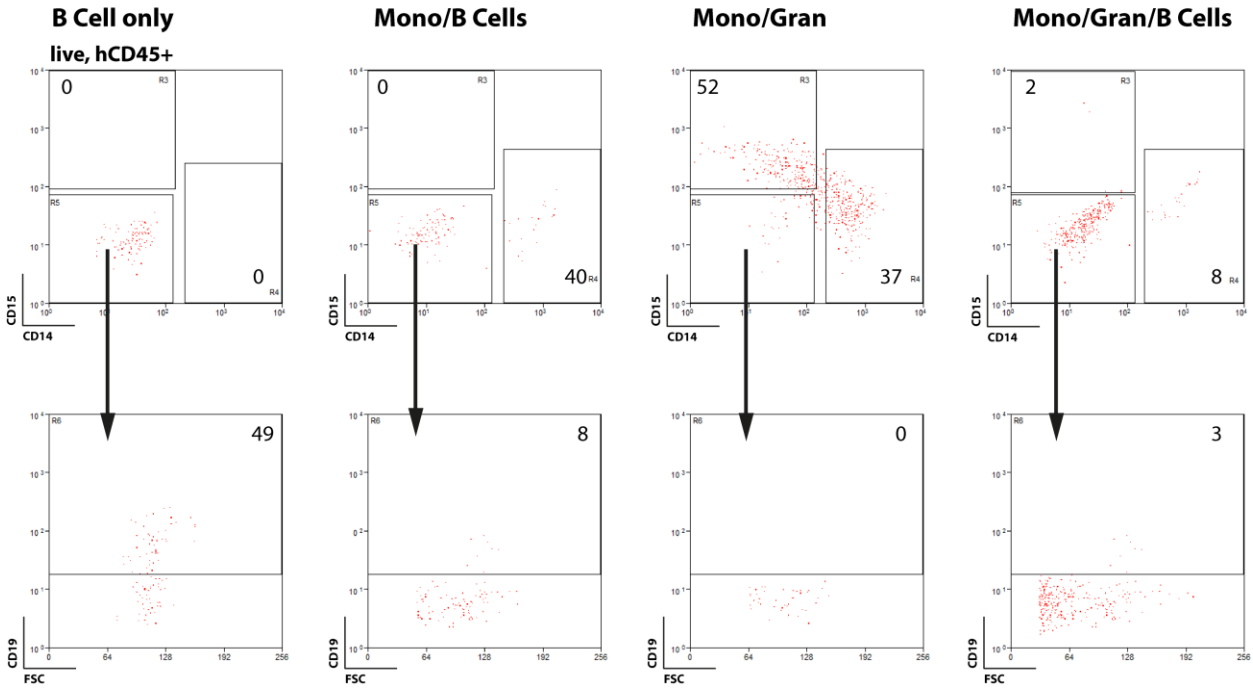

Figure 4.3. Progeny of single LMPPs after two weeks of culture on MS5 stromal monolayers. Single LMPPs were sorted directly onto MS5 stromal monolayers into a 96-well plate. Medium was changed weekly and supplemented with 20ng/mL SCF, 10ng/mL Flt3L, G-CSF and IL-15, as well as 10-7mM Dup697. Wells were harvested after 2 weeks by vigorous pipetting and stained with monoclonal antibodies directed against human CD45, CD14, CD15 and CD19. CD19+ B cells, CD14+ monocytes and CD15+ granulocytes could be detected by FACS analysis on a DAKO Cytomation CYAN flow cytometer. Wells were scored as positive if they contained a minimum of 30 human CD45+ cells. Percentages represent values from this particular experiment, 64 single LMPPs were assayed. Mono, monocytes; gran, granulocytes; hCD45, human CD45; LMPP, lymphoid-primed multipotent progenitor.

A

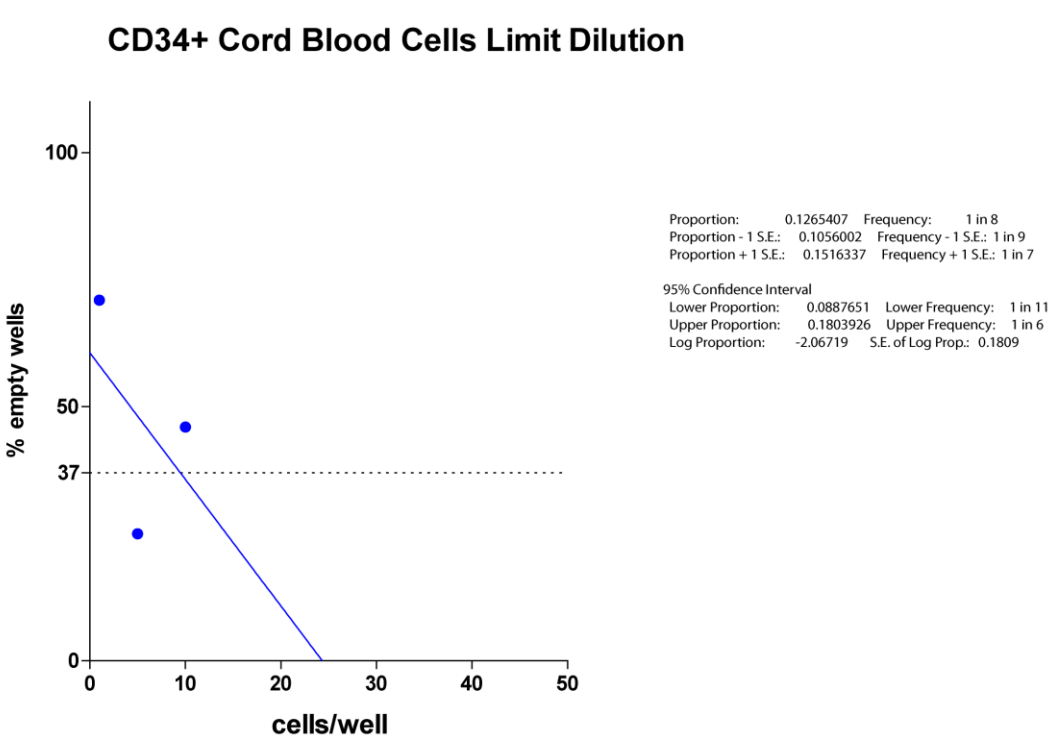

B

	1	2	3	4	5	6	7	8	9	10	11	12	
A	bm	bm	bm	bm	x	x	x	x	x	x	m	x	1 cell
B	m	bm	x	x	x	x	bm	x	x	x	bm	x	
C	bm	bm	bm	bm	bm	bm	bm	m	x	bm	bm	bm	5 cells
D	m	bm	bm	bm	bm	bm	bm	m	m	bm	bm	m	
E	m	bm	bm	m	bm	bm	bm	m	bm	m	m	bm	10 cells
F	bm	bm	m	bm	bm	x	m	bm	b	m	x	bm	
G	bm	bm	bm	bm	bm	bm	bm	bm	bm	bm	bm	bm	50 cells
H	bm	bm	bm	bm	bm	bm	bm	bm	bm	bm	m	bm	

x — empty well

m — well containing only CD33+ myeloid cells

bm — well containing both CD33+ myeloid and CD19+ B cells

b — well containing only CD19+ B cells

Figure 4.4. Limit Dilution Assay of CD34+ Cord Blood Cells.

1, 5, 10 and 50 CD34+ cells were sorted directly onto MS5 stromal layers and analysed by FACS after 3 weeks for the expression of CD19, CD33 and CD45. Only wells containing more than 30 hCD45+ cells were scored as positive.

A) shows the amount of cells plated per well against the proportion of empty wells. Poisson statistics were used to derive a frequency for cells in the CD34+ population with combined B cell and myeloid potential.

B) depicts a typical representation of a 96 well plate scoring sheet with examples of positive and negative wells.

4.2 Stromal Co-Cultures Expressing Delta-Like Ligands – T Cell Differentiation of HSPCs

Differentiation of human HSPCs into T cells in vitro without the complex 3D microenvironment of the thymus proved to be a difficult task. Cells do not only respond to growth factors and ligands in media, but also to 3D structures, which can provide additional stimuli for the cell to aid proliferation and survival. Foetal thymic organ cultures were the method of choice until the advent of Delta-Like-1 (DL1) transduced OP9 (osteopetrosis-9) stromal cells. This method was first published by JC Zuñiga-Pflücker for murine T cells[76] and later on also for cells from human CB[65].

Our group had failed previously to differentiate CD34+ HSPCs into CD4+CD8a+ T cells[19]. A number of different stromal support cell lines to derive T cells were used in this study to evaluate the most promising in vitro assay. The cell surface markers to look for T cell commitment, pre-T and mature cells were selected carefully. CD7 is thought to be expressed in early lymphoid cells[68] and CD1a+ is consistent with thymic commitment[77]. Mature T cells were scored as CD4+CD8a+, which are well known T cell markers[77].

The first cell line to be tested was an OP9-DL1 stromal cell line of undocumented passage number. Initial experiments to differentiate CD34+ CB cells into CD1a+CD7+ T cell committed cells failed (see Figure 4.5). The protocol used in this experiment was taken from Goardon et al[19], however no CD4+CD8a+ double positive cells were detected in any of their cultures. Half of the medium was changed weekly, cytokines supplemented were 5ng/mL of Flt3L and IL-7, and the cultures were propagated for 7 weeks. All conditions can be found in Table 2.9.

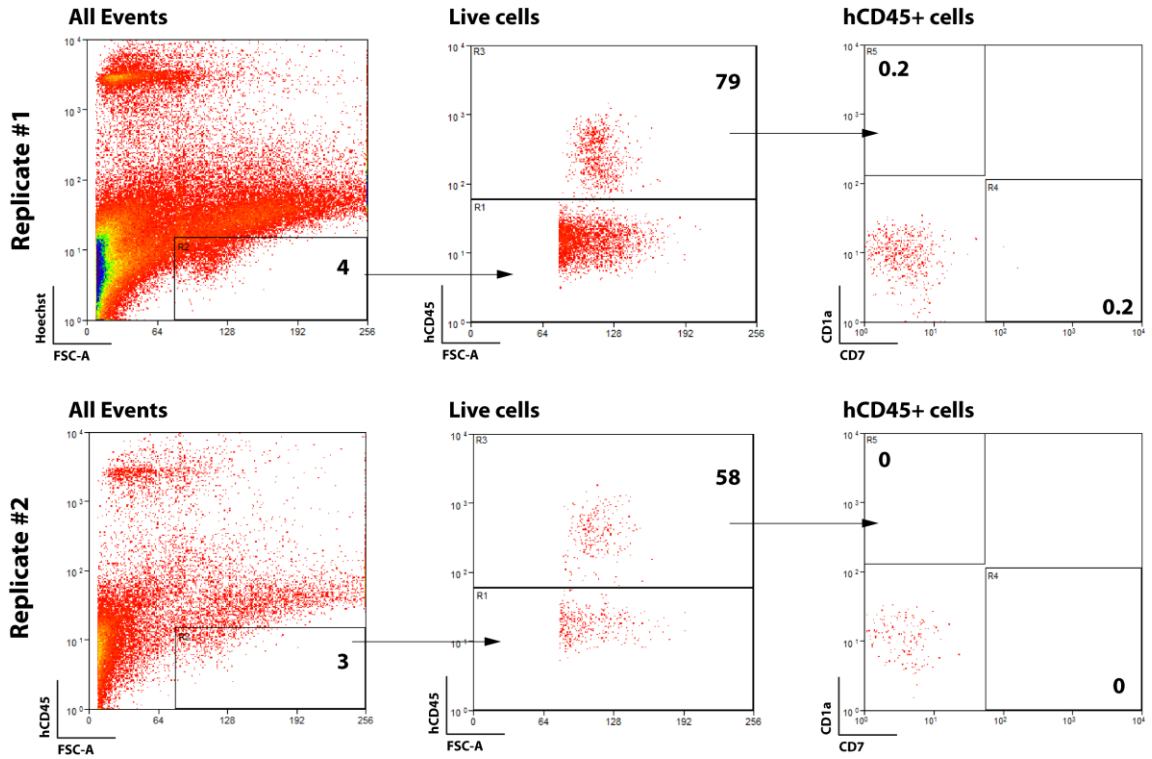

Figure 4.5. Progeny of CD34+ Cord Blood Cells Cultured On OP9-DL1 Stromal Cells for 7 Weeks.

Two replicates of CD34+ CB cells were plated at a concentration of 500 cells/mL on a monolayer of OP9-DL1 cells. Medium was changed weekly and supplemented with 5ng/mL IL-7 and Flt3L and 10% fetal calf serum. Wells were harvested and subjected to FACS analysis after 7 weeks. Cells were stained with anti-CD1a, CD7 and CD45. No CD1a+CD7+ T cell precursors could be detected.

OP9 cells are very fragile if handled incorrectly, they are susceptible to media components and should never reach confluency, as they will undergo adipocyte differentiation. Therefore, we tested a more robust DL1 transduced MS5 cell line which was kindly provided by Prof. Francoise Pflumio[78]. Culture conditions were adapted from Armstrong et al[78] (50ng/mL SCF, 5ng/mL Flt3L, 5ng/mL IL-7 and 150mM β-Insulin). In Figure 4.6, CD34+ CB cells were cultured on a MS5-DL1 monolayer for 7 weeks. This approach seemed to be promising at first, because after 2 weeks, CD7+ cells could be detected. However, at later time points, the CD7+ positive cells had disappeared. There also was a transient $CD1a^{hi}$ population which was suspected to contain dendritic cells. Later on, HLA-DR, expression could be

detected on these CD1a+ cells (data not shown). However, even after 7 weeks, no double positive T cells were present in cultures maintained on MS5-DL1 stromal layers.

Thus, we obtained new OP9-DL1 cells from Juan Carlos Zúñiga-Pflücker. We were not only provided with early passage OP9-DL1 cells, but also Delta-Like-4 (DL4) transduced OP9 cells. DL4 is thought to be the crucial Notch ligand involved in T cell differentiation in the thymus[79].

An experiment comparing OP9-DL1, OP9-DL4 and MS5-DL1 in parallel in different conditions was set up. CD34+ CB cells were plated at a concentration of 200 cells/mL, and maintained on a stromal layer for 7 weeks, in medium supplemented with 10% FSC (defined), 1% L-glutamine and 1% Pen-Strep. Figure 4.7 summarizes the results from this experiment, and all culture conditions are detailed in Table 2.9. Analysis after 5 weeks by FACS showed that CD1a+CD7+ cells could readily be detected in cultures initiated on OP9 based monolayers.

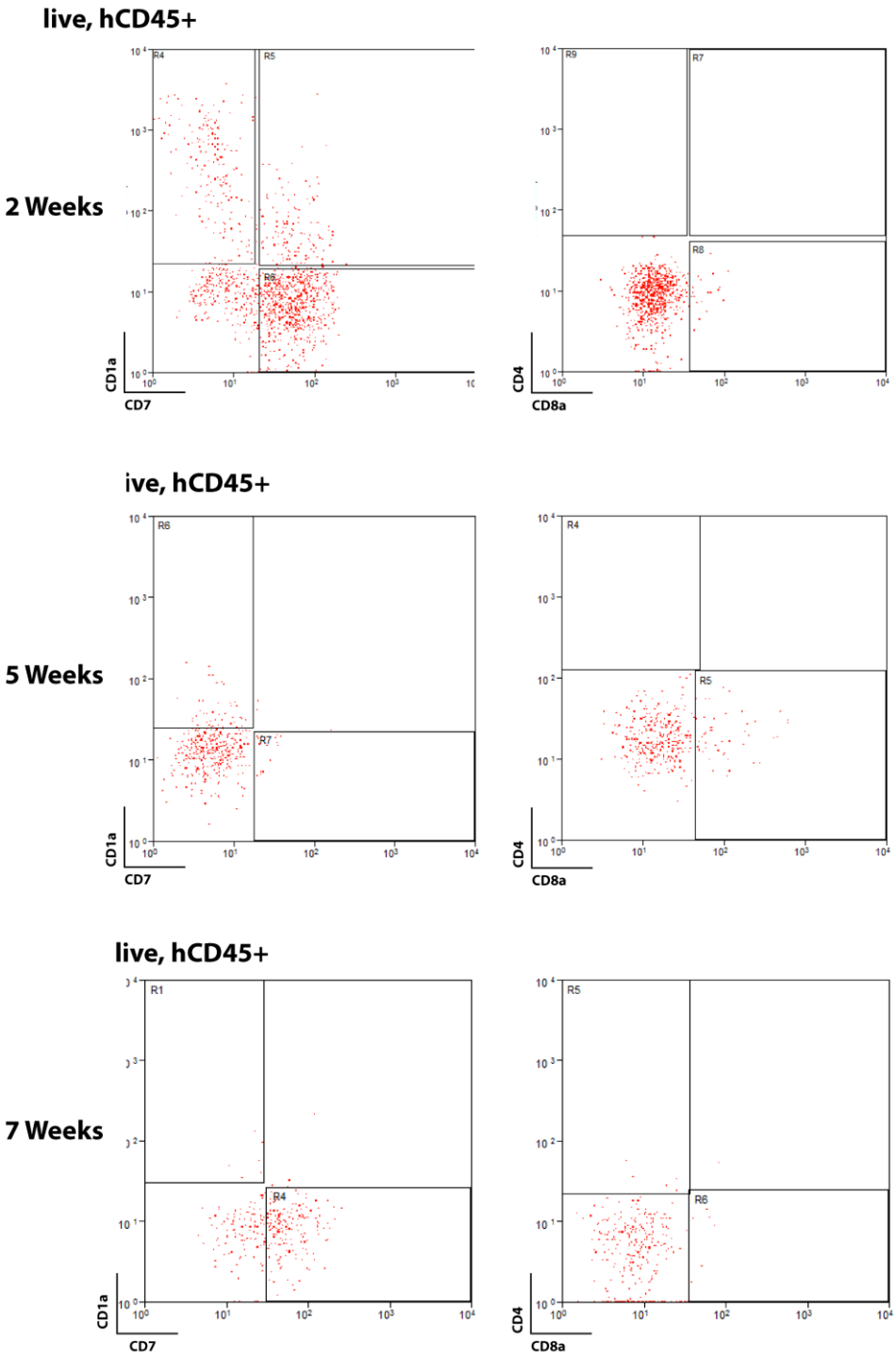

Figure 4.6: Progeny of CD34+ CB Cells Cultured on MS5-DL1 cells For 7 Weeks.
CD34+ CB cells were plated at a concentration of 200 cells/mL on a monolayer of MS5-DL1 cells. Medium was changed weekly and supplemented with 50ng/mL SCF, 5ng/mL IL-7 and Flt3L and 150mM β-insulin. At time points 2 weeks and 5 weeks, only the supernatant of the well was harvested and subjected to FACS analysis. After 7 weeks, the whole culture was dissociated and analysed. Cells were stained with anti-CD1a, CD4, CD7, CD8a and CD45. No CD1a+CD7+CD4+CD8a+ T cells could be detected. All plots are gated on live, human CD45+ cells.

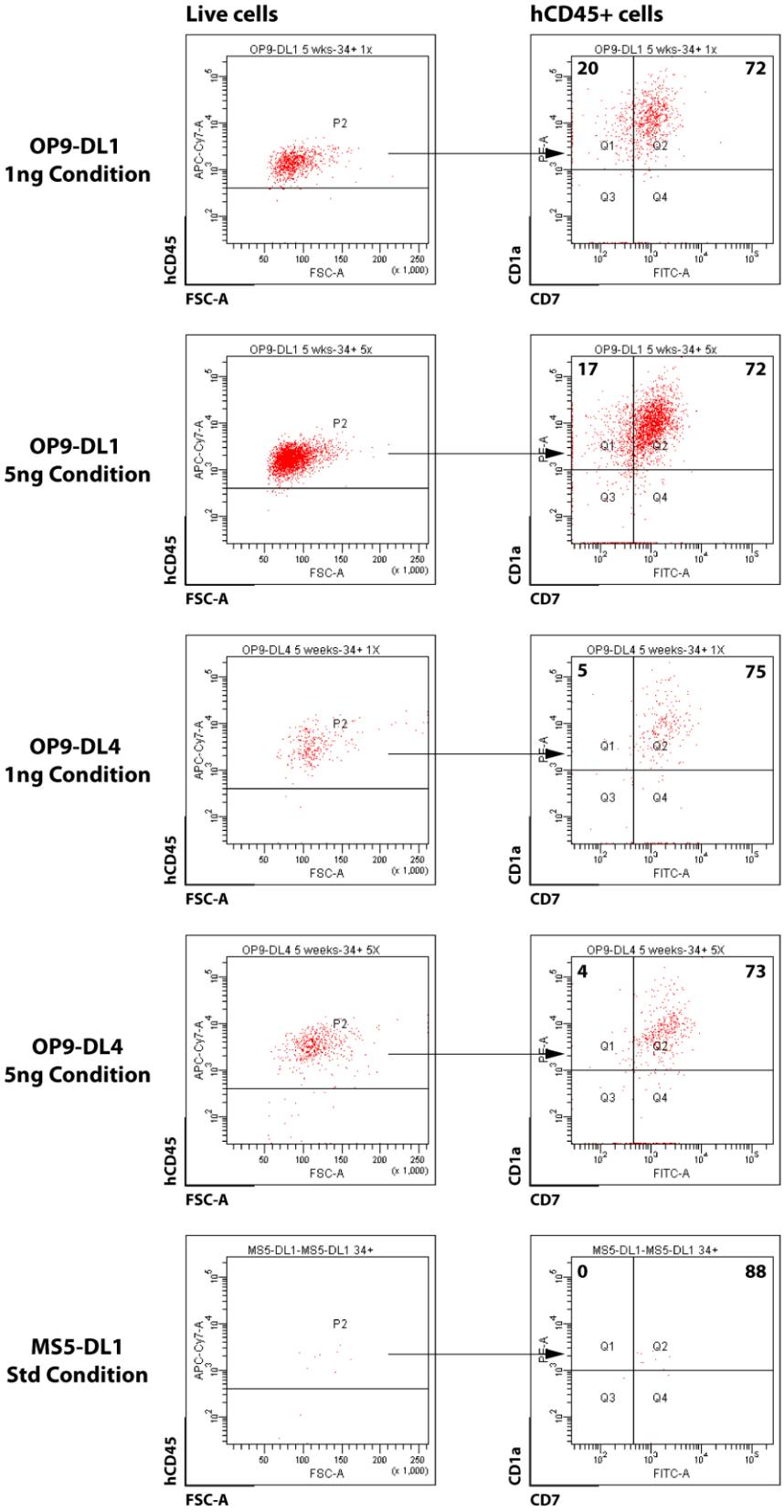

Figure 4.7: T Cell Differentiation Condition Screening Cultures. .

CD34+ cells from CB were cultured on stromal cell monolayers at a concentration of 200 cells/mL. Different concentrations of cytokines and monolayers were tested. After 5 weeks, wells were harvested and subjected to FACS analysis and stained with anti-CD1a, CD7 and CD45. Percentages are derived from a single trial experiment.

OP9-DL1 supported proliferation of CD34+ cells more efficiently than OP9-DL4 cells. MS5-DL1 cells failed to promote early T cell lineage commitment.

Discussion with one of the experts in the field of in vitro T cell differentiation, Dr. Emmanuelle Six, prompted me to batch test defined foetal calf serum (FCS). I was kindly supplied with serum tested to support T cell differentiation as a positive control ("Serum France") to obtain CD4+CD8a+ T cells.

Valuable advice also included the suggestion to prepare the media always fresh from αMEM powder and the recommendation to transfer the human cells to a fresh monolayer of OP9-DL1 cells weekly. From this point on, every T cell assay was performed in this manner[66].

Lin-CD34+CD38- and Lin-CD34+CD38+ cells were sorted from CB and plated on OP9-DL1 monolayers, in media (reconstituted from αMEM powder) supplemented with the positive "heat-inactivated" or "normal" control serum and FCS from Hyclone (Thermo Fisher). The aim of this experiment was to validate the most successful culture conditions for T Cells from HSPCs, with respect to media composition, heat-inactivation of serum and cytokine concentrations.

Historically, sera were heat-inactivated to eliminate mycoplasma and bacterial contaminants, and to inactivate complement, to prevent a complement reaction. Another effect of the heat-treatment of sera is the inactivation of other growth factors in the serum. It is hypothesized that through heat-inactivation growth factor which promote other cell fates than T cell development are rendered non-functional.

In further experiments, lineage negative cells were chosen to ensure that no committed T cell progenitors were amplified. Focussing on the normal, non-heat

inactivated serum first, it can be seen in Figure 4.8, that CD4+CD8a+ output ranges from 1-3% in the “Serum France” cultures and from 2-5% in the “Hyclone” cultures. Surprisingly, the addition of 10ng/mL SCF in the “Six Condition” did not impact greatly on the proliferation of the HSPCs in culture.

The comparison of the heat-inactivated sera can be found in Figure 4.9. CD4+CD8a+ cultured in the presence of the FCS from France constituted 6-16% of CD1a+CD7+ cells after 4 weeks, as opposed to a mere 1-3% in cultures supplemented with FCS from Hyclone. Again, there was no significant difference between the “5ng Condition” and the “Six Condition”.

In a final experiment to find the perfect T cell differentiation conditions, another batch of defined Hyclone supplied from Perbio was evaluated and compared it to the positive control serum from France. As it can be seen in Figure 4.10, the heat inactivated Perbio serum was capable of sustaining CD4+CD8a+ T cell differentiation even from highly purified CB progenitor populations, such as the LMPP, MPP and MLP already after 4 weeks, in both the “5ng Condition” (1-29% of CD4+CD8a+ cells) and the “Six Condition” (17-50% CD4+CD8a+ cells). MPPs did not successfully expand in this experiment, it was reasoned that due to unknown circumstances, they did not survive the transfer to fresh stromal monolayers.

Based on the above experiments, the following protocol for T cell differentiation was developed. It can be found in Materials and Method, Section 2.3.4.

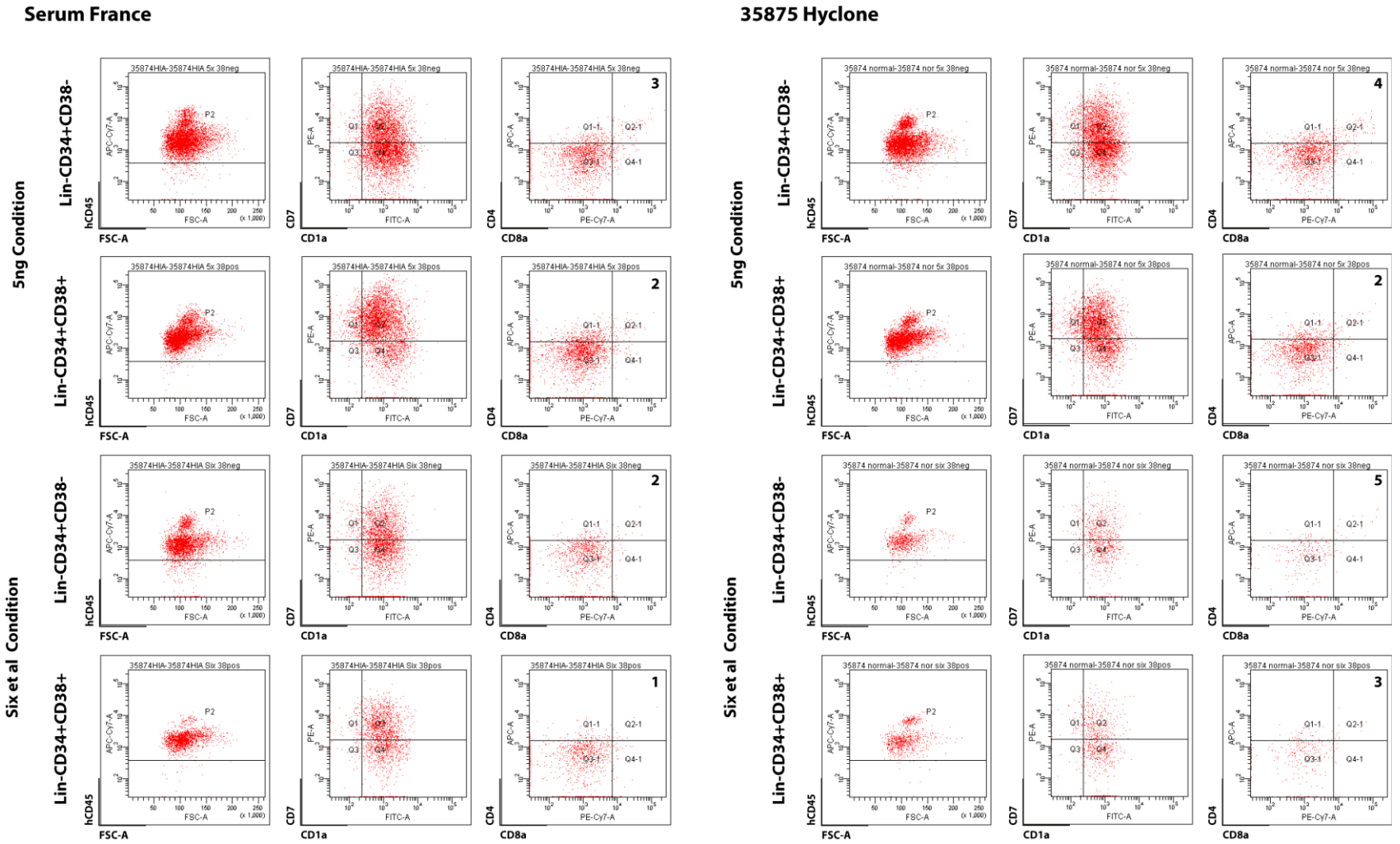

Figure 4.8. Serum Screening T Cell Cultures on OP9-DL1 Stromal Monolayers.

Serum, obtained from two different sources, was tested for the most effective condition supporting T cell differentiation. Lin- progenitors from cord blood were plated at a concentration of 200 cells/mL on OP9-DL1 monolayers. Medium and monolayers were changed weekly. Wells were harvested after 4 weeks by vigorous pipetting and subjected to FACS analysis. Cells were stained with anti-CD1a, CD4a, CD7, CD8a and CD45. CD1a+CD7+CD4+CD8a+ T cells could be successfully detected. N=1.

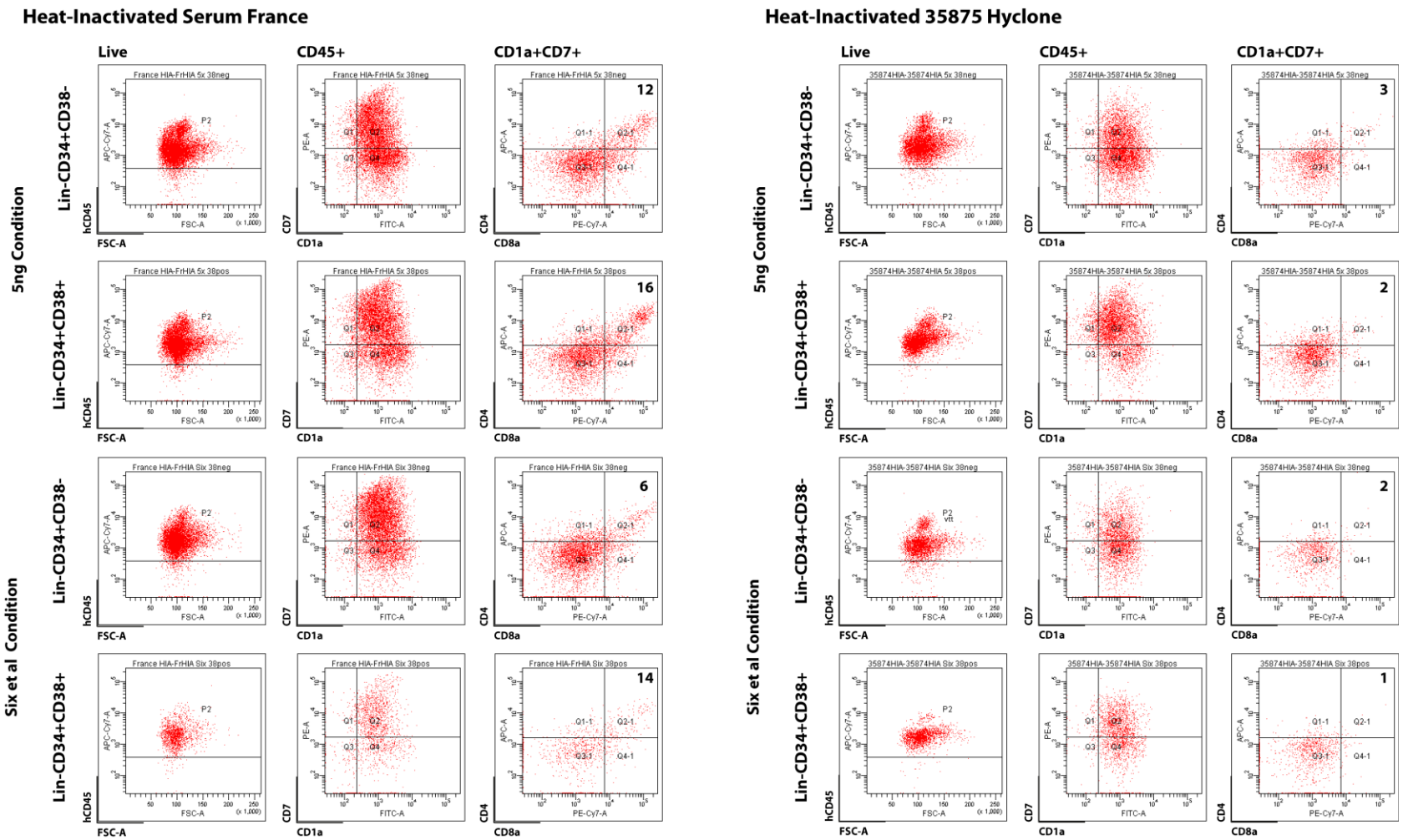

Figure 4.9. Heat-Inactivated Serum Screening T Cell Cultures On OP9-DL1 Stromal Monolayers.

Heat-inactivated serum, obtained from two different sources, was tested for the most effective condition supporting T cell differentiation. Lin- progenitors from cord blood were plated at a concentration of 200 cells/mL on OP9-DL1 monolayers. Medium and monolayers were changed weekly. Wells were harvested after 4 weeks by vigorous pipetting and subjected to FACS analysis. Cells were stained with anti-CD1a, CD4a, CD7, CD8a and CD45. CD1a+CD7+CD4+CD8a+ T cells could be successfully detected. N=1. .

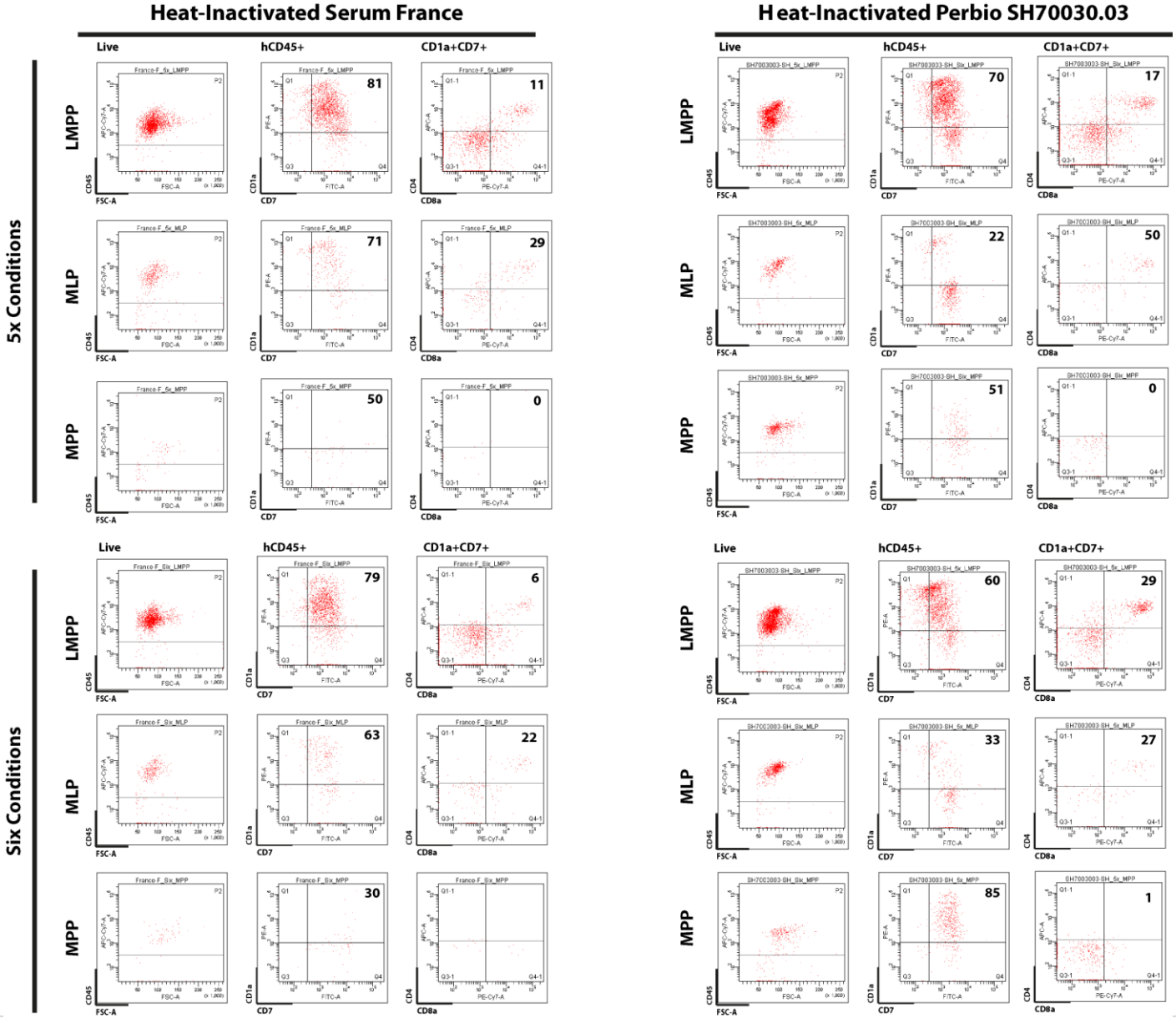
Heat-Inactivated Serum France
Heat-Inactivated Perbio SH70030.03
5x Conditions
Six Conditions
Live
hCD45+
CD1a+CD7+
LMPP
MLP
MPP
81
11
71
29
50
0
79
6
63
22
30
70
17
22
50
51
0
60
29
33
27
85
1

Figure 4.10. Final T Cell Culture Conditions on OP9-DL1 Stromal Monolayers.
Heat-inactivated serum, obtained from Emanuelle Six ('French Serum') and Perbio ('SH70030.03') was tested for the most effective condition supporting T cell differentiation. MPPs, LMPPs and MLPs from cord blood were plated at a concentration of 100 cells/mL on OP9-DL1 monolayers. Medium and monolayers were changed weekly. Wells were harvested after 4 weeks by vigorous pipetting and subjected to FACS analysis. Cells were stained with anti-CD1a, CD4a, CD7, CD8a and CD45. CD1a+CD7+CD4+CD8a+ T cells could be successfully detected. The numbers in the gates are percentages from this particular experiment. MPP, multipotent progenitor; LMPP, lymphoid primed multipotent progenitor; MLP, multilymphoid progenitor.

4.3 Dendritic Cell In Vitro Differentiation

Dendritic cells (DCs) are antigen presenting cells (APCs) and occupy an important function in innate immunity. In vitro differentiation of DCs proved to be a difficult task, and not many approaches have been published to differentiate them from stem and progenitor cells.

In order to derive DCs in vitro, progenitors sorted from CB were plated on MS5 stromal layers, in two different conditions. The first one was adapted from Galy et al and featured supplementation of the medium with Leukaemia Inhibitory factor (LIF), IL-3 and IL-6[67]. The second condition was "Our Condition" which was previously used to differentiate HSPCs into B, NK and myeloid cells. It was chosen as a means to compare it to the "Galy et al" condition, as well as DC output had not been previously assessed in this culture system.

After 3 weeks, the cultures were dissociated and stained with anti-CD45, CD1a (DC), CD15 (gran), CD14 (mono/DC) and CD19 (B cells). The results of 100 GMPs, MLPs and LMPPs plated in the Galy et al conditions can be seen in Figure 4.11 A. Populations expanded 3-fold (MLP), 5-fold (LMPP) up to 20-fold (GMP), and granulocytes and B cells could readily be detected in GMP and LMPP initiated

cultures. Monocyte output was low in all cases and no CD1a+ DCs could be detected.

Figure 4.11 B presents the counterpart experiment of the GMP, LMPP and MLP expansion in “Our Condition”. After 3 weeks, GMPs had expanded 10-fold , which suggests that the population is already exhausted, and most of the progeny which was still detectable were granulocytes. LMPPs expanded 100-fold and mainly gave rise to B cells. MLPs showed a 170-fold expansion and exclusively gave rise to B cells. DC generation was unsuccessful also in these culture conditions.

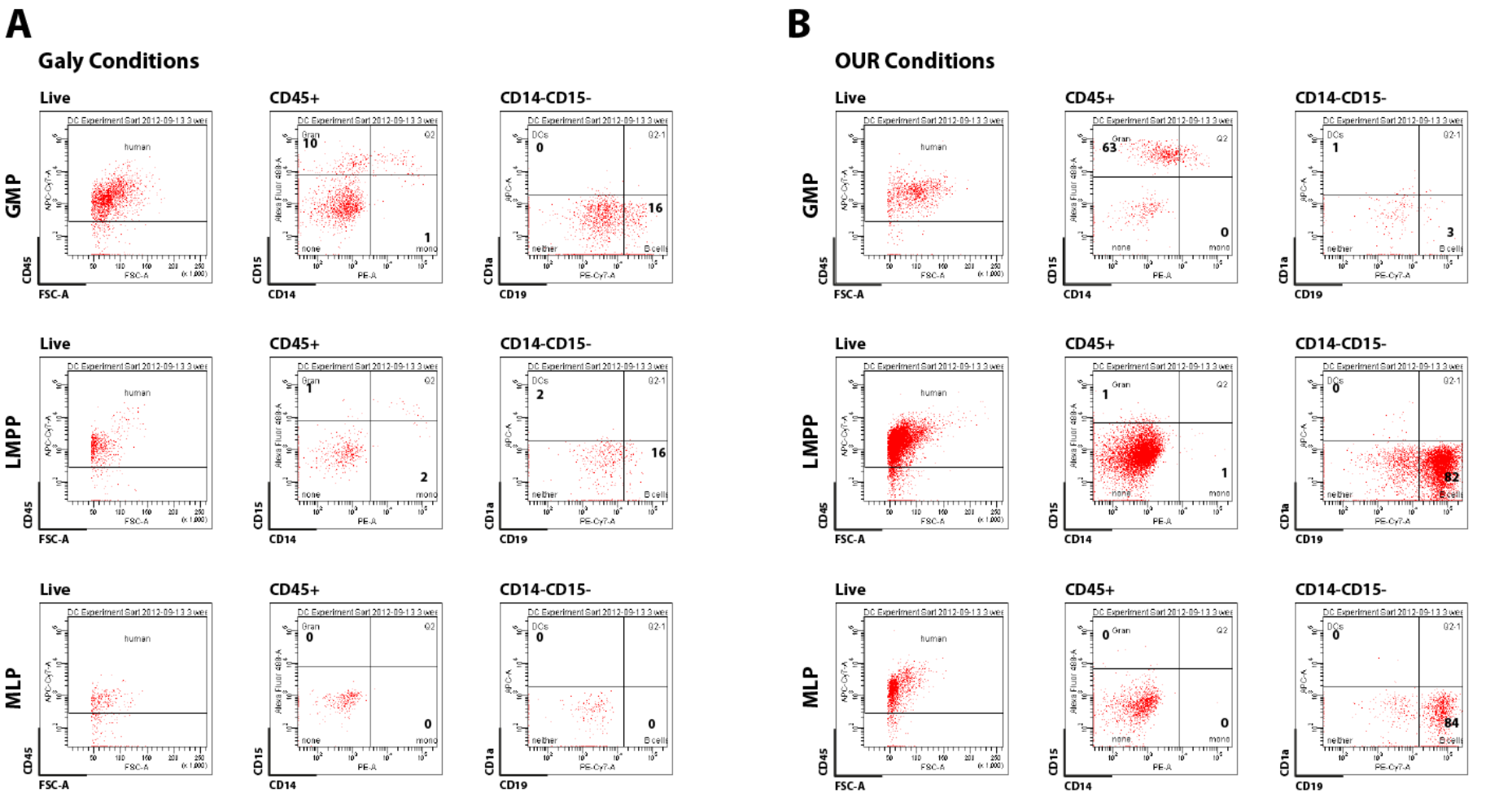

Figure 4.11. In Vitro Differentiation Of Dendritic Cells.

Sorted CB progenitors were placed in conditions adapted from Galy et al and into “Our Condition” to generate dendritic cells. After 3 weeks, cultures were dissociated and investigated for the expression of CD15 (granulocytes), CD14 (monocytes and DCs), CD19 (B Cells) and CD1a (DCs).

A) Results of GMP, LMPP and MLP cultured for 3 weeks in the Galy et al condition. No CD1a+CD14- DCs could be detected.

B) Results of GMP, LMPP and MLP cultured for 3 weeks in “Our Conditions”. No CD1a+CD14- DCs could be detected.

MLP, multilymphoid progenitor; LMPP, lymphoid-primed multipotent progenitor; GMP, granulocyte-maccrophage progenitor.

4.4 Multipotential In Vitro Functional Assay

In order to fully characterize a cell population, its differentiation potentials have to be assessed in parallel, ideally from a single cell. Based on a multipotential assay taken from Adolfsson et al[16], who expanded single, murine LMPPs on a supportive stromal layer and transferred fractions of the expanded clones to other culture conditions, I set out to translate this system to human cells.

Figure 4.12 A illustrates the experimental layout of this technique. Single or bulk cells are plated on MS5 stromal layers in high concentrations of SCF, Flt3L and TPO (100ng/mL each) to promote expansion. After 7 days, the culture is dissociated and split into three equal fractions, which are divided and plated in the "Six et al Condition" on OP9-DL1 cells to derive T cells, "Our Condition" to derive B, NK and myeloid cells and finally the "Galy et al Condition" to derive DCs. After the required culture period (7 weeks for T cells, and 2-3 weeks for myeloid, B, NK and DCs) the cultures are disaggregated and stained with appropriate mABs to identify the progeny generated in culture.

96 single LMPPs and MLPs were sorted onto MS5 stromal layers to 100% purity for expansion (Figure 4.12 B and C). After one week, wells were dissociated and transferred onto fresh OP9-DL1 and MS5 monolayers. Wells were inspected manually for growth; however no progeny could be detected under the inverted microscope. Nevertheless, the wells were fractionated into three parts and transferred to T cell, B/NK/myeloid cell and DC supporting conditions. After 7 weeks, T cell output was assessed by FACS, results of two representative wells can be found in Figure 4.12 D. However, in none of the 96 wells seeded, cells could be detected which fell into the live cell gate. Even though low numbers of

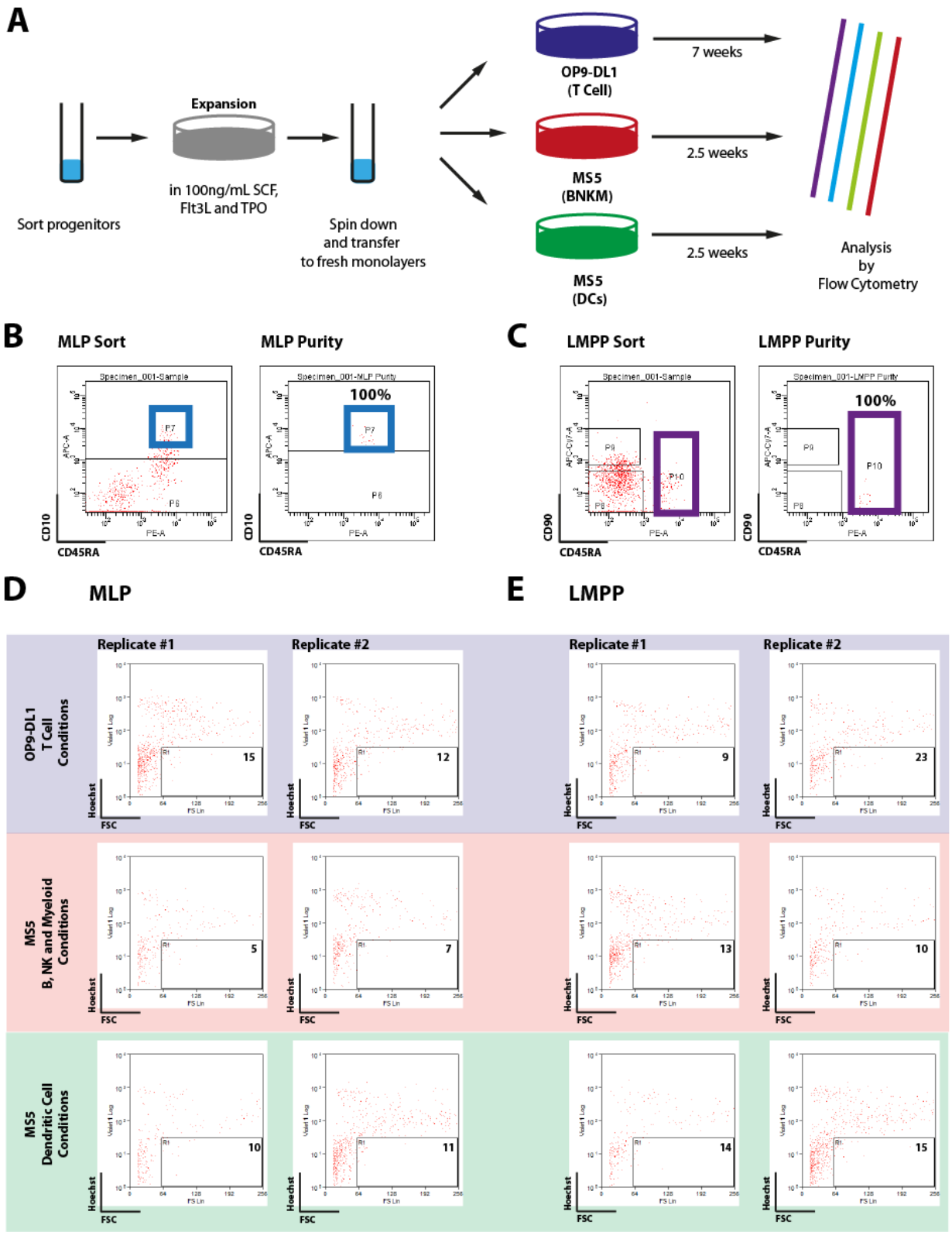

Figure 4.12. In Vitro Functional Assay To Detect Multiple Potentials In Parallel.
A) Shows the experimental set up of this assay. HSPCs are sorted by FACS (in bulk or as single cells) onto MS5 cells in 100ng/mL SCF, FLT3L and TPO and expanded for one week. After this, wells are dissociated and divided into three equal parts. Every fraction is transferred to a fresh monolayer in different conditions. OP9-DL1 cells in the "Six et al Conditions" to derive T Cells, MS5 cells in "Our Condition" to differentiate HSPCs into B, NK and myeloid cells and "Galy et al Condition" to derive dendritic cells.

After the designated culture periods (7 weeks for OP9-DL1, 2.5 for MS5 cells) the wells are harvested and subjected to flow cytometry for analysis. Only wells with more than 30 live hCD45+ cells were considered as successfully expanded.
B) Sort and purity plots of a single cell MLP sort into the expansion conditions on MS5 stromal cells.
C) Sort and purity analysis plots of a single cell LMPP sort into expansion conditions on MS5 stromal cells.
D) Results of the FACS analysis of two representative replicates of single MLPs cultured on OP9-DL1 cells (top row), MS5 cells in BMNK conditions (middle row) and MS5 cells in DC conditions (bottom row). Numbers refer to the amount of events in the live cell gate.
E) Results of the analysis by flow cytometry of two representative single LMPPs cultured in T cell conditions on OP9-DL1 cells (top row), BMNK conditions on MS5 cells (middle row) and DC conditions on MS5 cells (bottom row). Numbers refer to the amount of events in the live cell gate.
HSPC, haematopoietic stem and progenitor cell; MLP, multilymphoid progenitor; LMPP, lymphoid-primed multipotent progenitor; SCF, stem cell factor; Flt3L, fms-like tyrosine kinase 3 ligand; TPO, thrombopoeitin; BNKM, B cell, NK cell myeloid cell; DC, dendritic cell; OP9-DL1, osteopetrosis-9-delta ligand 1; MS5, murine stromal-5; FSC, forward scatter.

events could be detected, however, in order to score a well as positive, a threshold of 30 hCD45+ cells was set, which was never crossed.

The middle row summarises the results of MLPs cultured in “Our Condition” to derive B cells, NK cells and myeloid cells. No live cells could be detected after 2.5 weeks in culture (middle row). Also, the bottom row which illustrates the outcome of MLPs plated in Galy et al cultures to differentiate DCs, failed. Figure 4.12 E summarises similarly unsuccessful results of LMPPs cultured post-expansion in the “Six et al Condition”, “Our Condition” or “Galy et al” condition.

4.5 Methylcellulose Colony Forming Assays

Methylcellulose (MeC) is a semi solid culture medium that allows HSPCs to form colonies in culture, which can be identified according to their morphology. After a relatively short culture period of 14 days, fully formed colonies can be detected and counted. Subsequently, single colonies can be picked, centrifuged onto a glass slide and stained with a haematological stain, such as May Grunwald Giemsa or Wright's Stain.

MeC assays have been used previously in our group for assessing myeloid colony formation of BM HSPCs. However, the procedure for CB cells remained to be optimised. MeC of the brand Methocult© H4435 Enriched was selected, since it promotes balanced expansion of erythroid (E), granulocytic (G), monocytic (M), mixed GM and mixed GEM colonies. The supplier's manual recommends up 10^4 cells per plate (1.1mL of MeC).

A simple sort of CB CD34+ progenitors (all purity >95%) showed that 150 cells plated per 1.1mL of MeC generated just under 100 colonies, which could clearly be distinguished from each other. Figure 4.13 B demonstrates that the cloning efficiency of CD34+, CD34+CD38- and CD34+CD38+ lies between 55-60%, and that all three populations are able give rise to all types of erythroid, myeloid and mixed colonies. Also, typical for cells isolated from CB, erythroid potential is the most prominent. To assay also a more GM-primed population[80], CD34+CD45RA+CD19- cells were included. It was shown that they have a lower cloning efficiency (around 15%) than the more immature CD34+ populations and have only negligible erythroid potential.

MeC culture conditions were finally validated by culturing sorted HSPCs from CB in Methocult© H4435 Enriched for 14 days. Figure 2.7 summarises the results, as shown before. 150 cells from HSC, MPP, LMPP, CMP, GMP and MEP could be expanded. HSC and MPP have similarly high cloning efficiencies (~45%) and could give rise to all types of colonies, and both showed prominent erythroid output. The CMP had the highest cloning efficiency of all investigated populations (60%) and 3 out of 4 colonies generated by CMPs was scored as erythroid. The MEP mainly gave rise to erythroid colonies to (90% of colonies generated were red) and its cloning efficiency was around 40%. The LMPP did not produce any erythroid colonies, and showed cloning efficiencies around 30%, as expected. A single erythroid colony was detected in one of two technical replicates initiated with the GMP. It had a cloning efficiency of around 30% and gave rise to G, M and mixed GM colonies.

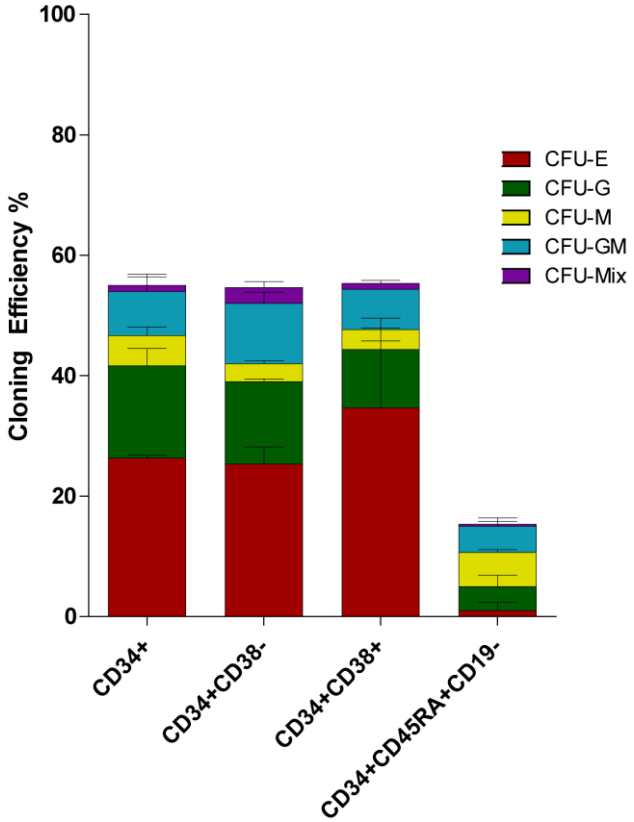

Figure 4.13. Initial Testing of Colony-Forming Assays
150 cells per sorted population from cord blood were plated in 1.1mL MeC. Colonies were scored and enumerated after 14 days. Bars represent mean plus standard deviation of 2 technical replicates.

4.6 Discussion:

An essential requirement in order to characterise HSPCs is the optimisation of isolation and purification procedures. Bearing in mind that the questions we are asking address human normal biology, there are only very limited resources of normal tissues available for research. In consequence, every normal tissue sample is precious and has to be treated accordingly. Efficiency of isolation, purification and in vitro assays is of vital importance. LMPPs, one of the populations of interest in this thesis, constitute only 1% of Lin-CD34+ cells in adult normal BM, and therefore every cell which can be extracted and assessed from a tissue donation counts.

The first step to a purified stem or progenitor population is successful isolation from the CB or BM sample. Typically, samples are subjected to density centrifugation first which enables purification of mononuclear cells (MNCs) e.g. in Ficoll. The MNC fraction not only contains CD34+ stem and progenitor cells, but also CD34- mature cells and precursors. In order to reduce flow sorting time, CD34+ cells are enriched by magnetic selection. We settled for the Miltenyi MACS CD34 microbead kit, because it extracted the most CD34+ cells and to the highest purity as compared to kits from two competitors. These were not the only advantages; processing time, which is crucial for cell viability, was shortest with this kit. Furthermore, the paratope of the CD34-recognising antibody binds to a class II epitope of CD34 on the cell surface, which is present on all CD34 glycoforms, which means that CD34 can be detected regardless of the glycosylation state. Class II epitopes can only be cleaved by glycoprotease, which

favours stability[81]. Moreover, the Miltenyi procedure also includes a F_c receptor blocking step, which can greatly reduce unspecific and background binding. Also, the microbead which is bound to the CD34+ cells of interest does not require an additional detachment step, due to its size (only 50nm in diameter).

Prior to sorting we introduced an overnight culture step to allow the cells to recover from the MNC and CD34+ isolation procedure. CD34+ cells are maintained at high concentrations of SCF, Flt3L and TPO (100ng/mL each) in StemSpan media at 37°C. This enables the cells to recover from the thawing and CD34+ isolation procedure, before exposing them to the cell sorting procedure, which also subjects the cells to great amounts of stress.

The populations of interest are then purified by FACS and subjected to in vitro functional assays.

In vitro differentiation of HSPCs has been extensively used to assess lineage potentials of distinct immunophenotypic populations of HSPCs. However, in vitro culture is limited by several factors.

It is still debated whether cytokines can instruct lineage fate decisions. The prevailing view in the field was that differentiation of HSCs occurred due to stochastic events, as first proposed by Till et al[28]. For example, noise in the transcriptome, as described by Chang et al[82], would prompt cells to gradually change from the average state and initiate lineage priming. Growth factors seemed important to permit the survival and proliferation of the already committed cells[83]. Recent work on the single cell level showed that certain cytokines are indeed able to instruct lineage fate[84,85] through imaging approaches. These factors have to be considered if stromal co-cultures are used as in vitro assays.

Addition of exogenous cytokines to the culture medium, as well as production and secretion of growth factors by the stromal cells will influence HSPCs in their decision to undergo differentiation into a particular cell type. Since it is impossible to perform a physiological in vivo experiment with human cells, we can only focus on interrogating the *differentiation potentials* of human stem and progenitor cells. We chose to provide an environment supporting multi-lineage differentiation in our assays to read out as many in vitro differentiation potentials as possible.

In MS5 cultures, the culture medium was supplemented with a variety of cytokines (See Table 2.8) to permit the generation of monocytes, granulocytes, B cells and NK cells in parallel from HSPCs[63,73,74]. Further additives to the culture medium which promote B cell differentiation were Dup697, which is a cyclooxygenase inhibitor[86] and all-*trans* retinoic acid (ATRA)[87]. ATRA has to be used with care however, because it is able to push myeloid progenitors towards differentiation, and mature granulocytes undergo apoptosis after a short time. This effect is also seen in culture of human acute promyelocytic leukaemia (APL) cells[88] and ATRA has been used to treat APL[89]. However, this might cause failure to detect granulocytes in culture and has to be considered when optimising culture periods.
Differentiation of T cells requires Notch signalling and IL-7[90]. Therefore, HSPCs are cultured on a monolayer of OP9 cells expressing DL1, which is a Notch ligand implicated in T lymphopoiesis, in medium supplemented with hIL-7. Cytokines, serum and media composition as well as correct maintenance of the stromal cells have prominent effects on the generation of double positive (DP) T cells (CD4+CD8a+). OP9 cells are characterised by a homozygous mutation in the gene encoding Macrophage-Colony Stimulating Factor (M-CSF). This cell line was used to support differentiation of embryonic stem (ES) cells in vitro without the

exogenous addition of cytokines[91]. Zúñiga-Pflücker and colleagues transduced OP9 with DL1 and DL4 to successfully derive functional T cells in vitro from immature murine[76] and human[65] cells. Substantial work has gone into clarifying which delta-like ligands are indispensable for T cell development. Research suggests that in vitro and in vivo requirements might not be the same.

The interplay between Notch and delta-like ligands orchestrates T lymphopoiesis. Mice with a cre-loxP mediated deletion of Notch-1 show absence of T cells and elevated numbers of B cells in the thymus, for example[92]. Interestingly, cre-loxP deletion of DL1 in mice does not result in ablation of T cells. DL4, which belongs to the same family of Notch ligands, seemingly compensates for DL1 and T cell differentiation is not affected[93]. This suggests that DL4 might be the physiological Notch ligand of choice to initiate T lymphopoiesis. Additional evidence comes from a study in which DL4 was specifically deleted in thymic epithelial cells, which resulted in absence of T cells in the thymus[94]. We validated both DL1 and DL4 expressing cell lines and in vitro in our hands, DL1 provides the best stimulus for T cell differentiation of human HSPCs.

Interestingly, the OP9-DL1 cell line used in this study, expresses the murine DL1. Experiments on MS5 cells with exogenously supplied human Dll1 were not successful (data not shown) however we did not pinpoint the exact reason for this. The missing cell-cell contact could be a possible explanation. HSPCs need an array of different signals to survive, proliferate and differentiate, which are not only supplied in the form of soluble factors, hormones or external stimuli, but also by direct cell to cell contact[77].

In the normal BM microenvironment, HSPCs reside in contact with the stroma, which can provide the clues for survival, proliferation or differentiation.

Furthermore, the microenvironment in different organs supports different cell fates, for example Dll4 expression in thymic epithelial cells promotes T cell differentiation[94]. This is one of the reasons why stromal cells are indispensable for in vitro differentiation assays.

Another caveat in this study is the missing dendritic cell data. Dendritic cells (DCs) are antigen presenting cells[95], can produce interferon and can be derived via lymphoid and myeloid differentiation pathways[96]. More research is needed in order to characterise them to a greater extent in the human system. Approaches to differentiate HSPCs from CB or BM into DCs were not fruitful in my hands, Figure 4.11. Low cloning efficiencies and difficulties to find specific markers for analysis post-culture hampered my progress. Future efforts will be concentrated on finding an in vitro assay permissive for DC development.

Another point I would like to address is the optimisation of assays to read out co-potentials in parallel. B, Myeloid and NK cells can be derived in culture with relative ease on monolayers of MS5 cells. However, reading out B, T, myeloid, NK and dendritic cell potential from a single cell in vitro proved very difficult indeed. An approach developed for this study had been tested to assess as many differentiation potentials from a single cell as possible. On the population level, I succeeded in expanding LMPPs and other progenitor cells on MS5 cells for one week. Subsequently, the culture was dissociated and the progeny transferred to fresh layers of MS5 or OP9-DL1 cells, to initiate differentiation into B cells, T cells, NK cells, granulocytes and monocytes. However, I was not able to reproduce this on the single cell level, as it can be seen in Figure 4.12. It is unclear where the problem with this assay system lies. One possible problem is the nature of the

cells to be assessed. Progenitors differentiate rapidly and therefore lose differentiation potential very quickly. Expansion of progenitors in culture is very difficult while maintaining their differentiation capacity, as they do not self-renew. Through the disruption of the culture after the brief expansion culture, the cells are subjected to additional stress which might harm them through mechanical stress or induction of apoptosis.

Table 4.1 summarises all conditions of lineage differentiation cultures evaluated in this study.

I am aware of the need of an assay to read out multipotential progenitors on a clonal level in vitro; future efforts will focus on this requirement.

Combining pre-enrichment of CD34+ cells with multi-parametric flow cytometry enabled me to highly purify stem and progenitor populations from human CB and BM. Paired with an array of in vitro cultures we can address questions concerning the differentiation potential of stem and progenitor populations. Furthermore, we can perform limit dilution assays, which not only provide us with clonal readouts of single cells but also result in a frequency of cells with a certain potential within a population defined by immunophenotyping.

Name	Culture Method	Output	Stromal Cells	Cytokines	Culture Period	Markers used for lineage evaluation (Flow cytometry)	Successful?
OUR Condition 1	co-culture	B, Gran, Mono, NK	MS5	20ng/mL SCF, 10ng/mL FL3TL, IL-15, G-CSF, 10^{-7}M Dup697	2-5 weeks	CD19 (B), CD14 (Mono), CD15 (Gran), CD56 (NK)	yes
OUR Condition 2	co-culture	B, Gran, Mono, NK	MS5	20ng/mL SCF, 10ng/mL FL3TL, IL-15, IL-2 G-CSF, 10^{-7} M Dup697, ATRA	2-5 weeks	CD19 (B), CD14 (Mono), CD15 (Gran), CD56 (NK)	yes
JED1 (John E. Dick 1)	co-culture	B, Gran, Mono, NK	MS5	100ng/mL SCF, 50ng/ml TPO, 20ng/mL GM-CSF, G-CSF, IL-7, IL-2, M-CSF	4 weeks	CD19 (B), CD14 (Mono), CD15 (Gran), CD56 (NK)	yes
JED2 (John E. Dick 2)	co-culture	B, Gran, Mono, NK	MS5	100ng/mL SCF, 50ng/mL TPO, 20ng/mL IL-7, 10ng/mL IL-2	4 weeks	CD19 (B), CD14 (Mono), CD15 (Gran), CD56 (NK)	yes
Granulocyte 1	co-culture	Gran: neutrophil	MS5	50ng/mL G-CSF	3 weeks	CD45, CD15, CD11b	no
Granulocyte 2	co-culture	B, Mono, NK, Gran: neutrophil, basophil, eosinophil	MS5	50ng/ml GM-CSF, 20ng/mL IL-3, IL-5, TPO, SCF, 4U/mL EPO	3-5 weeks	CD19 (B), CD14 (Mono), CD15 (Gran/neutro), CCR3 (eo), FcERI (Baso) CD56 (NK)	yes
MS5-DL1 1	co-culture	T cells	MS5-DL1	50ng/mL SCF, 5ng/mL Flt3L, 5ng/mL IL-7 and 150mM β-Insulin	5-7 weeks	CD1a, CD7, CD4, CD8a, CD3 (all T cell markers)	no
5ng Condition	co-culture	T cells	OP9-DL1 or OP9-DL4	5ng/mL IL-7, Flt3L	7 weeks	CD1a, CD7, CD4, CD8a, CD3 (all T cell markers)	yes
1ng Condition	co-culture	T cells	OP9-DL1 or OP9-DL4	1ng/mL IL-7, Flt3L	7 weeks	CD1a, CD7, CD4, CD8a, CD3 (all T cell markers)	yes

Six et al Condition	co-culture	T cells	OP9-DL1	10ng/mL SCF, 5ng/mL IL-7, Flt3L	7-8 weeks	CD1a, CD7, CD4, CD8a, CD3 (all T cell markers)	yes
T/Mye 1	co-culture	T cells, myeloid cells	MS5+MS5-DL1 (1:1)	50ng/mL SCF, GM-CSF, 5ng/mL IL-7, Flt3L	5-7 weeks	CD14, CD15, CD1a, CD7, CD4, CD8a	no
T/Mye 2	co-culture	T cells, myeloid cells	OP9+OP9-DL1 (1:1) or OP9+OP9-DL4 (1:1)	50ng/mL SCF, GM-CSF, 5ng/mL IL-7, Flt3L	5-7 weeks	CD14, CD15, CD1a, CD7, CD4, CD8a	no
T/Mye 3	co-culture	T cells, myeloid cells	OP9+OP9-DL1 (1:3) or OP9+OP9-DL4 (1:3)	50ng/mL SCF, GM-CSF, 5ng/mL IL-7, Flt3L	5-7 weeks	CD14, CD15, CD1a, CD7, CD4, CD8a	no
T/Mye 4	co-culture	T cells, myeloid cells	MS5+OP9-DL1 (1:1) or MS5+OP9-DL4 (1:1)	50ng/mL SCF, GM-CSF, 5ng/mL IL-7, Flt3L	5-7 weeks	CD14, CD15, CD1a, CD7, CD4, CD8a	no
T/Mye 5	co-culture	T cells, myeloid cells	MS5+OP9-DL1 (1:3) or MS5+OP9-DL4 (1:3)	50ng/mL SCF, GM-CSF, 5ng/mL IL-7, Flt3L	5-7 weeks	CD14, CD15, CD1a, CD7, CD4, CD8a	no
Galy et al	co-culture	Dendritic cells	MS5	10ng/mL IL-3, IL-5, LIF	3 weeks	CD11c, CD14, CD1a, HLA-DR, CD15, CD83	no
Multipotential	pre + co-culture	T cells, B, NK, Gran, Mono	expansion on MS5, then split of culture and transfer to MS5 & OP9-Dl1	pre-culture: 100ng/mL SCF, FLt3L, 50gn/mL TPO, then Our Condition for B/Mye/NK and Six et al for T cells	1 week + 2 weeks/6 weeks	CD19 (B), CD14 (Mono), CD15 (Gran), CD56 (NK) and CD1a, CD7, CD4, CD8a, CD3 (all T cell markers)	Bulk: yes; Single cells: no

Table 4.1. Summary of All Culture Conditions Evaluated In This Study.

5 Lymphoid Primed Multipotent Progenitor Vs. Multilymphoid Progenitor

The research described in this section focuses on clarifying the relationship of two different classes of human haematopoietic progenitor cells on the phenotypic, functional and molecular level.

In recent years, work from different groups defined many different progenitor populations in human umbilical cord blood (CB) and/or bone marrow (BM). These differed in their immunophenotype and functional properties assessed in vitro and in vivo. However, little is known about how these populations are related to each other and if there is a hierarchical relationship between them. We set out to answer these questions to establish a comprehensive roadmap for human haematopoiesis.

A publication from our group first described the human CD45RA+ compartment in the Lin-CD34+CD38- fraction of human normal BM as sharing the same functional properties[19] as the lymphoid-primed multipotent progenitor (LMPP) in murine haematopoiesis[16]. This human counterpart was subsequently also referred to as LMPP. Furthermore it was found that this immunophenotypic compartment is expanded in a relevant proportion of AMLs and contains leukaemic stem cells (LSCs)[19]. The LMPP retains all lymphoid as well as granulocytic and monocytic differentiation potential; however it lacks erythroid and megakaryocytic capacity. It resides in the Lin-CD34+CD38-CD90-CD45RA+ compartment in BM and CB. About 1 in 6 cells with this surface phenotype can give rise to B and myeloid cells, 1 in 12 give rise to CD1a+CD7+ T cell committed cells. No erythroid progeny could be detected in MeC colony forming assays, nor any megakaryocytic colonies in Mega-Cult clonogenic assays[19].

Importantly, it does not express the lymphoid marker CD10. CD10 expression on progenitors has been linked to lymphoid potential previously[22,68,97].

Doulatov et al published a multilymphoid progenitor (MLP) which also resides in the CD45RA+ compartment in BM and CB and only differs from the LMPP by expressing CD10 and not being able to give rise to granulocytic cells. This MLP does not proliferate strongly in culture and has prominent lymphoid potential and only retains very little monocytic potential, fully lacking granulocytic differentiation capacity[20].

One of the questions I wanted to address in my thesis was how these two populations are related with respect to each other.

5.1 Phenotypic Analysis Of The CD45RA+ Compartment In CB

As discussed extensively in a previous chapter, flow cytometry is the first step to the purification of highly pure progenitor populations. Naturally, I started with evaluating the differences in the FACS published by Doulatov et al[20] and our group, to pinpoint why the CD45RA+ compartment is mostly CD10+ in the MLP paper.

CB was stained with the standard antibody panel from our group, the one published by Doulatov et al[20]. A summary of these FACS panels detailing the fluorochromes used can be found in Table 2.5.

The aim of this experiment was to reproduce the staining patterns seen in Doulatov et al, and compare how they relate to the patterns in our FACS panel. Furthermore, expression of CD7 had not yet been defined in my hands before.

Figure 5.1 illustrates the profiles acquired with the 2 different panels. The gating strategy is very similar in its approach to the gating strategy in Figure 3.1. In the first panels of each example, live, single and lineage negative cells are obtained and then plotted relative to their expression of the markers CD34 and CD38. The immature, CD38- cells are taken into the next plot and investigated for the expression of CD45RA and CD90. The LMPP and MLP both reside in the CD45RA+ compartment which is taken into the fifth plot, which shows CD7 and CD10 expression on CD45RA+ cells.

The most striking fact about this figure that we could never reproduce the finding in Doulatov et al which shows that the entire CD45RA+ fraction is CD10+ as well. The second part of this figure compares the Doulatov et al staining to the staining used in this study. In the Expanded MLP Panel (see Table 2.5), there is a dead cell, doublet and lineage exclusion step. Separation was better on CD34-PerCP in this panel, as was CD90 resolution. On the other hand, using CD38-PeCy7, as in the Doulatov et al Panel, provides strong resolution on CD38.

However, CD7 expression was very variable in both panels. As published[20], CD7 did not contribute to separating the MLP from any other functionally different population, therefore it was omitted in subsequent experiments.

The Doulatov et al[20] panel proved very unsuccessful in general, for example CD90-Qdot605 (a biotin streptavidin system) did not exhibit convincing fluorescence above background level. Furthermore, the published protocol does not include a lineage exclusion step in the FACS procedure, which might permit mature and/or committed cells to contaminate the stem and progenitor populations. From this point forward, it was chosen to slightly modify the panel we

had in our use previously (omit CD7, and substitute CD38 Alexa Fluor 700 with CD38 FITC) to conduct the remainder of this study.

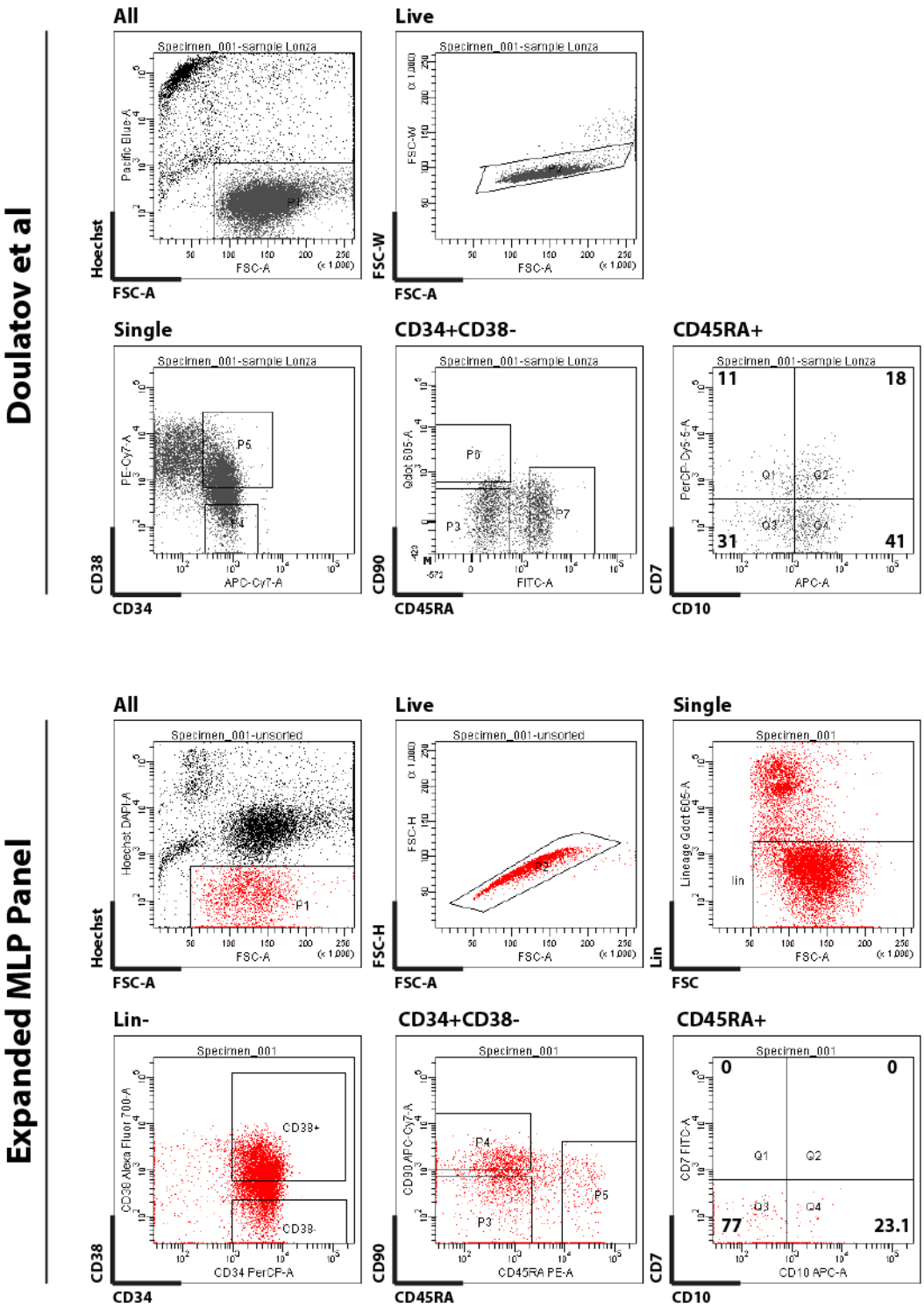

Figure 5.1. Summary Of CD10 And CD7 Expression Analysis In Human Cord Blood And Evaluation Of Optimum Staining Panel.
In the top row, the antibody staining panel (Panel B) used in Doulatov et al[20] as applied to minimise variation due to differences in antibody-clone or fluorochrome. Shown is one representative example of three experiments. The bottom row depicts human CB analysed with the Expanded MLP panel used in our lab. N=3.

To illustrate the phenotypic characteristics of the CD45RA+ compartment of human CB, 5 representative examples of CB samples stained with mABs and analysed on a flow cytometer can be found in Figure 5.2. A details how live, single, Lin-CD34+CD38-CD90-CD45RA+ cells are selected and can be further split on their basis of CD10 expression into LMPP (CD10-) and MLP (CD10+). B presents 5 representative CB samples.

Overall the profiles look relatively similar. Slight variations can be attributed to the nature of biological specimens from different individuals. The aim of these immunophenotyping experiments was to show that in the human CB CD45RA+ compartment, a CD10- LMPP and a CD10+MLP can be consistently detected. The LMPP accounts for about 70-80% of the CD45RA+ compartment and the MLP for 30-20%. Both populations could be sorted to high purities.

A summary of 10 independent LMPP/MLP sorts can be found in Figure 5.3. Dead cells, doublets and lineage positive cells are excluded from the analysis in the first 3 panels. The CD34+CD38- immature cells are separated from any CD10+ and the MLP is isolated. The CD10- negative remaining cells are further analysed for CD45RA and CD90 expression. The CD45RA+CD90-CD10- LMPP can thus be separated.

Figure 5.3 B provides a summary of the proportion of all isolated populations as percentage of the Lin-CD34+ fraction. The values are averages from 10 independent experiments. In Figure 5.3 C, a representative example of one such progenitor sort can be found, with the average percentages of HSPC populations (as percentage of Lin-CD34+) added to the gates. These experiments provided the basis on which we could move forward and assess the functional potential of LMPPs and MLPs in greater detail.

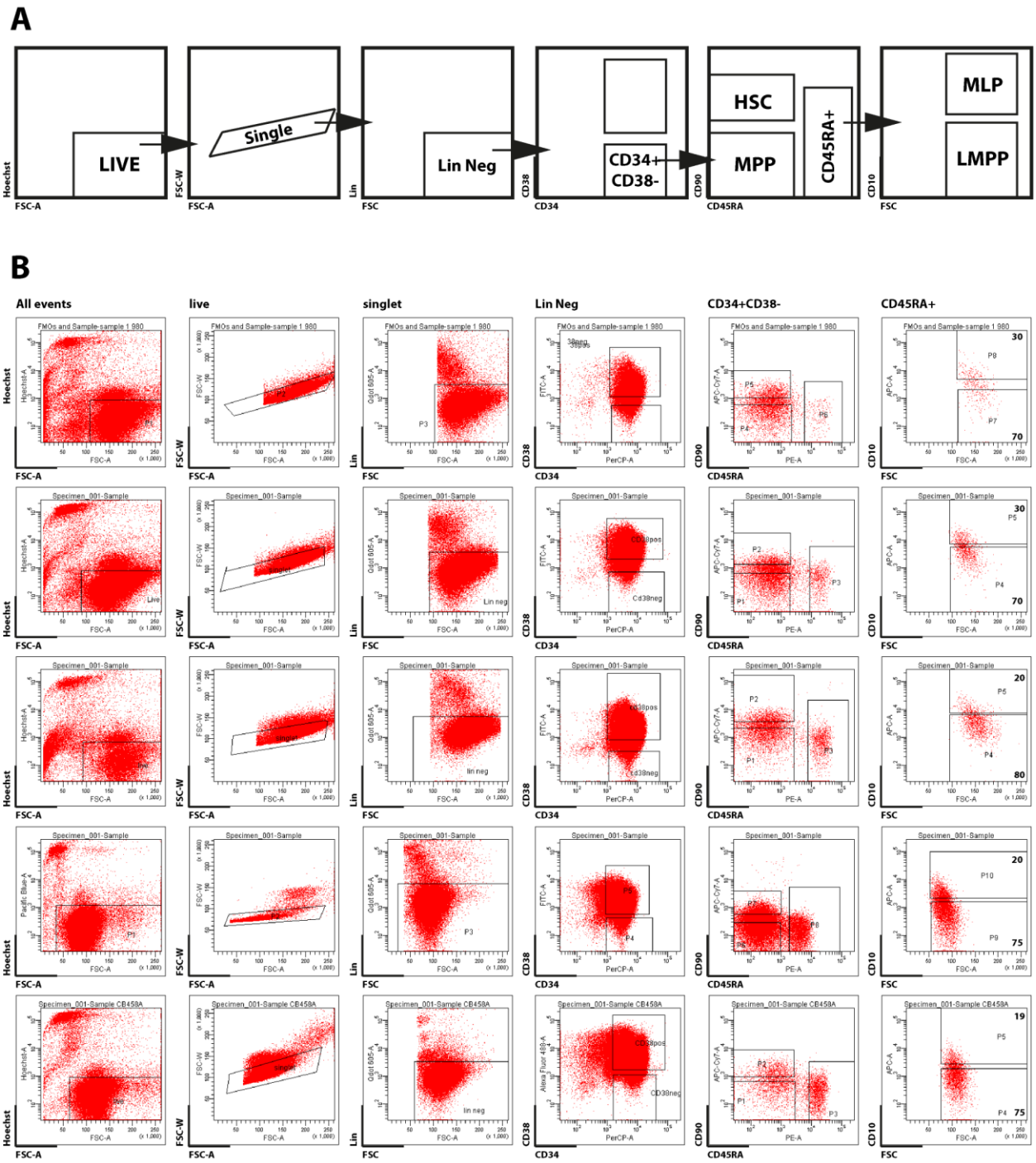

Figure 5.2. Phenotypic Analysis of 5 Individual Cord Blood Samples By Flow Cytometry To Separate The CD10- LMPP from the CD10+ MLP.

Different cord blood samples were stained with a set of monoclonal antibodies to separate haematopoietic stem and progenitor populations.

5 examples are shown here. In all cases, cells were first gated for live, single and lineage negative cells and further divided with respect to CD38 expression. CD34+CD38- stem and progenitor cells can be further separated according to their CD45RA and CD90 expression. HSCs are CD45RA-CD90+ and MPPs are CD45RA-CD90-. The CD45RA+ compartment, which contains the LMPP, can then be plotted with respect to its CD10 expression. In all cases, a CD10- LMPP and a CD10+ MLP could be detected. Numbers in the gates indicate the % of the LMPP or MLP from the CD45RA+ compartment.

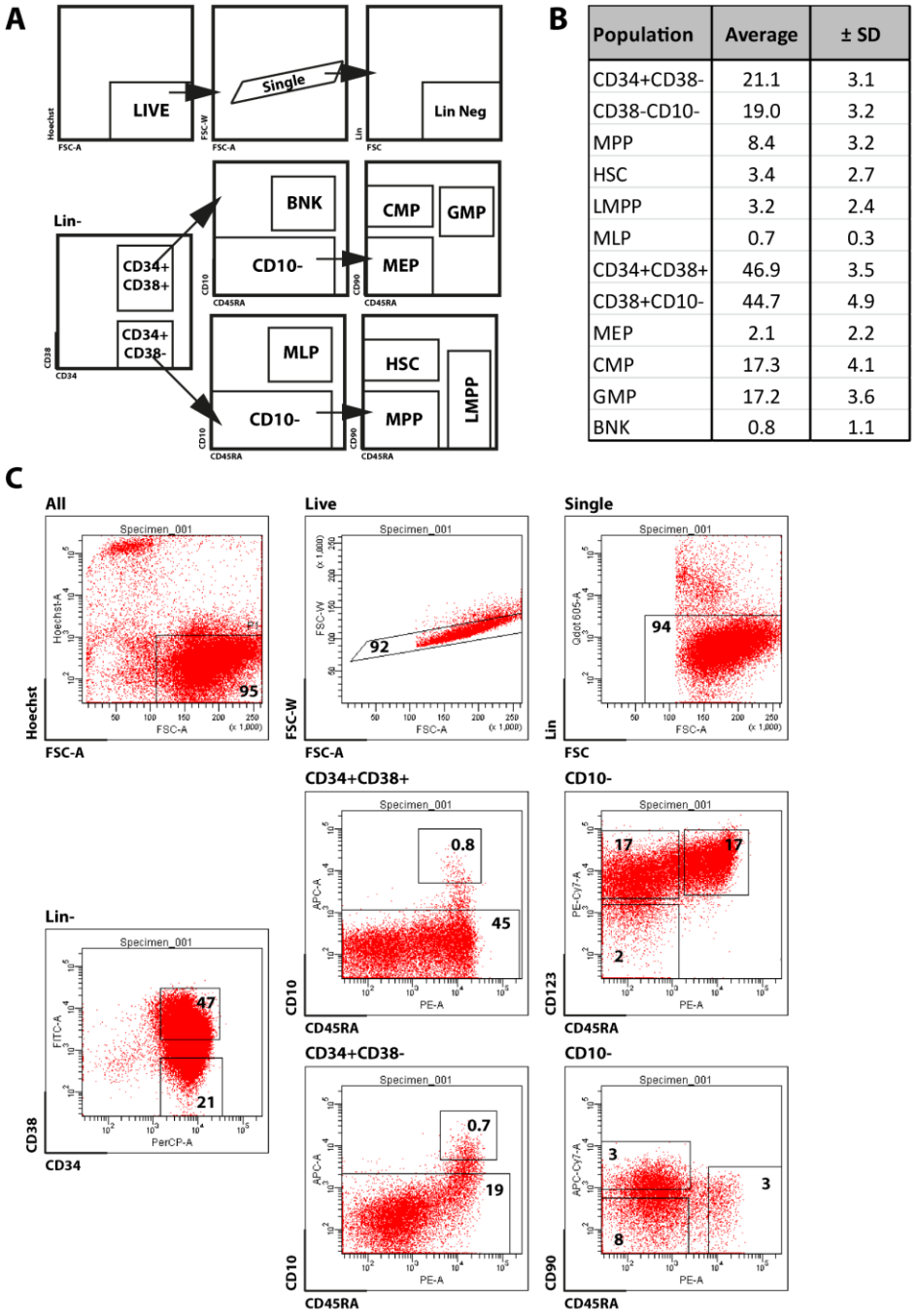

Population	Average	± SD
CD34+CD38-	21.1	3.1
CD38-CD10-	19.0	3.2
MPP	8.4	3.2
HSC	3.4	2.7
LMPP	3.2	2.4
MLP	0.7	0.3
CD34+CD38+	46.9	3.5
CD38+CD10-	44.7	4.9
MEP	2.1	2.2
CMP	17.3	4.1
GMP	17.2	3.6
BNK	0.8	1.1

Figure 5.3. LMPP and MLP Gating Strategy and Immunophenotyping.
A) The gating strategy to isolate and sort the LMPP and MLP is illustrated here. LIve, single, lineage negative cells are analysed for CD34 and CD38 expression. CD34+CD38- cells are further analysed for CD45RA and CD10 expression. The CD45RA+CD10+ MLP can be excluded. CD10- cells are then separated with respect to CD45RA and CD90 expression. CD90-CD45RA+CD10- LMPPs can be identified. Furthermore, the isolation strategies for HSC, MPP, CMP, GMP, MEP and BNK are also shown in this figure.
B) summarizes the average proportion of the immunophenotypic compartments as percentage of the Lin-CD34+ fraction of CB. N=10.
C) A representative example of a LMPP-MLP sort of CB is shown. The percentages are averages (N=10) given as percentages of the Lin-CD34+ fraction. HSC, haematopoietic stem cell; MPP, multipotent progenitor; LMPP lymphoid primed multipotent progenitor; MLP, multilymphoid progenitor; CMP, common myeloid progenitor; GMP, granulocyte-monocyte progenitor; MEP, megakaryocyte-erythroid progenitor; BNK, B-NK cell progenitor; SD, standard deviation.

5.2 B Cell, NK Cell, Monocytic And Granulocytic Differentiation Potential Of LMPPs and MLPs

Due to the differences in published literature, I sought to investigate if I could determine the lineage potentials of LMPPs and MLPs in liquid culture and compare them. Furthermore, previous characterisation of the LMPP was incomplete and NK cell potential had yet to be confirmed. In addition to this, we sought to identify the nature of the myeloid progeny generated from LMPPs and verify that they belonged to both the granulocytic (gran) and monocytic (mono) lineages. The MLP had been extensively characterised in Doulatov et al, however, relating to the significantly different FACS profiles, it was decided to ascertain its functional potential in my hands.

B, NK, granulocytic and monocytic differentiation potential was evaluated on the population level at first. Importantly, every lineage follows its own kinetics. Therefore it has to be kept in mind that granulocytes undergo apoptosis after maturation, and hence might not be detectable at later time points in a culture system. Lymphoid cells generally take longer to develop than myeloid cells, so a compromise has to be found when the culture is analysed.

Figure 5.4 illustrates this compromise. Here, sorted LMPPs and MLPs were plated on MS5 stromal monolayers in media supplemented with SCF, Flt3L, G-CSF, IL-2, IL-15 and Dup697 (for detailed cytokine concentration and media composition, please refer to Table 2.8). The experimental layout is depicted in Figure 5.4 A. The progenitors were cultured for up to 3 weeks with twice weekly media changes. Every week, half of the culture medium was aspirated and subjected to FACS

analysis. Supernatants were stained with mABs directed against hCD45, and lineage specific antigens, namely CD14 (mono), CD15 (gran), CD19 (B cell) and CD56 (NK cell).

After one week, only few events (>100) could be detected and identified as progeny from LMPP or MLP (Figure 5.4 B). No lymphoid output was present in either culture at this early time point. Two weeks after initiation of the culture (see Figure 5.4 C), both LMPP and MLP had proliferated and differentiated; the number of hCD45+ cells present in the culture supernatant was much increased. The LMPP had generated granulocytes, monocytes and even lymphoid progeny was detectable at low levels. The MLP showed prominent B cell generation and residual monocytic potential. Importantly, no granulocytes could be detected at any point in time in cultures initiated with MLPs.

In Figure 5.4 D, analysis of the same experiment is shown, after 3 weeks. Most notably, the CD15+ granulocytes which were present in the LMPP culture at 2 weeks, have now disappeared. The lymphoid progeny is more prominent, and CD19+ B cells and CD56+ NK cells can be detected. Overall cell numbers detected were also increased. The MLP gave rise to high numbers of B and NK cells, and low levels of monocytic cells.

Therefore we could validate, on the population level that LMPPs retain full myeloid differentiation capacity, and the MLP lacks granulocytic potential in liquid culture.

To verify the cell surface markers we used to assess functional potentials in vitro, we cultured sorted HSCs, LMPPs, MLPs and GMPs in “Our Condition” or in “JED2 Condition” for 2.5 weeks. After the culture period, monolayers were dissociated and the resulting single cell suspensions were stained with mABs against CD45,

CD14, CD15, CD19 and CD56 and individual lineage+ progeny sorted. The sorted cells were centrifuged onto glass slides and stained with the Modified Wright's staining protocol to all lineage verification.

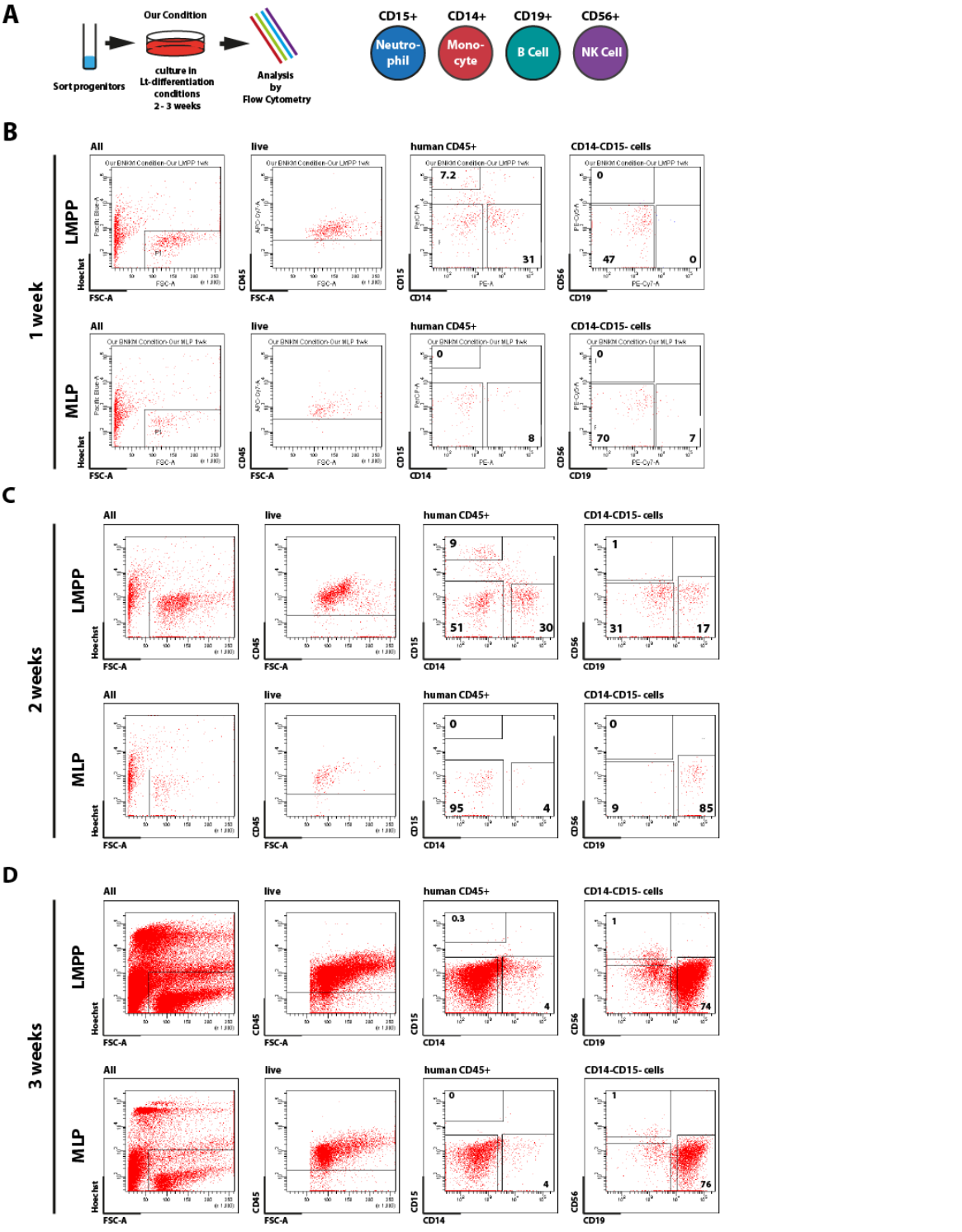

Figure 5.4. Optimum Timepoint for Analysis Evaluation In Myeloid Culture of LMPPs and MLPs On MS5 Stromal Cells.

A) Experimental outline of MS5 assays. 100 cells/well were plated on MS5 stromal monolayers in "Our Condition". At the designated time points, cultures were dissociated and analysed by FACS. The markers to identify each lineage are displayed on the right.

B) Analysis of LMPP and MLP progeny after 1 week by flow cytometry (N=1).

C) Analysis of LMPP and MLP progeny after 2 weeks by flow cytometry (N=3).

A) Analysis of LMPP and MLP progeny after 3 weeks by flow cytometry (N=1).

LMPP, lymphoid-primed multipotent progenitor; MLP, multilymphoid progenitor; NK, natural killer; lt, long-term.

Figure 5.5 A details the results from the cells differentiated in “Our Condition”. HSCs had the greatest output in culture and sufficient numbers for the cytospin could easily be sorted and imaged. The other, more committed progenitors, such as the LMPP gave rise to mainly lymphoid and monocytic cells. Even though granulocytes were detectable by flow cytometry, it was not possible to sort enough events to detect them on the slides. Granulocytes featured a typical bilobed nucleus, monocytes were easily identified due to their size and the vacuoles in their cytoplasm, B cells were small and round and NK cells were intermediate in size between the smaller B cells and the larger myeloid cells and granules could be seen in their cytoplasm.

Figure 5.5 B shows the progeny of cells cultured in the “JED2 Condition”. Due to the high concentration of SCF in this culture system, B cell differentiation was increased as compared to “Our Condition”. The GMP also gave rise to lymphoid cells, which is due to the residual lymphoid potential in this incompletely characterised progenitor. The MLP and LMPP populations only generated sufficient numbers of B and monocytes in this culture condition to be detected upon imaging. This condition is also less permissive for granulocyte differentiation, if the granulocytic output from the HSC population is compared between “Our Condition” and “JED2 Condition”. These results confirmed that the cell surface markers used for lineage evaluation in this study correlated with the morphology of these cells in culture.

Moreover, single cell limit dilution assays were performed to assess the frequencies of cells within the immunophenotypic compartments of LMPP and MLP with one or more certain differentiation potentials. LMPPs and MLPs were sorted directly into wells seeded with a MS5 stromal layer at 1, 2, 5 and 10 cells.

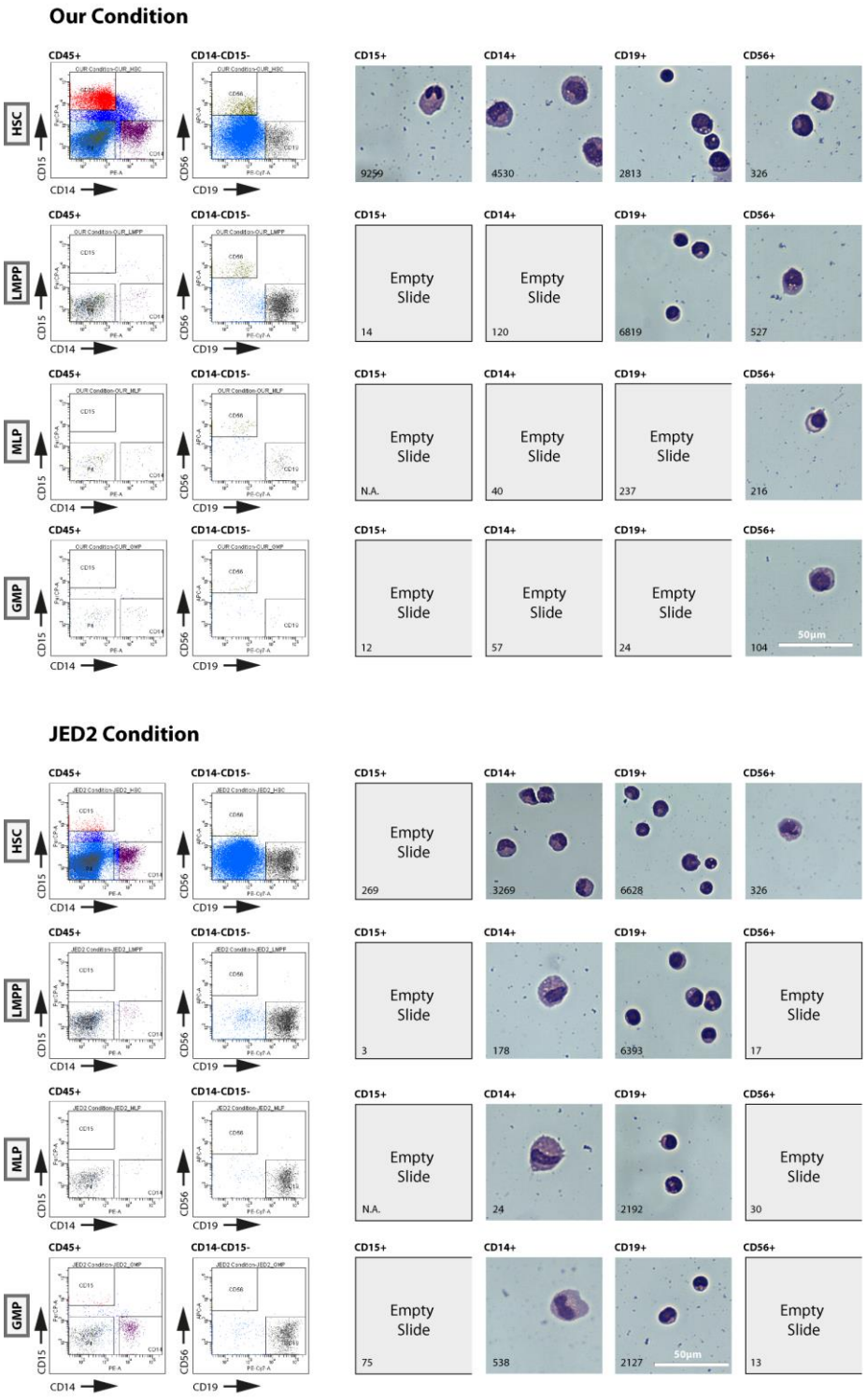

Figure 5.5. Morphology of B Cells, NK Cells, Monocytes and Granulocytes differentiated on MS5 Stromal Monolayers From Sorted HSPCs.

HSPCs were sorted and cultured in two different culture conditions. After 2.5 weeks, cultures were dissociated, stained for B cells (CD19), NK cells (CD56), monocytes (CD14) and granulocytes (CD15) and linage positive cells were sorted and centrifuged on glass slides. Subsequent Modified Wright's staining allowed for identification of progeny in culture. The number in the lower left corner of the images indicates the number of events sorted as recorded by the FACS sorter. All images were taken with the same magnification (see scale bar). HSC, haematopoietic stem cell; LMPP lymphoid-primed multipotent progenitor; MLP, multilymphoid progenitor; GMP, granulocyte-macrophage progenitor. N=1.

Cells were maintained in “Our Condition” or “JED2 Condition” for 2.5 weeks and analysed well for well on a CYAN flow cytometer. Wells were scored and frequencies derived as described in Materials and Methods.

As shown in Figure 5.6 A, the LMPP was calculated to have a frequency of 1 in 10 to 1 in 13 to give rise to B, Mono and Gran cells (N=3) whereas the MLP never gave rise to all three cell types in culture. As seen in Figure 5.6 B, the MLP showed a B cell frequency of 1 in 11, and a very low mono frequency at 1 in 117. No wells with both myeloid and B cells were detected in any well initiated with MLPs. A summary of all single and combined frequencies is shown in Table 5.1.

This data confirmed what was already suspected from the bulk data – that the LMPP is a multipotential progenitor which retains myeloid and lymphoid differentiation potential and the MLP is a mainly lymphoid committed progenitor.

5.3 T Cell Differentiation Potential Of LMPPs and MLPs

In order to contribute to a more complete characterisation of LMPP and MLP, T cell assays on OP9-DL1 stromal cells were also carried out. Previously this in vitro differentiation method was thoroughly optimised to allow CD4+CD8+ double positive T cell generation in culture, which had not yet been shown for the LMPP in vitro. Therefore, LMPPs and MLPs were isolated from human CB by FACS and plated on OP9-DL1 stromal monolayers at a concentration of 200 cells/mL.

The progenitor cells were maintained in the “5ng Condition” and “Six et al Condition” for 5 weeks with weekly stromal layer and media changes. (Please refer to the Materials and Methods for protocols and cytokine concentrations in Table 2.9). After the end of the culture period, the layers were dissociated, filtered

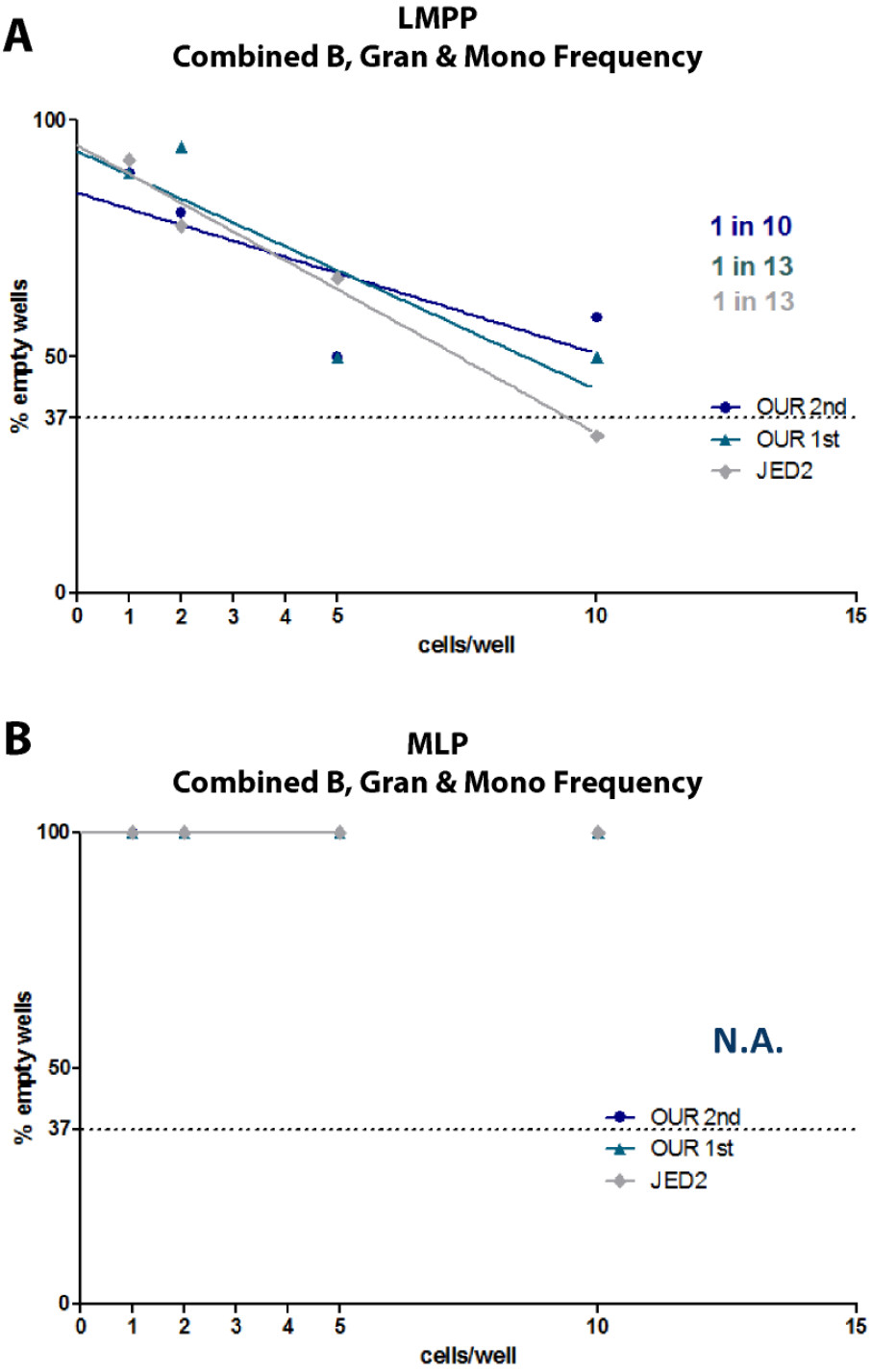

Figure 5.6. Limit Dilution Assay of CD34+ Cord Blood Cells.
A) 1, 2, 5 and 10 sorted LMPPs from CB were sorted directly onto MS5 stromal layers into "Our Condition" or "JED2 Condition" and analysed by FACS after 2.5 weeks for the expression of CD19, CD33 and CD45. Only wells containing more than 30 hCD45+ cells were scored as positive.
B) 1, 2, 5 and 10 sorted MLPs from CB were sorted directly onto MS5 stromal layers into "Our Condition" or "JED2 Condition" and analysed by FACS after 2.5 weeks for the expression of CD19, CD33 and CD45.
The graphs show the amount of cells plated per well against the proportion of empty wells. Poisson statistics were used to derive a frequency for cells in the LMPP or MLP population with combined B cell, monocytic and granulocytic potential. Three replicates per population are shown.

Frequency	LMPP	MLP
B	2	11
mono	3	117
gran	6	N.A.
B/gran	8	N.A.
B/Mono	6	N.A.
Gran/Mono	8	N.A.
Combined	10	N.A.

Table 5.1. Frequencies of LMPP and MLP In MS5-Stromal Co-Culture To Evaluate Lineage Differentiation Potentials.
1, 2, 5, or 10 LMPPs and MLPs were cultured on MS5 cells and after 2.5 weeks, all wells were dissociated and analysed for B, monocytic and granulocytic differentiation potential. Frequencies of how many cells in a specific immunophenotypic compartment gave rise to B, mono, gran or dual- or multi-lineage output. Frequencies were calculated with L-Calc. All numbers are expressed in 1 in X cells can give rise to.

through a 70µm strainer and stained with mABs directed against a range of different T Cell antibodies denoting specific T cell maturation stages. (Please see Table 2.5 for the staining panels).

Figure 5.7 A depicts the progeny of LMPPs, MLPs and GMPs cultured for 5 weeks in the “5ng Condition”. After the exclusion of CD45- murine cells from the stromal layer, all three populations had given rise to CD45+CD1a+CD7+ T cell committed cells. Furthermore, the MLP generated the highest proportion of CD4+CD8a+ T cells (10% of the CD1a+CD7+ cells), followed by LMPP (6%) and GMP(4%). As mentioned before, the relatively prominent T cell output in GMP-initiated cultures stems from the inherent lymphoid potential of this class of progenitors.

Figure 5.7 B demonstrates the results of the progeny generated in the “Six et al Condition”. Proliferation seemed to be increased slightly under this condition as compared to “5ng Condition” and cell numbers were elevated. Confirming what was seen in the “5ng Condition”, all three progenitors gave rise to fully differentiated T Cell progeny (CD4+CD8a+), constituting 13% of CD1a+CD&+ for LMPPs, 16% for MLPs and 8% for GMPs.

These experiments proved that both the LMPP and the MLP can give rise to double positive T cells in vitro. Hereby we also complemented the findings in Goardon et al, by showing that also in human umbilical cord blood, an LMPP-like population resides in the CD45RA+ compartment which retains all lymphoid differentiation potentials, as well as granulocytic and monocytic potential, but has lost megakaryocytic/erythroid differentiation capacity.

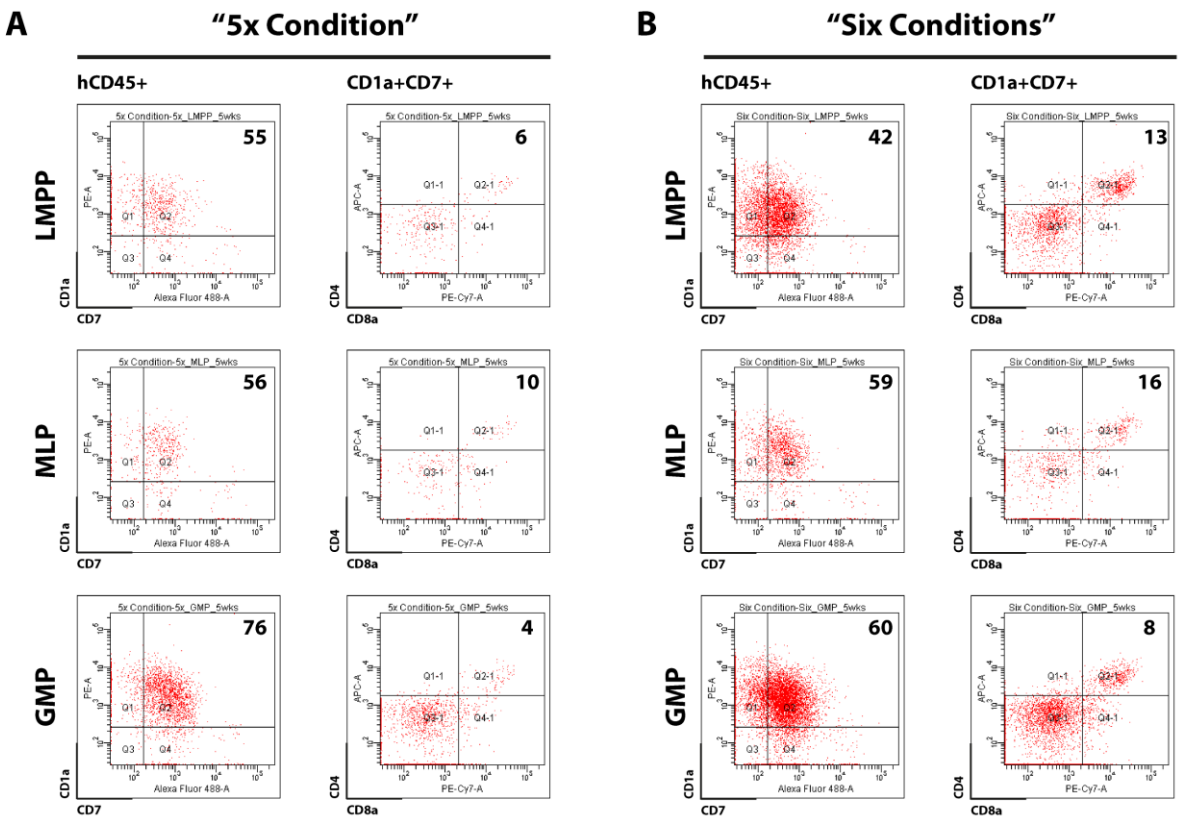

Figure 5.7.T Lymphoid Potential of LMPPs and MLPs.
100 LMPPs, MLPs or GMPs were cultured on OP9-DL1 cells for 5 weeks with weekly stromal monolayer changes. In the 5x condition, the medium was supplemented with 5ng/µL IL-7 and Flt3L. The "Six Condition" was taken from a paper by Emanuelle Six et al[66]; medium was supplemented with 10ng/µL SCF, 5ng/µLIL-7 and Flt3L. After 5 weeks, stromal monolayers were dissociated and filtered through a 70µm strainer, stained with monoclonal antibodies and analysed by flow cytometry. N=3.

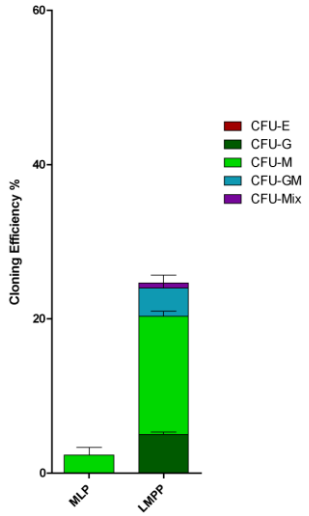

Figure 5.8. Cloning Efficiency Of LMPP And MLP Cultured In Methylcellulose For 14 Days.
150 sorted progenitors were cultured per plate in 1.1mL methylcellulose supplemented with cytokines (see Materials and Methods) in duplicate for 14 days. Colonies were scored and the cloning efficiency calculated. Bars represent mean plus standard deviation of two technical replicates.

5.4 Clonogenic Colony Forming Assays Of LMPPs And MLPs From Cord Blood

In order to investigate myeloid and erythroid colony forming potential of LMPPs and MLPs in more detail, MeC assays were performed. 150 cells were plated in 1.1mL (equals one 35mm dish). After 14 days, colonies were scored and counted and the cloning efficiency was calculated. Figure 5.8 shows the cloning efficiency and the nature of the colonies detected from sorted LMPPs and MLPs plated in MeC.

The MLP exclusively gave rise to CFU-M, and its cloning efficiency was only 3%. The LMPP could give rise to CFU-G, CFU-M and CFU-GM, with a cloning efficiency of 26%. Also, in a single sample, one individual mixed colony was detected.

This confirms that neither LMPP nor MLP have erythroid potential in cord blood and adds another proof that the MLP is lacking granulocytic potential.

5.5 Short-Term In Vitro Differentiation

5.5.1 Optimisation of Culture Conditions

Human haematopoiesis is usually depicted as a hierarchy, where arrows mimic the transition of one cell type to the next. In order to define the hierarchical relationship between the LMPP and MLP, I tried to differentiate LMPP and MLP in culture and catch the intermediate stages by FACS analysis. A similar approach was performed by Majeti et al[37] who defined the relationship between HSC, MPP and the Lin-CD34+CD38-CD90-CD45RA+ compartment in CB.

First of all, conditions permissive for the differentiation of HSPCs had to be found. Initial culture conditions were adapted from Majeti et al, however progenitors were

plated on a layer of MS5 stromal cells. Precise culture conditions can be found in Table 2.10. The experimental layout is depicted in Figure 5.9 A. Sorted stem and progenitor cells were plated on MS5 cells in triplicate, wells were harvested at designated time points and subjected to progenitor FACS analysis.

Figure 5.9 B and C show the FACS analysis plots of a first trial experiment to find the right time points and media composition. The sorting plots to initially isolate HSPCs can be seen in Figure 5.9 B. HSC, LMPP and GMP were sorted and plated in the “Majeti Condition” in StemSpan medium and analysed by flow cytometry after 1 (not shown), 2 and 4 days in culture, which is displayed in C. Live, human cells (hCD45+) cells were considered for analysis and investigated for the expression of CD34, CD38, CD10 and CD45RA+. Already after two days in culture, the plated HSPCs had divided and generated more progeny. However, as clearly visible in the top row of C, CD38 expression, which is a sign of proliferation and can be detected on more mature cells, was not upregulated on the progeny of HSCs and LMPPs. Even more drastically, GMPs, which are sorted as CD38+, lost CD38 expression in culture. The CD10/CD45RA plots after two days showed that the HSC had not yet differentiated into any CD45RA+ or CD10+ progeny, whereas a minor fraction of cells generated from LMPP expressed CD10.

After 4 days, as in Figure 5.9 C, the proportion of CD38+ cells was still very low, irrespective of the starting population. Furthermore, the cells generated in culture slowly started to lose CD34 expression, which is an indication of progressing differentiation. This was more prominent in the progeny derived from GMPs, which is consistent with its relatively committed nature. The offspring of HSCs could

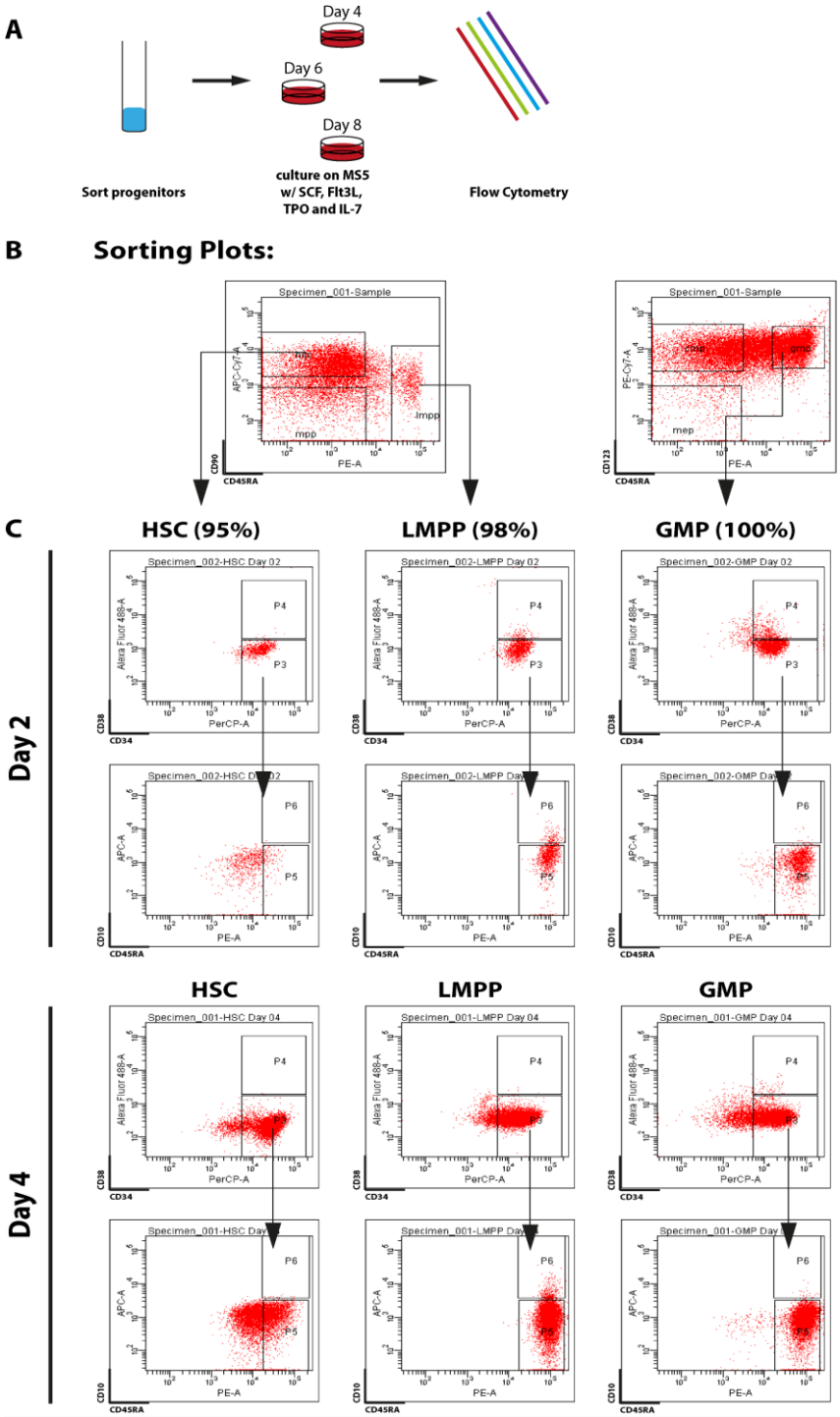

Figure 5.9. Short Term Differentiation Culture.
A) Scheme of the experimental procedure.
B) Stem and progenitor cells from cord blood were stained with monoclonal antibodies conjugated to fluorophores and sorted on a BD FACS Aria and plated on a monolayer of MS5 cells StemSpan medium supplemented with 100ng/mL SCF, 100ng/mL FLT3L, 50ng/mL TPO, 20ng/mL IL-3, 20ng/mL IL-6 and 40μg/mL LDL. C) Cultures were dissociated and analysed after 2 and 4 days by FACS. FACS analysis revealed loss of CD38 expression after 2 days in culture.
SCF, stem cell factor; IL, interleukin; MS5, murine stromal -5; TPO, thrombopoietin; FLT3L, fms-like tyrosine kinase 3 ligand; LDL, Low density lipoprotein; HSC, haematopoietic stem cell; LMPP, lymphoid-primed multipotent progenitor; GMP, granulocyte-macrophage progenitor. (N=1)

slowly be seen to upregulate CD45RA+ which suggests passing through a LMPP or GMP intermediate stage. The LMPP progeny finally started to generate CD10+ cells, as well as CD34- precursors/ mature cells.

In order to maintain expression of the crucial marker of differentiation and proliferation in culture, the composition of culture medium and cytokine concentrations were optimised. The media which yielded the most successful outcome was the standard differentiation medium used in assays on MS5 cells to derive, B, NK and myeloid cells, substituted with 10% defined FCS and supplemented with SCF, TPO, Flt3L, IL-7 and LDL. All concentrations can be found in Table 2.10.

Results of a successful differentiation experiment can be found in Figure 5.10. HSCs, LMPPs and MLPs cultured in short-term differentiation conditions were analysed after 4 and 6 days. All three populations had acquired a CD34+CD38+ fraction after 4 days; the HSC with the slowest kinetics, and the MLP with the fastest. The LMPP gave rise to 20% CD10+ immunophenotypic MLPs after 4 days in culture and this population reached its highest proportion after 6 days with 30% of all CD34+CD38-CD45RA+ cells from LMPP plated. The MLP on the other hand does not lose CD10 expression, and differentiates quickly into CD38+ and CD34-negative cells.

This experiment confirms the hypothesis that the LMPP lies upstream of the MLP in the human haematopoietic hierarchy, and that the LMPP can differentiate through an MLP intermediate.

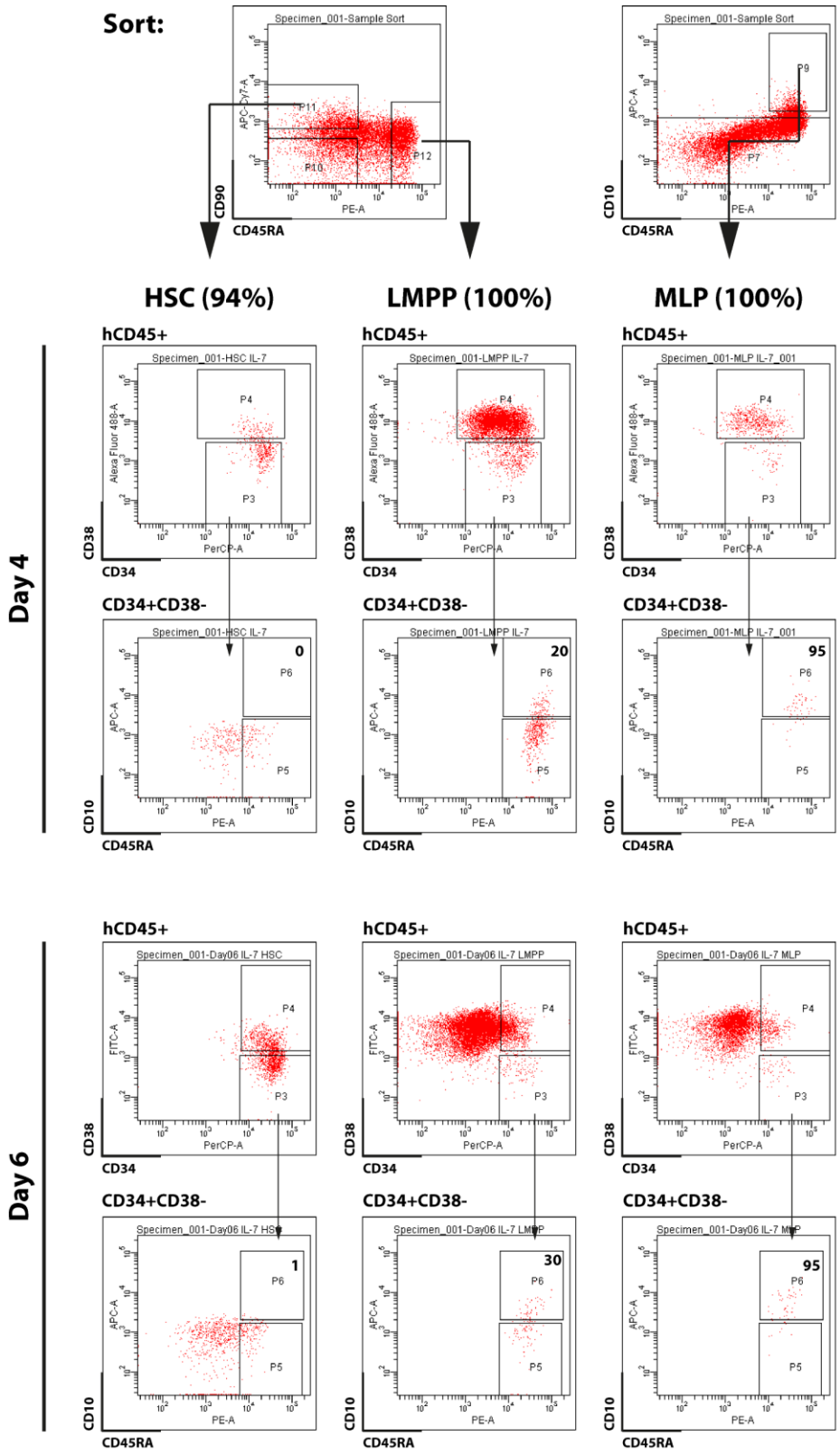

Figure 5.10. Short-Term In Vitro Differentiation of HSPCs.
Sorted stem and progenitor cells were cultured on MS5 monolayers in aMEM medium supplemented with 20% serum, 100ng/µL SCF, 100ng/µL FLT3L, 50ng/µL TPO and 20ng/µL IL-7 and 40ug/µL LDL. Wells were analysed at the designated time points and subjected to FACS analysis to monitor differentiation by loss/acquisition of cell surface markers. Events are gated on single, live and human cells. (N=1)

5.5.2 In Vitro Live Tracking – Choice Of FACS Antibodies

As to refine this in vitro differentiation approach, sought to use an in vitro live imaging set up which allows for continuous tracking of single cells in collaboration with Timm Schroeder's group[98]. This experimental set up features the culture of cells on a feeder layer. Up to 6 different fluorochromes can be tracked in parallel, in addition to phase contrast microscopy. The fluorescently labelled antibodies are directly added to the culture medium and replenished at defined intervals. Fluorochromes used for this purpose have to be particularly stable and resistant to photo-bleaching.

Tandem-dyes, such as PE-Cy7, are inapplicable due to their tendency to decay into their two components if exposed to light[99]. Also, organic fluorochromes, such as PE, can degrade over time and bleach quickly when exposed to the excitation laser beam. These limitations are less of an issue in conventional flow cytometry, since the time between staining and sorting/analysis usually does not excess 6-8 hours. Bearing these considerations in mind, it became evident that our standard staining panels would have to be adapted to allow for stable tracking of differentiation in liquid culture.

5.5.3 BD Biosciences Custom Conjugated Antibodies For In Vitro Live Tracking

One option are Alexa Fluor© conjugated antibodies which offer a widely-used alternative to traditional fluorochromes and they exhibit particular stability and

photo-bleaching resistance. BD Biosciences custom conjugated CD38, CD45RA and CD10 to Alexa Fluor dyes for this purpose. Details can be found in Table 5.2. Antibodies were titrated on normal BM MNCs, and the optimum concentration per test was evaluated. Validation had to be performed to ensure the custom conjugated antibodies marked the same populations as our “Standard Panel”. Therefore, HSPC sorts were prepared. Subsequently, sorted HSPCs were placed in liquid culture under the short-term differentiation culture conditions. CB cells were stained to compare the “Standard Panel” to the “BD Panel”.

Table 5.3 summarizes the core antibodies, clones, fluorochromes and suppliers of both the “Standard Panel” and the “BD Panel”. Figure 5.11 shows examples of different CB stains. On the left (A), the CB was stained with the “Standard Panel”. The gating was performed as described before (Figure 5.3). Clearly, a CD10+ MLP can be recognized and separated from the $CD10^{dim/-}$ LMPP. Numbers represent averages from 10 independent experiments.

In B, the cells were stained with the “BD Panel” and the same gating strategy was followed. The custom conjugated antibodies are highlighted in red (AF647), yellow (AF555) and green (AF488). After the exclusion of dead cells, doublets and lin+ progeny, the cells are analysed for the CD34 and CD38 expression. Surprisingly, CD38 AF647 (which is analysed in the APC channel on a flow cytometer) was not quite as bright as CD38 FITC in the “Standard Panel”.

Also, the separation on CD45RA AF488 was not as strong as with CD45RA PE, understandably, as PE is the brightest fluorochrome available. CD10 was conjugated to AF555, which is a substitute for PE and is analysed in the same channel on a flow cytometer. AF555 conjugation of CD10 would allow not only for

Antigen	Clone	Alexa Fluor	Concentration supplied (mg/mL)	Titrated Concentration (ng/test)
CD45RA	L481	AF488	0.25	1000
CD10	W8E7	AF555	0.25	25
CD38	HB7	AF647	0.25	25

Table 5.2. Summary Of BD Biosciences Custom Conjugated Antibodies.

Standard MLP Panel				BD Custom Conjugated AB Panel			
Antigen detected	**Clone**	**Fluorochrome**	**Supplier**	**Antigen detected**	**Clone**	**Fluorochrome**	**Supplier**
CD10	eBio CB CALLA	APC	eBioscience	CD10	W8E7	Alexa Fluor 555	BD Biosciences
CD34	581	PerCP	Biolegend	CD34	581	PerCP	Biolegend
CD38	HIT2	FITC	eBioscience	CD38	HB7	Alexa Fluor 647	BD Biosciences
CD45RA	HI100	PE	eBioscience	CD45RA	L481	Alexa Fluor 488	BD Biosciences
CD90	eBio5E10	Biotin	eBioscience	CD90	eBio5E10	Biotin	eBioscience
CD123	6H6	PE Cy7	eBioscience	CD123	6H6	PE Cy7	eBioscience

Table 5.3. Comparison Of The Standard MLP Panel And The BD Biosciences Custom Conjugated AB Panel.

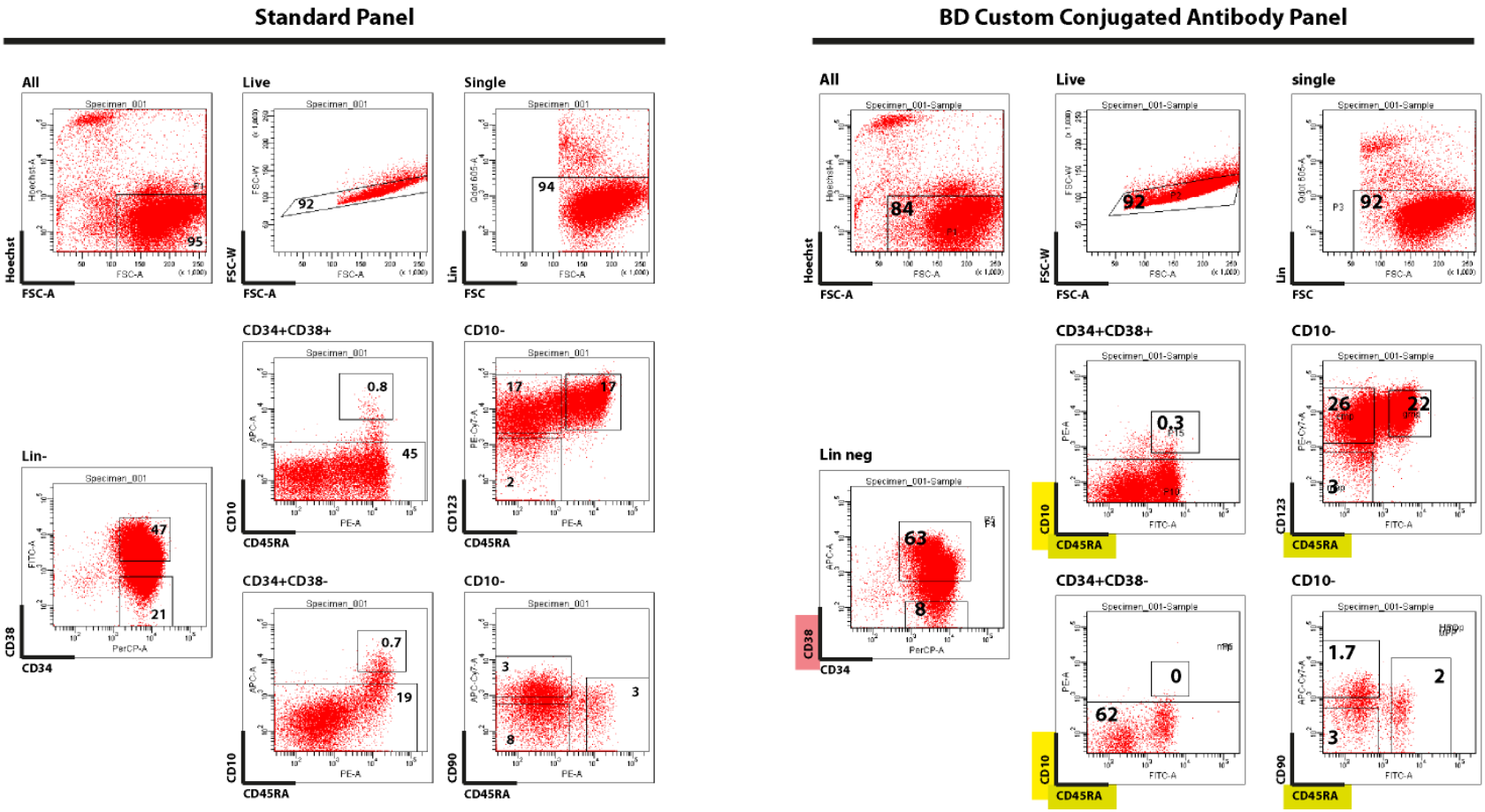

Figure 5.11. Standard Panel and BD Custom Panel Comparison.
Cord blood CD34+ enriched cells were stained with monoclonal antibodies directed against antigens known to separate human stem and progenitor cells on basis of their expression. A) depicts the standard panel used in this thesis, with a well characterized profile. Percentages shown are averages from 10 independent experiments. B) shows a staining panel substituted with Alexa Fluor 555 conjugated CD10, Alexa Fluor 647 conjugated CD38 and Alexa Fluor 488 conjugated CD45RA. (N=1)

in vitro live imaging, but also provide a higher degree of separation due to the brightness of the fluorochrome.

However, regarding the FACS plots of the CB in Figure 5.11 B, the CD10 AF555 staining showed high background levels, if compared to the “Standard Panel”. CD10+ cells were detected in the CD45RA- fraction which is something that was never observed before. Furthermore, it was increasingly difficult to place the gates for the CD10-/CD10+ fractions, as the staining does not exceed the threshold of the AF555 FMO control. The CD10 staining resembles unspecific background staining.

HSPCs were sorted to verify that these populations showed functional potential according to their immunophenotype, populations from both sorts were plated in short-term differentiation culture conditions and analysed at different time points.

LMPPs were plated at a concentration of 500 cells per mL, analysed after 6 days by flow cytometry. “Standard” and “BD Panels” were evaluated in parallel. Figure 5.12 A shows both sorting plots for the “Standard Panel” LMPP (post-sort purity: 95%) and the “BD Panel” LMPP (post-sort purity: 96%) with the sorted populations outlined in red. In B, progeny from both LMPP sorts is evaluated with the use of the standard panel.

The top row in B shows the positive control, with the “Standard Panel” used for sorting and analysis. There are three major populations in culture of LMPPs after 6 days with respect to CD34 and CD38. There is the CD34+CD38- fraction, which still contains undifferentiated LMPPs (CD45RA+CD10-) and CD10+ MLPs (37% of CD38-). Furthermore, the CD34+CD38+ populations contains CD45RA+ cells which immunophenotypically resemble the GMP and a minor proportion of CD10+,

which might be committed B/NK progenitor cells. The third fraction holds CD34- cells, which have already started to differentiate; these cells slowly start to lose CD45RA expression and a small percentage starts to upregulate CD10 expression which marks early B cell commitment. The results from the LMPP sorted with the "BD Panel" do not differ greatly from the positive control.

C focusses on the results of the analysis performed with the "BD Panel". Interestingly, from the sorted cells selected by the "Standard Panel" antibodies, the CD34+CD38- immature fraction seemed to be similar to the control, however both in the CD34+CD38+ and CD34- populations, a $CD45RA^{int}CD10+$ population could be detected (marked in blue).

The same pattern was evident in the progeny of "BD Panel" sorted LMPPs. CD10+ expression can denote early B lineage commitment, however this CD34- $CD45RA^{int}CD10+$ population did not correlate with previously seen B cell differentiation data. The same population could be found in cultures initiated with both "Standard Panel" sorted and "BD Panel" sorted GMPs which suggested that the CD10 W8E7 clone is not binding the same antigen as the clones CD10 CB CALLA (eBioscience) or CD10 HI10a (BD Biosciences), which were previously used in this study. Figure 5.13 illustrates the sorting and purity plots for the GMP and the analysis results after 6 days with both antibody panels.

These CD10+ populations were also re-sorted and plated in conditions permissive for B, myeloid and NK cells development, however, no lineage affiliated cell surface markers could be identified after 1 week in culture (data not shown).

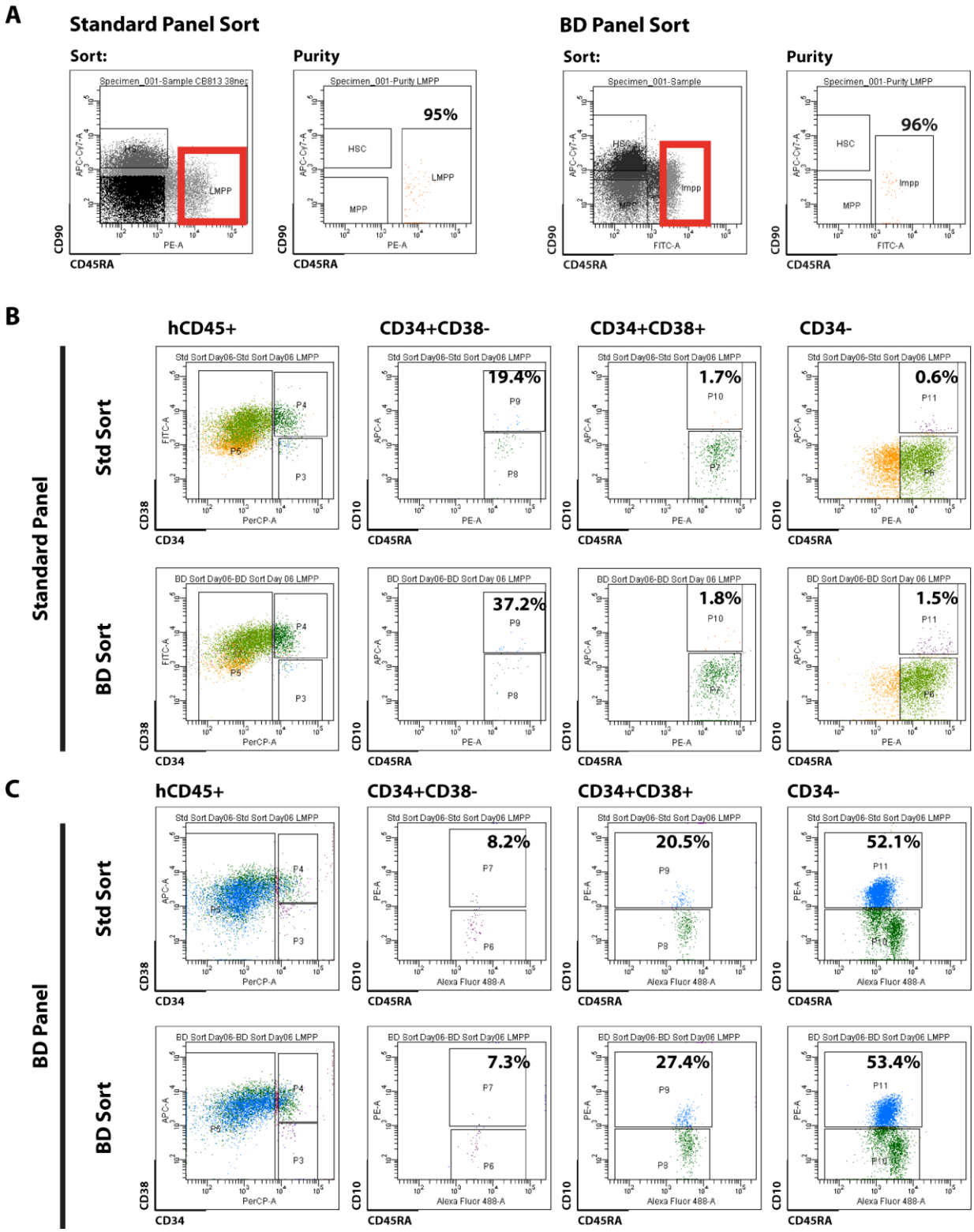

Figure 5.12. Comparison Of Standard And BD Antibody Panels In Short-Term Differentiation Conditions.

A) CB cells were stained with the STD (left) or BD Panel (right). The post-sort purity is shown next to the sort plots. The sorted LMPPs were placed into the IL-7 Short Term Differentiation Conditions. B) Analysis of cultured cells after 6 days with the standard panel.

C) Analysis of cultured cells after 6 days with the BD panel. LMPP, lymphoid-primed multipotent progenitor. N=1

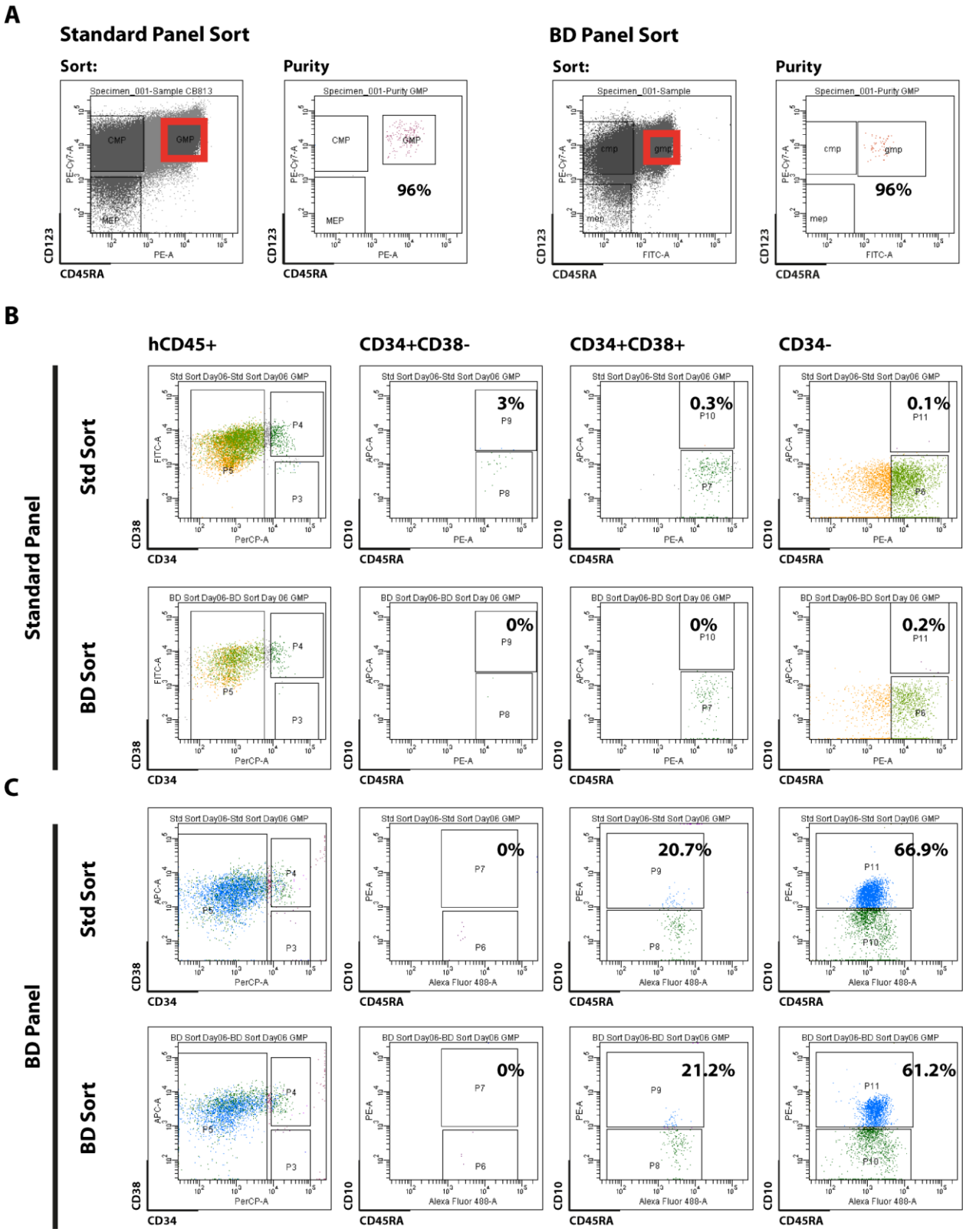

Figure 5.13. Comparison Of Standard And BD Antibody Panels In Short-Term Differentiation Conditions.

A) CB cells were stained with the STD (left) or BD Panel (right). The post-sort purity is shown next to the sort plots. The sorted GMPs were placed into the IL-7 Short Term Differentiation Conditions. B) Analysis of cultured cells after 6 days with the standard panel. C) Analysis of cultured cells after 6 days with the BD panel. GMP, granulocyte-macrophage progenitor. N=1

5.5.4 Anti-CD10 Antibody Clone Testing

These findings prompted me to look further into the differences between the antibody clones used. In Figure 5.14, 3 examples of mAB stainings with three different CD10 antibody clones are shown which are gated as described in A. The CD10 clone HI10a, which is depicted in B was used in Doulatov et al[20], as well as in this study, and it separates the MLP from the LMPP faithfully. CD10 CB CALLA, illustrated in D, has also been used in this study and verified to bind the correct CD10 antigen by subsequent in vitro differentiation experiments. CD10 W8E7 however, the clone custom conjugated to AF555 by BD Biosciences for this study, shows poor staining and high background binding.

In a final experiment concerning the issues related to finding a bright, photo-bleaching resistant CD10 antibody for single cell live in vitro tracking, I conjugated purified CD10 clones to AF555 myself.

Figure 5.15 demonstrates the results. Two different antibody clones were conjugated in this experiment, CD10 CB CALLA as a known control and CD10 W8E7 to be tested. As a positive control, CD10 CB CALLA conjugated to APC commercially was used. The conjugation was performed with the ZENON ALEXA Fluor 555 MOUSE Ig (Z25205) kit, which was selected to fit the isotype of the antibodies to be conjugated. Different fluorophore to antibody ratios (6:1 and 3:1) were tested to find the optimum concentration. MNCs from CB were stained with custom conjugated and control antibodies to evaluate their functionality.

Figure 5.15 A shows the controls used for the analysis of this experiment and to achieve an understanding of the staining patterns. The first panel is the Unstained Control, with CD10 AF555 on the y-axis and CD10 APC on the x-axis. The second

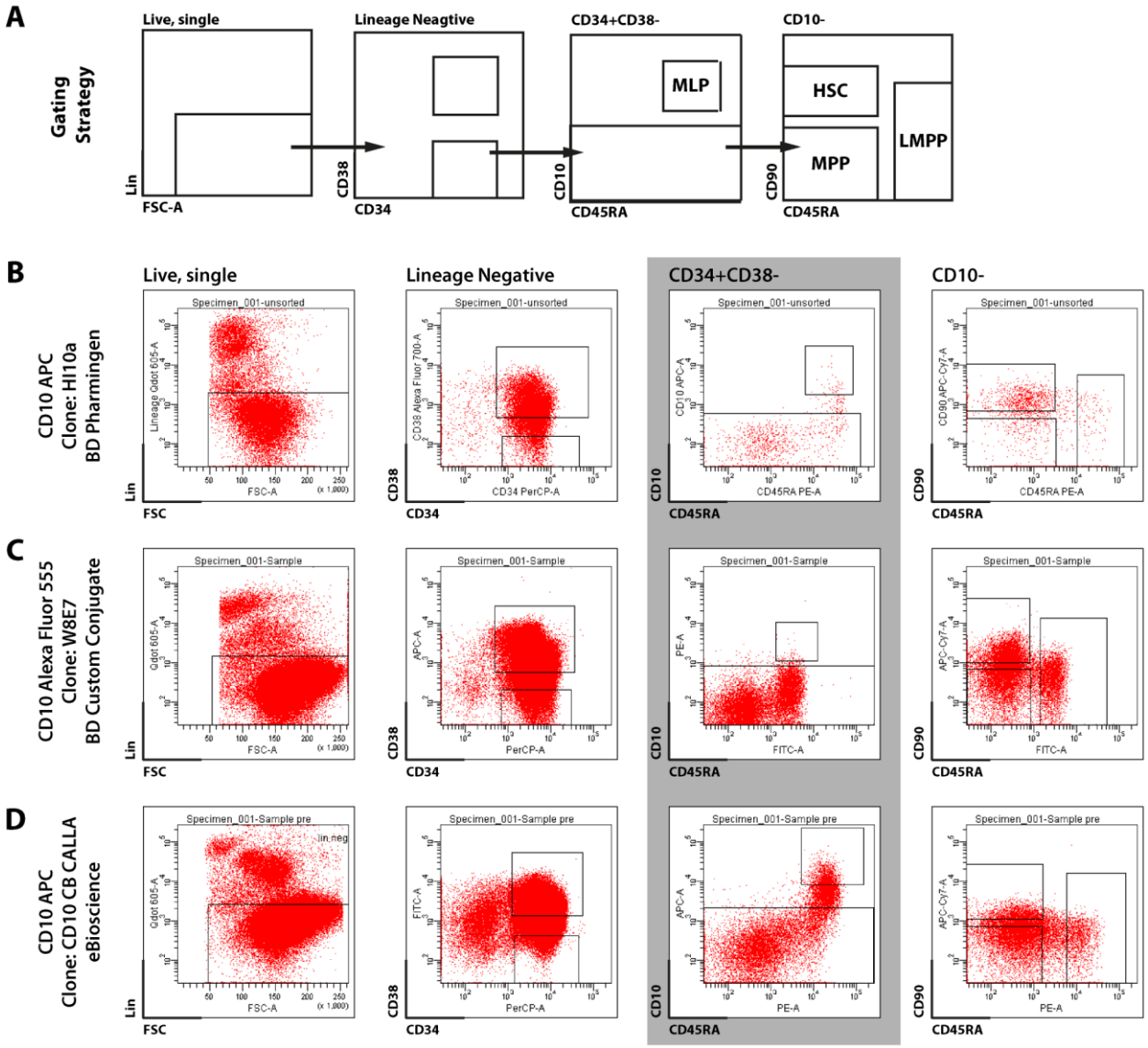

Figure 5.14. Comparison Of Different Clones And Fluorophores To Investigate CD10 Antigen Expression On CD34+ Cord Blood Cells.

A) depicts the gating strategy for this experiment. CD34+ cells from CB were stained with monoclonal antibodies. The grey shaded area highlights the CD45RA and CD10 plots. Single, live cells are investigated for their expression of common lineage markers, and lineage negative are further plotted against CD34 and CD38 to separate early stem and progenitors (CD34+CD38-) and more mature progenitors (CD34+CD38+). CD34+CD38- cells are further gated on basis of their CD10 and CD45RA expression to separate the MLP from the HSC, MPP and LMPP. CD90 and CD45RA expression can separate the latter three stem/progenitor populations.

B) CD10 APC (clone HI10a) supplied by BD Pharmingen was used in this staining process.

C) CD10 Alexa Fluor 555 (clone W8E7) supplied by BD Biosciences as a custom conjugate was used in this experiment.

D) CD10 APC (clone eBio CD10 CB CALLA) supplied by eBioscience was used in this staining.

CB, cord blood; MLP, multilymphoid progenitor; HSC, haematopoietic stem cell; MPP, multipotent progenitor; LMPP, lymphoid primed multipotent progenitor; APC, allophycocyanin; Lin, lineage. N=1

panel depicts the single stain with the positive control, the commercially conjugated CD10 CB CALLA APC. The third one shows CD10 W8E7 conjugated by BD Biosciences, in order to get a measure for the staining pattern of this antibody in CB MNCs.

In B, different concentrations of the newly conjugated antibodies were used for staining. The top row shows BD clone W8E7 conjugated to Alexa Fluor 555 at a 3:1 ratio, from 5µL/test to 1µL/test. The most prominent staining was detected at the highest ratio and concentration per test. The second row shows the 6:1 ratio conjugation of CD10 W8E7, which was less successful than the previous one. The bottom row demonstrates the 3:1 ratio conjugation of CD10 CB CALLA to AF555, where a clearly stained CD10+ population can be seen.

This data had to be put in context with known staining patterns to yield a proper conclusion. In Figure 5.15 C, the custom-conjugated antibodies were counterstained with the known CD10 CB CALLA APC (eBioscience).

The top row shows W8E7 at the 3:1 ratio conjugation (y-axis) counterstained with CD10 CB CALLA APC (x-axis). Interestingly, as best demonstrated at the 5µL/test concentration, low degrees of blocking can be seen, which means that both clones bind to a similar/related antigen. However, the signal exhibited by CD10 W8E7 AF555 is very weak, and random background staining could be detected too.

The second row illustrates CD10 W8E7 at the 6:1 conjugation ratio, which shows a similar pattern to the 3:1 ratio, albeit weaker. The bottom row focusses shows CD10 CB CALLA AF555 and CD10 CB CALLA APC counterstained MNCs. As it can be clearly seen, blocking occurs to a high degree in these samples, since both antibodies bind to the same antigen. The skew towards the x-axis in the plot on

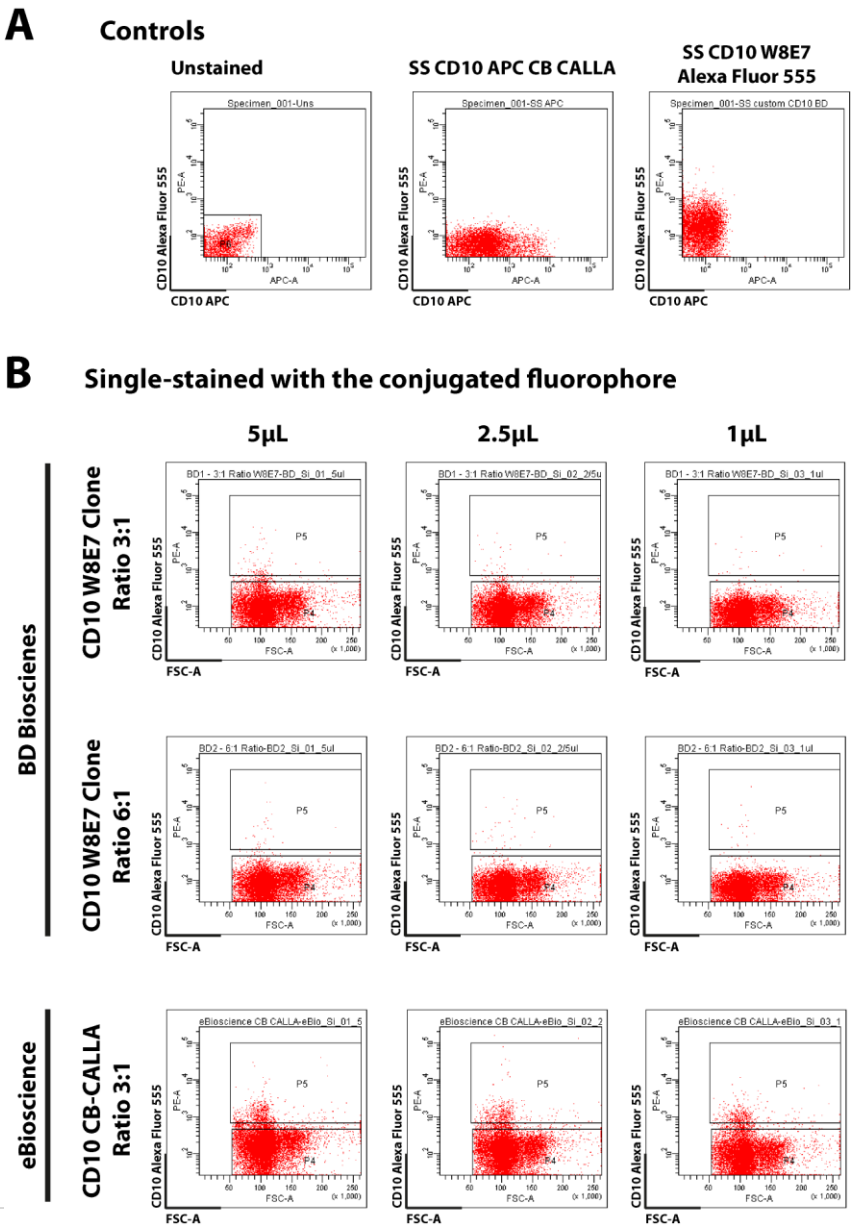

Figure 5.15. Conjugation Of Alexa Fluor 555 To Different CD10 Antibody Clones. (A) Unstained and single stained (SS) controls. Human mononuclear cells (MNCs) from umbilical cord blood were stained with monoclonal antibodies, CD10 APC (eBioscience CB-CALLA), commercially conjugated and a separate control, stained with CD10 Alexa Fluor555 (W8E7) custom conjugated by BD Biosciences. Dead cells were excluded by Hoechst staining (data not shown). (B) MNCs from cord blood stained with different amounts of antibody which was conjugated in house to Alexa Fluor 555. The ratio is the antibody to fluorochrome ratio which was used in the conjugation process. (C) MNCs from cord blood stained CD10 W8E7-conjugated in house to Alexa Fluor 555 or CD10 CB CALLA-conjugated in house to Alexa Fluor 555 for comparison.

the right can be explained by the saturation of antigen binding due to the higher concentrations of CD10 APC present.

The conclusion which was drawn from this experiment was that CD10 W8E7 binds the CD10 antigen, however staining only results in weak signals which are riddled by high background.

Furthermore, the manufacturer of the conjugation kits recommends the use of freshly conjugated antibodies for analysis. Stability issues will have to be addressed if custom conjugated antibodies are to be used over prolonged periods of time in single cell live in vitro tracking experiments.

5.6 Discussion and Future Perspectives

The aim of these experiments was to characterise progenitor populations residing in the CD45RA+ compartment of CB and dissect their relationship. It could be established that there are two distinct populations in the CD45RA+ compartment, which can be separated on basis of their expression of the early lymphoid marker CD10.

The CD10- LMPP, as published by our lab before, in human bone marrow[19], retains all lymphoid functional potentials and can also give rise to granulocytes and monocytes on a single cell level. In the Lin-CD34+CD38-CD45RA+CD10- compartment, 1 in 11 cells can give rise to B, mono and gran cells. Furthermore, we could verify T cell and NK cell potential on the population level and the absence of erythroid cells in MeC culture.

The MLP on the other hand, is only a fraction of the CD45RA+ compartment (20-30%) and has less proliferative potential than the LMPP in culture. Furthermore, even though it has full lymphoid differentiation capacity, it retains only very little monocytic differentiation potential in our hands. In limit dilution cultures, about 1 in 11 cells maintained in “Our Condition” give rise to B cells, and only 1 in 117 cells to monocytes. The MLP never gave rise to both lymphoid and myeloid cells from the same well. We could confirm the NK and T cell potential for the MLP as well as validate its poor colony forming ability in MeC.

Importantly, the LMPP and the MLP not only differ in their immunophenotype, but also in their functional and proliferative potential, as I have shown in this chapter. Future efforts are focussing on the generation of RNA sequencing profiles and gene expression profiles from real time PCR.

I am aware of the caveats in my data. First of all, no single cell T cell assays could successfully be performed; I succeeded in expanding single HSCs and MPPs on OP9-DL1 monolayers, however, with very low frequencies and could not make this procedure work with single LMPPs and MLPs (data not shown).

Furthermore, as mentioned in the discussion of the previous chapter, a multipotential assay, which would be able to quantify T cell, B cell, NK cell, monocytic and granulocytic differentiation capacity in parallel would be a very important tool to pinpoint the exact differences between MLP and LMPP. Furthermore, dendritic cell potential will need to be assessed in the LMPP, as it is said that the MLP has prominent dendritic potential in culture[20]. Dendritic cells could not be derived successfully in my hands in this study, due to limitations discussed in this study before.

In vivo models to read out short lived progenitor are sparse. There is a variety of mouse models available for the transplantation of cancer cells and stem cells, engraftment of progenitors however remains difficult to achieve. Immune-deficient mice have mainly been used for this purpose. They are characterised by mutations in the IL-2R gamma chain (IL2γ), the RAG or SCID gene, in a non-obese diabetic background[100,101] which will render them with very little residual immune function. B, T and NK cells are ablated, preventing clearance of the injected HSPCs by the host immune system.

Furthermore, “humanised mice” engineered to express human cytokines have been used to boost engraftment of stem cells[102]. Progenitors still pose a challenge to be assessed, even in these mouse models.

One possible approach to enhance engraftment of progenitors is the creation of a human environment in the model organism. Foetal bone implants are one way of achieving an environment supportive of early human haematopoiesis[103]. Similar set-ups used as breast[104] and prostate[105] cancer metastasis models have been published before. Combining these approaches with administration of exogenous cytokines to enable mobilization of the supporting graft to colonise the murine BM could be a new model to engraft human HSPCs.

Another possible system proposed the injection of human mesenchymal stem cells, which can give rise to pericytes, myofibroblasts, osteocytes, osteoblasts, endothelial cells and bone marrow stromal cells[106,107]. In theory, this should provide stem and progenitor cells with the perfect conditions, as found in the niche. Limitations in this model stem from the difficulty to obtain MSCs, as their isolation procedure has not been standardised. Furthermore, there is no consent concerning their surface markers or other criteria used for purification.

Another point which has to be kept in mind is the timing of the injections of MSCs and haematopoietic cells. Would it be advantageous to inject the MSCs ahead of the haematopoietic cells to allow for differentiation? Furthermore, the lineage evaluation of cells generated by HSPCs will have to be separately marked from the MSCs. Even if MSCs and their progeny should not express antigens found on blood cells, background binding might falsify results. A fluorescent tag applied to the MSCs would be a way to circumvent this problem.

Taken together, this data confirms the existence of a human lymphoid-primed multipotent progenitor in neonatal cord blood. Therefore we have acquired additional evidence which validates the haematopoietic hierarchy first proposed by Adolfsson[16] et al, which features a split between the Meg-E branch and all other cell types, which differentiate through an LMPP intermediate.

My work highlights another facet in the on-going evolution of the human haematopoietic hierarchy. The LMPP in cord blood is the counterpart to the BM LMPP; they share the same properties and differentiation capacities. Furthermore, we were the first group to dissect the relationship between the LMPP and the MLP. I could confirm that the LMPP lies upstream of the MLP in the haematopoietic hierarchy in in vitro assays.

Additional experiments to assess gene expression signatures in these two populations will be carried out in the near future. The data which was acquired so far by us[19] and Doulatov et al suggests that LMPP and MLP also differ in their gene expression profiles. While the MLP was shown to highly express Pax5, which is a B cell specific gene, its expression could not be detected in LMPPs. To identify additional differences in gene expression of LMPP and MLP qPCR as well as RNA sequencing experiments will be performed.

With the help of the Fluidigm C1 Single Cell Capture System, I plan to interrogate gene expression of single LMPPs and MLPs. In a trial experiment, I could capture and amplify single LMPPs and investigate the expression of 94 individual genes. This very preliminary data points toward an underlying lymphoid priming also in the cord blood LMPP (expression of Notch 1 – Notch 4, Runx3), expression of gran/mono genes (MPO, SPI1, IFR8), absence of erythroid genes vWF and TAL1, however residual GATA-1 expression could be detected.

All in all, more time will be spent to acquire more single cell gene expression data of both LMPP and MLP, once the installation of the C1 system is finalized. The set of 96 genes which was selected in order to perform this real time PCR experiment were picked from the literature and previously acquired microarray data of the LMPP. Going forward, RNA sequencing data from the LMPP and MLP will be used to complete the genes validated on the C1 system.

Initial profiles have already been acquired for LMPP populations, which will be discussed and presented in detail in the next section. mRNA expression profiles provide a starting point to filter out differences between cell populations, as a basis for RT-PCR. One of the most challenging limitations encountered in this study was the difficulty to sort enough cells for all applications. RNA sequencing on the Illumina HiSeq Platform requires at least 20ng of high quality input RNA in a small volume (1µL) to take it through cDNA preparation and the sequencing procedure. 5,000 cells sorted per populations are required at the very least to isolate such an amount of RNA. Furthermore, immature and less proliferating cells contain smaller amounts of RNA than more mature populations.

Moreover, the LMPP only contributes about up to 5% of all lin- cells in CB. In a quick calculation, CB CD34+ sample size usually ranges around $1x10^6$ cells.

Following the necessary CD34+ separation, cells are cultured in StemSpan supplemented with SCF, FLt3L and TPO overnight. On the day of sorting only about 70% of cells can be recovered. Throughout the staining procedure, an additional 10-20% of cells will be lost in the centrifugation and filtration steps.

Up to 10% of the cells still present at this stage will be dead or dying and excluded by Hoechst and a further 8% will be excluded as debris or doublets. Lineage exclusion also eliminates another 10% of the remaining cells. If $1x10^6$ cells were present at the start, only about 460,000 cells are left at this stage. The proportion of LMPPs can be variable in CB, if 5% of lin- cells are assumed to be LMPPs, in this example, 23,000 LMPPs would be left to be sorted.

However, only about 50% of acquired events can be sorted (depending on the cytometer settings, i.e. purity masks used etc.). Even more devastating, after counting tests, it was found that also only about 50% of events recorded as "sorted", were actually present in the sorting tube. In this example, 5750 LMPPs would be left at the end. For MLPs, which constitute about 1% of the Lin- fraction, only 1150 MLPs could be sorted in this example. For in vitro assays, small numbers of cells are sufficient to perform bulk co-culture assays and MeC assays.

On the other hand, most molecular biology techniques require great numbers of cells, which are virtually unobtainable from a single sample. MLP RNA sequencing will have to be performed on samples pooled from multiple CB samples. In normal progenitor biology, it can be acceptable to pool samples under circumstances such as these.

In order to obtain a quantitative readout of progenitor differentiation potential frequencies in culture, limit dilution assays have to be performed. Great numbers of cells are required to sort multiple replicates of since, two, five and ten cells per

well. Therefore, the live in vitro tracking system would be a great way to evaluate the frequencies of cells on the single cell level without the need for large samples. However, limitations with the antibodies used for imaging have hampered progress in this facet of this study. Custom-conjugation by BD Biosciences proved unsuccessful, the clone of CD10 antibody (W8E7) which was supplied could not be verified to bind the same antigen as the previously used clones, CD10 CB CALLA and CD10 HI10a. Furthermore, the fluorochrome conjugated to CD10 W8E7, Alexa Fluor 555, was not bright enough to yield a clearly distinguishable signal in FACS analysis. In tests with compensation beads, which are engineered to bind all mABs in order to provide a comparable control, signals emitted by AF555 could be clearly detected in the PE channel. The most promising solution to this problem would be conjugation of CD10 CB CALLA or CD10 HI10a to AF555 by a commercial laboratory in conjunction with performing the same set of short term differentiation experiments again.

As a future outlook, these experiments have set the basis to purify the LMPP and MLP and characterised their functional potential on bulk and single cell level. Initial gene expression profiling has been performed and further analysis of RNA Sequencing profiles will follow. Validation of genes identified by RNA Seq will be helpful to establish gene expression signatures specific to LMPP or MLP. Furthermore, RNA Seq will also aid the selection of a list of cell surface markers, which might be of use in separating the LMPP and MLP and other haematopoietic populations. These can be verified by flow cytometry and subsequent functional in vitro assays.

6 Prospective Markers To Purify The LMPP Further

The lymphoid-primed multipotent progenitor (LMPP) can be isolated from human CB and BM. Its frequency in the CD10-CD45RA+ compartment is about 1 in 6 in BM and 1 in 11 in CB. In order to increase the frequency, the purification method has to be improved. Antigens differentially expressed on the LMPP fraction were picked from previous microarray studies and/or the literature and the LMPP subpopulations assayed to evaluate their functional potential in vitro.

6.1 CD53

CD53 is a pan leukocyte antigen and member of the tetrasparin surface protein family. Tetrasparins (such as CD9, CD37 and CD63) are highly evolutionally conserved proteins and characteristically have 4 hydrophobic transmembrane domains and an N-glycosylated extracellular loop, with both C- and N-termini in the cell interior[108]. CD53 has been implemented in having activating effects on certain cell types upon crosslinking; e.g. it can induce resting B cells to enter the G1 phase of the cell cycle[109].

Goardon et al found it differentially expressed in microarray analyses between HSC and MPP and it seemed a promising target, considering it also associates with VLA-4 (very late antigen 4 or integrin $\alpha_4\beta_1$) amongst other members of the tetrasparin family[110]. VLA-4 can bind ligands expressed by BM stromal cells in the niche, such as fibronectin. In experiments with leukaemic cell lines, VLA-4 and VLA-5 expressing cells could bind to fibronectin coated plates and therefore showed a higher viability than cells on control (BSA-coated) plates. In vivo, if VLA-4 blocking antibodies are administered in conjunction with an anticancer drug,

eradication of minimal residual disease is achieved, and no remaining human cells could be detected in the mouse bone marrow by PCR[111]. Due to these reasons, I hypothesized that CD53 might be an interesting candidate cell surface antigen to separate functionally distinct LMPP populations also in CB.

6.1.1 Immunophenotypic Analysis

Initially, CB was stained with a slightly modified version of the Standard LMPP Staining Panel, detailed information can be found in Table 2.5. The immunophenotypic profile can be seen in Figure 6.1 A. Live, single, lin-CD34+CD38- cells are plotted in relation to their CD45RA and CD90 expression, which enables separation of HSC, MPP and LMPP. The CD45RA+ LMPP is further analysed for its CD53 expression. CD53 expression segregates the LMPP into a CD53+ population (55% of LMPPs) and a CD53- population (45% of LMPPs). These populations could be sorted to high purity on a FACS Aria II, as is shown in Figure 6.1 B.

6.1.2 Methylcellulose Colony Forming Assays

CD53+ LMPP and CD53+ LMPP were assayed for their in vitro CFU-ability. 150 sorted cells were plated in MeC per plate. As a control for the assay system, normal MPP was sorted. Figure 6.1 C shows the results of the colony forming assay. MPPs had a high cloning efficiency of around 80%, whereas both LMPP populations ranged around 20%. MPPs could give rise to CFU-G, CFU-M, CFU-GM, CFU-E and CFU-mixed, as expected. CD53+ LMPP and CD53- LMPP mainly gave rise to CFU-G and CFU-M after 14 days in culture. No erythroid and/or mixed colonies were detected on any plate initiated with LMPPs.

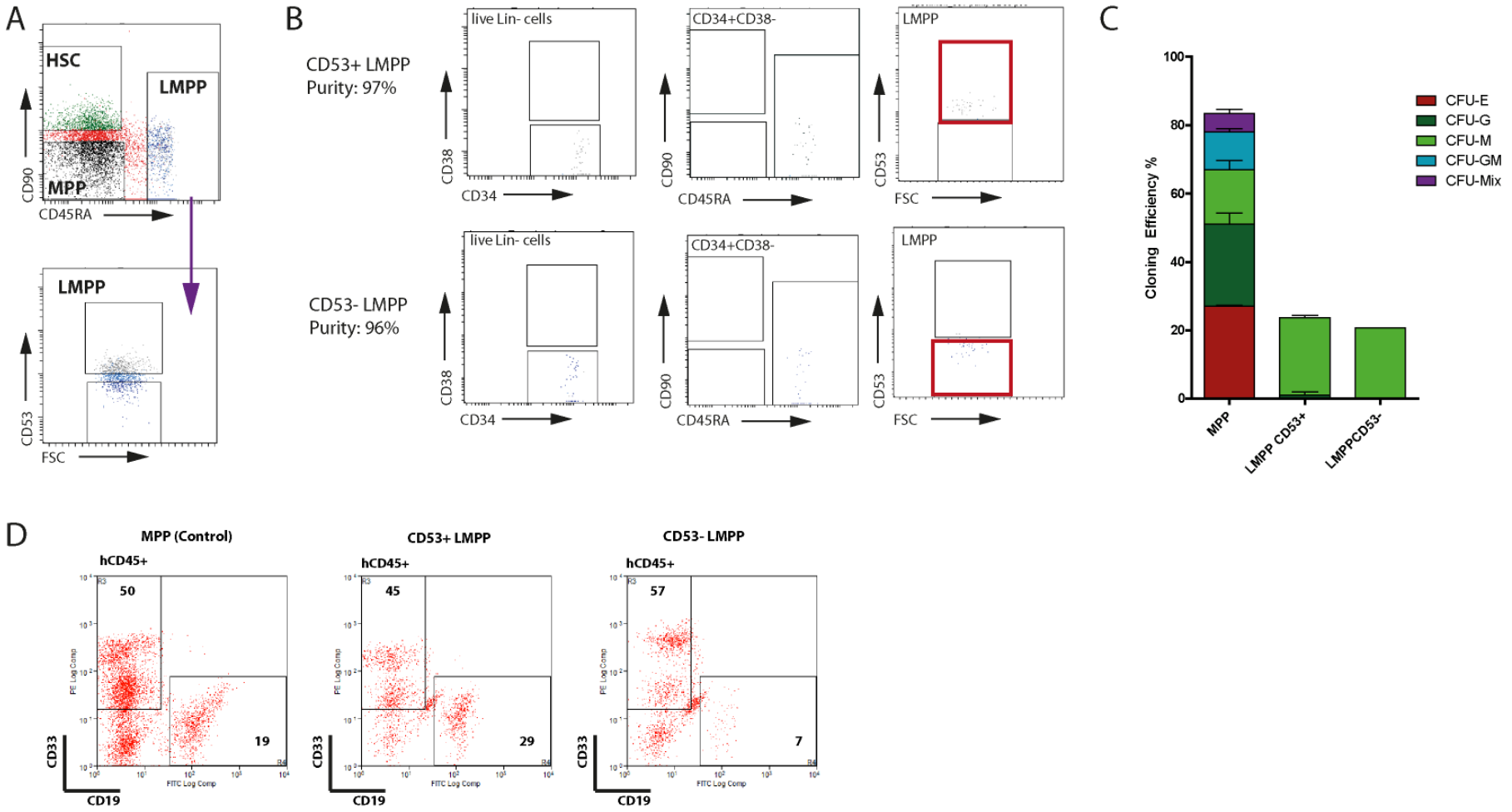

Figure 6.1. Summary Of Immunophenotypic And Functional Analysis Of CD53 LMPP Subpopulations.
A) Human UCB was stained with a panel of lineage exclusion and HSPC-markers and sorted for CD53+ LMPP and CD53- LMPP. MPP was sorted as a control. Sorted cells were placed into MS5 stromal co-culture and cultured in methylcellulose. B) Purity resort plots of the CD53+ LMPP and CD53- LMPP fractions. The purity was 97% for CD53+ LMPP and 93% for LMPP CD53-, respectively. C) Sorted progenitors growing in methylcellulose. Colonies were enumerated after 14 days of culture. Both LMPP populations mainly gave rise to macrophage colonies and also showed granulocytic potential. MPP

6.1.3 B Cell and Myeloid Differentiation Potential Of CD53 LMPP Subpopulations

In order to assess B and myeloid functional in vitro differentiation potential of CD53+ LMPP and CD53- LMPP, both populations were sorted to high purity from CB and plated on MS5 monolayers. If CD53 expression on the LMPP segregated functional myeloid or B cell differentiation potentials, it would be possible to detect this in this assay.

After 5 weeks, wells were harvested and subjected to FACS analysis. Monoclonal antibodies directed against cell type specific antigens were used to mark B cells (CD19+) and myeloid cells (CD33+). In order to differentiate from the murine stromal layer, the human pan blood cell marker, CD45, was included in the analysis panel. As a control, sorted MPPs were included, because they can give rise to B and myeloid cells. Figure 6.1 D demonstrates the outcome of MS5 in vitro assays. MPPs generated both CD33+ myeloid cells and CD19+ B cells in culture after 5 weeks. The CD53 subpopulations of the LMPP did not differ greatly in their bulk in vitro differentiation potentials on MS5 cells, both could differentiate into B and myeloid cells. However, to quantify a possible difference in differentiation capacity, limit dilution assays were performed. 1, 5, 10 or 50 CD53+ LMPP or CD53- LMPP were plated per well and analysed after 5 weeks in culture. Figure 6.2 shows the results from this experiment. With the help of Poisson statistics, it was evaluated that 1 in 8 CD53+ LMPPs have the capacity to generate both B and myeloid cells in culture. On the other hand, 1 in 10 CD53- LMPPs can generate both cell types in culture as well.

Due to the fact that T cell differentiation potentials could not be assessed in vitro at this time, it was decided to halt experiments on CD53 at this point and continue

with other markers, since there was no obvious difference between the CD53+ and the CD53- LMPP subpopulation.

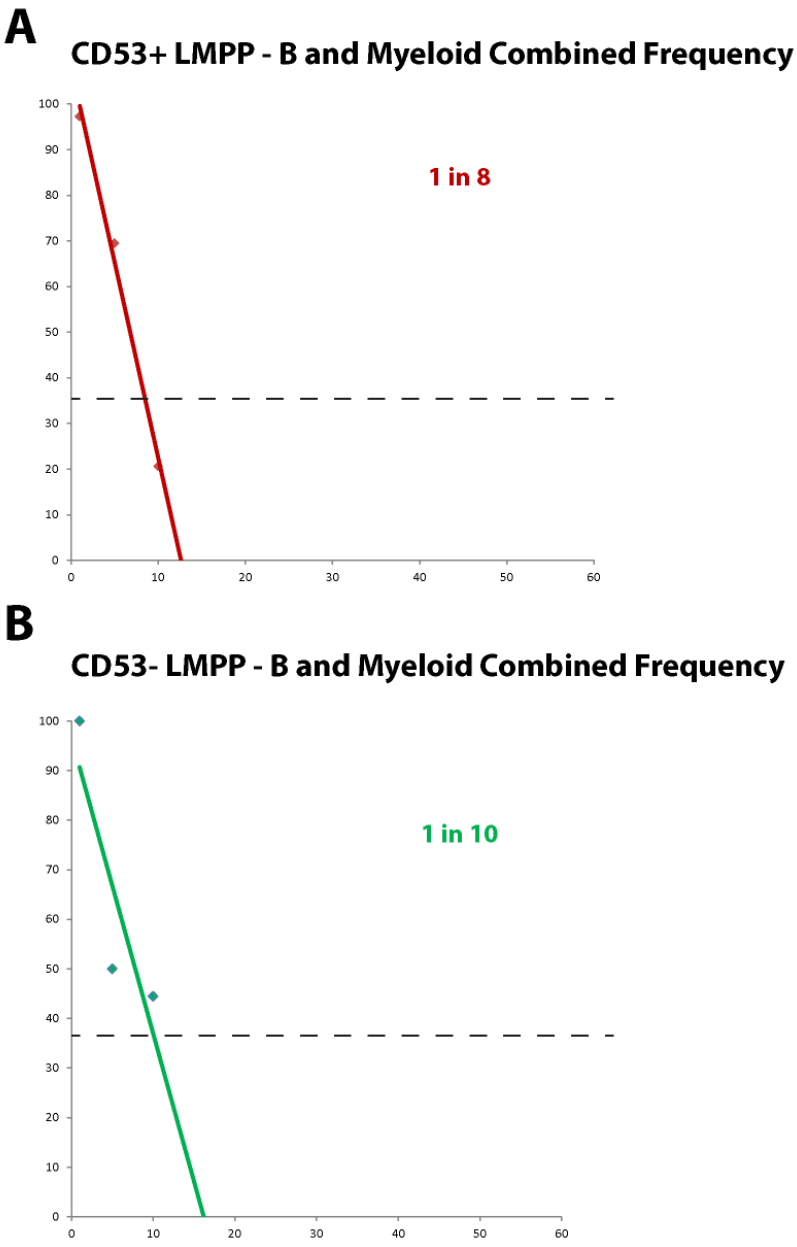

Figure 6.2. Limit Dilution Analysis Of CD53 LMPP Subpopulations On MS5 Stromal Monolayers.
CD53+LMPPs and CD53-LMPPs were sorted directly onto stromal monolayers (1, 5, 10 or 50 cells per well), maintained in culture for 5 weeks and subsequently analysed by FACS for B cell progeny (CD19+) and/or myeloid progeny (CD33+). Only wells with more than 30 hCD45+ cells were scored as positive. Frequencies were calculated with Poisson statistics in L-Calc. A) The combined B and myeloid frequency of the CD53+ LMPP after 5 weeks in culture is 1 in 8 cells. B) 1 in 10 CD53- LMPPs give rise to B and myeloid cells after 5 weeks in culture.
LMPP, lymphoid primed multipotent progenitor.

6.2 CD84

CD84 (SLAMF4) is a member of the SLAM (signalling lymphocyte activation molecule) family of receptors. Other important SLAMs are CD150 (SLAMF1), CD244 (SLAMF4), CD229 (SLAMF3) etc. Structurally, they belong into the group of type I transmembrane proteins, and they have extracellular immunoglobulin-like domains.

Furthermore, they can only be found on the surface of immune cells; their presence has never been confirmed on the surface of non-immune cells[112,113]. In murine bone marrow, a so called “SLAM code” has been used to enrich for HSCs (Lin-Sca-1+c-kit+CD150+CD48-CD244-), MPPs (LSK CD150-CD244+) and more committed progenitors, which are all CD48+[3]. These considerations, as well as the fact that CD84 was found to be differentially expressed between MPP and HSC by microarray analysis of bone marrow stem and progenitor cells initiated analysis of this particular antigen on LMPPs.

6.2.1 Immunophenotypic Analysis

Cord blood was subjected to flow cytometric analysis. Samples were stained with a slightly modified standard LMPP panel (“CD84 Sorting Panel”, see Table 2.5, which details the fluorochromes, clones and lineage panel) to separate the basic stem and progenitor populations, as well as investigate expression of the CD84 antigen on the LMPP.

Lin-CD34+CD38- immature cells were plotted with respect to their CD45RA and CD90 expression. The CD45RA+CD90- LMPP is further interrogated for CD84

expression in a FSC/CD84 plot. Low CD84 expression could be detected on the LMPP (12% CD84+), whereas the majority of this population was CD84- (78%). Sort plots are demonstrated in Figure 6.3 A. Even though CD84 was conjugated to PE, which is the brightest fluorochrome available, the signal emitted by CD84+ LMPPs was very low, and CD84 expression resembled a continuum. Due to these reasons, sorting a highly pure population proved to be a challenge. CD84+ LMPP could be sorted to a purity of 64%, which is very low. The main contaminating cells were $CD84^{neg/low}$ expressing LMPPs. The CD84- LMPP had a post-sort purity of roughly 90%. Post sort purity data can be seen in Figure 6.3 B. Nevertheless, both populations were sorted and subjected to in vitro assays.

6.2.2 Methylcellulose Colony Forming Assays

In order to determine myeloid differentiation potential and cloning efficiency, CD84+ LMPP, CD84- LMPP and MPP as control were plated in 1.1mL of MeC and maintained in a humidified atmosphere for 14 days. Colonies were counted and scored as CFU-E, CFU-G, CFU-M, CFU-GM or CFU-Mixed.

The results of this experiment are demonstrated in Figure 6.3

C. MPPs had a cloning efficiency of 47%, and they gave rise to all types of colonies, most prominently 20% of CFU-E. Neither LMPP population gave rise to any mixed or erythroid colonies in vitro, however both showed strong monocytic

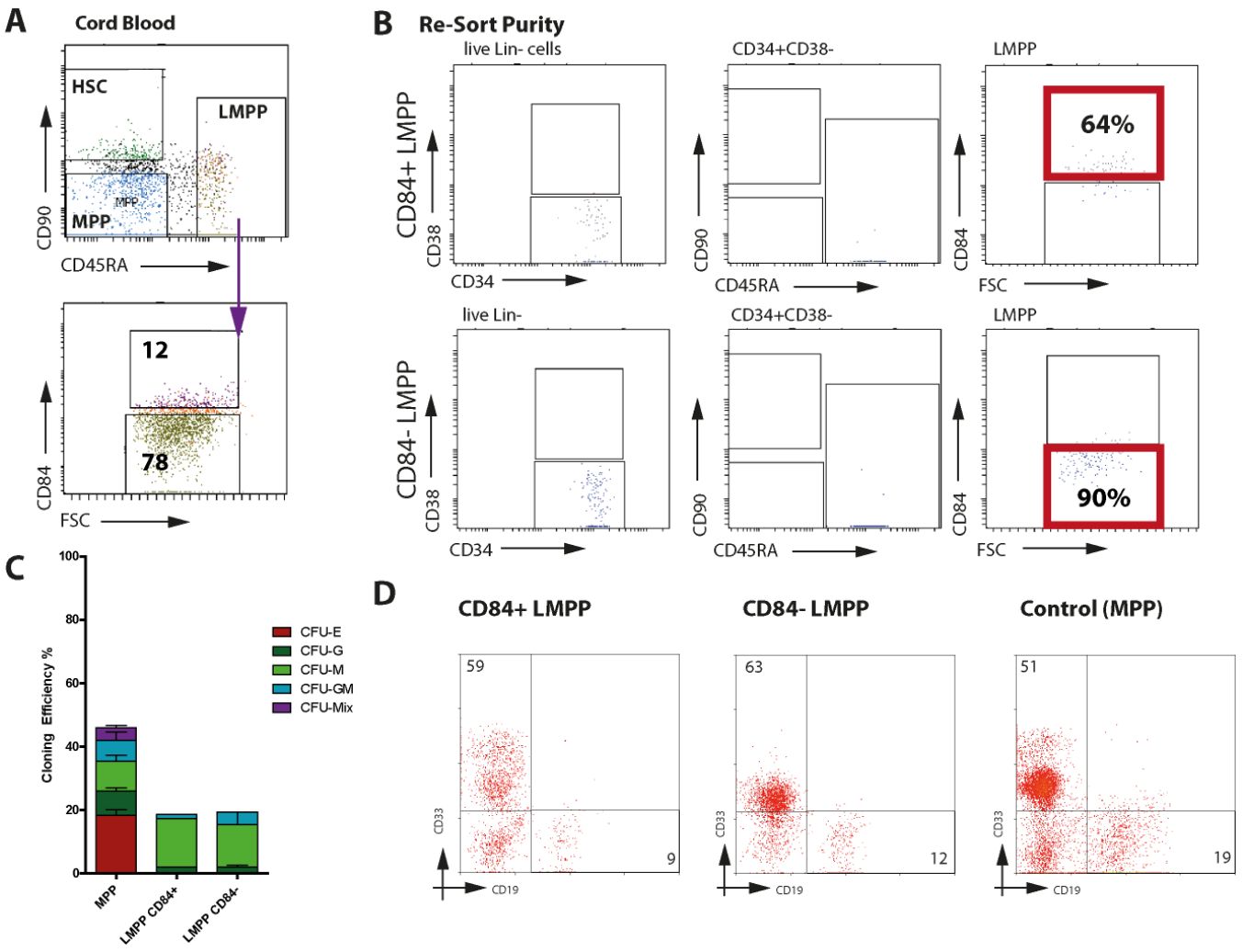

Figure 6.3. Phenotypic And Functional Analysis Of CD84+ LMPP And CD84- LMPP.

A) Human UCB was stained with a panel of lineage exclusion and HSPC-markers and sorted for CD84+ LMPP and CD84- LMPP. MPP was sorted as a control. Sorted cells were placed into MS5 stromal co-culture and cultured in methylcellulose.

B) Purity resort plots of the CD84+ LMPP and CD84- LMPP fractions. The purity was 64% for CD84+ LMPP and 90% for LMPP CD84-, respectively.

C) Sorted progenitors grown in methylcellulose. Colonies were enumerated after 14 days of culture. Both LMPP populations mainly gave rise to macrophage colonies and also showed granulocytic potential and mixed GM potential. Multipotent progenitor (MPP) served as a multilineage control. Data derived from biological replicates, error bars represent SEM.

D) Bulk populations of 100 CD84+ LMPP or 100 CD84- LMPP, respectively, were cultured on MS5 stroma for 5 weeks and analysed by FACS. Staining with antibodies characteristic for different haematopoietic lineages (CD19 –B cell lineage, CD33 – myeloid cells), revealed lineage potentials of the cultured cells. CD84+ LMPP showed bipotential progeny, whereas CD84- LMPP seemed to give rise to B cells rather than myeloid cells. LMPP, lymphoid primed multipotent progenitor

potential and also gave rise to granulocyte-monocytic colonies and pure granulocyte colonies. Their overall cloning efficiency ranged around 18-19%. Therefore, CD84+ LMPP and CD84- LMPP do no differ significantly in their cloning efficiencies or myeloid differentiation potential in MeC culture.

6.2.3 B Cell and Myeloid Differentiation Potential Of CD84 LMPP Subpopulations

To investigate lymphoid and myeloid differentiation potential, CD84 LMPP subpopulations were plated in liquid culture assays on MS5 stromal cells in “Our Condition” (Table 2.8). After 5 weeks with twice weekly change of the medium, wells were harvested and scored by FACS. Cells which stained for hCD45 were further investigated for expression of CD33 (myeloid cells) and CD19 (B lymphoid cells). In Figure 6.3 D, MPPs plated as control population gave rise to CD33+ and CD19+ cells after 5 weeks. Both LMPP populations could also give rise to CD19+ B cells and CD33+ myeloid cells. Interestingly, the CD84-LMPP lacked the $CD33^{hi}$ population which is present in both the MPP and the CD84+ LMPP.
However, due to the low purity of this population and the fact that both populations can give rise to CD33+ cells, it was decided to move on to a more promising set of markers.

6.3 CD127 and Other Prospective Markers To Purify The LMPP Further

Extensive search of the literature yielded another 3 promising candidate cell surface markers which might improve purification of the LMPP. CD127, also

known as IL-7 receptor alpha, CD150 (SLAMF1) and Notch-1 were also investigated.

CD127 is expressed on the murine CLP[6], it was hypothesized that a similar expression pattern is possible in human. LMPPs might be a heterogeneous mixture of a GMP-like cell and a CLP, and therefore read out in culture as a cell with granulocytic, monocytic and all lymphoid potentials. CD127 was included in the analysis panel to test this theory. Furthermore, it is the receptor for IL-7, which is a crucial lymphoid cytokine and might influence early lymphoid lineage decisions. It is expressed on early T cell and B cell progenitors and absence of IL-7 in T cell cultures can inhibit T cell development[77,114].

Notch-1 is indispensable for the development of lymphoid cells, especially of the T cell lineage[92,115]. It was decided to evaluate expression of Notch-1 on LMPPs from CB.

Furthermore, CD150 was evaluated for its expression on human LMPPs. As mentioned above, SLAM markers are a useful tool to separate early stem and progenitor cells in murine BM[3]. Even though their expression had been previously investigated in human with little to no success[116], it was chosen to include it for preliminary analysis and validate its expression on LMPPs.

Figure 6.4 summarizes expression of the three antigens described above on the LMPP from CB. One CB sample was divided in three equal parts and stained with mABs to enable separation of stem and progenitor cells. Staining Panels can be found in Table 2.5. The gating strategy was the same as shown before; the first plot is gated on live, single and lineage negative cells. CD34+CD38- are taken on

further to be analysed for CD45RA and CD90 expression. The CD45RA+ LMPP is shown in the last panel of each row.

Figure 6.4 A illustrates CD127 expression on the LMPP from CB. 12% of LMPPs exhibit low level expression of CD127, whereas the majority is negative for the marker CD127. Notch-1 on the other hand was detected on virtually all LMPPs in this experiment, as demonstrated in Figure 6.4 B. CD150, could only be detected on 9% of LMPPs, as is shown in Figure 6.4 C.

These results indicated that Notch-1 would not be useful for further analysis, since it does not split the LMPP population. The CD150 and CD127 subpopulations were further investigated and their functional potentials evaluated in vitro. Unfortunately, the CD150+ LMPP could never be sorted to any respectable purity (data not shown), therefore it was impossible to obtain interpretable and reliable in vitro data.

6.3.1 CD127 Phenotypic Analysis

CB was stained with an array of fluorescently labelled mABs, see Table 2.5 for the panel. It was chosen to investigate the expression of CD127 on LMPPs in context with expression of CD10, which, as discussed extensively before, marks human MLPs.

Therefore, CD10 was omitted from the mAB lineage cocktail and the panel slightly modified to permit parallel analysis of CD127 and CD10. The standard gating strategy was followed. The CD45RA+ compartment contains LMPP and MLP, as CD10+ cells have not been excluded by the lineage. Four populations could be discerned in the CD45RA+ compartment with respect to CD127 and CD10:

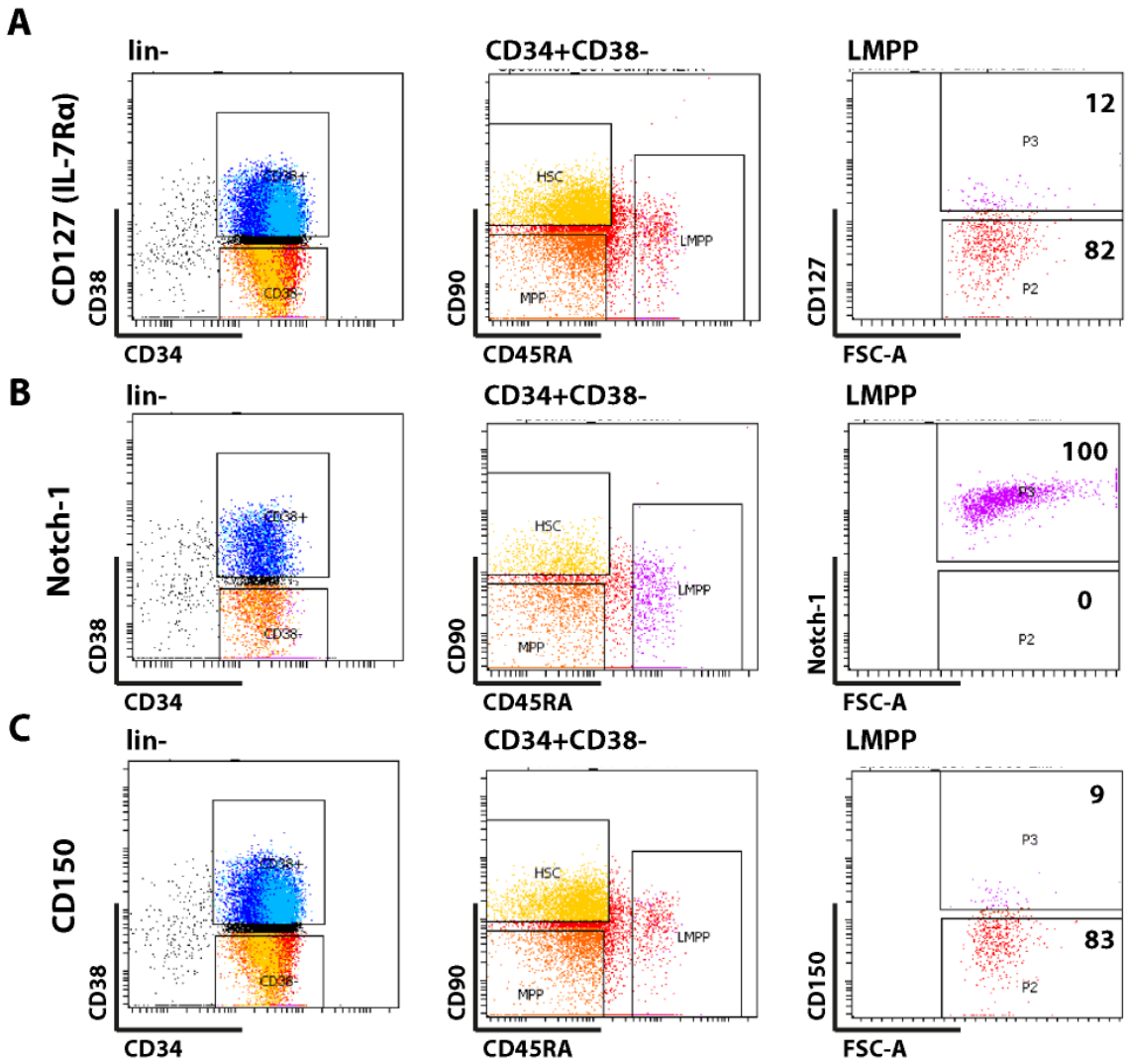

Figure 6.4. Immunophenotyping Of LMPPs - Investigation of Expression of CD127, Notch-1 And CD150.

Cells from CB were stained with mABs in order to separate stem and progenitor cells. Live, single and lineage negative cells were gated on CD34 and CD38 to obtain the CD38- early stem/progenitor cells. CD45RA+ LMPPs were gated on three different prospective markers to obtain a more pure population. A CD127 (IL-7Ra) expression on the LMPP from CB. 12% of LMPPs express low levels of CD127. B Notch-1 expression on the LMPP. All LMPPs expressed Notch-1 in this experiment. C Only 9% of LMPPs expressed low levels of the SLAM marker CD150.

LMPP, lymphoid primed multipotent progenitor; SLAM, signalling lymphocyte activation molecule; IL-7Rα, inter-leukin-7 receptor alpha.

CD127-CD10- (66%), CD127-CD10+ (18%), CD127+CD10-(14%) and CD127+CD10+ (2%).

The results of the immunophenotypic analysis are displayed in Figure 6.5 A. All four populations were sorted and plated in “Our Condition” (see Appendix A, Table 3). Due to the size of these populations, only very small numbers of cells could be obtained (180 and 340, for the 2 CD127+ populations) which made a purity check virtually impossible. The CD127-CD10- population could be sorted to nearly 100%, however no assumption can be made about the purity of the other populations. The low cell numbers also tie in with the fact that no MeC colony forming assay could be performed, as there were not enough cells available to plate at a sufficient concentration.

6.3.2 B Cell and Myeloid Differentiation Potential Of CD127 and CD10 CD45RA+ Compartment Subpopulations

The four immunophenotypically distinct subpopulations separated from the CD45RA+ compartment of human normal CB were plated in “our Condition” on MS5 monolayers and analysed by FACS after 2 weeks. The wells were harvested and the resulting cell suspension stained with mABs against CD45, CD14, CD15, CD56 and CD19. Live, single hCD45+ cells were detected in all wells initiated with any of the four CD127/CD10 populations. Figure 6.5 B also shows that all four populations could give rise to CD56+ NK cells and CD19+ B cells.

In the myeloid compartment, every single of the four initial populations showed rather prominent monocytic differentiation potential. Both CD10+ populations (CD127+ and CD127-) had very little granulocytic potential, as expected for the

MLP in these in vitro cultures. The residual granulocytic potential which was detected can most likely be attributed to low purity which could not be evaluated in the CD127 sorts, because the cell numbers were very limited.

Both CD10- populations could give rise to B cells, NK cells, granulocytes and monocytes on MS5 stromal layers, irrespective of their CD127 expression status. Therefore, CD127 expression on MLP and LMPP does not yield any additional benefit in sequestering any differentiation potential in vitro on MS5 stromal layers.

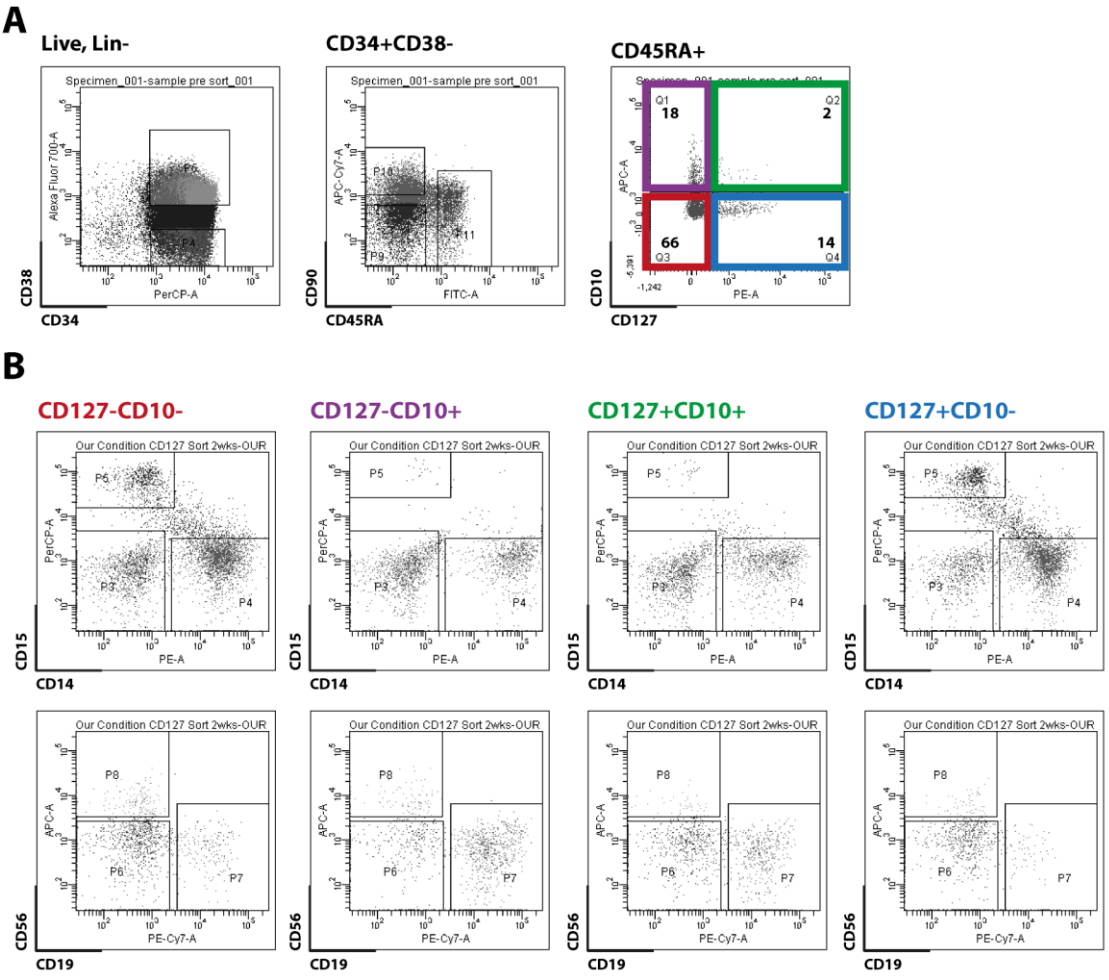

Figure 6.5. CD127 As An Additional Marker To Separate Functionally Distinct Populations In The CD45RA+ Compartment In Cord Blood.
A) Cord blood cells were stained and sorted to separate the CD45RA+ compartment with respect to CD10 and CD127 (IL-7Rα), whereas the last plot is on bi-exponential display in order to visualize the four populations more clearly. B) Sorted CD45RA+ populations were plated at a concentration of 200/mL on a MS5 stromal monolayer and cultured in the presence of cytokines (20ng/mL SCF, 10ng/mL Flt3L, G-CSF, IL-15, IL-2 and 10-7 Dup697) for 2 weeks. Wells were harvested and analysed by FACS after the culture period.

6.4 CD62L (L-Selectin)

Very recently, Kohn et al published a cell type with features similar to the LMPP. With the help of CD62L expression, a CD45RA+CD62L^{hi} population could be identified which shows similar functional potentials as the LMPP[21]. Disregarding CD38 expression, this group claims that CD62L expression is enough to mark lymphoid priming in human bone marrow from young donors. CD62L is also known as L-selectin and is expressed on mature lymphoid cells, as well as lymphoid organs, and is involved in the homing mechanism[117]. They subjected the CD62L^{hi} population to functional and molecular assays and confirmed myeloid (not clearly specified if granulocytic and monocytic), DC, B, T and NK differentiation potential in vitro. Furthermore, they also show low level short term engraftment of CD62L^{hi} cells (0.03% of NSG host BM). Microarray analysis of global gene expression data showed that the CD62L^{hi} population clustered intermediate between immature CD34+CD38- and more mature CD10+ cells[21].

It was decided that CD62L expression had to be interrogated in human CB and BM in our hands as well. CD62L might have the potential to purify the LMPP further, or maybe segregate the residual lymphoid potential in the GMP.

6.4.1 Immunophenotypic Analysis of Bone Marrow And Cord Blood Samples

CB and BM were processed as usual, and stained with a combination of mABs to reproduce the findings by Kohn et al in context with my staining panel[21]. Therefore a staining panel was devised which allowed parallel analysis of CD62L, CD38,

CD45RA and CD10 amongst other cell surface markers. A detailed description of clones and fluorochromes can be found in Table 6.1.

Two samples of each tissue were analysed initially. The gating strategy, which differs slightly from previous approaches, is detailed in Figure 6.6 A. First, live and single cells are gated with respect to Lin and CD34 expression. Lin-CD34+ cells are further depleted of any CD10+ cells, which contain the MLP as well as a CD38+ BNK progenitor. CD10- cells are then analysed for CD62L and CD45RA expression levels. If the $CD62L^{hi}$CD45RA+ population is back-gated on CD34/CD38, GMP and LMPP can be detected.

Figure 6.6 B illustrates the results of two cord blood samples. $CD62L^{hi}$CD45RA+ cells could be detected in both tissues; however the profiles differed from the ones published by Kohn et al. Approximately 99% of Lin-CD34+ cells were CD10-, and 9% were $CD62L^{hi}$CD45RA+ (see Table 6.2).

If this population was taken further onto a CD34/CD38 plot, a continuum of CD38 expression can be detected, just like the LMPP-GMP continuum. This suggests that the $CD62L^{hi}$CD45RA+ population is in truth a mixture of the LMPP and GMP, which would explain the functional readout and the results of the microarray data by Kohn et al.

The results of the immunophenotypic analysis of BM cells were very similar. As shown in Figure 6.6 C, a $CD62L^{hi}$CD45RA+ population could be detected in the bone marrow of elderly donors. The CD10- population occupies on average 91% of the Lin-CD34+, and the $CD62L^{hi}$CD45RA+ 15.6% (see Table 6.2). As expected for bone marrow, the proportion of GMPs vs LMPPs in the $CD62L^{hi}$CD45RA+ fraction is higher, as the numbers of LMPPs decline with age.

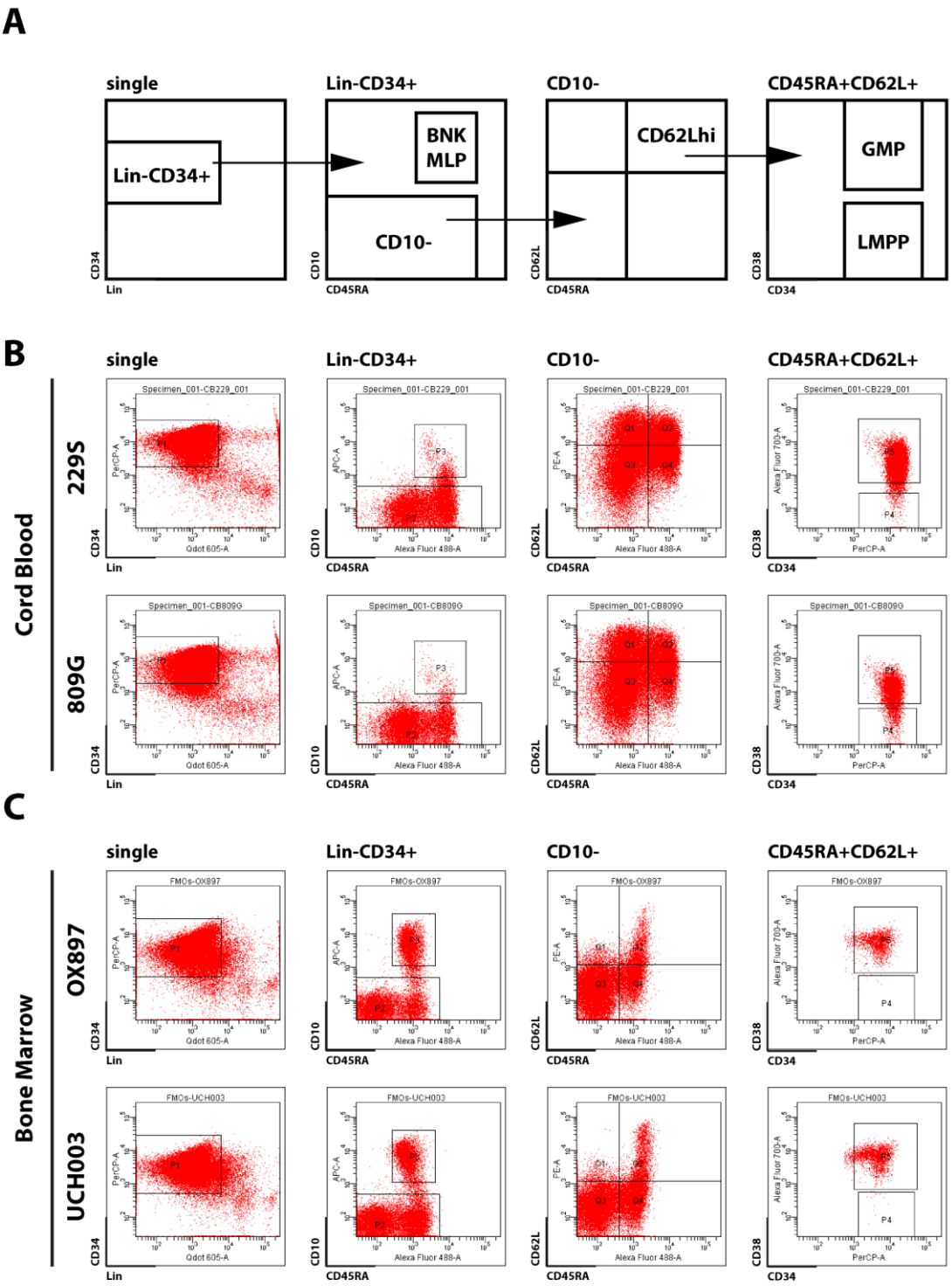

Figure 6.6. Immunophenotypic Analysis Of CD45RA+CD62Lhi Cells From Cord Blood And Bone Marrow.

Cord blood and bone marrow were processed and stained for FACS analysis following the standard procedure. CD62L was included in the analysis panel and the gating strategy by Kohn et al was followed[21]. A) Live and single cells were selected to exclude CD34- and lin+ cells. Furthermore, Lin-CD34+CD10- cells were analysed for expression of CD45RA and CD62L. CD45RA+CD62Lhi cells were further analysed for expression of CD38, to separate the CD38+ GMP and CD38- LMPP. B) Two representative examples of the HSPC stain including CD62L in CB.C) Two representative examples of the HSPC stain including CD62L in BM.

HSC, haematopoietic stem cell; MPP, multipotent progenitor; LMPP lymphoid primed multipotent progenitor; MLP, multilymphoid progenitor; CMP, common myeloid progenitor; GMP, granulocyte-monocyte progenitor; BNK, B-NK cell progenitor; BM, bone marrow; CB, cord blood; lin, lineage.

CD62L Sorting Panel		
Antigen	**Fluorochrome**	**Clone**
CD10	APC	eBioscience CB CALLA or HI10a
CD34	PerCP	581
CD38	AF700	HIT2
CD90	Biotin +APC CY7	eBio5E10
CD45RA	Alexa Fluor 488	HI100
CD123	PE Cy7	6H6
CD62L	PE	DREG-56
Lineage	QDot605	N.A.
Hoechst	Pacific Blue	N.A.

Our Lineage			
Antigen	**Clone**	**Antigen**	**Clone**
CD2	RPA-2.10	CD14	61D3
CD3	HIT3a	CD19	HIB19
CD4	RPA-T4	CD20	2H7
CD7	eBio124-1d1	CD56	MEM188
CD8a	RPA-T8	CD235a	HIR2
CD11b	ICRF44		

Table 6.1 CD62L Sorting Panel Plus Lineage

Cord Blood	Average	Standard Deviation	
CD10-	98.9	1.1	
CD62Lhi	9	4.8	**N=10**

Bone Marrow	Average	Standard Deviation	
CD10-	90.8	3.9	
CD62Lhi	15.6	10.1	**N=8**

Table 6.2. Proportions Of CD10- and CD62Lhi Fractions of Cord Blood And Bone Marrow.
Expressed as % of Lin-CD34+CD38-.

To eliminate as many variables as possible, samples were divided and stained with the standard lineage panel in use in our lab, and the lineage panel as published by Kohn et al. Table 6.3 compares both lineage cocktails.

A

Our Lineage			
Antigen	**Clone**	**Antigen**	**Clone**
CD2	RPA-2.10	CD11b	ICRF44
CD3	HIT3a	CD14	61D3
CD4	RPA-T4	CD19	HIB19
CD7	eBio124-1d1	CD20	2H7
CD8a	RPA-T8	CD56	MEM188
CD10	eBio CB CALLA	CD235a	HIR2

B

Kohn et al Lineage	
Antigen	**Clone**
CD3	SK7
CD14	M2E3
CD19	4G7
CD56	MY31
CD235a	GA-R2

Table 6.3. Comparison Of Our Lineage Panel vs. Kohn et al Lineage Panel.
Summary of lineage exclusion Abs used in this study, from our lab[19] and Kohn et al.[21] CD235a; glycophorin a.

The results of the analysis can be seen in Figure 6.7. The standard lineage cocktail used in this study is very extensive, CD34+ cells are depleted of B cells, T cells, NK cells, myeloid cells, granulocytes, nucleated erythroid cells, DCs and even more committed progenitors are excluded. Kohn et al, on the other hand, use a reduced lineage exclusion panel, which selects for B, T, NK, erythroid and monocytic cells. Figure 6.7 A shows the results from the analysis of a CB sample which was not pre-enriched for CD34+ cells, which explains the large number of CD34- negative cells. The FACS plots are gated as in Figure 6.6; however the dead cell and doublet exclusion is shown as well. The top row demonstrates our standard lineage panel, and the second row the lineage panel used by Kohn et al. The numbers in the CD45RA/CD62L plots are the percentages of the respective

populations, of the Lin-CD34+CD10-. Interestingly, there was no difference in the proportions of the four different CD62L/CD45RA populations between the two lineage panels in CB.

A similar observation was made in bone marrow. Irrespective of the lineage exclusion cocktail, the proportions of the populations of interest did not change significantly, as can be seen in Figure 6.7 B. It was decided to continue the use of the lineage exclusion panel which had already been optimised in this study, to maintain comparability with previous experiments.

The gating and sorting strategy was modified slightly, instead of sorting a CD62Lhi mixture of GMP and LMPP, both of these populations were divided into their CD62L+ and CD62L- components in both bone marrow and cord blood.

Furthermore, it was planned to subject as many populations as possible from the haematopoietic hierarchy to functional assays, as well as extract RNA from sorted populations and sequence it to obtain comparative gene expression data.

Examples of the phenotypic analysis and also the sorting plots of a representative CB and BM can be found in Figure 6.8.

A demonstrates the FACS profile of a bone marrow, which was CD34 enriched and stained with mABs (see Table 2.5). Dead cells, doublets and lineage positive cells are excluded. The CD34+CD38+ more mature progenitors are taken through exclusion of CD10+ B-NK cell progenitors and can be separated into GMP, CMP and MEP with the help of CD123 and CD45RA. The CD45RA+CD123+ GMP is further analysed for expression of CD62L. A CD62L- GMP and a CD62L+ GMP can be detected. On the other hand, CD34+CD38- immature stem and progenitor cells are subjected to the exclusion of the CD10+ MLP, and further on separated

into HSC, MPP, and LMPP with CD90 and CD45RA. LMPPs can further be divided on basis of their CD62L expression.

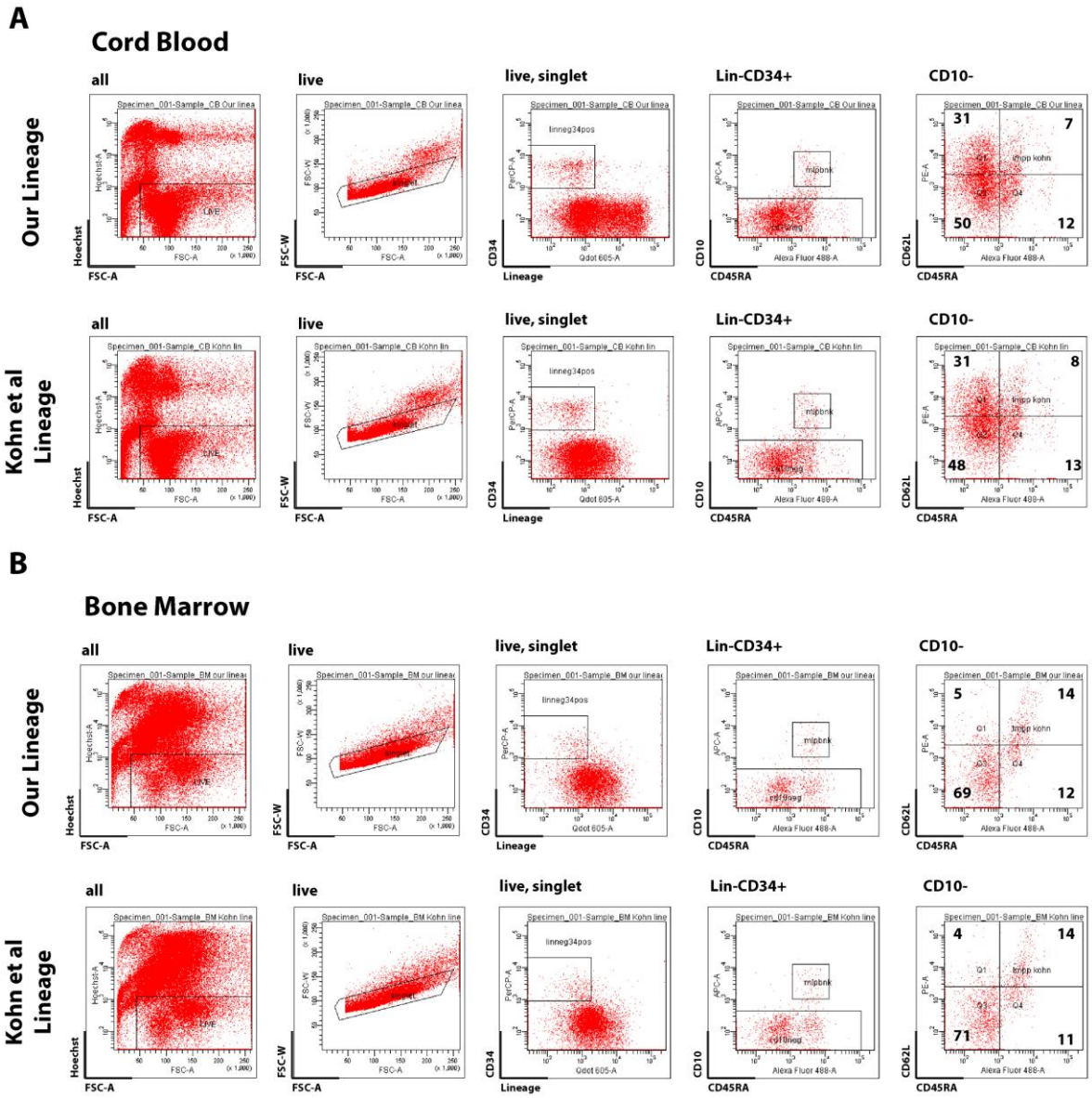

Figure 6.7. Comparison Of Standard vs Kohn et al Lineage Panels In Cord Blood And Bone Marrow.

CB and BM samples were divided in half and were stained with our standard panel or the lineage panel as devised by Kohn et al[21] and analysed by flow cytometry.

Gating strategy shows exclusion of dead cells and doublets and the profile of the lineage positive cells.CD10+ cells were further excluded from the Lin-CD34+ population and analysed for CD45RA and CD62L expression. A) Example of one CB sample stained with our lineage panel (top row) or the Kohn et al lineage panel (bottom row).B) Example of one BM sample stained with our lineage panel (top row) or the Kohn et al lineage panel (bottom row).The numbers in the CD62L/CD45RA plot express percentages of Lin-CD34+CD10-.

BM, bone marrow; CB, cord blood; lin, lineage.

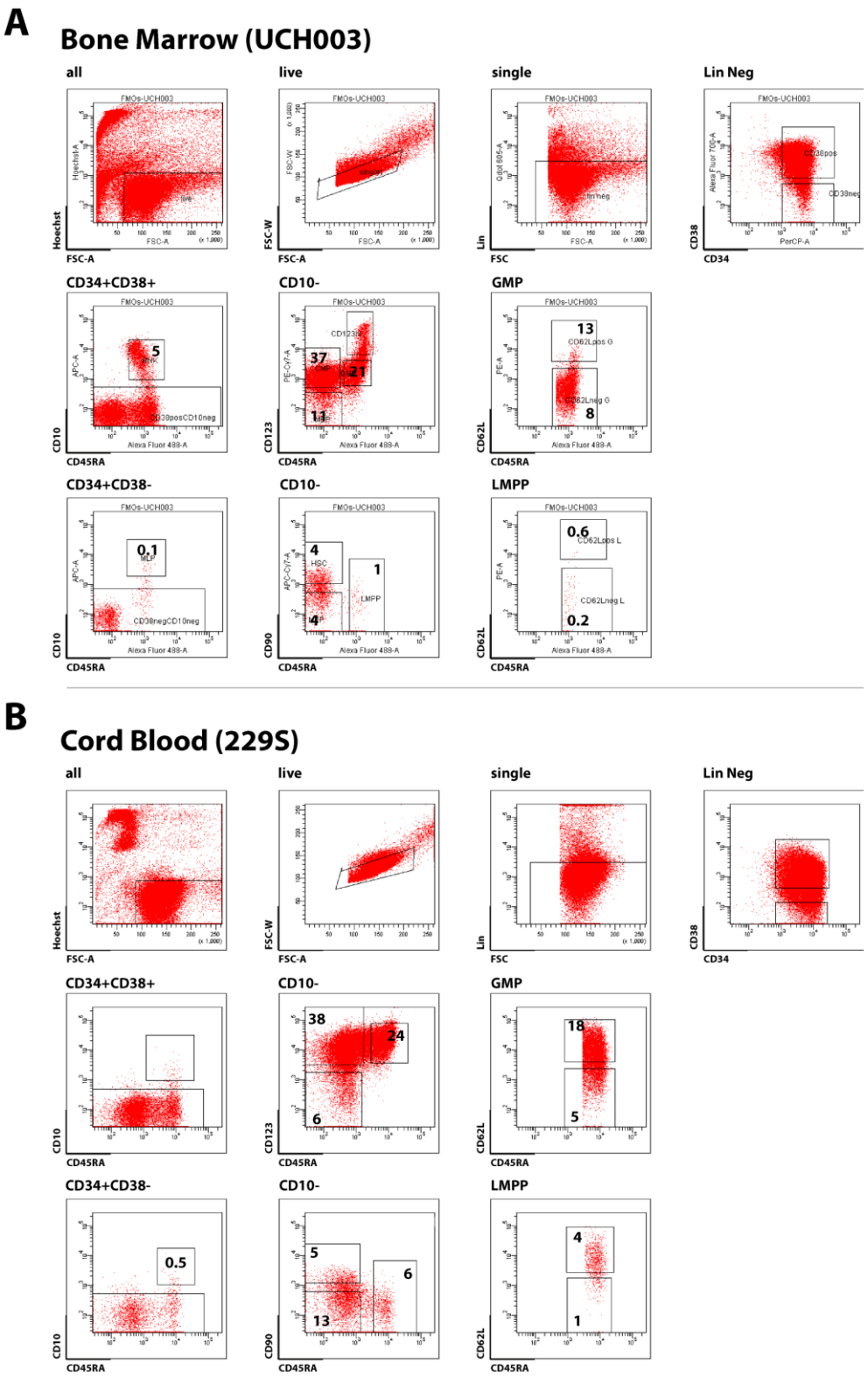

Figure 6.8. Sorting Profiles For CD62L Subpopulations Of GMP, LMPP And Other HSPCs From Cord Blood And Bone Marrow.

A) An example of a typical BM sorting profile is shown. B) This is a profile of a typical CB sorting profile. Proportions of HSPC populations are given as percentages of total Lin-CD34+ cells.
LMPP lymphoid primed multipotent progenitor; GMP, granulocyte-monocyte progenitor; BM, bone marrow; CB, cord blood; lin, lineage.

Proportions of all HSPCs are given as average percentages of Lin-CD34+ (N=6). Detailed numbers and standard deviations can be found in Table 6.4. B shows an example of a CB sort, which follows the same gating strategy as described for Figure 6.8 A. As it can be seen, the proportions of immature cells are higher in CB than in BM, therefore certain populations could be more successfully acquired from CB than from BM.

Population	BM (N=6)		CB (N=7)	
	Average	SD	Average	SD
HSC	4.1	1.5	5.1	3.2
MPP	3.6	1.9	13.6	7.6
LMPP	0.8	0.9	5.9	5.4
LMPP CD62Lneg	0.2	0.2	1.4	1.8
LMPP CD62L pos	0.6	0.8	4.4	3.8
MLP	0.1	0.1	0.5	0.5
CMP	37.1	10.0	38.2	10.1
GMP	21.3	4.9	23.9	12.6
GMP CD62Lneg	8.3	6.3	5.2	2.6
GMP CD62L pos	12.6	7.2	18.2	11.0
BNK	5.4	2.3	0.5	0.4
MEP	10.8	2.4	6.0	3.4

Table 6.4. Percentages Of HSPCs In CD62L Sorts From Bone Marrow And Cord Blood.
Percentages are expressed as fraction of live, single and lineage negative cells.

The complex sorting strategy to sort up to 10 different HSPC populations from a single sample is illustrated in Figure 3.3. It features three consecutive rounds of sorting, whereas the smallest populations are sorted in the first run (for example

the MLP) and the remaining populations are sorted into a bulk tube. The bulk cell suspensions are sequentially re-sorted to obtain all desired populations. The post-sorting purity was always checked, whenever enough cells were available. Table 2.4 summarizes all acquired sorting purities for all CD62L HSPC sorts from CB and BM. The purities of all 9 HSPC populations ranged from 92% to 98%.

6.4.2 Methylcellulose Colony Forming Assays

Sorted HSPCs from CB and BM were plated in MeC, at a concentration of 150 cells per dish. After 14 days, colonies were counted and scored for E, G, M and mixed progeny.

Cloning efficiencies from four different CB HSPC sorts can be found in Figure 6.9. HSC and MPP had the highest cloning efficiency (45% and 43%) and they could give rise to all cell lineages evaluated in this assay. Both LMPP subpopulations could give rise to GFU-G, CFU-M and CFU-GM, the individual CFU-E and CFU-mixed colonies which could be detected were attributed to a sorting impurity.

CD62L+ LMPP had a cloning efficiency around 25% and CD62L- LMPP ranged around 15%, however due to the relatively high SEM, these two populations do not differ significantly in their cloning efficiencies.

MLPs exclusively gave rise to monocytic colonies with a low cloning efficiency (8%); due to limited cell numbers only 2 MLPs could be assayed. CMPs surprisingly gave rise to erythroid colonies with great efficiency (23%) and barely any other cells. CD62L+ GMP and CD62L- GMP showed similar cloning efficiency (33% and 27%) and gave rise to gran, mono and gran-mono colonies, and a few mixed as well as erythroid colonies, which reflects issues with the sorting purity.

The MEP consistently gave rise to very small, erythroid colonies at a cloning efficiency of 10%.

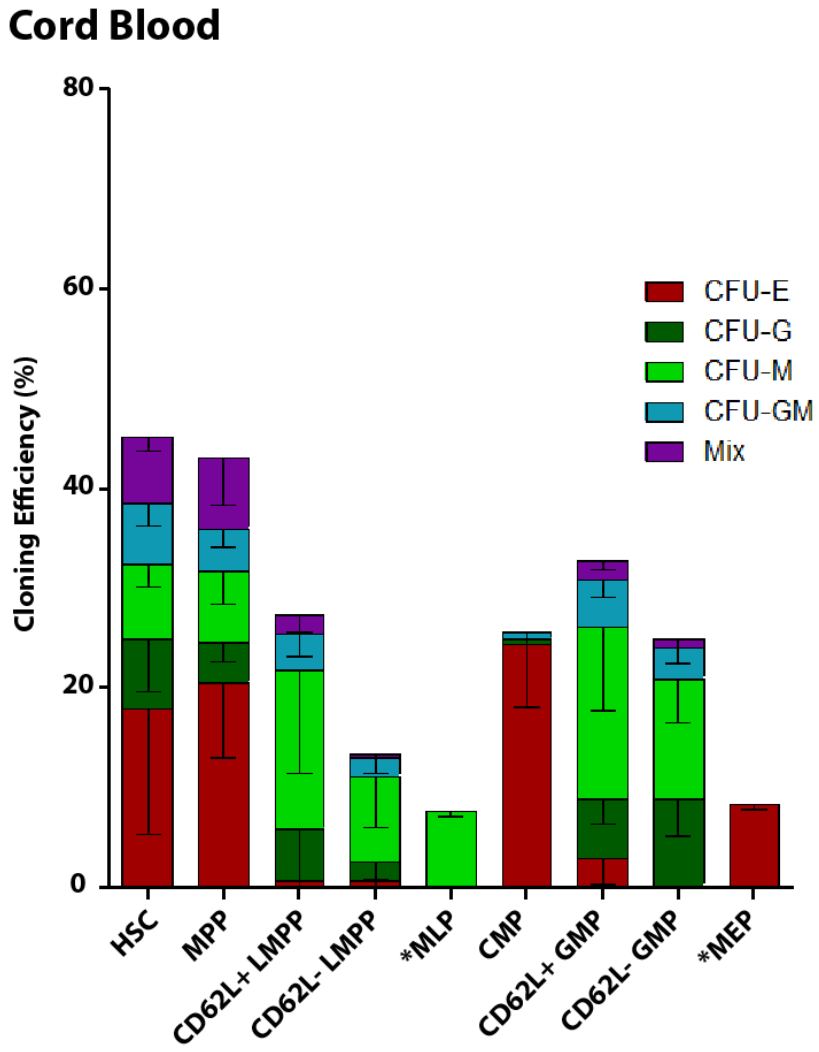

Figure 6.9. Methylcellulose Colony Forming Assay Of HSPCs and CD62L Subpopulations from Cord Blood.
150 cells of each sorted population were plated into MeC per dish. Colonies were counted after 14 days and scored for CFU-G, CFU-E, CFU-M, CFU-GM and CFU-mixed. N=4, *N=2. HSC, haematopoietic stem cell; MPP, multipotent progenitor; LMPP lymphoid primed multipotent progenitor; MLP, multilymphoid progenitor; CMP, common myeloid progenitor; GMP, granulocyte-monocyte progenitor; MEP, megakaryocyte-erythroid progenitor; CFU, colony forming unit; E, erythroid; G, granulocyte; M, macrophage; GM, granulocyte-macrophage.

Bone Marrow was also subjected to MeC colony forming assays, results are displayed in Figure 6.10. The cloning efficiency of the sorted HSPCs was lower than in CB (up to 15% as compared to 45% in CB). HSCs (15% cloning efficiency) gave rise to all different types of colonies with fairly equal frequencies; as did

MPPs, however with lower cloning efficiency (8%). LMPPs proliferated very poorly, if at all, in MeC. CD62L+ LMPP did not grow at all and CD62L- LMPP gave rise to CFU-G, CFU-M and CFU-GM at a cloning efficiency of 3%. CMP could differentiate into all types of colonies and ranged around 15% for cloning efficiency. Both GMP populations exclusively gave rise to gran, mono and gran-mono colonies. CD62L+ GMP (5%) and CD62L- GMP (15%) seemed to differ in their cloning efficiency, however, due to variable results; it is not possible to draw a reliable conclusion.

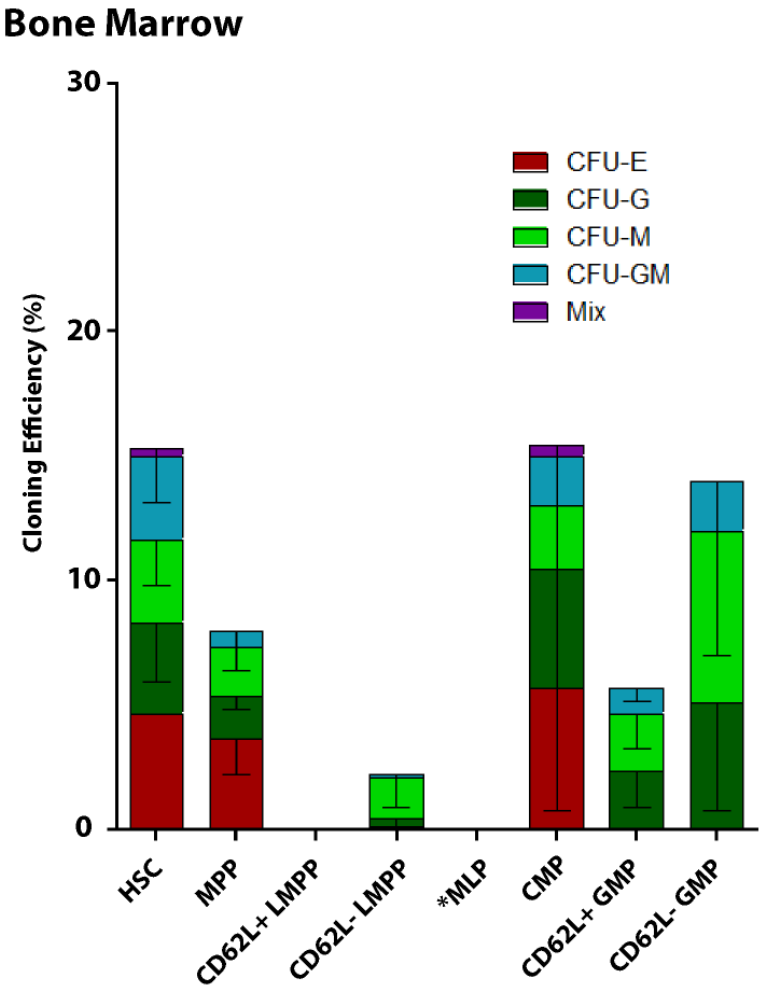

Figure 6.10. Methylcellulose Colony Forming Assay Of HSPCs and CD62L Subpopulations from Bone Marrow.
150 cells of each sorted population were plated into MeC per dish. Colonies were counted after 14 days and scored for CFU-G, CFU-E, CFU-M, CFU-GM and CFU-mixed. N=3, *N=2. HSC, haematopoietic stem cell; MPP, multipotent progenitor; LMPP lymphoid primed multipotent progenitor; MLP, multilymphoid progenitor; CMP, common myeloid progenitor; GMP, granulocyte-monocyte progenitor; CFU, colony forming unit; E, erythroid; G, granulocyte; M, macrophage; GM, granulocyte-macrophage.

6.4.3 B Cell, NK Cell, Monocytic And Granulocytic Differentiation Potential Of CD62L GMP and LMPP Subpopulations And Other HSPCs

To evaluate functional potentials of bulk HSPCs, in particular to investigate the differentiation potentials of the CD62L subpopulations of LMPP and GMP in detail, in vitro assays on MS5 stromal layers were carried out. As usual, 100 cells were plated per well and maintained for 2-3 weeks in “Our Condition” (see Appendix B Table 3 for detailed cytokine concentration and media composition). Analysis was performed by FACS, for scoring progeny for CD45+ (human) cells, CD14+ monocytes, CD15+ granulocytes, CD19+ B cells and CD56+ NK cells.

Figure 6.11 summarizes the results of cultured HSPCs on MS5 stromal monolayers for 2.5 weeks. First, dead cells and doublets were excluded, and only human CD45+ cells selected for analysis (not shown). Human CD45+ cells were then analysed for CD14 and CD15 expression, and CD14-CD15- were further separated with respect to their CD19 and CD56 expression. This figure shows a representative example of 3 individual experiments, with average percentages.

HSCs could give rise to B, NK, monocytes and granulocytes in these culture conditions. B cell output was relatively weak (1% on average), which will amplify over time, since the differentiation kinetics of HSCs are relatively slow compared to more committed progenitors. MPPs showed similar kinetics, and differentiated into all four assayed lineages. CD62L+ LMPP and CD62L- LMPP did not differ in their culture output; both populations gave rise to B, NK, mono and gran cells.

Furthermore, even the proportions of the differentiated cells were remarkably similar. MLPs, as expected, did not differentiate into granulocytes, had minimal monocytic differentiation ability, but faithfully gave rise to lymphoid cells. The CMP mainly gave rise to monocytes and granulocytes. Both GMP populations had

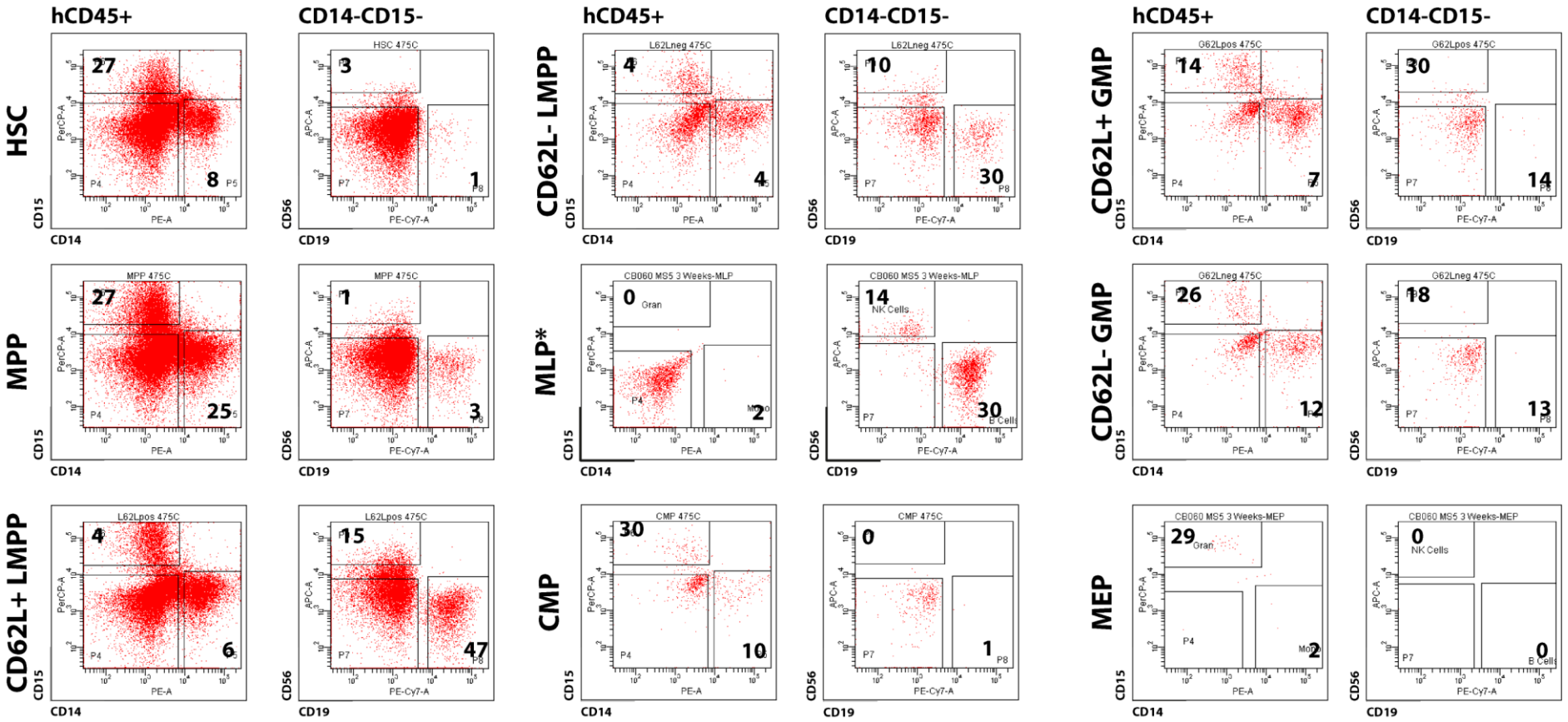

Figure 6.11. B Cell, NK Cell, Monocytic And Granulocytic Differentiation Potential of HSPCs And CD62L GMP And LMPP Subpopulations In Cord Blood.

100 sorted HSPCs were cultured for 2.5 weeks in “Our Condition” on MS5 stromal monolayers. After the designated culture period, wells were harvested and subjected to FACS analysis. Wells were scored for human (CD45+) cells, CD15+ granulocytes, CD14+ monocytes, CD19+ B cells and CD56+ NK cells. The first plot was gated on live, single and hCD45+ cells. The numbers are averages from 3 individual experiments. *N=2. HSC, haematopoietic stem cell; MPP, multipotent progenitor; LMPP lymphoid primed multipotent progenitor; MLP, multilymphoid progenitor; CMP, common myeloid progenitor; GMP, granulocyte-monocyte progenitor; MEP, megakaryocyte-erythroid progenitor; NK, natural killer.

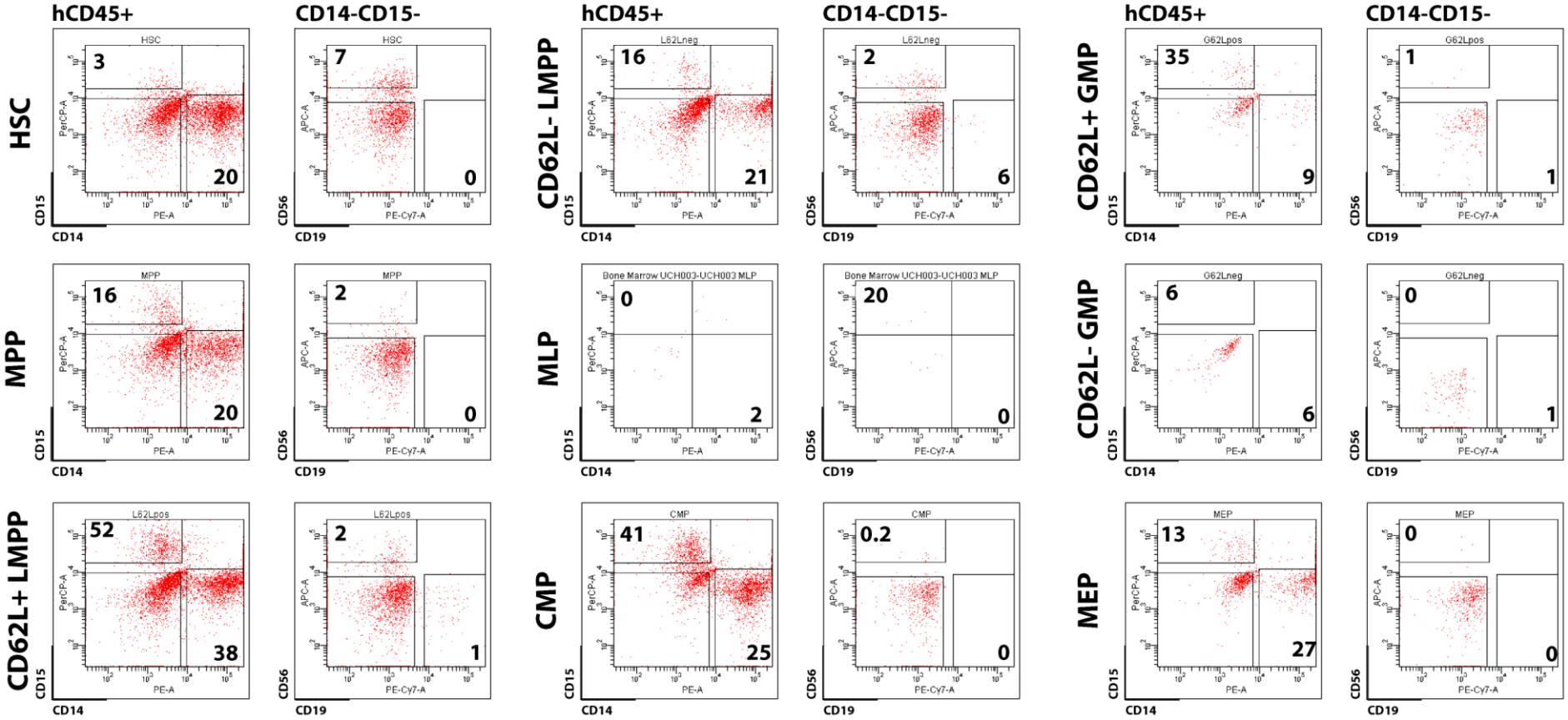

Figure 6.12. B Cell, NK Cell, Monocytic And Granulocytic Differentiation Potential of HSPCs And CD62L GMP And LMPP Subpopulations In Bone Marrow.

100 sorted HSPCs were cultured for 2.5 weeks in “Our Condition” on MS5 stromal monolayers. After the designated culture period, wells were harvested and subjected to FACS analysis. Wells were scored for human (CD45+) cells, CD15+ granulocytes, CD14+ monocytes, CD19+ B cells and CD56+ NK cells. The first plot was gated on live, single and hCD45+ cells. The numbers are averages from 3 individual experiments. *N=2. HSC, haematopoietic stem cell; MPP, multipotent progenitor; LMPP lymphoid primed multipotent progenitor; MLP, multilymphoid progenitor; CMP, common myeloid progenitor; GMP, granulocyte-monocyte progenitor; MEP, megakaryocyte-erythroid progenitor; NK, natural killer.

prominent myeloid potential, but also both of them gave rise to varying numbers of B and NK cells. The hypothesis that CD62L expression might be valuable in separating the lymphoid potential in GMP could therefore not be confirmed in these initial experiments. MEPs, which were contaminated with functional CMPs, gave rise to very low numbers of granulocytes and monocytes in culture.

The results from BM HSPCs are displayed in Figure 6.12. HSCs and MPPs differentiated into myeloid cells and low numbers of NK cells. B cells could not be detected at this relatively early time point from either one of these populations. This is consistent with the hypothesis that HSPCs isolated from adult BM is more myeloid biased than CB, and therefore it takes longer for lymphoid cells to develop.

CD62L+ LMPP and CD62L- LMPP both gave rise to granulocytic, monocytic, B and NK cells, with no significant difference in frequency or cell number. The MLP from BM barely proliferated at all in MS5 culture, residual numbers of NK and monocytic cells could be detected. CMPs on the other hand gave rise to monocytes and granulocytes with minimal contamination of NK cells, which most like stem from a sorting impurity. The CD62L subpopulations of the GMP proliferated poorly in culture on MS5 cells, and differentiated into variable numbers of monocytes, granulocytes, NK cells and B cells. Therefore, neither in cells isolated from CB nor BM does the expression of CD62L on GMPs sequester lymphoid potential in vitro on MS5 stromal monolayers.

MEPs, as expected, only showed very little proliferative potential and exclusively gave rise to myeloid cells.

6.4.4 T Cell Differentiation Potential Of CD62L GMP and LMPP Subpopulations And Other HSPCs

In order to complete the evaluation of functional potentials of HSPCs and CD62L subpopulations of GMP and LMPP, their in vitro T cell differentiation ability was investigated.

As described before, 100 sorted cells were plated on OP9-DL1 stromal monolayers in the “Six et al” condition. Cultures were maintained for 7 to 8 weeks with weekly changes of the stromal layer and culture medium. HSC-initiated wells were maintained for 8 weeks, the progeny of any other progenitor cell could be assessed after 7 weeks. Wells were harvested and stained with mABs against CD1a, CD3, CD4, CD7, CD8a and CD45 to discern various stages of T cell development. Presence of double positive T cells (CD45+CD1a+CD7+CD4+CD8a+) was necessary to attribute T cell differentiation capacity to a population.

Figure 6.13 summarizes 3 individual experiments of cultured HSPCs on OP9-DL1 monolayers. HSCs gave rise to DP T cells after 8 weeks in culture, however with a relatively low proportion of CD1a+CD7+ cells (on average 18%). 33% of CD1a+CD7+ cells differentiated from the MPP were CD4+CD8a+. Both CD62L+ LMPP and CD62L- LMPP generated DP T cells after seven weeks in culture, constituting 63% (CD62L+ LMPP) or 43% (CD62L- LMPP) of CD1a+CD7+ cells. Furthermore, both CD62L+ GMP and CD62L- GMP also differentiated into CD4+CD8a+ T cells. Cell numbers however were relatively low at this point in time, because the progeny of GMPs is prone to disappear after a few weeks in culture.

Again, the hypothesis that CD62L might segregate lymphoid potential in the GMP proved unsuccessful. Finally, the MLP proliferated extensively on OP9-DL1 stromal monolayers and consistently gave rise to DP T cells, which accounted for 54% of CD1a+CD7+ cells on average.

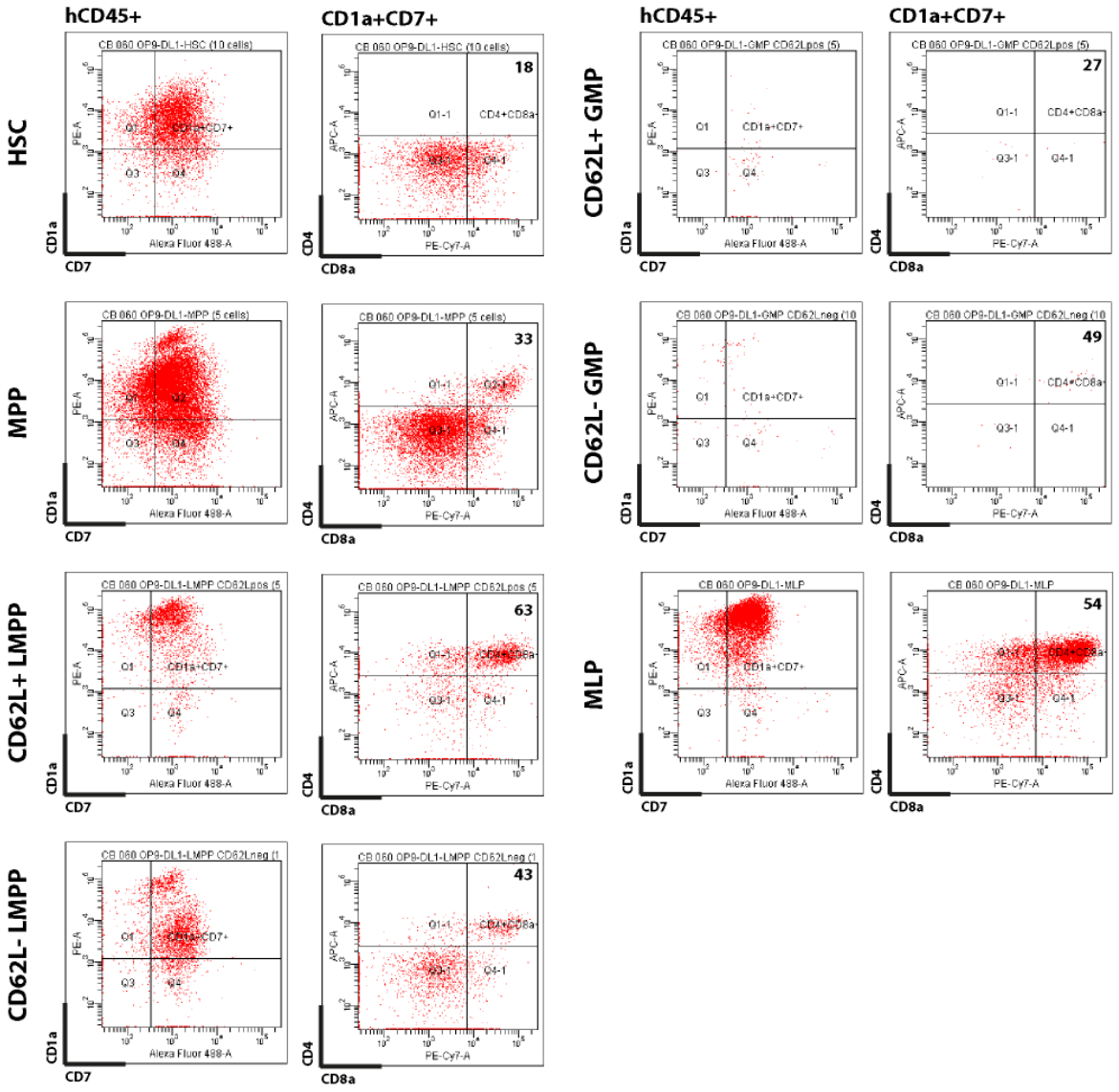

Figure 6.13. T Cell In Vitro Differentiation Potential Of CD62L LMPP And GMP Subpopulations And Other HSPCs From Cord Blood.
100 sorted HSPCs were cultured on OP9-DL1 stromal monolayers with weekly media changes. Haematopoietic cells were transferred weekly to a fresh layer of OP9-DL1 cells. After 7 weeks wells were harvested and analysed by FACS for expression of hCD45, CD1a, CD4, CD7, CD8a and CD3. Percentages of double positive T cells (CD4+CD8a+) were evaluated as proportion of CD45+CD1a+CD7+ cells. Numbers shown are averages of 3 independent experiments. Cultures initiated with HSCs were analysed after 8 weeks. HSC, haematopoietic stem cell; MPP, multipotent

progenitor; LMPP lymphoid primed multipotent progenitor; MLP, multilymphoid progenitor; CMP, common myeloid progenitor; GMP, granulocyte-monocyte progenitor.

The same set of experiments was performed for BM, however only two samples could be successfully propagated on OP9-DL1 cells in vitro. Figure 6.14 provides a summary of these two experiments. HSCs, which were cultured for 8 weeks due their delayed differentiation kinetics, could give rise to DP T cells on OP9-DL1 stromal monolayers, albeit with low efficiency (1.1% of CD1a+CD7+). MPPs showed similar results after 7 weeks and generated DP T cells, which constituted on average 3% of CD1a+CD7+ cells. Disappointingly, both CD62L+ LMPP and CD62L- LMPP generated CD4+CD8a+ T cells with similar efficiency (as of CD1a+CD7+, 2% for CD62L+ LMPP and 4% for CD62L- LMPP).

Consistent with the results already seen in CB, the CD62L subpopulations of GMPs sorted from BM both generated T cells after 7 weeks in culture. MLPs were omitted in this assay, because of the limited cell numbers which were obtained in the sorting procedure.

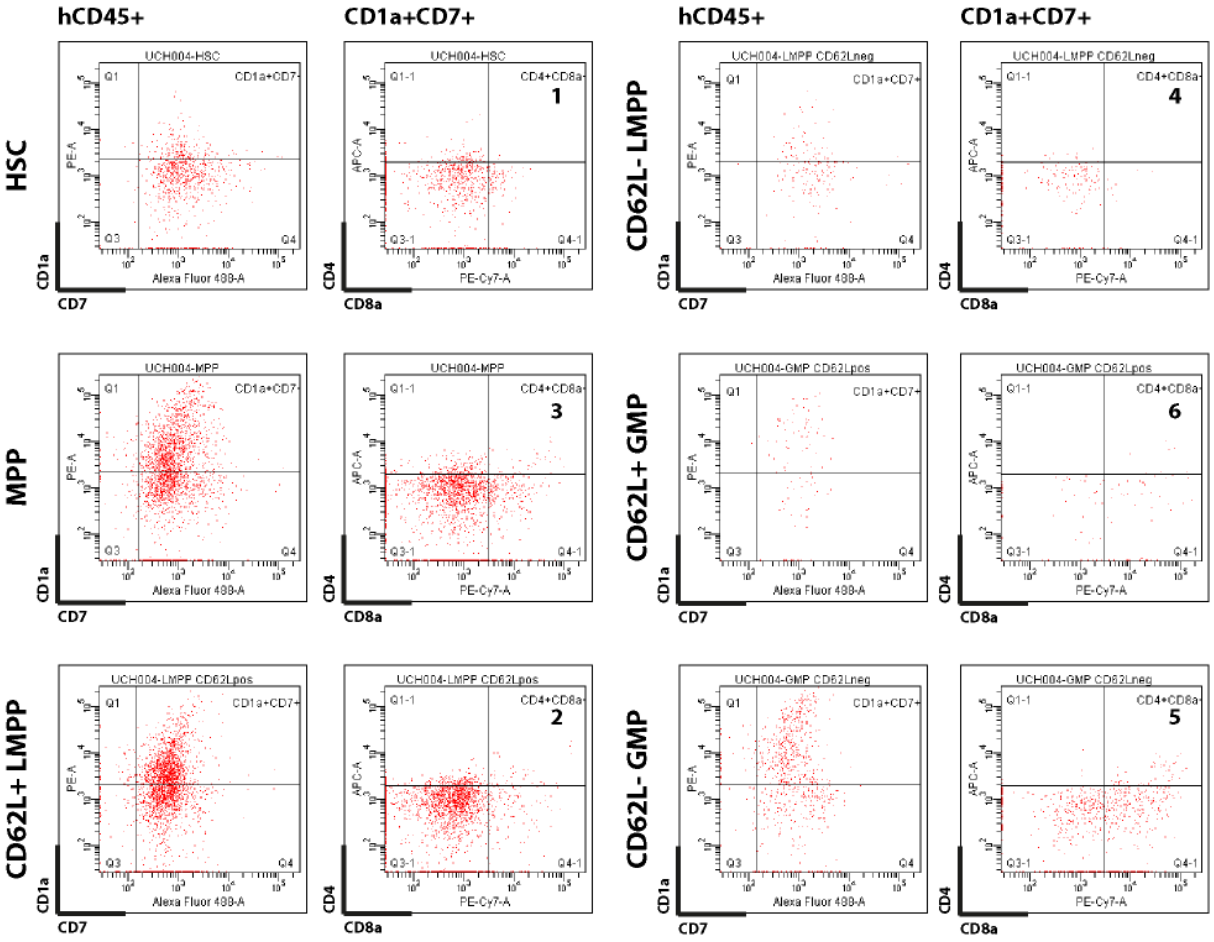

Figure 6.14. T Cell In Vitro Differentiation Potential Of CD62L LMPP And GMP Subpopulations And Other HSPCs From Bone Marrow.
100 sorted HSPCs were cultured on OP9-DL1 stromal monolayers with weekly media changes. Haematopoietic cells were transferred weekly to a fresh layer of OP9-DL1 cells. After 7 weeks wells were harvested and analysed by FACS for expression of hCD45, CD1a, CD4, CD7, CD8a and CD3. Percentages of double positive T cells (CD4+CD8a+) were evaluated as proportion of CD45+CD1a+CD7+ cells. Numbers shown are averages of 2 independent experiments. Cultures initiated with HSCs were analysed after 8 weeks. HSC, haematopoietic stem cell; MPP, multipotent progenitor; LMPP lymphoid primed multipotent progenitor; CMP, common myeloid progenitor; GMP, granulocyte-monocyte progenitor.

6.5 Discussion

6.5.1 CD53 and CD84

The tetrasparin CD53 seemed to be a promising marker with the potential to mark functionally distinct progenitor populations. Analysis of CD53 expression on the LMPP by flow cytometry revealed a continuum of CD53 expression. CD53+ LMPPs and CD53- LMPPs could be sorted to high purity and were subjected to a range of in vitro assays to determine their functional potentials. In the assays performed, both CD53+ LMPP and CD53+ LMPP showed the same in vitro differentiation potential, with very similar frequencies.

Even though in vitro assays are hampered by extensive disadvantages, for example the inability of reading out multiple lineage potentials in parallel, their use can be justified to compare the functional potentials of two immunophenotypically distinct populations in vitro. Since both populations are subjected to the same condition, a conclusion can be drawn regarding their lineage potential. However, this does not necessarily address the question if the lineage potentials, as defined in in vitro assays, reflect what would happen in a truly physiological environment. CD53 however proved unsuccessful in separating two functionally distinct populations in the CD45RA+ compartment of Lin-CD34+CD38- CB cells.

Analysis of the SLAM marker CD84 in the LMPP compartment showed rather similar results. No functional difference between CD84+ LMPP and CD84- LMPP could be detected. Even though SLAM markers are widely used to separate murine haematopoietic stem and progenitor cells, and might be implicated in separation of human CD34- AML stem cells (Quek et al, unpublished data), CD84 failed to contribute to the purification of LMPPs from human CB.

On MS5 stromal cells as well as in MeC, CD84+ LMPP and CD84- LMPP could give rise to the same cell types at virtually the same cloning efficiencies. Furthermore, expression of CD84 was very dim, and CD84+ populations could only be sorted to 64% purity, which renders the results obtained from these sorts very difficult to interpret.

These sorts were performed prior to the upgrade of the ARIA II; which means that PE was excited by the blue laser. Even though PE is a very bright fluorochrome, excitation with the blue 488nm laser might not be strong enough to separate populations which only weakly express a certain antigen. This combination of expression density of the antigen of interest, choice of fluorochrome and laser used to excite it, impacts greatly on the populations which can be separated. In the case of the CD84 subpopulations of the LMPP, the available resolution on the 488nm laser was not enough to fully separate the CD84- LMPP from the CD84+ LMPP, which reflects in the poor sorting purity.

In both cases of CD53 and CD84, the antigens to be tested were picked from microarray studies. Microarrays can provide a guide about gene expression; however it is difficult to translate this knowledge to the protein level. Post-transcriptional regulation of mRNAs, internalization or shedding of surface markers and post-translational modifications of proteins control protein levels and may be the case for discrepancies between the gene expression and the protein level. Nevertheless, gene expression levels of cell surface antigens are a first indicator to select potential new markers.

Multiplex-analysis of cell surface markers, for example in antibody coated plates would be a way to assess great numbers of cell surface antigens. A few limitations have to be kept in mind however; first, the large numbers of cells which would be

necessary to provide enough LMPPs; second, the choice of antigens and third, the potentially very high cost of such a custom designed assay.

In the years to come, Cytometry by Time-of-Flight (CyTOF) will complement flow cytometry. This mass spectrometry based technique allows immuno-labelling of cells with antibodies stably conjugated to elemental isotopes. Through vaporisation of single cells in a stream, not unlike flow cytometry, the cellular components are ionised and these ions are analysed by a time-of-flight mass spectrometer. Up to 34 parameters could be analysed in parallel, with virtually no compensation requirements; including assessment of viability, DNA content and relative cell size[118]. With the help of extensive data analysis and the correct algorithm, the authors were able to construct a 2D representation of the expression of cell surface markers on different cell types.

This would be a very powerful tool to not only assess the expression of new cell surface markers on known populations, but also to map the emergence/loss of already known markers during differentiation. Single cell resolution as well as the possibility to investigate intracellular epitopes (for example signalling molecules as in Bendall et al[118]) in the context of their surface markers will provide an unparallelled in depth look at haematopoietic stem and progenitor cells. Of course, there are also limitations, such as the destructive nature of this means of analysis. Populations of interest can only be analysed by CyTOF, it is not possible to sort them and subject them to functional in vitro assays. A way around this limitation would be the translation of the CyTOF analysis panel to a common flow cytometry antibody panel in a simplified version. At the moment, it is yet unclear how many cells would be needed for such an experiment and how difficult the stable

conjugation of antibodies to elemental marker proves, but this is a promising technique for the future nevertheless.

Combining a surface marker panel with an array of differentiation specific transcription factors/intracellular molecules, with added markers to assess proliferation, DNA content as well as apoptosis on a single cell level would be possible by CyTOF.

6.5.2 CD150, Notch-1 and CD127

CD150, Notch-1 and CD127 all hold significant positions in haematopoiesis. CD150 is expressed on murine HSCs[3,119], Notch-1 is involved in differentiation and essential particularly for lymphopoiesis[90]. CD127, also known as IL-7Rα, can bind and initiate the response to a crucial lymphoid cytokine, IL-7[114,120,121]; and is furthermore expressed on the murine common lymphoid progenitor[6]. These were the reasons which initiated expression analysis of these cell surface markers in the LMPP compartment in CB.

Expression of CD150 had been investigated on human haematopoietic cells before[116], this result was verified in our hands and with our standard FACS analysis panels. Expression of CD150 on the human LMPP from CB resembled a continuum, with 90% being CD150-. The remaining 10% of $CD150^{+/low}$ LMPPs could not be sorted to satisfying purity and therefore in vitro functional assay results are not reliable. CD150 did not prove to be a useful marker in separating out any functional potential in the LMPP, in tested in vitro conditions. Cell surface markers expression may differ between species, knowledge acquired in one species does not necessarily translate to another[1]. An example would be CD34,

which is expressed on early human HSPCs[19,37,72], however in mouse it marks more committed myeloid progenitors, such as the GMP[10].

Notch-1 was expressed on virtually all LMPPs in CB, therefore it was not possible to sort subpopulations of the LMPP. It was hypothesized that Notch-1 is too crucial in early differentiation, which might explain its presence on all investigated cells.

CD127 however was expressed on a fraction of LMPPs and MLPs. In this round of experiments, CD10 was included to permit simultaneous analysis of the MLP as well. The CD45RA compartment in human CB contained 4 distinct populations if analysed for the expression of the markers CD127 and CD10: double negative (CD127-CD10-), CD127+CD10-, CD127-CD10+ and a double positive (CD127+CD10+) population. It has to be kept in mind that especially the CD10+ populations were very small and therefore not enough cells could be obtained to subject them to a range of in vitro assays or check the post-sort purity.

Nevertheless, results from MS5 culture assays, indicate that CD127 does not contribute, under these conditions, to a segregation of particular potentials. The only difference which could be discerned was attributed to CD10, the upregulation of which coincides with loss of granulocytic potential, as extensively shown before in Chapter 5.

Unfortunately, CD127 failed to isolate a human common lymphoid progenitor in the Lin-CD34+CD38-CD45RA+ compartment. Later research reported the identification of a human CD38+CD127+ human CLP in BM, however it was not extensively characterised and single cell data is missing[15]. In this study, no CD38+CD127+ cells could be detected.

6.5.3 CD62L (L-Selectin)

A report published by Kohn et al[21] proposed that CD62L is the earliest cell surface marker associated with lymphoid priming, in contrast to previous work which suggested CD7 and/or CD7 are linked to early lymphoid potential[22,67,68,97]. It was shown that a the Lin-CD34+CD45RA+CD62L^{hi} population isolated from BM (referred to as "CD62L^{hi}" from now on) retained myeloid and lymphoid in vitro differentiation potential; could even engraft for short periods of time at low levels in immunocompromised mice and clustered intermediate between the immature CD34+CD38- fraction and the more committed CD10+ population in gene expression analysis[21].

However, the immunophenotyping approach was different from previous efforts; disregarding well-defined markers for this purpose, such as CD38 and CD90[37] or CD123[41]. I set out to place the CD62L^{hi} population into context with my current and our previous work[19] and determine how it correlated with the Lin-CD34+CD38-CD90-CD45RA+ LMPP in BM and CB. Immunophenotyping revealed that the CD62Lhi population was a mixture of GMP and LMPP, and it read out in functional assays accordingly. Therefore, rather than investigating this imperfectly purified population, CD62L+ and CD62L- subpopulations of LMPP and GMP were sorted and their functional potentials determined in vitro, as well as RNA sequencing profiles were acquired.

In human, as well as mouse, previous research showed that the GMP still has considerable residual lymphoid differentiation potential[19,43]. CD62L seemed to be a promising marker in sequestering GMPs with lymphoid potential, assuming the GMP is a heterogeneous population. There is increasing evidence, that at least in

murine haematopoiesis, the GMP is a mixture of at least two, if not more populations[85]. It is important to acquire an understanding of the heterogeneity of a population. This can be achieved through limit dilution assays and other single cell assays on the functional level. On the molecular level, an increasing choice of single cell qPCR and even RNA-Sequencing applications is available and might provide a means to investigate the heterogeneity of HSPC populations.

On the functional level, no evidence could be found that CD62L is associated with lymphoid priming in the GMP or the LMPP. The CD62L+ GMP did not retain any more lymphoid differentiation capacity than the CD62L- GMP in in vitro functional assays. Both could give rise to B and NK cells in MS5 cultures, as well as T Cells on OP9-DL1 stromal monolayers with similar efficiencies. GMPs isolated from cord blood seemed to have higher proliferative potential and showed more lymphoid progeny than their adult bone marrow counterparts. While lymphoid progeny could be detected in BM GMP cultures, it was not as abundant as from CB GMPs. This is consistent with the hypothesis that bone marrow stem and progenitor cells are increasingly myeloid-biased with age, which in turn means diminished lymphoid potential[122,123].

Research performed on murine BM from aged mice revealed that there are multiple different types of lineage biased (or balanced) HSCs present, with myeloid biased HSCs occupying the largest proportion[122]. HSCs from aged mice are not only myeloid biased but also show engraftment deficiencies in transplantation experiments. Furthermore, they exhibit decreased activity and delayed proliferation kinetics in stromal co-cultures[122], which is consistent with results from this study. In addition, the HSC compartment in aged murine BM is enlarged, at least immunophenotypically; however it is hypothesized that the

frequency of true HSCs is reduced and the number of primitive progenitors are elevated.

It is yet unclear if this aging mechanism is triggered by cell intrinsic changes, alterations of the microenvironment or a combination of these and possible other factors. The first theory could at least in part be confirmed by research from Dykstra et al, when they aged HSCs through serial transplantations and could therefore re-establish the myeloid-biased phenotype[122].

It has to kept in mind however, that most of the aging research has been performed in mouse models, due to ethical and practical reasons, but there is evidence from studies with human bone marrow suggest similar tendencies[15,124]. If it is assumed that the GMPs from BM assayed in this study are derived from myeloid-biased HSCs, it would explain their diminished lymphoid potential and in general lower proliferative ability in these experiments. It is widely known that the human immune system declines with age ("immunesenescence"), especially number of B[125], T[126], NK cells[127] and DCs[128] are decreased with age. Myeloid cells one the other hand, are more prominent which can lead to a pro-inflammatory environment which might be harmful for the individual[129,130].

Cord blood, on the contrary, is very proliferative, and a mixture of adult and foetal cells. Cells from foetal tissues have very high proliferative potential and can contain foetal stem cells[131,132] (FSC). A number of studies have confirmed that stem and progenitor cells isolated from CB have high cloning efficiency in liquid and semi-solid culture media[133-135]. If compared to cells of the same immunophenotype from BM, CB stem and progenitors generate higher numbers of progeny cells in culture. Furthermore, CB cells have higher proliferative and replating potential in the immature stem and progenitor compartment[135,136].

Interestingly, the earlier in ontogeny stem and progenitor cells are isolated, the higher their proliferative potential rises. In a study comparing foetal liver HSCs to HSCs isolated from CB and BM, foetal liver HSCs had the highest proliferative index.

Furthermore, they were also the first to lose CD34 expression in culture, indicating differentiation of foetal liver HSCs and hinting at fast differentiation kinetics[131]. This trend of decreasing proliferative potential and delayed differentiation kinetics seems to continue through neonatal CB up to adult BM. If these observations are examined in the context of ontology they make perfect sense, considering how rapidly an individual evolves from the single cell stage up until birth.

Moreover, CB is not only a source for HSPCs, FCSs as well as MSCs can be isolated. Further evidence also suggests that under the right conditions, CB cells can be differentiated into neuron-like cells[137], which suggests a certain plasticity in cell fate decisions which is retained in primitive cells in CB. This might also tie in with the increased lymphoid potential of cells isolated from neonatal tissues and a degree of plasticity, even in immunophenotypic compartments of more committed progenitors in adult tissues.

A combination of these reasons might explain the difference in cloning efficiency from CB and BM in this study, as well as the discrepancies in the in vitro differentiation potentials of HSPC populations isolated on basis of their immunophenotype from CB and BM.

Another point I would like to address was the low but persistent frequency with which the GMP gave rise to erythroid cells. It was hypothesized that this might be attributed to low sorting purities, but also due to the fact that the marker BAH-1 is missing in the FACS panel used to isolate HSPCs in this study.

BAH-1 was first marketed as antibody directed against the TPO-receptor (CD110). In conjunction with CD123 and CD45RA, these three markers enable purification of functional GMP (CD123+CD45RA+BAH-1-), CMP (CD123+CD45RA-BAH-1) and MEP (CD123-CD45RA-BAH-1-)[19,42]. However, it was retracted by the manufacturer, since evidence accumulated that BAH-1 does not bind the CD110 antigen. Including this marker into my FACS panels might provide additional separation especially in the myeloid compartment and therefore allow me to isolate highly pure progenitor populations.

In order to obtain all the populations of the human haematopoietic hierarchy to subject them to molecular and functional assays, an extensive sorting protocol is required,

Sorting up to 10 different HSPC populations poses a set of issues which have to be solved in order to obtain highly pure and viable populations. As mentioned previously, the struggle to sort sufficient cell numbers for particular populations can be very challenging. To maximise yield, the sorting strategy to sort HSC, MPP, CD62L+ LMPP, CD62L- LMPP, MLP, CMP, CD62L+ GMP, CD62L- GMP and MEP from a single sample had to be adapted. Only four different populations can be sorted at any one time, therefore it has to be carefully planned which population will be sorted in the first, second etc. round of sorting. As mentioned before, the loss per single round of sorting is about 50%, therefore cell types which are more abundant should be sorted in later rounds. This problem was solved by first sorting LMPP subpopulations and MLP in the first round, with everything else being sorted into a bulk tube (CD38+ and HSC/MPP for example). CD38+/HSC/MPP was then resorted into HSC, MPP and MEP, with GMP/CMP going into the bulk tube. The final sort then separated CMP, CD62L+ GMP and

CD62L- GMP. To illustrate this process and other, less complex sorting strategies, Figure 3.3 was included.

It has to be mentioned that the purity of sorted populations increases with every round of sorting. If sample numbers are high enough, the losses during each round of sorting can be tolerated in order to achieve highly pure populations.

All in all, these results summarize different efforts to purify the LMPP population further, through the addition of another cell surface marker. Until now, I was not successful in doing so however. RNA sequencing, as discussed in the next chapter, might promise a better way to solve this question.

7 Preliminary RNA Sequencing Data Analysis

7.1 Sorting of CD62L LMPP and GMP Subpopulations and Other HSPCs For RNA Sequencing and RNA Isolation

HSPCs were sorted to high purity from cord blood and bone marrow samples following the usual procedure, with only a few changes. To extract RNA from sorted HSPCs, they are sorted directly into RLT buffer, which will lyse the cells and provides a more favourable environment to stabilize RNA. Because the cells were lysed directly, the purity of the populations had to be assessed before the sort. After the desired number of cells per population was sorted, cells in RLT buffer were snap frozen on dry ice and stored at -80°C until RNA was extracted.

RNA was extracted through column purification and eluted in nuclease free water. RNA integrity (RIN) scores were determined with the Agilent Bioanalyzer to assess RNA quality. The higher the RIN score, the higher the RNA quality is. The Bioanalyzer is also capable of providing a value for the RNA concentration. Samples with a RIN score of at least 8 and at a minimum concentration of 20 pg/µL were used in this study. 24 samples were selected for RNA sequencing. A detailed summary of the characteristics of these samples can be found in Table 7.1. 17 of these populations were sorted from CB, from 3 different biological specimens. 7 populations were sorted from BM, from only one sample so far. Number of cells sorted per sample ranged from 3,500 to 20,000 and they were sorted with an average purity of 96% (+/- 3.54%). The lowest RIN score was 8.4, the highest 10, and the average RIN score was 9.63 (+/- 0.45). On average, the RNA concentration was 265 pg/µL (+/- 205.4), however it ranged from 24 pg/µL to

686 pg/µL. All Bioanalyzer traces and images of the gels can be found in Figure 7.1.

Sample ID	Population	# sorted cells	Purity (%)	RIN score	RNA [c] pg/uL	Sequencing ID
959Z	CD62L+ LMPP	5000	99	10	364	H
	CD62L- LMPP	5000	85	8.9	91	I
	CMP	5000	96	10	106	J
	CD62L+ GMP	5000	96	9.1	132	K
	CD62L- GMP	5000	97	8.7	101	L
229S	HSC	4000	95	8.4	33	A
	MPP	8000	93	10	108	B
	CD62L+ LMPP	10000	93	9.9	168	C
	CMP	12000	99	9.8	235	D
	CD62L+ GMP	10000	98	9.7	276	E
	CD62L- GMP	10000	99	9.9	281	F
	MEP	11500	99	9.9	352	G
809G	MPP	10000	97	9.7	258	M
	CD62L+ LMPP	12000	99	10	760	N
	CD62L- LMPP	5000	93	9.7	182	O
	CD62L+ GMP	10000	90	10	518	P
	CD62L- GMP	8000	95	9.9	686	Q
UCH003	HSC	10000	96	9.3	105	R
	MPP	10000	99	9.4	102	S
	CD62L- LMPP	3500	N.A.	9.6	24	T
	CMP	20000	99	9.9	624	U
	CD62L- GMP	10000	98	9.4	194	V
	MEP	10000	98	10	426	W
	CD123hi	10000	N.A.	9.9	246	X

Average:	96.05	9.63	265.44
SD:	3.54	0.45	205.40

Table 7.1. Summary Of All Populations Sorted For RNA Sequencing.
This table shows all populations sent for RNA Sequencing, the respective purity, amount of cells sorted, RIN score as acquired on the Agilent Bioanalyzer, RNA concentration in pg/µL and the code for sequencing. 959Z, 229S and 809G are CB samples, UCH003 is a BM from a young donor. The average purity, RIN score and RNA concentration are stated at the bottom, +/- standard deviation.
RIN, RNA integrity score; HSC, haematopoietic stem cell; MPP, multipotent progenitor; LMPP, lymphoid-primed multipotent progenitor; CMP, common myeloid progenitor; GMP, granulocyte-monocyte progenitor; MEP, megakaryocyte-erythroid progenitor; BM, bone marrow; CB, cord blood.

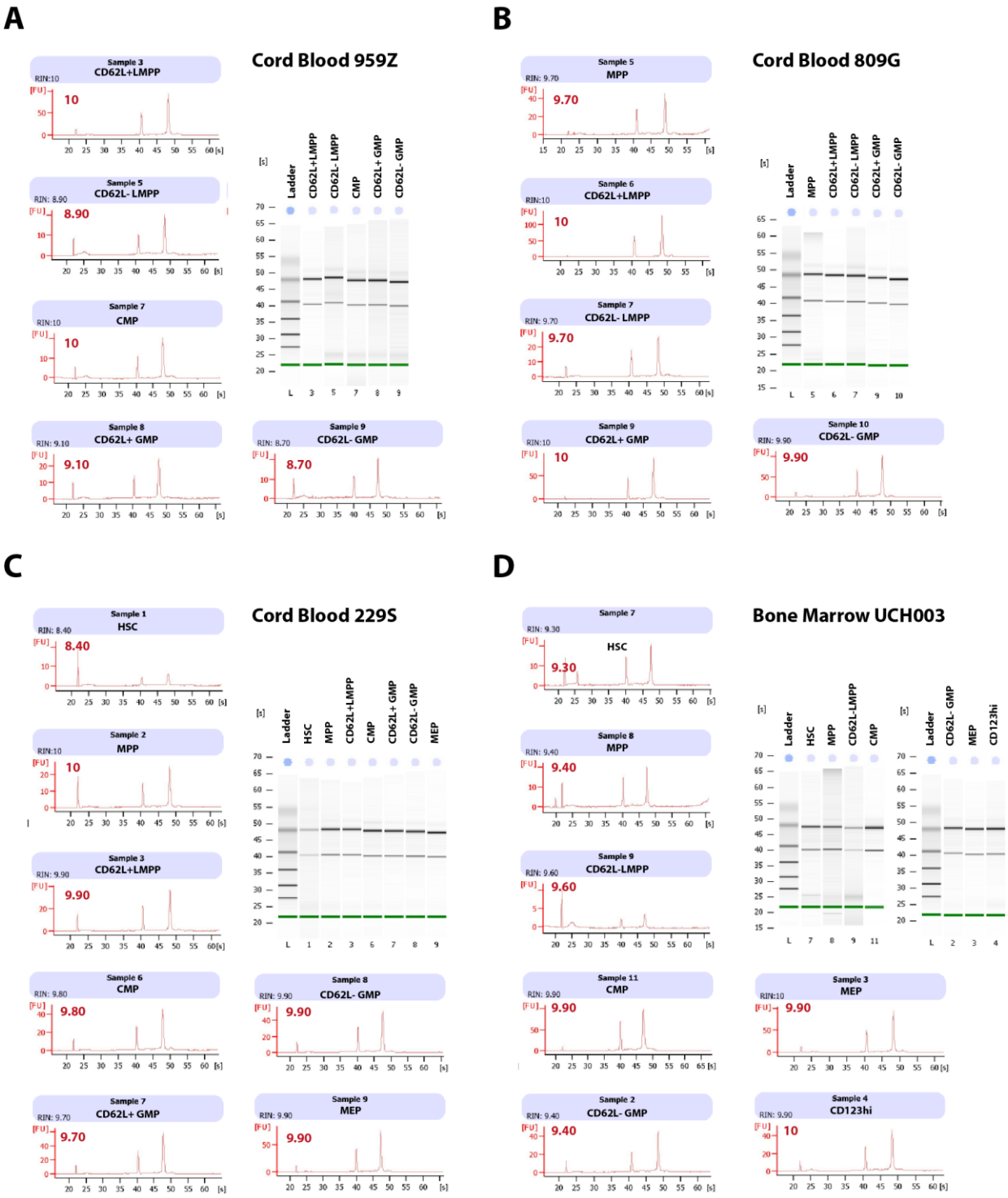

Figure 7.1. Quality Checking Of RNA Extracted From Sorted HSPCs From Bone Marrow And Cord Blood.

5,000-10,000 progenitors were sorted directly into RNA-later solution, snap frozen and stored at -80ºC. RNA was extracted with the QIAgen RNeasy micro kit and eluted in 12µL nuclease free water. RIN scores were acquired on the Agilent Bioanalyzer. Shown here are Bioanalyzer traces and the gels on which the RNA was analysed. RIN scores are shown in red. CB sample 959Z is shown in A), CB 809G in B), CB 229S in C) and BM UCH003 in D).

RIN, RNA integrity score; HSC, haematopoietic stem cell; MPP, multipotent progenitor; LMPP, lymphoid-primed multipotent progenitor; CMP, common myeloid progenitor; GMP, granulocyte-monocyte progenitor; MEP, megakaryocyte-erythroid progenitor.

7.2 cDNA Preparation and RNA Sequencing At The WTCHG

The 24 samples were coded and 3µL of each transferred to a 96-well plate and passed on to the Wellcome Trust Centre for Human Genetics. There, all samples were subjected to cDNA generation with the SMARTer kit and library preparation. Figure 7.2 summarizes the principle of the cDNA generation. In brief, mRNA is added to the reaction mix containing, enzymes, the SMARTer-oligonucleotide, oligo-dT primers, and nucleotides. The oligo-dT primer as well as the SMARTer oligonucleotide can be coupled to a sequencing adapter. First strand synthesis occurs after priming with the oligo-dT primer and the extension of the first strand by the SMARTScribe enzyme. This enzyme is capable of generating a short overhang which can then be primed by the SMARTer-oligonucleotide to enable second strand synthesis. At this point, template switching occurs and the second strand is amplified, which contains both sequencing primers at the end.

Sequencing was performed on the Illumina HiSeq 2000 sequencer. The output was mapped with the help of TopHat, merged and trimmed for unmapped reads in SAMtools. One sample failed to sequence for unknown reasons, sequencing ID “l”, one biological replicate of a CD62L- LMPP, which left 23 data sets for analysis. Table 7.2 contains the read counts of both technical replicates for all sequenced samples. On average, 26,585,823 reads per sample were acquired (SD: +/- 3,360,230), and the average difference between the two technical replicates was 1,443,681 reads (+/- 609,190).

Sequencing data was returned in a trimmed, mapped and merged format.

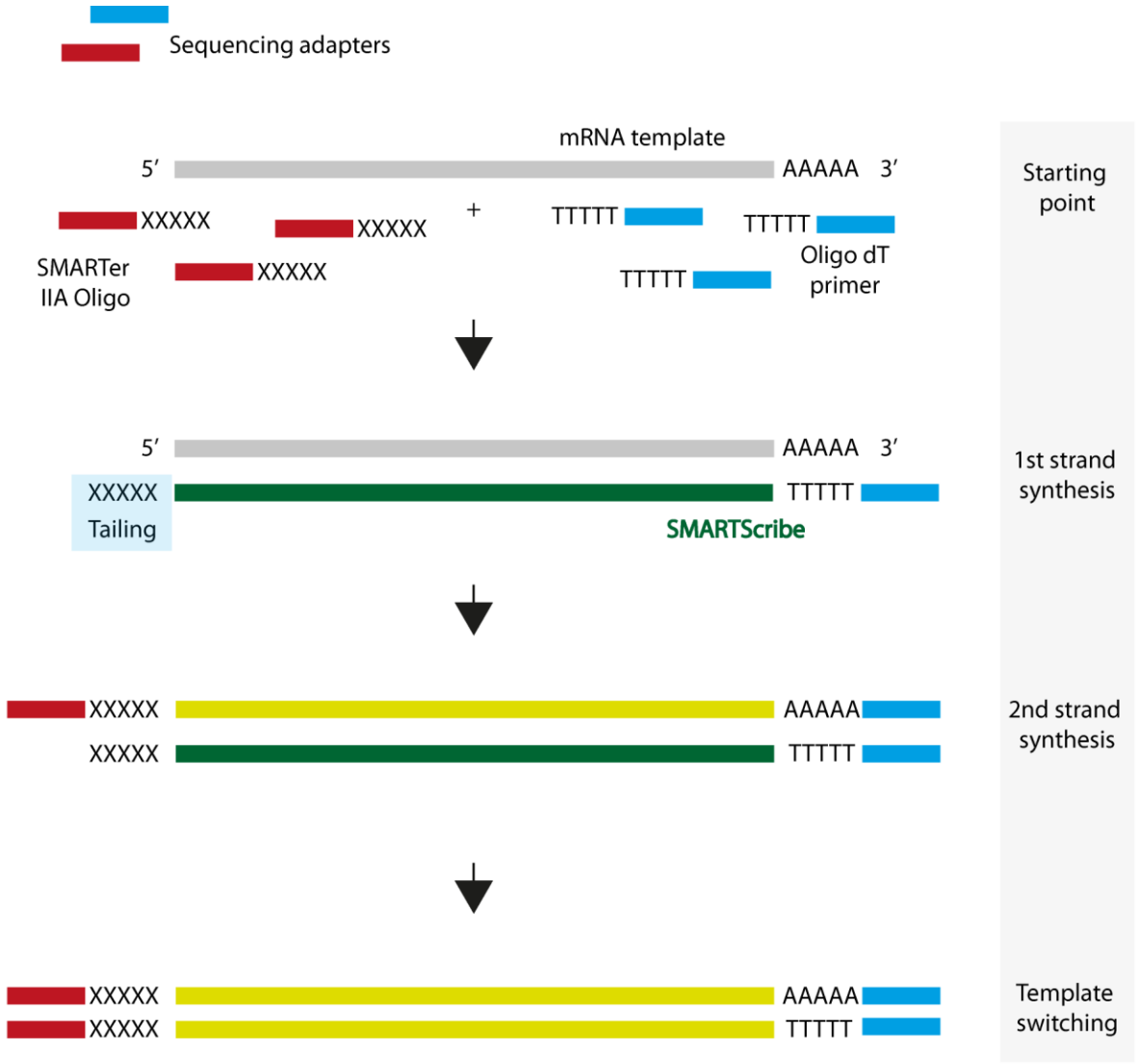

Figure 7.2. cDNA Generation With The SMARTer Kit.
SMART (Switching Mechanism at 5' End of RNA Template) is a technique which permits the incorporation of known sequences at the end of cDNA during first and second strand synthesis. First, the mRNA template is added to the reaction mix containing enzymes, nucleotides and SMARTer-oligos coupled to the sequencing adapters and to an oligo-dT primer. The SMARTScribe enzyme is capable of extending the oligo-dT primer and synthesising the first strand of cDNA. It also generates an overhang (XXX). The SMARTer-oligo can then pair with the overhang therefore incorporate the second sequencing adapter, while the second strand is synthesised. Then, template switching occurs and the second strand is amplified.
cDNA, copy-DNA; mRNA, messenger RNA.

Population	Replicate 1		Replicate 2		Difference between Replicates
	Name	Counts	Name	Counts	
HSC	WTCHG_47712_225 Sample:A	25,899,885	WTCHG_47649_225 Sample:A	23,769,740	2,130,145
MPP	WTCHG_47712_226 Sample:B	23,833,281	WTCHG_47649_226 Sample:B	21,946,084	1,887,197
CD62Lpos LMPP	WTCHG_47712_227 Sample:C	23,124,795	WTCHG_47649_227 Sample:C	21,659,688	1,465,107
CMP	WTCHG_47712_228 Sample:D	27,902,176	WTCHG_47649_228 Sample:D	25,572,798	2,329,378
CD62Lpos GMP	WTCHG_47712_229 Sample:E	24,981,532	WTCHG_47649_229 Sample:E	23,302,486	1,679,046
CD62Lneg GMP	WTCHG_47712_230 Sample:F	27,923,289	WTCHG_47649_230 Sample:F	25,491,375	2,431,914
MEP	WTCHG_47712_231 Sample:G	29,031,315	WTCHG_47649_231 Sample:G	26,611,616	2,419,699
CD62Lpos LMPP	WTCHG_47712_232 Sample:H	25,218,144	WTCHG_47649_232 Sample:H	22,934,348	2,283,796
CMP	WTCHG_47713_234 Sample:J	31,370,153	WTCHG_47650_234 Sample:J	30,255,760	1,114,393
CD62Lpos GMP	WTCHG_47713_235 Sample:K	29,455,092	WTCHG_47650_235 Sample:K	28,614,536	840,556
CD62Lneg GMP	WTCHG_47713_236 Sample:L	28,341,105	WTCHG_47650_236 Sample:L	27,446,442	894,663
MPP	WTCHG_47713_237 Sample:M	32,428,201	WTCHG_47650_237 Sample:M	30,920,711	1,507,490
CD62Lpos LMPP	WTCHG_47713_238 Sample:N	32,027,801	WTCHG_47650_238 Sample:N	30,750,424	1,277,377
CD62Lneg LMPP	WTCHG_47713_239 Sample:O	23,888,690	WTCHG_47650_239 Sample:O	23,259,963	628,727
CD62Lpos GMP	WTCHG_47713_240 Sample:P	33,791,140	WTCHG_47650_240 Sample:P	32,399,683	1,391,457
CD62Lneg GMP	WTCHG_47714_241 Sample:Q	29,645,909	WTCHG_47651_241 Sample:Q	28,220,612	1,425,297
HSC	WTCHG_47714_242 Sample:R	27,165,265	WTCHG_47651_242 Sample:R	25,648,971	1,516,294
MPP	WTCHG_47714_243 Sample:S	23,518,975	WTCHG_47651_243 Sample:S	23,117,410	401,565
CD62Lneg LMPP	WTCHG_47714_244 Sample:T	27,514,531	WTCHG_47651_244 Sample:T	26,042,510	1,472,021
CMP	WTCHG_47714_245 Sample:U	28,524,252	WTCHG_47651_245 Sample:U	27,205,988	1,318,264
CD62Lneg GMP	WTCHG_47714_246 Sample:V	27,092,033	WTCHG_47651_246 Sample:V	25,708,744	1,383,289
MEP	WTCHG_47714_247 Sample:W	20,039,434	WTCHG_47651_247 Sample:W	19,749,130	290,304
123hi	WTCHG_47714_248 Sample:X	25,359,270	WTCHG_47651_248 Sample:X	24,242,588	1,116,682
			Average:	26,585,823	1,443,681
			Std. Deviation:	3,360,230	609,190

Table 7.2. Summary Of All Sequenced Populations.

Samples were sequenced in two technical replicates. This table shows the range of read counts acquired (see colour coded cells for lowest and highest read count), the average number of reads (+/- SD) as well as the difference of reads between two technical replicates.

7.3 Quality Check With the FASTQC Quality Tools

The quality of sequenced data before mapping was assessed with the help of the FASTQC quality tools, which provide a means to check overall base calling quality, GC contents, duplication levels, per base sequence quality, read length and per base sequence content.

The first measure of quality which was focused on is the base calling quality, which is expressed in a Phred score as defined by the sequencer, the Illumina HiSeq in this case. Automated sequencers assign a quality score to each base call; historically this was done by the Phred programme[138]. Also known as the Q-score, the Phred score indicates the probability that the base call was not correct[139]. Q(20) means that the base was called with 99% accuracy, and Q(30) even indicates a 99.9% accuracy of the base call. Generally, Phred scores above 30 are considered high quality calls and will virtually have no errors[139]. Figure 7.3 A shows 3 representative Phred score plots of 3 populations sequenced from CB. The x-axis shows the position in the 50 base pair read and the actual Phred score is given on the y-axis. The yellow boxes indicate the 25^{th}/75^{th} percentile of each value, with the median in depicted as a red line, the mean as a blue line and the standard deviation visualized as black error bars.

Towards the start and end of the read, base calling quality decreases slightly in all three samples, to a Phred score of about 31, reaching a maximum of 40 in the centre of the read. Outliers still remained above a Phred score of 20, which indicates sufficient base calling quality.

A different representation of the base calling quality is given in Figure 7.3 B. The average quality per read is shown on the x-axis and the number of reads is depicted on the y-axis. This results in a curve which shows the average quality per

read. As it can be seen for all three populations sorted from CB, the peak lies between Phred score 38-40, which suggests the overall base calling quality is excellent. The data could be trimmed to allow only high quality base called reads for analysis.

In Figure 7.3 C, the per base sequence content is shown. The graph shows the position in the read on the x-axis and the sequence content on the y-axis. Roughly, the sequence content for each base should be 25%, and the fluctuations at the start of the read can be explained by the primers used for RNA sequencing.

In populations sorted from BM, the quality measures looked similar. Figure 7.4 A illustrates the Phred scores for three BM populations, which was in the same range as the ones from CB. The mean Q-score ranged from 31 to 37, and the lowest outliers stayed above 22.

Looking at the distribution of Phred scores, Figure 7.4 B shows that, similar to CB, the average lay between 38 and 40 which correlates with excellent base calling quality.

The per base sequence content in Figure 7.4 C in the BM populations shows fluctuations at the start of the read, which, as mentioned before, is due to the nature of the sequencing primers used and equilibrates roughly around 22-25% for all four types of bases.

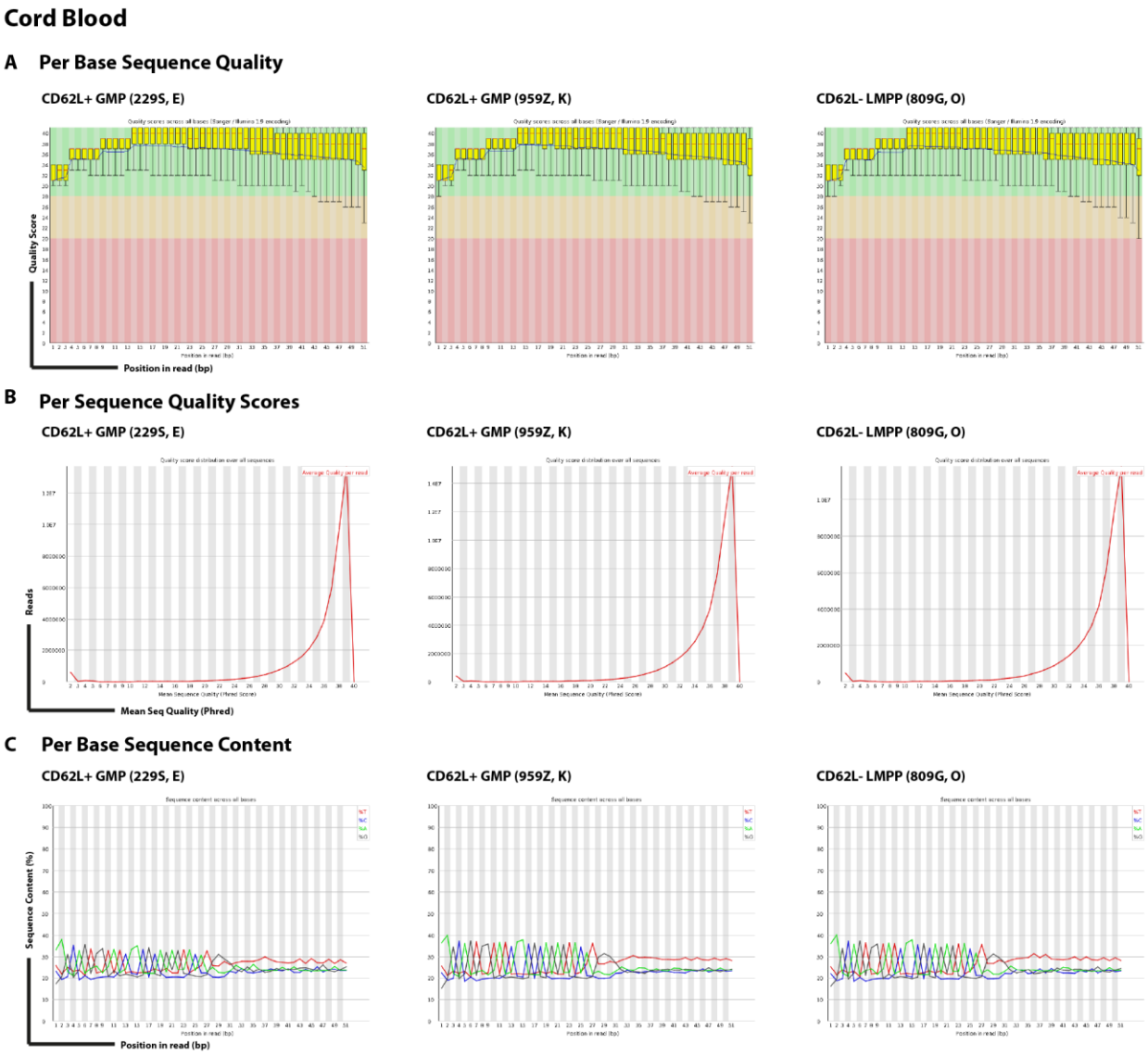

Figure 7.3. RNA Sequencing Data Quality Check In FASTQC Of Populations Sorted From Cord Blood.

Raw data from Illumina sequencing was subjected to quality analysis in FASTQC. Three representative examples from cord blood are shown.

A) demonstrates the per base sequence qualities with the Phred scores generated by the sequencer, with the quality score on the y-axis and the position in the read (bp) on the y-axis.The yellow boxes quantify the 25th/75th percentile, the red line is the median quality score per base and the blue line is the mean. Phred scores above 20 are considered successful.

B) The per sequence quality score distribution is shown, with reads on the y-axis and the mean sequencing quality on the x-axis.

C) These graphs illustrate the per base sequence content, showing the sequence content on the y-axis and the position in the read (bp) on the x-axis. T is shown in red, C in blue, A in green and G in black.

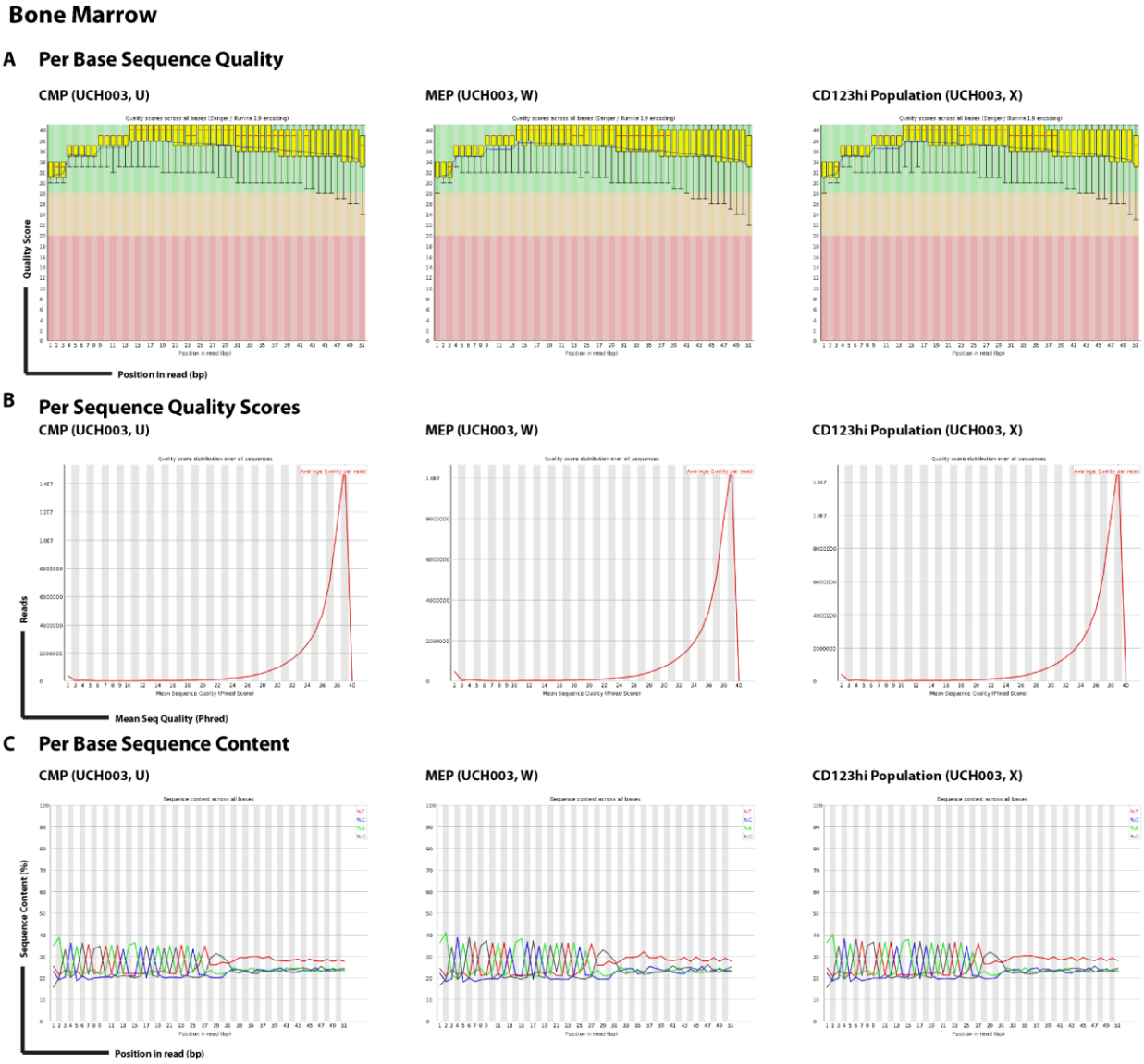

Figure 7.4. RNA Sequencing Data Quality Check In FASTQC Of Populations Sorted From Bone Marrow.

Raw data from Illumina sequencing was subjected to quality analysis in FASTQC. Three representative examples from bone marrow are shown.

A) demonstrates the per base sequence qualities with the Phred scores generated by the sequencer, with the quality score on the y-axis and the position in the read (bp) on the y-axis.The yellow boxes quantify the 25th/75th percentile, the red line is the median quality score per base and the blue line is the mean. Phred scores above 20 are considered successful.

B) The per sequence quality score distribution is shown, with reads on the y-axis and the mean sequencing quality on the x-axis.

C) These graphs illustrate the per base sequence content, showing the sequence content on the y-axis and the position in the read (bp) on the x-axis. T is shown in red, C in blue, A in green and G in black.

Moving on from the per base sequence content, the GC content was assessed next in FastQC. Figure 7.5 A shows again three representative samples sorted from CB samples. The x-axis shows the position in the read and the GC content is displayed on the y-axis. Ideally, the GC content should be around 50%, and the fluctuations at the start of the read can again be explained by the use of sequencing primers. The average GC content for all samples sequenced in this sample was 47% (+/- 0.3%; N=24), as demonstrated in Table 7.3.

The distribution shown in Figure 7.5 B is a representation of the GC content over all sequences, with the GC content on the x-axis and the number of reads assayed on the y-axis. The blue line is a hypothetical distribution derived from the mean and standard deviation of the real data; the red line shows the actual distribution. The higher the overlap, the better the indication of the quality of the data is. The spikes, which are present in all populations, are most likely contaminations of genomic DNA.

Another important quality measure is the sequence duplication level. It will give an indication of how many sequences are overrepresented in the sequencing data and how many unique sequences are present.

Figure 7.5 C shows three typical sequence duplication level graphs. The sequence duplication level is depicted on the x-axis and the y-axis shows the percentage. Sequence duplication levels in all populations sequenced in this study ranged from 57% to 72%, with an average of 66.8% (+/- 4.3%; N=24), see Table 7.3.

In the populations sequenced from BM, the results were similar. Figure 7.6 A shows the per base GC content, which rests around 47% after the fluctuations at the start of the read.

The distribution of the GC content aligns relatively well with the theoretical distribution, but the spikes which indicate genomic DNA amplification contamination are also present in all samples sequenced from BM, as it can be seen in Figure 7.6 B. Figure 7.6 C also shows the sequence duplication levels which range in the same ballpark as the values from CB.

Overrepresented sequences in all sequences samples were also analysed for their potential origin. In every sample, see Table 7.4, the SMARTer II A Oligonucleotide (with the oligo dT primer at the end)[140] was detected as overrepresented sequence. 30% of the samples (7 out of 23) had the poly-A tail among the overrepresented sequences. Furthermore, a specific Tru Seq Illumina adapter was also present in the overrepresented sequences in every sample.

All in all, the quality measures showed satisfactory data quality.

ID	Duplication (%)	GC content
225	60.39	47
226	59.03	47
227	61.81	47
228	64.33	47
229	63.56	47
230	67.67	48
231	67.01	47
232	68.87	47
234	71.9	47
235	71.19	47
236	71.46	47
237	66.54	47
238	69.96	47
239	63.21	47
240	71.51	47
241	70.05	47
242	57.38	46
243	70.2	47
244	72.17	47
245	66.47	47
246	65.95	47
247	65.93	47
248	70.17	47
Av	66.8	47.0
SD	4.3	0.3

Table 7.3. Duplication Levels and GC Content of Sequenced Populations.

Cord Blood

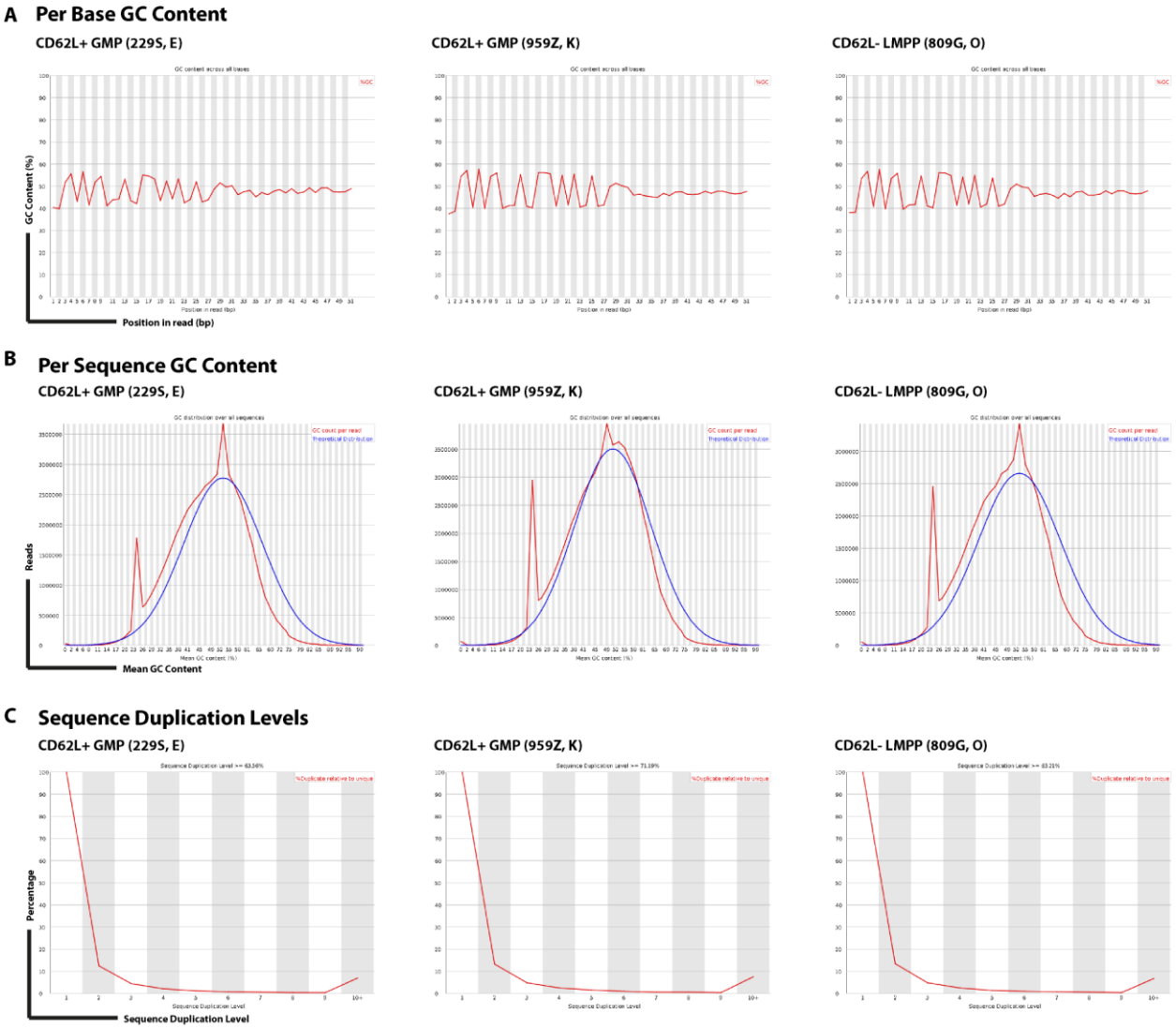

Figure 7.5. RNA Sequencing Data Quality Check In FASTQC Of Populations Sorted From Cord Blood.

Raw data from Illumina sequencing was subjected to quality analysis in FASTQC. Three representative examples from cord blood are shown.

A) demonstrates the GC content (y-axis) across the read (x-axis).

B) This graph demonstrates the per sequence GC content, with the relative GC content on the x-axis and the reads on the y-axis. The blue line shows the theoretical distribution of the GC content with the same mean and standard deviation as your real data, whereas the red line is a representation of the actual data.

C) The sequence duplication levels are shown on the x-axis and the relative percentage is displayed on the y-axis.

Bone Marrow

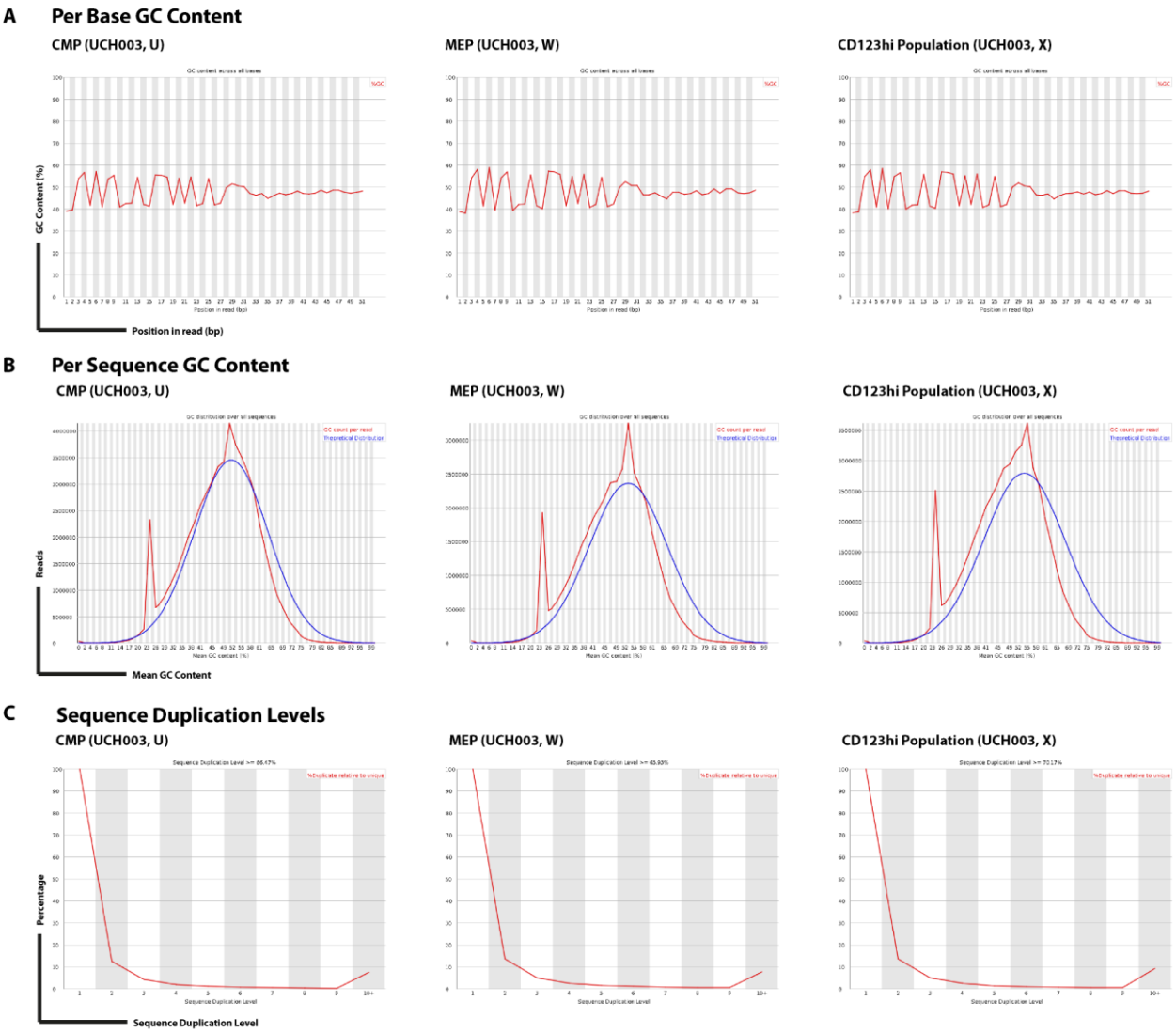

Figure 7.6. RNA Sequencing Data Quality Check In FASTQC Of Populations Sorted From Bone Marrow.

Raw data from Illumina sequencing was subjected to quality analysis in FASTQC. Three representative examples from bone marrow are shown.

A) demonstrates the GC content (y-axis) across the read (x-axis).

B) This graph demonstrates the per sequence GC content, with the relative GC content on the x-axis and the reads on the y-axis. The blue line shows the theoretical distribution of the GC content with the same mean and standard deviation as your real data, whereas the red line is a representation of the actual data.

C) The sequence duplication levels are shown on the x-axis and the relative percentage is displayed on the y-axis.

Sample ID	Sequencing ID	Population	Sequences	Count	%	Possible Source
229S	225	HSC	AAGCAGTGGTATCAACGCAGAGTACTTTTTTTTTTTTTTTTTTTTTTTT	1568020	3.2984	SMARTer II A Oligonucleotide
			GATCGGAAGAGCACACGTCTGAACTCCAGTCACTGCCGGCTATCTCGTATG	563935	1.1862	TruSeq Adapter, Index 4 (97% over 37bp)
	226	MPP	AAGCAGTGGTATCAACGCAGAGTACTTTTTTTTTTTTTTTTTTTTTTTT	1542682	3.5147	SMARTer II A Oligonucleotide
			GATCGGAAGAGCACACGTCTGAACTCCAGTCACTCCATGGTATCTCGTATG	1084228	2.4702	TruSeq Adapter, Index 6 (97% over 37bp)
	227	CD62L+ LMPP	AAGCAGTGGTATCAACGCAGAGTACTTTTTTTTTTTTTTTTTTTTTTTT	1567884	3.6194	SMARTer II A Oligonucleotide
			GATCGGAAGAGCACACGTCTGAACTCCAGTCACTACTCTAGATCTCGTATG	379769	0.8767	TruSeq Adapter, Index 7 (97% over 35bp)
			AAAAAAAAAAAAAAAAAAAAAAAAAAAAAAAAAAAAAAAAAAAAAAAA	59018	0.1362	Poly (A) Tail
	228	CMP	AAGCAGTGGTATCAACGCAGAGTACTTTTTTTTTTTTTTTTTTTTTTTT	1771392	3.4634	SMARTer II A Oligonucleotide
			GATCGGAAGAGCACACGTCTGAACTCCAGTCACGCGAGACTATCTCGTATG	490493	0.9590	TruSeq Adapter, Index 6 (97% over 37bp)
			AAAAAAAAAAAAAAAAAAAAAAAAAAAAAAAAAAAAAAAAAAAAAAAA	60132	0.1176	No Hit
	229	CD62L+ GMP	AAGCAGTGGTATCAACGCAGAGTACTTTTTTTTTTTTTTTTTTTTTTTT	1371394	2.9426	SMARTer II A Oligonucleotide
			GATCGGAAGAGCACACGTCTGAACTCCAGTCACGAGTCGACATCTCGTATG	760782	1.6324	TruSeq Adapter, Index 7 (97% over 36bp)
	230	CD62L- GMP	AAGCAGTGGTATCAACGCAGAGTACTTTTTTTTTTTTTTTTTTTTTTTT	1543315	3.0271	SMARTer II A Oligonucleotide
			GATCGGAAGAGCACACGTCTGAACTCCAGTCACCTTGCAACATCTCGTATG	910948	1.7868	TruSeq Adapter, Index 12 (97% over 40bp)
	231	MEP	AAGCAGTGGTATCAACGCAGAGTACTTTTTTTTTTTTTTTTTTTTTTTT	1890046	3.5512	SMARTer II A Oligonucleotide
			GATCGGAAGAGCACACGTCTGAACTCCAGTCACCTATCACAATCTCGTATG	389284	0.7314	TruSeq Adapter, Index 2 (97% over 37bp)
			AAAAAAAAAAAAAAAAAAAAAAAAAAAAAAAAAAAAAAAAAAAAAAAA	60622	0.1139	Poly (A) Tail
959Z	232	CD62L+ LMPP	AAGCAGTGGTATCAACGCAGAGTACTTTTTTTTTTTTTTTTTTTTTTTT	1503091	3.2769	SMARTer II A Oligonucleotide
			GATCGGAAGAGCACACGTCTGAACTCCAGTCACCAGGCCTCATCTCGTATG	600450	1.3091	TruSeq Adapter, Index 7 (97% over 36bp)
	234	CMP	AAGCAGTGGTATCAACGCAGAGTACTTTTTTTTTTTTTTTTTTTTTTTT	2123264	3.5089	SMARTer II A Oligonucleotide
			GATCGGAAGAGCACACGTCTGAACTCCAGTCACTCCAGCCAATCTCGTATG	464427	0.7675	TruSeq Adapter, Index 6 (97% over 37bp)
			AAAAAAAAAAAAAAAAAAAAAAAAAAAAAAAAAAAAAAAAAAAAAAAA	75154	0.1242	Poly (A) Tail
	235	CD62L+ GMP	AAGCAGTGGTATCAACGCAGAGTACTTTTTTTTTTTTTTTTTTTTTTTT	2404130	4.2009	SMARTer II A Oligonucleotide
			GATCGGAAGAGCACACGTCTGAACTCCAGTCACTAAGAGGAATCTCGTATG	510454	0.8919	TruSeq Adapter, Index 3 (97% over 37bp)
			AAAAAAAAAAAAAAAAAAAAAAAAAAAAAAAAAAAAAAAAAAAAAAAA	65119	0.1138	Poly (A) Tail
	236	CD62L- GMP	AAGCAGTGGTATCAACGCAGAGTACTTTTTTTTTTTTTTTTTTTTTTTT	2022452	3.6844	SMARTer II A Oligonucleotide
			GATCGGAAGAGCACACGTCTGAACTCCAGTCACGCCTTCCTATCTCGTATG	484401	0.8824	TruSeq Adapter, Index 11 (97% over 37bp)
			AAAAAAAAAAAAAAAAAAAAAAAAAAAAAAAAAAAAAAAAAAAAAAAA	61472	0.1120	Poly (A) Tail
809G	237	MPP	AAGCAGTGGTATCAACGCAGAGTACTTTTTTTTTTTTTTTTTTTTTTTT	1680437	2.7173	SMARTer II A Oligonucleotide

			GATCGGAAGAGCACACGTCTGAACTCCAGTCACGACGACGTATCTCGTATG	532621	0.8613	TruSeq Adapter, Index 6 (97% over 36bp)
	238	CD62L+ LMPP	AAGCAGTGGTATCAACGCAGAGTACTTTTTTTTTTTTTTTTTTTTTTTT	1656682	2.6938	SMARTer II A Oligonucleotide
			GATCGGAAGAGCACACGTCTGAACTCCAGTCACCTGCATGTATCTCGTATG	410348	0.6672	TruSeq Adapter, Index 7 (97% over 36bp)
	239	CD62L- LMPP	AAGCAGTGGTATCAACGCAGAGTACTTTTTTTTTTTTTTTTTTTTTTTT	1986619	4.2705	SMARTer II A Oligonucleotide
			GATCGGAAGAGCACACGTCTGAACTCCAGTCACCGTCTCGAATCTCGTATG	532021	1.1436	TruSeq Adapter, Index 12 (97% over 36bp)
			AAAAAAAAAAAAAAAAAAAAAAAAAAAAAAAAAAAAAAAAAAAAAAAA	53094	0.1141	No Hit
	240	CD62L+ GMP	AAGCAGTGGTATCAACGCAGAGTACTTTTTTTTTTTTTTTTTTTTTTTT	2235714	3.4502	SMARTer II A Oligonucleotide
			GATCGGAAGAGCACACGTCTGAACTCCAGTCACCACCAACTATCTCGTATG	446372	0.6889	TruSeq Adapter, Index 7 (97% over 35bp)
	241	CD62L- GMP	AAGCAGTGGTATCAACGCAGAGTACTTTTTTTTTTTTTTTTTTTTTTTT	1667080	2.9537	SMARTer II A Oligonucleotide
			GATCGGAAGAGCACACGTCTGAACTCCAGTCACTGAACCTCATCTCGTATG	280957	0.4978	TruSeq Adapter, Index 4 (97% over 38bp)
UCH003	242	HSC	AAGCAGTGGTATCAACGCAGAGTACTTTTTTTTTTTTTTTTTTTTTTTT	2057463	4.0108	SMARTer II A Oligonucleotide
			GATCGGAAGAGCACACGTCTGAACTCCAGTCACTCCACAACATCTCGTATG	612950	1.1949	TruSeq Adapter, Index 6 (97% over 37bp)
	243	MPP	AAGCAGTGGTATCAACGCAGAGTACTTTTTTTTTTTTTTTTTTTTTTTT	1998458	4.3224	SMARTer II A Oligonucleotide
			GATCGGAAGAGCACACGTCTGAACTCCAGTCACTAAGGAAGATCTCGTATG	650649	1.4073	TruSeq Adapter, Index 3 (97% over 38bp)
	244	CD62L- LMPP	AAGCAGTGGTATCAACGCAGAGTACTTTTTTTTTTTTTTTTTTTTTTTT	2917494	5.6014	SMARTer II A Oligonucleotide
			GATCGGAAGAGCACACGTCTGAACTCCAGTCACGCCTCTTCATCTCGTATG	858048	1.6474	TruSeq Adapter, Index 11 (97% over 37bp)
			AAAAAAAAAAAAAAAAAAAAAAAAAAAAAAAAAAAAAAAAAAAAAAAA	123873	0.2378	Poly (A) Tail
	245	CMP	AAGCAGTGGTATCAACGCAGAGTACTTTTTTTTTTTTTTTTTTTTTTTT	1883415	3.4614	SMARTer II A Oligonucleotide
			GATCGGAAGAGCACACGTCTGAACTCCAGTCACGACGTACAATCTCGTATG	493620	0.9072	TruSeq Adapter, Index 6 (97% over 36bp)
	246	CD62L- GMP	AAGCAGTGGTATCAACGCAGAGTACTTTTTTTTTTTTTTTTTTTTTTTT	2040081	3.9677	SMARTer II A Oligonucleotide
			GATCGGAAGAGCACACGTCTGAACTCCAGTCACCTGCTGCAATCTCGTATG	912020	1.7738	TruSeq Adapter, Index 7 (97% over 36bp)
	247	MEP	AAGCAGTGGTATCAACGCAGAGTACTTTTTTTTTTTTTTTTTTTTTTTT	1600383	4.0518	SMARTer II A Oligonucleotide
			GATCGGAAGAGCACACGTCTGAACTCCAGTCACCGTCCTAGATCTCGTATG	616073	1.5597	TruSeq Adapter, Index 12 (97% over 36bp)
	248	CD123hi	AAGCAGTGGTATCAACGCAGAGTACTTTTTTTTTTTTTTTTTTTTTTTT	2090089	4.3108	SMARTer II A Oligonucleotide
			GATCGGAAGAGCACACGTCTGAACTCCAGTCACCACCGGTCATCTCGTATG	522069	1.0768	TruSeq Adapter, Index 7 (97% over 35bp)

Table 7.4. Summary Overrepresented Sequences Across All Samples.

7.4 Preliminary Analysis In SeqMonk

Preliminary analysis was performed in SeqMonk (SeqMonk Mapped Sequence Data Analyser, version: 0.24.1), after aligning the data to human reference genome GRCh37. Probes were quantified according to the RNA sequencing pipeline function in SeqMonk, which is optimised to quantitate mRNA probes. To exclude probes which were not expressed in any samples, only probes with a value above 1 in at least one sample was considered. Other probes were excluded from the analysis. Samples from cord blood and bone marrow were analysed separately. Table 7.3 summarizes the total read counts of all samples from BM and CB, with averages and SD. On average, in BM, 20,728,894 reads could be mapped (+/- 3,121,184). This means that compared to the average number of reads of the two technical replicates from BM, 83% of all reads could be mapped. In CB, on average 24,163,448 reads were mapped (+/- 3,169,263), which was 89% of the total acquired reads.

In order to visualise the probe value distribution across the different samples, cumulative distribution plots with the previously quantified probes for each sample were generated. This way of visualisation will allow the researcher to judge if normalization is necessary, in order to compare the samples to each other. In this study, populations sorted from CB and populations sorted from BM were always analysed separately, due to the different natures of the tissues.

Figure 7.7 A shows the cumulative distribution plot which was acquired for all CB populations. With exception of the CB HSC profile acquired, all CB populations lie very close together. In B, the distribution of BM population derived probe values is shown. Again, the cumulative distribution function has a very similar shape in all

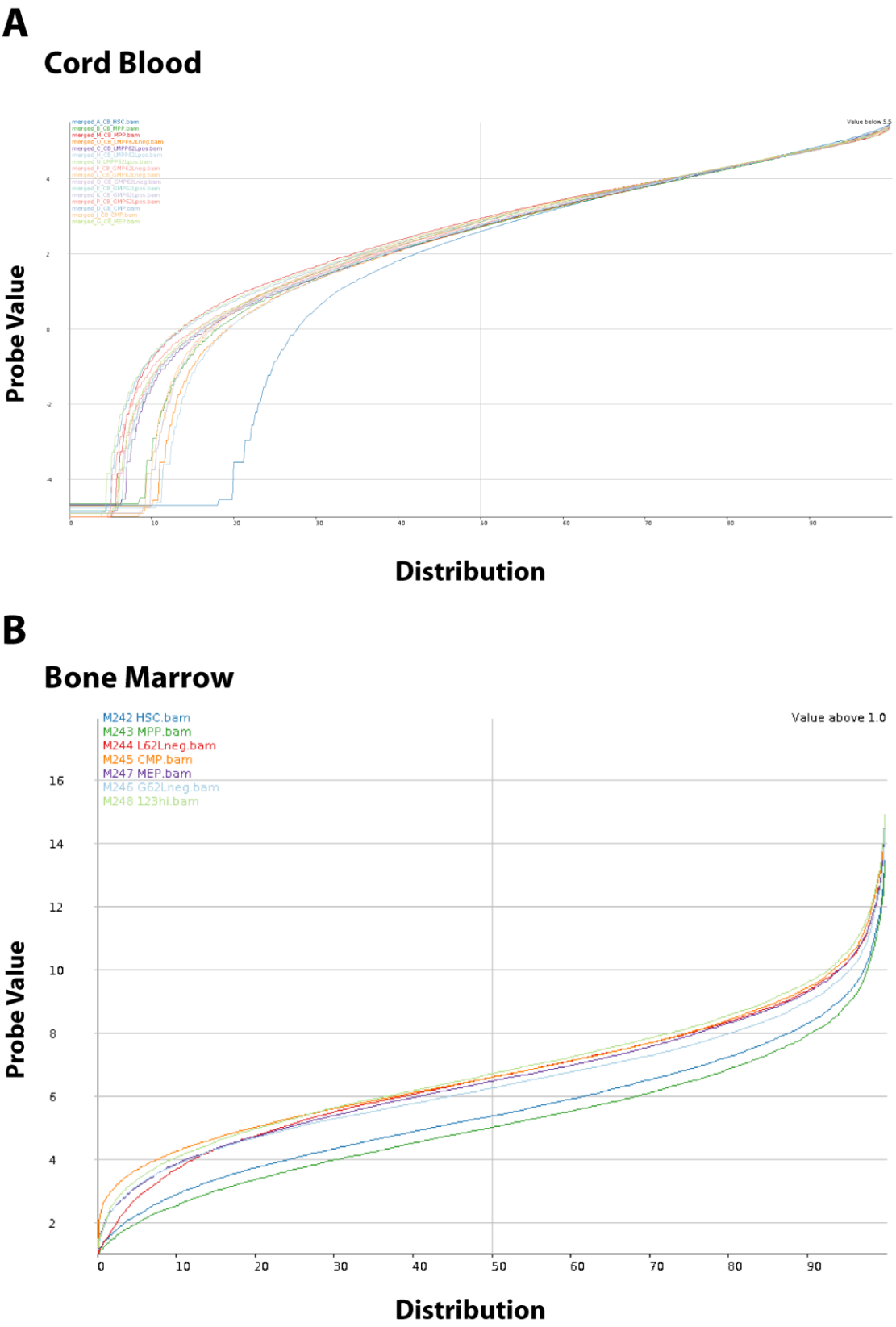

Figure 7.7. Seqmonk - Cumulative Distribution Plot To Visualize Probe Value Distribution.
Populations from CB and BM were sequenced on the Illumina HiSeq and mapped with TopHat. In Seqmonk, probes were quantified according to the RNA Sequencing pipeline. Probes which were not expressed in at least one sample with a value of 1.0 were excluded.
A) Distribution of probe values from CB.
B) Distribution of probe values from BM.

samples, however, the MPP and HSC cluster together and slightly away from the more mature cell populations. This could possibly be explained by the fact that HSCs and MPPs might contain less RNA due to their quiescent cell cycle status.

Another way of visualising probe value distributions is utilising the box whisker plot. In this representation, the probe value distribution is shown across several datastores (i.e. populations), whereas the line across the grey box signifies the median, the size of the box correlates with the $25^{th}/75^{th}$ percentile and the whiskers show the median plus/minus the interquartile range multiplied by two. Any probe which falls out of this range is represented by a circle. Comparing both CB and BM, it was found that the medians were relatively similar, ranging from 3.5 to 5 in CB and generally the median probe value was in the range from 5 to 6.5 in BM. Figure 7.8 A shows the distribution of the datastores from CB. Looking across all samples, the median range for CB is relatively similar and also the variation is in the same order for all the samples, which suggests quantification and probe values are similar across all samples in CB, even from different biological replicates (sample colour code: CB 229S – green; CB 959Z – black; CB 809G – red).

For samples derived from BM, a summary is provided in Figure 7.8 B. Here, the $25^{th}/75^{th}$ percentiles for all samples are smaller than in CB. As seen before, the HSC and MPP lie slightly lower in their median probe value than the other, more committed progenitors.

These probe value distribution plots provided a guide to recognise equal coverage and quantification of the probes sequenced in all samples.

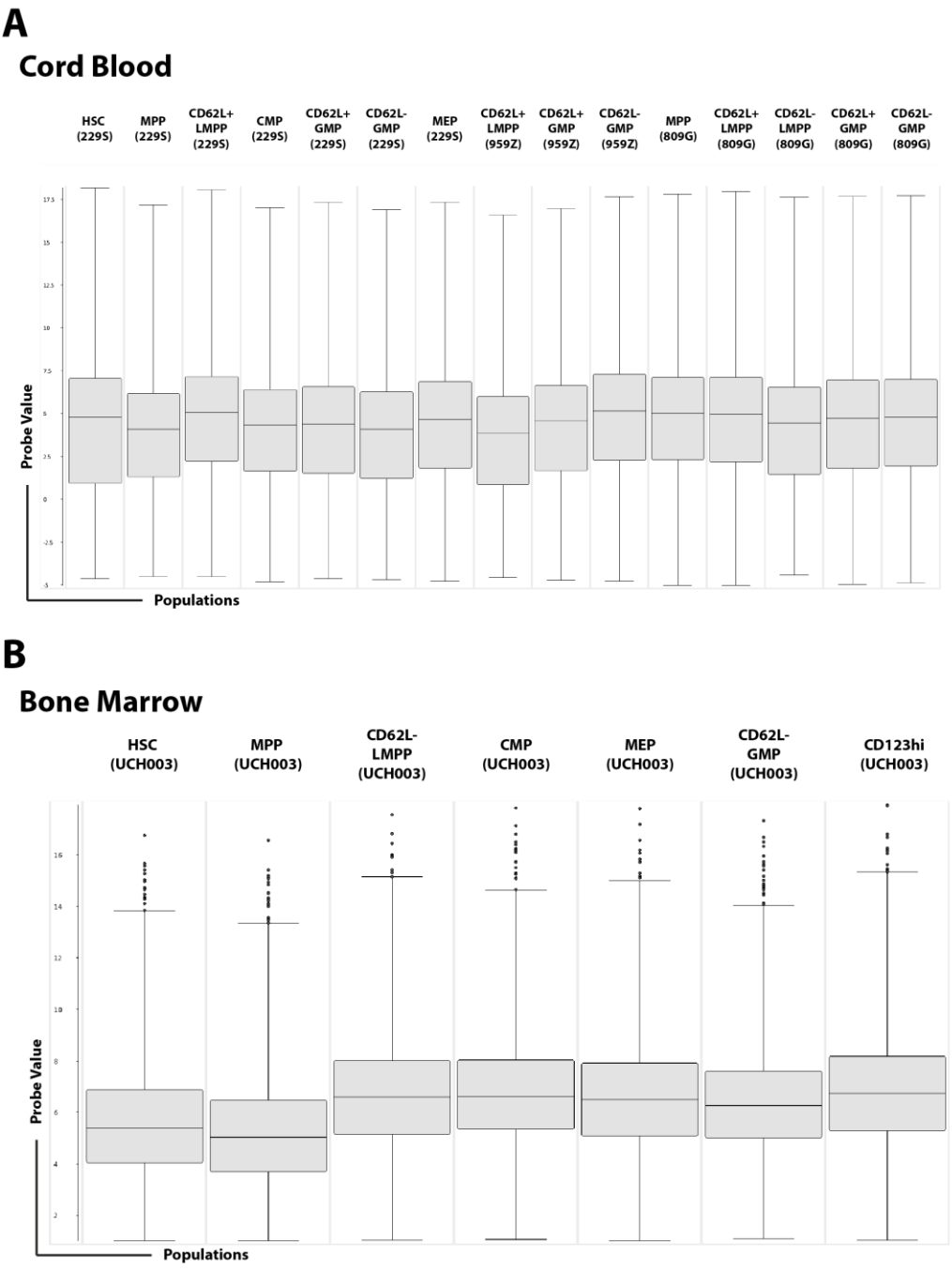

Figure 7.8. Probe Value Distribution Across Multiple Populations In Cord Blood And Bone Marrow.

RNA extracted from sorted populations fron CB and BM, cDNA generated from it by SMARTer cDNA Synthesis was then sequenced on the Illumina HiSeq Sequencer and reads were mapped with TopHat and trimmed in SAMtools. Bam-files were imported into SeqMonk and quantified with the RNA sequencing pipeline. Here, the probe value distribution across all sequenced populations is visualised as a box whisker plot for the initially quantified probe list (only probes which are expressed in at least one sample at a value of >1).

A) Details all the populations sorted from CB with respect to their probe value distribution in the initially quantified probe list.

B) Summary of all populations sorted from BM.

The grey boxes signify the 25th/75th percentile, and the line across the middle is median and the whiskers are the median plus/minus the interquartile range multiplied by two. Filled circles outside the whiskers represent single probes.

CB, cord blood; BM, bone marrow; SMART, Switching Mechanism at 5' End of RNA Template.

Furthermore, datastore trees are a way of visualising how similar or related different populations with respect to each other. With the help of Pearson correlation, the programme establishes a matrix and then generates a tree which adjoins the different populations. It is a simple way to acquire a sense for the similarity of several populations.

Figure 7.9 A focusses on the datastore tree which visualises the samples sorted from three different samples from CB first. Again, the samples are colour coded as in the previous figure; green – CB 229S, black – CB 959Z and red – CB 809G.

The first major division can be seen between the branch on the lower part of the tree, which comprises two replicates of MPP, one HSC and one CD62L- LMPP. These three different, immature cell types seem to be more related to each other than the other populations on the upper branch. The second big division is located between the CMP and MEP and the remaining LMPP and GMP populations. It is difficult to interpret the data regarding the CD62L+ and CD62L- populations, since sometimes they seem to cluster within samples, and sometimes with regard to CD62L or CD38 expression (LMPP with LMPP, GMP with GMP).

Figure 7.9 B illustrates the BM datastore tree with all samples which have been sequenced so far. Again, the tree can be divided into two major parts – the immature stem/multipotent progenitor compartment at the bottom and the more committed progenitors at the top. HSC and MPP cluster together in their own fork. The CD62L- LMPP lies slightly off to the side. On the upper, more committed branch of the datastore tree, another split between the CMP-MEP group and the CD123hi population (which is suspected to be a dendritic cell progenitor) and the CD62L- GMP can be seen.

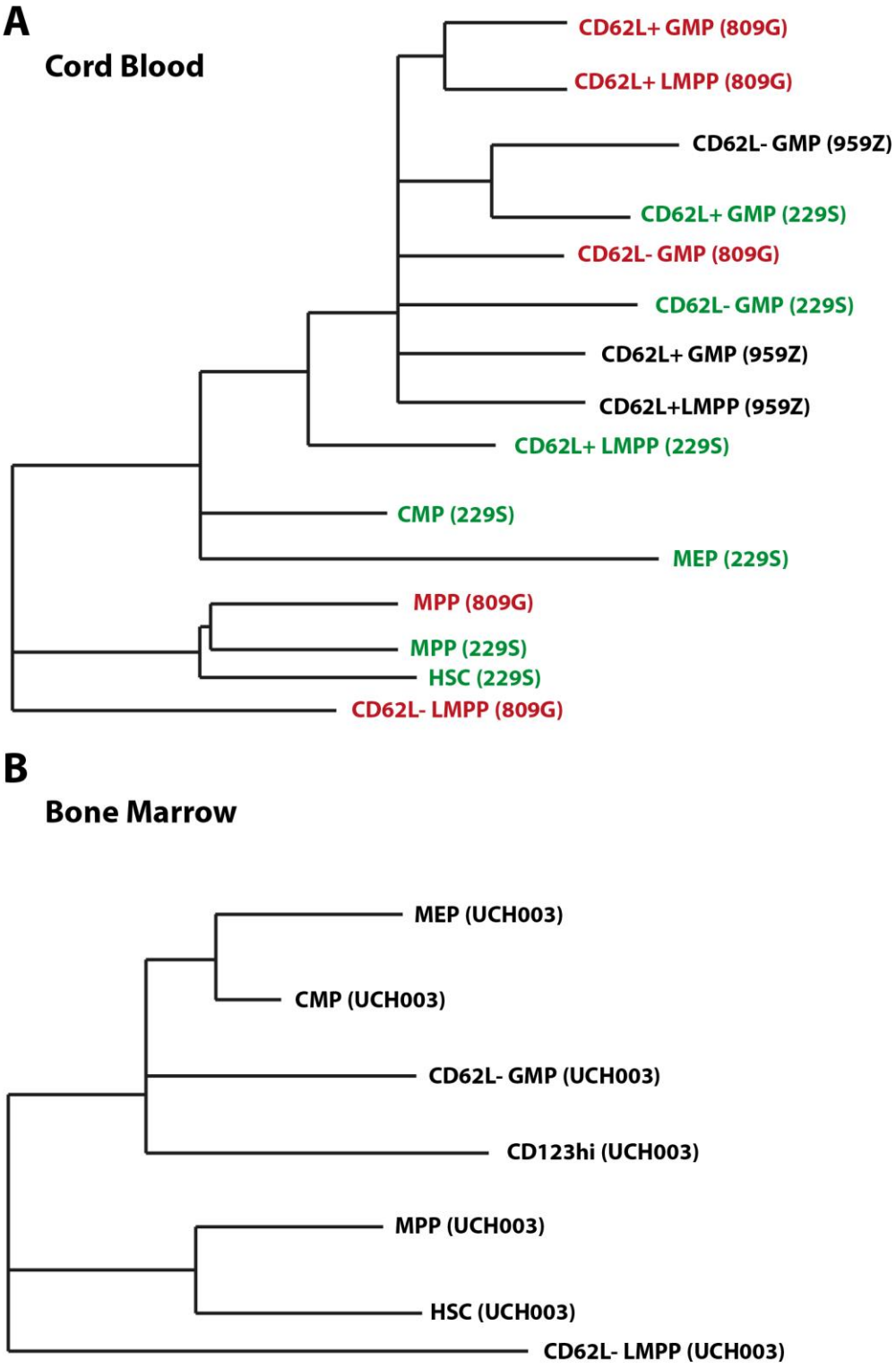

Figure 7.9. Datastore Trees Of Cord Blood And Bone Marrow Populations.
RNA was extracted from sorted populations from CB and BM, cDNA generated by SMARTer cDNA Synthesis, it was then sequenced on the Illumina HiSeq Sequencer and reads were mapped with TopHat and trimmed in SAMtools. Bam-files were imported into SeqMonk and quantified with the RNA sequencing pipeline. Quantified values were analysed with Pearson Correlation to establish a datastore tree.
A) The datastore tree for all sequenced populations from CB is shown here. Different CB samples are colour-coded: green, CB 229S; black, CB 959Z and red, CB 809G.
B) The datastore tree for all sequenced populations from BM is depicted here. At present only one biological replicate of BM has been sorted. CB, cord blood; BM, bone marrow.

This data is consistent with what would be expected from the literature and recapitulates the split between the immature stem/multipotent progenitor compartment and more committed progenitors. Moreover, progenitors with erythro-myeloid potential consistently cluster together in both adult bone marrow and neonatal cord blood.

Gene expression signatures which correlate with specific cell differentiation potentials were also investigated. With the help of the basic statistical Intensity Difference Filter in SeqMonk probe values from one or more data sets can be compared to the remaining data sets. This filter generates a local distribution of differences of probes which share a similar average intensity to the probe examined. A normal distribution is calculated which models the set of differences. With this model, a p-value can be assigned to the probe which signifies the probability of this particular probe falling into the distribution. The p-value can be adjusted to fit specific data.

In Figure 7.10 A, probes from HSC, MPP, CMP and MEP were compared to probes from LMPP and GMP populations, with a user-specified p-value of 0.001. They were subsequently displayed in a heatmap which depicts the probe values by the genes expressed. The genes which are differentially expressed can be found in Table 7.5. For the samples from CB, it can clearly be seen that the CMP and MEP differ from the CD62L+/CD62L- subpopulations of LMPP and GMP, with clusters of genes differentially up- and down-regulated. The two MPP replicates share some of the gene expression profile of the MEP and CMP, and there are a handful of genes which are also found to be expressed in the HSC. Examples of genes with the lowest p-value and enriched in MEP/CMP in CB samples are CD36, ANK1, KEL, HBA1, HBA2, GATA1, ALDH1, ITAGA2B. Significantly down

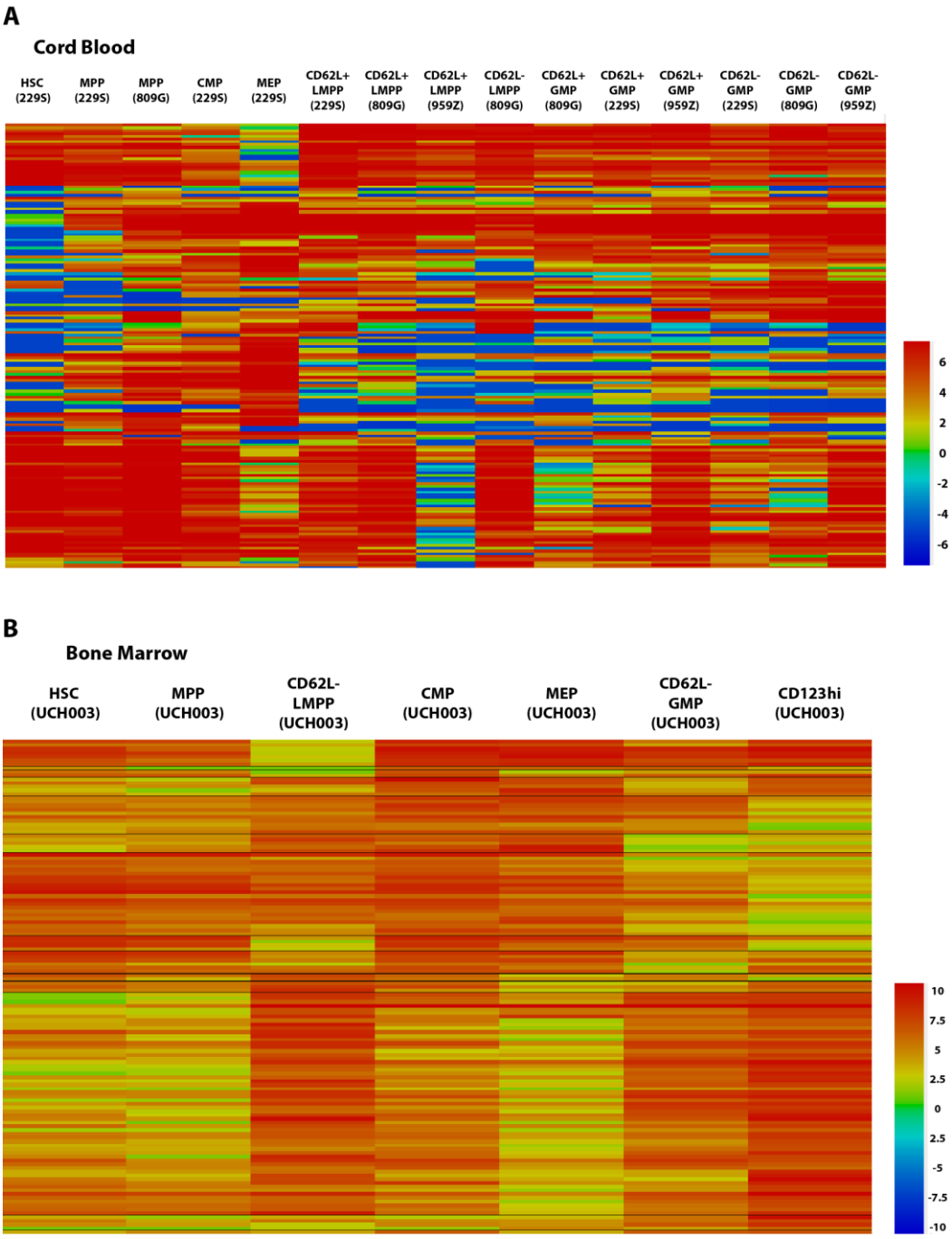

Figure 7.10. Genes Enriched And Downregulated In Cells With Megakaryocyte-Erythroid Differentiation Potential.

RNA was extracted from sorted populations from CB and BM, cDNA generated by SMARTer cDNA Synthesis, it was then sequenced on the Illumina HiSeq Sequencer and reads were mapped with TopHat and trimmed in SAMtools. Bam-files were imported into SeqMonk and quantified with the RNA sequencing pipeline. Only probes which were expressed in at least one data set with a value of >1.0 were used for analysis. Probes were filtered according to the statistical difference with a user specified p-value. One or more datasets can be compared against other data sets.

A) Heatmap of genes with different p-values of HSC, MPP, CMP and MEP are compared to all LMPP and GMP populations with a threshold p-value of 0.001 from cord blood.

B) Heatmap of genes with different p-values of HSC, MPP, CMP and MEP which are compared to LMPP and GMP populations with a threshold p-value of 0.01.

The colours represent the relative probe value.

regulated when compared to GMP and LMPP populations were SLAMF1, CD52, AMICA1, CLEC5a which correlate with the differentiation potentials of the investigated populations.

Figure 7.10 B shows a very similar analysis for samples derived from bone marrow tissue. Similarly, HSC, MPP, CMP and MEP were investigated with the Intensity Difference Filter in SeqMonk, with a specified p-value of 0.01. Visualising the differences in probe value expression, the heatmap in 7.10 B is generated. Macroscopically, it can be seen that there are roughly the top half of all genes displayed in this heatmap is upregulated in CMP and MEP, whereas the genes in the bottom half are expressed on a lower level. In LMPP, GMP and the CD123hi population this is vice versa. HSC and MPP on the other hand reflect the CMP and MEP more than LMPP, GMP and CD123 do.

The top 50 genes with the lowest p-values can be found in Table 7.5. Amongst the upregulated genes in the MkE-primed populations, ITGA2B, ALDH1A1, GATA2 and SERPINB8 were found. FLT3L, IL3Ra and AMICA1 were downregulated.

This preliminary analysis suggests that the data is sufficient to derive lineage specific gene expression signatures from CB and BM populations.

Cord Blood		
Probe	**Chr**	**Diff p-value**
FOS	14	4.84E-12
MPO	17	7.26E-12
CD36	7	1.94E-11
ANK1	8	1.35E-10
CLU	8	1.74E-10
FAM178B	2	3.99E-10
GZMB	14	5.42E-10
KEL	7	7.01E-10
GATA1	X	2.50E-09
LAT	16	3.01E-09
HBA2	16	7.61E-09
CLEC5A	7	1.19E-08
IL8	4	1.49E-08
AMICA1	11	1.55E-08
FOSB	19	2.12E-08
DHRS9	2	2.93E-08
TPSAB1	16	2.96E-08
CCL3L1	17	3.11E-08
KIF23	15	4.01E-08
RP11-1280I22.1	5	6.15E-08
PLAT	8	1.09E-07
CCL3	17	1.36E-07
KCNH2	7	1.39E-07
HBG2	11	1.39E-07
CXCL13	4	1.65E-07
STEAP4	7	3.01E-07
C9orf125	9	3.12E-07
ITGA2B	17	3.27E-07
SPTA1	1	3.34E-07
IL6	7	4.32E-07
CD1E	1	5.73E-07
CXCL1	4	6.46E-07
RNASE1	14	7.51E-07
HBA1	16	9.32E-07
CCL1	17	1.00E-06
FCER1A	1	1.33E-06
SLC2A5	1	1.64E-06
SLC39A4	8	1.67E-06
GATSL3	22	1.83E-06
CSF1R	5	2.70E-06
C3AR1	12	2.70E-06
UMODL1	21	3.14E-06
INHBA	7	3.46E-06
SLFN5	17	3.51E-06
HBD	11	3.88E-06
EPB49	8	3.96E-06
CNRIP1	2	4.60E-06
RAPGEF3	12	5.01E-06
AMHR2	12	6.13E-06
FAM65C	20	8.10E-06

Bone Marrow		
Probe	**Chr**	**Diff p-value**
SAMHD1	20	1.81E-07
MPO	17	6.37E-07
PTPRS	19	2.23E-06
ITGA2B	17	2.80E-06
CRHBP	5	8.38E-06
LGMN	14	1.22E-05
SPP1	4	2.41E-05
HLA-DMB	6	3.27E-05
CALN1	7	3.98E-05
LGALS1	22	5.17E-05
RP11-354E11.2	10	6.02E-05
SLC7A7	14	6.02E-05
FAM19A2	12	7.91E-05
GUCY1B3	4	1.08E-04
ZC3H14	14	1.88E-04
PPIP5K1	15	1.95E-04
TP53I11	11	2.04E-04
ALDH1A1	9	2.61E-04
RGS1	1	3.53E-04
PLOD2	3	4.68E-04
UBAP2	9	7.94E-04
SOCS2	12	1.00E-03
SORBS1	10	0.00118
AIM1	6	0.00119
PTGS1	9	0.00135
PRG2	11	0.00135
AXL	19	0.00137
CSF2RB	22	0.00159
CA2	8	0.00179
MLLT3	9	0.00244
CSF2RA	X	0.00267
GAS7	17	0.00272
SERPINB8	18	0.00292
STON2	14	0.00296
FCER1G	1	0.00319
HMGCR	5	0.00357
B3GNT7	2	0.00461
ZHX2	8	0.00463
EGR1	5	0.00565
CYTH4	22	0.00565
FLT3	13	0.00569
MAPKBP1	15	0.00675
TNFRSF14	1	0.00684
TTYH2	17	0.00684
BEX1	X	0.00684
YES1	18	0.00703
FGR	1	0.00734
ZNF154	19	0.00772
TNFRSF1B	1	0.00784
SPNS3	17	0.00793

Table 7.5. Genes Differentially Expressed In Populations With Megakaryocyte-Erythroid Potential Vs. LMPP and GMP Ordered By P-Value. The 50 genes with the lowest p-value for both cord blood and bone marrow are shown here. This list was generated with the Intensity Difference Filter in SeqMonk with an upper p-value threshold of 0.001.

7.5 Discussion

RNA sequencing is a rapidly advancing technique[141] and recently efforts to take it down to the single cell level have been made[142,143]. Here, RNA extracted from populations sorted from neonatal cord blood and adult bone marrow was sequenced on the Illumina HiSeq sequencer. Distinct immunophenotypic populations were chosen for transcriptome analysis, including the HSC, MPP, CMP, MEP, CD62L+ LMPP, CD62L- LMPP, CD62L+ GMP and CD62L- GMP from CB, as well as HSC, MPP, CMP, MEP, CD62L- LMPP, CD62L- GMP and the $CD123^{hi}$CD45RA+ population from BM.

Limitations in the cell numbers which could be sorted per population, as well as limited availability of BM samples of sufficient cell number constrained the number of the populations which were sent for sequencing so far. Furthermore, the cost of the sequencing preparation and reaction is not to be underestimated either and has to be taken into account when planning a study. Therefore, a compromise was found where 24 samples would be sequenced. At least 3,500 cells were sorted for RNA sequencing per population, up to a maximum of 20,000. To also get an understanding for the variation in tissues in development, populations from both CB and BM were sequenced. This however will require more biological replicates of various populations to be analysed as well. The researchers are aware of the caveats in this data.

First, there are only a handful of populations which have been sent for sequences in multiple biological replicates. The reason for sending the 24 initial samples as it was done here, is due to the fact that it can take a long time for sequencing data to be returned. Furthermore, this preliminary data would provide a guide for to plan

further experiments, i.e. it might hint if the splitting of GMP and LMPP with CD62L is useful in separating distinct populations or if the quality of the RNA had to be improved.

Second, the MLP population has not been sequenced yet. This is due to the fact that the MLP population in CB and even more so in BM is very small (>1% of Lin-CD34+ cells). Sorting sufficient cells to extract RNA is very challenging. To circumvent this problem, I propose to pool MLP RNA from different cord blood samples. Since this research is done in normal tissue specimens, the variation would not be an issue. In fact, it might overcome small sample specific fluctuations in gene expression and provide an averaged view. Data from this chapter also suggests that clearly defined populations purified with the help of a specific surface immunophenotype cluster together, and not with respect to the biological sample they originate from.

Third, the quality check and data analysis discussed in this chapter is only a preliminary step, however it is beyond the scope of this project to analyse bioinformatics data in depth. Currently, the data is being analysed by a bioinformatics expert. There are a few questions I would like to ask in collaboration with the bioinformatician.

The first one is if there are any signatures which can be found in distinct cell populations, i.e. underlying lineage priming signatures; this might enable us to find a lymphoid signature on the LMPP level, which is missing on the CMP/MEP branch of the hierarchy and vice versa. Moreover, this approach might enable me to detect which genes segregate the LMPP from the GMP and MLP populations and if there are differences in the gene expression of CD62L+ LMPP and CD62L- LMPP (as well as CD62L+ GMP and CD62L-). Even if the CD62L subpopulations

of LMPP and GMP were found to have similar functional potential in in vitro assays, there could be a possible difference in the respective gene expression signatures.

Also, the question of MkE-priming in the HSC and MPP remains to be solved. This might lend evidence to the hypothesis of the erythro-megakaryocytic lineage branching off early, either at the HSC or MPP level. With gene expression data from different stages in the haematopoietic hierarchy, an in vitro functional assay can be developed to test this hypothesis, i.e. in the live in vitro tracking experiment as published before[98].

Furthermore, since this research lab also has profound interest in the biology of AML stem cells, this data acquired in normal tissues will be compared to data sets from AML samples. Since the data to specific immunophenotypic compartments in AML as well as normal samples is available, it will be possible to compare immunophenotypic compartments which are enriched in LSCs, to their exact normal counterpart. This might provide an idea for which gene expression is altered with respect to the normal environment and might identify potential genes which could be targeted in therapy. A related question is the identification of a self-renewal signature which is upregulated in the LSC-compartments as shown by microarray analysis before[19] and could be validated by RNA sequencing.

As shown in the results section, MkE signatures could be detected with the help of very basic filtering tools in SeqMonk. Genes specific for MkE primed cells were detected to be significantly upregulated in MEP and CMP from CB and BM. For example, HBA1 and HBA2 were significantly upregulated, which both encode haemoglobin isoforms and are erythroid genes. KEL also is found on erythroid

cells[144] and GATA1 is well known for its important role in erythropoiesis[145] and megakaryopoiesis[146]. This evidence adds to the credibility of this data.

The FASTQC data is discussed here. The initial base calling quality as supplied in the format of a Phred score by the Illumina sequencer was found to be of satisfactory quality, with even outliers remaining above a Q score of 20. The 25th/75th percentile was found to be above a Q score of 30 in all cases which correlates with a base cassling accuracy of at least 99.9%. The vast majority of all phred scores ranged around 38.

The per base sequence and GC content were also checked and in the per base sequence content, fluctuations can be detected in first half of the read, which can be attributed to the RNA sequencing primers used. The percentage of T-bases is also slightly elevated which might be due to the SMARTer II oligonucleotide, which contains an oligo dT primer (sequence: AAG CAG TGG TAT CAA CGC AGA GTA CTTTTTTTTTTTTTTTTTTTTTTTTT[140]) and should theoretically be present in each template.

The per sequence GC content aligned in most cases very well with the modelled theoretical distribution, however spikes which denote contamination with genomic DNA could be detected. RNA was extracted with the RNeasy kit from Qiagen. The protocol contains a DNAse treatment step at room temperature which is, according to the manufacturer, sufficient to remove all genomic contamination[147]. However, for future reference, an additional DNase treatment step could be validated to eliminate genomic contamination.

Sequence duplication levels are a useful guide to investigate overrepresented sequences in RNA sequencing data. The first reason for the relatively high

sequence duplication content in this study is due to the requirement for massively parallel sequencing to be able to detect rare transcripts. Second, the small starting amount of RNA (from 20pg/µL to 686pg/µL) will also affect the sequence duplication levels. The higher the RNA concentration is in the starting preparation, the smaller the sequence duplication level will be.

For all overrepresented sequences detected in FASTQC, matches could be found. The specific TruSeq adapters used by Illumina were overrepresented in every sample, as was the SMARTer II oligonucleotide, which is expected due to the nature of the cDNA synthesis and sequencing principles. The poly-A tail was also detected in a proportion of samples as an overrepresented sequence. This is consistent with the notion that poly-A selected RNA was used as templates for cDNA generation.

If the mapped data is then re-analysed in FASTQC, all the unmapped sequences disappear and with them, the genomic contamination in the per sequence GC content, as well as all the duplicate reads. Therefore it was chosen to show the FASTQC files from the raw data.

At first, the RNA sequencing data was mapped with the Stampy programme, which is the default mapping software used for many applications, including Chip-Seq and RNA seq and is optimised to align short reads from Illumina sequencing[148]. It is however not able to map reads spanning an exon boundary. To be able to map different splice variants and reads spanning exon boundaries, TopHat was chosen to align the data to the genome. TopHat first maps everything with the help of BowTie, and then re-assigns initially unmapped reads (IUMs) to potential splices via seed and extend. This means that a small seed up and

downstream of the exon-exon junction is, which is subsequently queried for the IUM reads. The sequences adjacent to the original seed are then interrogated for extended alignment within the IUM read with specified number of mismatches. If the IUM read passes this number, it will be mapped to this exon junction[149]. This method proved more successful for our RNA sequencing data than the initial alignment with Stampy.

Data from SeqMonk showed that after RNA sequencing pipeline quantitation, the probe value distribution was similar within tissues. Comparing CB and BM, it was found that the 25^{th}/75^{th} percentile from the median probe value were larger in CB, which suggests that gene expression in CB is more dynamic as in steady-state BM. Furthermore, also the range of probe value expression was larger than in BM. The initial clustering with Pearson correlation and subsequent visualisation in a datastore tree provides a basic understanding of the "relatedness" of different data sets/populations. On a simple level, HSCs and MPPs cluster together, as do MEP and CMP. The GMP and LMPP subpopulations with respect to CD62L expression cluster seemingly random, sometimes with respect to the biological sample, sometimes with respect to the immunophenotype. This suggests, that on functional, as well as molecular level, CD62L does not add any benefit in separating distinct populations in the LMPP and GMP compartment.
Principle component analysis (PCA) would be another way of clustering data sets in 2 or more dimensions to visualise their degree of relatedness. Currently, other methods are being employed in to investigate this RNA sequencing data.

The next step from sequencing populations from CB and BM would be single cell analysis. With the new C1 platform from Fluidigm, it will be possible to capture

single cells and synthesise cDNA on a single cell level. This amplified material could then be used for RNA sequencing as well. Analysis on single cell level is the only way to tackle the ever arising question of heterogeneity. Even though cells express the same markers on their surface, which allows for purification, their gene expression profiles might look quite different, since protein and gene expression level can be differentially regulated. Data from studies in the murine system suggests that many populations which are readily referred to as “CMP” or “LMPP” for instance, might contain different progenitors with heterogeneous properties. There is accumulating evidence that the CMP might be a heterogeneous population, which consists of a selection of bi-potential progenitors, where one is MkE-primed and the other GM-primed[11]. Furthermore, a recent study shows that the murine LMPP is a mixture of differentially primed progenitor populations[40]. In human, in vivo lineage fate mapping is not applicable; therefore alternatives have to be found to address the heterogeneity of human stem and progenitor populations.

A way around the fate mapping would be the labelling of single cells with random, fluorescently labelled lentiviral barcodes[150] with a subsequent in vivo assay. This would permit the tracking of single cells and their progeny in a near physiological environment. However, the labelling technique has only been optimised for murine cells so far and in vivo assays to faithfully engraft short term progenitors remain challenging. Also, lentiviral transduction procedures for low numbers of human progenitors can be problematic. However, a combined approach of the C1 single cell RNA sequencing and qPCR gene expression with a single cell in vivo fate mapping system would answer these questions in a scientifically valid way.

To make the most of this data, an in depth analysis by a qualified bioinformatician will enable us to derive cell type specific signatures which can then be validated on a population level by Taqman qPCR with appropriate positive and negative controls. RNA from all sequenced samples is still stored in appropriate conditions to enable validation.

Going further from there, single cell qPCR can then be done with the Fluidigm C1 system which would address the question of heterogeneity, as discussed before. In the meanwhile, more populations have been sorted from both BM and CB, the RNA of which has been extracted and is ready to be sent for sequencing.

8 Discussion and Future Directions

8.1 Final Discussion

The aim of this thesis was the identification and characterisation of early human myelo-lymphoid multipotent progenitors in human umbilical cord blood and bone marrow. These questions were answered with the help of purification of candidate populations by flow cytometry, in vitro functional assays and molecular techniques. In order to carry out these experiments, purification methods and in vitro functional assays had to be developed and/r optimised, which could be successfully accomplished; as it is shown in Chapters 3 and 4.

The main focus was concentrated on identifying the progenitors residing in the Lin-CD34+CD38-CD45RA+ compartment of BM and CB. Previously identified in this lab[19], the human lymphoid-primed multipotent progenitor (LMPP) remained incompletely characterised in BM and yet to be investigated in CB. I succeeded in showing functional in vitro T cell potential, NK cell potential and could also confirm that the LMPP from BM and CB gives rise to monocytic and granulocytic myeloid cells. Limit dilution assays showed that the LMPP can give rise to B and myeloid cells on a clonal level with a frequency of 1 in 12.

Moreover, it was confirmed that the LMPP CD10 -LMPP and the CD10+ multilymphoid progenitor (MLP)[20] are two distinct progenitors with different functional potentials. The LMPP can give rise to granulocytes as well monocytes, whereas the MLP is heavily lymphoid primed and only retains residual monocytic potentials. In vitro single cell assays confirmed that no MLP gave rise to granulocytes in stromal co-culture experiments or in methylcellulose culture.

Furthermore, I could place the CD10 -LMPP and the CD10+ MLP[20] into a hierarchical relationship. The LMPP can generate CD10+ MLPs after 4-6 days in vitro, whereas the MLP does not lose CD10 expression and differentiates with faster kinetics than the LMPP. This data combined with the results from the functional assays suggests that the LMPP is more immature than the MLP and can differentiate through an MLP intermediate. I propose therefore that the existence of the LMPP has now been confirmed in bone marrow and also cord blood. It is a human progenitor with B, NK, granulocytic, monocytic and T cell differentiation potential and it can give rise to CD10+ MLPs in vitro.

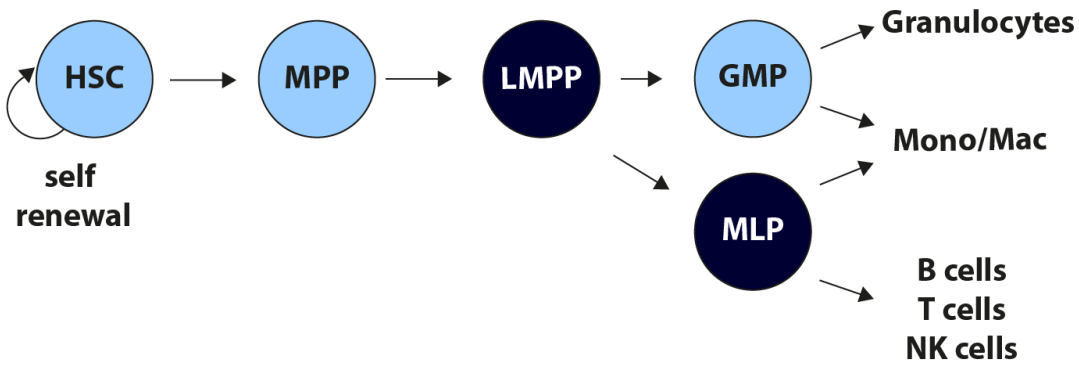

Fig. 8.1 Illustration of the Hierarchical Relationship of LMPP and MLP.
In vitro differentiation experiments suggest in the haematopoietic hierarchy, a LMPP and MLP can be found. The LMPP was confirmed to give rise to MLPs in in vitro differentiation assays.
HSC, haematopoietic stem cell; MPP, multipotent progenitor; LMPP lymphoid primed multipotent progenitor; MLP, multilymphoid progenitor; GMP, granulocyte-monocyte progenitor; NK, natural killer.

The second major aim of this research was the identification of a marker to purify the human LMPP further. As mentioned before, the frequency of functional LMPP in the immunophenotypic Lin-CD34+CD38-CD45RA+ compartment is relatively low. With the correct set of cell surface markers, it might be possible to enrich even more for LMPPs. I validated a selection of cell surface markers and subjected LMPP subpopulations to in vitro functional assays to potentially purify differentially primed populations. CD53, a tetrasparin, and CD84, one of the SLAM markers, were found to be differentially expressed between stem and progenitor populations, so I validated their expression on the LMPP. Both divided the LMPP into a negative and a positive fraction. CD53+ LMPP and CD53- LMPP did not show any difference in functional potential when cultured on MS5 cells or in methylcellulose. No difference could be found also in the CD84+ LMPP and CD84- LMPP populations. Further markers tested unsuccessfully to split the LMPP into two populations with functionally distinct properties included CD127 (IL-7Ra), Notch-1 and CD150.

Furthermore, CD62L (L-selectin) was evaluated for its significance in lymphoid priming, as published by Kohn et al[21]. Neither in the GMP nor in the LMPP population did CD62L coincide with lymphoid priming. All subpopulations were cultured in assay systems permitted B/NK/myeloid readouts, T cell readout or E/G/M/Mixed readouts. Additionally, RNA of different HSPC populations was isolated from BM and CB and subjected to next generation sequencing after cDNA generation. Transcriptional profiles could be acquired for HSC, MPP, CD62L+ LMPP, CD62L- LMPP, CMP, MEP, CD62L+ GMP and CD62L- GMP successfully. The quality measures showed satisfactory quality of the sequencing data and

preliminary data analysis suggests that lineage specific priming signatures can be detected.

Taken together, this data provide a toolkit to purify and characterise the function and molecular properties of human stem and progenitor cells in haematopoietic tissues.

Findings from the normal LMPP can be implicated into AML research, and the global RNA transcription profiles will be useful to pinpoint the differences between normal progenitors and their LSC-activity containing leukaemic counterparts in AML.

I could also confirm that LMPP and MLP are two separate progenitors with distinct functional potentials, with the LMPP giving rise to the MLP. This first approach to define hierarchical relationships in vitro assays in our group has laid the foundation to dissect the complex haematopoietic hierarchy.

Even though all attempts to purify the LMPP have been unfruitful, the RNA sequencing data generated in this study can be used to find candidate surface markers which can be validated experimentally. Similarly, it can be used to find a differentially expressed marker to enhance separation of GMP and LMPP.

8.2 Future Directions

As mentioned before, this data provides a comprehensive foundation to investigate human haematopoietic progenitor biology.

In terms of the LMPP vs. MLP question, there are a few things which would be worth doing. As I have succeeded in optimising the in vitro differentiation conditions to model the differentiation of LMPP to the MLP, the next step would be pairing this approach with the in vitro live tracking system published by Timm Schroeder's group[98]. This would allow for a quantitative readout of how many LMPP pass through an MLP intermediate and provide a frequency. Furthermore, this system can be translated to LMPP – GMP differentiation or HSC – MPP – LMPP or even the myeloid and erythroid-megakaryocytic branches of the hierarchy.

Furthermore, I am aware of the caveat in this study that there is no single cell T cell differentiation data of MLP and LMPP. Also, multipotential assays would have to be optimised to permit parallel assessment of B/myeloid/T/NK differentiation potential at best on a clonal level. Furthermore, I could not succeed in finding culture conditions permissive to read out dendritic cell (DC) potential.

The single cell capture system C1 from Fluidigm, which is capable of capturing single cells and subjecting them to pre-amplification, cDNA synthesis and subsequent multiplex qPCR can be used in the future to interrogate single cell gene expression programs of LMPP and MLP to filter out the differences between these populations on a molecular level. RNA from MLP has been prepared for next generation sequencing and with RNA profiles from MLP and LMPP, it will be possible in identifying candidate genes of surface markers to purify both populations further.

The LMPP-MLP data has mainly been acquired in samples from CB. The MLP and LMPP compartment are smaller in bone marrow, therefore extending this research to BM LMPP and MLP will be challenging. Cell yields are very low, which

would impact on techniques requiring large amounts of cells, such as RNA sequencing or limit dilution assays. Pooling of individual samples would have to be considered.

With respect to the surface marker question, the best way to identify candidate markers to improve purification would be in silico analysis of the RNA sequencing data acquired and mine it for potential surface markers. A large scale approach to test an array of different surface markers for expression on leukaemia cells has been set up in our group; it could be adapted for analysis of normal stem and progenitor populations to screen for surface markers. After the initial screening process, candidate markers can be picked and LMPP/GMP subpopulations assayed for functional and molecular properties.

Furthermore, the RNA sequencing data from various populations can be completed to include three biological replicates of every population in CB and BM. Due to the limited availability of normal bone marrow samples, there are replicates still missing for populations sorted from BM. I have extracted RNA from additional populations from BM and it is ready to be subjected to RNA sequencing. With a completed dataset for CB and BM, it will be easy to compare the neonatal to the adult tissue and filter out differences. Moreover, a similar approach as published by our group before[19] of comparing global gene expression data of normal progenitor populations and their leukaemic counterparts can also be done with RNA sequencing data. Potential differences in normal and leukaemic cells can be evaluated for their value to target them.

One point which has not been addressed in this thesis is the in vivo engraftment potential of human HSPCs. Since engraftment of progenitors is very poorly in most

immunocompromised mouse strains in the short term[20,21] as well as intermediate term[19] a new alternative to those xenograft models has to be found. Potential systems include subcutaneous implantation of foetal human bone, co-transplantation of mesenchymal stem cells and the usage of humanised mice to improve engraftment of early human progenitor cells.

9 References

1. Payne, K.J. & Crooks, G.M. Immune-Cell Lineage Commitment: Translation from Mice to Humans. *Immunity* **26**, 674-677 (2007).
2. Terstappen, L., Huang, S., Safford, M., Lansdorp, P. & Loken, M. Sequential generations of hematopoietic colonies derived from single nonlineage-committed CD34+CD38- progenitor cells. *Blood* **77**, 1218-1227 (1991).
3. Kiel, M.J., Yilmaz, Ö.H., Iwashita, T., Yilmaz, O.H., Terhorst, C. & Morrison, S.J. SLAM Family Receptors Distinguish Hematopoietic Stem and Progenitor Cells and Reveal Endothelial Niches for Stem Cells. *Cell* **121**, 1109-1121 (2005).
4. Notta, F., Doulatov, S. & Dick, J.E. Engraftment of human hematopoietic stem cells is more efficient in female NOD/SCID/IL-2Rgc-null recipients. *Blood* **115**, 3704-3707 (2010).
5. Kawamoto, H. & Katsura, Y. A new paradigm for hematopoietic cell lineages: revision of the classical concept of the myeloid–lymphoid dichotomy. *Trends in Immunology* **30**, 193-200 (2009).
6. Kondo, M., Weissman, I.L. & Akashi, K. Identification of Clonogenic Common Lymphoid Progenitors in Mouse Bone Marrow. *Cell* **91**, 661-672 (1997).
7. Akashi, K., Traver, D., Miyamoto, T. & Weissman, I.L. A clonogenic common myeloid progenitor that gives rise to all myeloid lineages. *Nature* **404**, 193-197 (2000).
8. Wu, L., Antica, M., Johnson, G.R., Scollay, R. & Shortman, K. Developmental potential of the earliest precursor cells from the adult mouse thymus. *The Journal of Experimental Medicine* **174**, 1617-1627 (1991).
9. Nutt, S.L., Metcalf, D., D'Amico, A., Polli, M. & Wu, L. Dynamic regulation of PU.1 expression in multipotent hematopoietic progenitors. *The Journal of Experimental Medicine* **201**, 221-231 (2005).
10. Pronk, C.J.H., Rossi, D.J., Månsson, R., Attema, J.L., Norddahl, G.L., Chan, C.K.F., Sigvardsson, M., Weissman, I.L. & Bryder, D. Elucidation of the Phenotypic, Functional, and Molecular Topography of a Myeloerythroid Progenitor Cell Hierarchy. *Cell Stem Cell* **1**, 428-442 (2007).
11. Arinobu, Y., Mizuno, S.-i., Chong, Y., Shigematsu, H., Iino, T., Iwasaki, H., Graf, T., Mayfield, R., Chan, S., Kastner, P. & Akashi, K. Reciprocal Activation of GATA-1 and PU.1 Marks Initial Specification of Hematopoietic Stem Cells into Myeloerythroid and Myelolymphoid Lineages. *Cell Stem Cell* **1**, 416-427 (2007).
12. Borghesi, L., Hsu, L.-Y., Miller, J.P., Anderson, M., Herzenberg, L., Herzenberg, L., Schlissel, M.S., Allman, D. & Gerstein, R.M. B Lineage–specific Regulation of V(D)J Recombinase Activity Is Established in Common Lymphoid Progenitors. *The Journal of Experimental Medicine* **199**, 491-502 (2004).
13. Rumfelt, L.L., Zhou, Y., Rowley, B.M., Shinton, S.A. & Hardy, R.R. Lineage specification and plasticity in CD19− early B cell precursors. *The Journal of Experimental Medicine* **203**, 675-687 (2006).
14. Balciunaite, G., Ceredig, R., Massa, S. & Rolink, A.G. A B220+ CD117+ CD19± hematopoietic progenitor with potent lymphoid and myeloid developmental potential. *European Journal of Immunology* **35**, 2019-2030 (2005).
15. Pang, W.W., Price, E.A., Sahoo, D., Beerman, I., Maloney, W.J., Rossi, D.J., Schrier, S.L. & Weissman, I.L. Human bone marrow hematopoietic stem cells are increased in frequency and myeloid-biased with age. *Proceedings of the National Academy of Sciences* (2011).
16. Adolfsson, J., Månsson, R., Buza-Vidas, N., Hultquist, A., Liuba, K., Jensen, C.T., Bryder, D., Yang, L., Borge, O.-J., Thoren, L.A.M., Anderson, K., Sitnicka, E., Sasaki, Y., Sigvardsson, M. & Jacobsen, S.E.W. Identification of Flt3+ Lympho-Myeloid Stem Cells Lacking Erythro-

Megakaryocytic Potential: A Revised Road Map for Adult Blood Lineage Commitment. *Cell* **121**, 295-306 (2005).
17. Adolfsson, J., Borge, O.J., Bryder, D., Theilgaard-Mönch, K., Åstrand-Grundström, I., Sitnicka, E., Sasaki, Y. & Jacobsen, S.E.W. Upregulation of Flt3 Expression within the Bone Marrow Lin-Sca1+c-kit+ Stem Cell Compartment Is Accompanied by Loss of Self-Renewal Capacity. *Immunity* **15**, 659-669 (2001).
18. Luc, S., Luis, T.C., Boukarabila, H., Macaulay, I.C., Buza-Vidas, N., Bouriez-Jones, T., Lutteropp, M., Woll, P.S., Loughran, S.J., Mead, A.J., Hultquist, A., Brown, J., Mizukami, T., Matsuoka, S., Ferry, H., Anderson, K., Duarte, S., Atkinson, D., Soneji, S., Domanski, A., Farley, A., Sanjuan-Pla, A., Carella, C., Patient, R., de Bruijn, M., Enver, T., Nerlov, C., Blackburn, C., Godin, I. & Jacobsen, S.E.W. The earliest thymic T cell progenitors sustain B cell and myeloid lineage potential. *Nat Immunol* **13**, 412-419 (2012).
19. Goardon, N., Marchi, E., Atzberger, A., Quek, L., Schuh, A., Soneji, S., Woll, P., Mead, A., Alford, K.A., Rout, R., Chaudhury, S., Gilkes, A., Knapper, S., Beldjord, K., Begum, S., Rose, S., Geddes, N., Griffiths, M., Standen, G., Sternberg, A., Cavenagh, J., Hunter, H., Bowen, D., Killick, S., Robinson, L., Price, A., Macintyre, E., Virgo, P., Burnett, A., Craddock, C., Enver, T., Jacobsen, S.E.W., Porcher, C. & Vyas, P. Coexistence of LMPP-like and GMP-like Leukemia Stem Cells in Acute Myeloid Leukemia. *Cancer Cell* **19**, 138-152 (2011).
20. Doulatov, S., Notta, F., Eppert, K., Nguyen, L.T., Ohashi, P.S. & Dick, J.E. Revised map of the human progenitor hierarchy shows the origin of macrophages and dendritic cells in early lymphoid development. *Nat Immunol* **11**, 585-593 (2010).
21. Kohn, L.A., Hao, Q.-L., Sasidharan, R., Parekh, C., Ge, S., Zhu, Y., Mikkola, H.K.A. & Crooks, G.M. Lymphoid priming in human bone marrow begins before expression of CD10 with upregulation of L-selectin. *Nat Immunol* **13**, 963-971 (2012).
22. Six, E.M., Bonhomme, D., Monteiro, M., Beldjord, K., Jurkowska, M., Cordier-Garcia, C., Garrigue, A., Dal Cortivo, L., Rocha, B., Fischer, A., Cavazzana-Calvo, M. & André-Schmutz, I. A human postnatal lymphoid progenitor capable of circulating and seeding the thymus. *The Journal of Experimental Medicine* **204**, 3085-3093 (2007).
23. Kawamoto, H., Ikawa, T., Masuda, K., Wada, H. & Katsura, Y. A map for lineage restriction of progenitors during hematopoiesis: the essence of the myeloid-based model. *Immunological Reviews* **238**, 23-36 (2010).
24. Kawamoto, H. & Katsura, Y. A new paradigm for hematopoietic cell lineages: revision of the classical concept of the myeloid-lymphoid dichotomy. *Trends in Immunology* **30**, 193-200 (2009).
25. Kawamoto, H., Ohmura, K. & Katsura, Y. Direct evidence for the commitment of hematopoietic stem cells to T, B and myeloid lineages in murine fetal liver. *International Immunology* **9**, 1011-1019 (1997).
26. Kawamoto, H., Wada, H. & Katsura, Y. A revised scheme for developmental pathways of hematopoietic cells: the myeloid-based model. *International Immunology* **22**, 65-70 (2010).
27. Montecino-Rodriguez, E., Leathers, H. & Dorshkind, K. Bipotential B-macrophage progenitors are present in adult bone marrow. *Nat Immunol* **2**, 83-88 (2001).
28. Till, J.E., McCulloch, E.A. & Siminovitch, L. A STOCHASTIC MODEL OF STEM CELL PROLIFERATION, BASED ON THE GROWTH OF SPLEEN COLONY-FORMING CELLS. *Proceedings of the National Academy of Sciences* **51**, 29-36 (1964).
29. Nicola, N. & Johnson, G. The production of committed hemopoietic colony-forming cells from multipotential precursor cells in vitro. *Blood* **60**, 1019-1029 (1982).
30. Brown, G., Bunce, C.M. & Guy, G.R. Sequential determination of lineage potentials during haemopoiesis. *Br J Cancer* **52**, 681-686 (1985).
31. Brown, G., Hughes, P.J., Michell, R.H., Rolink, A.G. & Ceredig, R. The sequential determination model of hematopoiesis. *Trends in Immunology* **28**, 442-448 (2007).

32. Lu, L., Walker, D., Broxmeyer, H.E., Hoffman, R., Hu, W. & Walker, E. Characterization of adult human marrow hematopoietic progenitors highly enriched by two-color cell sorting with My10 and major histocompatibility class II monoclonal antibodies. *The Journal of Immunology* **139**, 1823-1829 (1987).
33. Civin, C.I., Strauss, L.C., Brovall, C., Fackler, M.J., Schwartz, J.F. & Shaper, J.H. Antigenic analysis of hematopoiesis. III. A hematopoietic progenitor cell surface antigen defined by a monoclonal antibody raised against KG-1a cells. *The Journal of Immunology* **133**, 157-165 (1984).
34. Peault, B., Weissman, I.L., Baum, C., McCune, J.M. & Tsukamoto, A. Lymphoid Reconstitution of the Human Fetal Thymus in SCID Mice with CD34+ Precursor Cells. *Journal of Experimental Medicine* **174**, 1283-1286 (1991).
35. Baum, C.M., Weissman, I.L., Tsukamoto, A.S., Buckle, A.M. & Peault, B. Isolation of a candidate human hematopoietic stem-cell population. *Proceedings of the National Academy of Sciences* **89**, 2804-2808 (1992).
36. Bhatia, M., Wang, J.C.Y., Kapp, U., Bonnet, D. & Dick, J.E. Purification of primitive human hematopoietic cells capable of repopulating immune-deficient mice. *Proceedings of the National Academy of Sciences* **94**, 5320-5325 (1997).
37. Majeti, R., Park, C.Y. & Weissman, I.L. Identification of a Hierarchy of Multipotent Hematopoietic Progenitors in Human Cord Blood. *Cell Stem Cell* **1**, 635-645 (2007).
38. Scott, E.W., Simon, M.C., Anastasi, J. & Singh, H. Requirement of Transcription Factor PU.1 in the Development of Multiple Hematopoietic Lineages. *Science* **265**, 1573-1577 (1994).
39. Laurenti, E., Doulatov, S., Zandi, S., Plumb, I., Chen, J., April, C., Fan, J.-B. & Dick, J.E. The transcriptional architecture of early human hematopoiesis identifies multilevel control of lymphoid commitment. *Nat Immunol* **14**, 756-763 (2013).
40. Naik, S.H., Perie, L., Swart, E., Gerlach, C., van Rooij, N., de Boer, R.J. & Schumacher, T.N. Diverse and heritable lineage imprinting of early haematopoietic progenitors. *Nature* **496**, 229-232 (2013).
41. Manz, M.G., Miyamoto, T., Akashi, K. & Weissman, I.L. Prospective isolation of human clonogenic common myeloid progenitors. *Proceedings of the National Academy of Sciences* **99**, 11872-11877 (2002).
42. Edvardsson, L., Dykes, J. & Olofsson, T. Isolation and characterization of human myeloid progenitor populations—TpoR as discriminator between common myeloid and megakaryocyte/erythroid progenitors. *Experimental Hematology* **34**, 599-609 (2006).
43. Ng, S.Y.-M., Yoshida, T., Zhang, J. & Georgopoulos, K. Genome-wide Lineage-Specific Transcriptional Networks Underscore Ikaros-Dependent Lymphoid Priming in Hematopoietic Stem Cells. *Immunity* **30**, 493-507 (2009).
44. UK, N. in *NHS UK*, Vol. 2013 (NHS UK).
45. UK, C.R., Vol. 2013 (2013).
46. Hoffbrand, A.V., Pettit, J.E. & Vyas, P. *Clinical Hematology*, (MOSBY Elsevier, 2010).
47. Tenen, D.G. Disruption of differentiation in human cancer: AML shows the way. *Nat Rev Cancer* **3**, 89-101 (2003).
48. Estey, E. & Döhner, H. Acute myeloid leukaemia. *The Lancet* **368**, 1894-1907.
49. Grimwade, D., Walker, H., Harrison, G., Oliver, F., Chatters, S., Harrison, C.J., Wheatley, K., Burnett, A.K. & Goldstone, A.H. The predictive value of hierarchical cytogenetic classification in older adults with acute myeloid leukemia (AML): analysis of 1065 patients entered into the United Kingdom Medical Research Council AML11 trial. *Blood* **98**, 1312-1320 (2001).
50. Grimwade, D., Walker, H., Oliver, F., Wheatley, K., Harrison, C., Harrison, G., Rees, J., Hann, I., Stevens, R., Burnett, A. & Goldstone, A. The Importance of Diagnostic

Cytogenetics on Outcome in AML: Analysis of 1,612 Patients Entered Into the MRC AML 10 Trial. *Blood* **92**, 2322-2333 (1998).

51. Byrd, J.C., Mrózek, K., Dodge, R.K., Carroll, A.J., Edwards, C.G., Arthur, D.C., Pettenati, M.J., Patil, S.R., Rao, K.W., Watson, M.S., Koduru, P.R.K., Moore, J.O., Stone, R.M., Mayer, R.J., Feldman, E.J., Davey, F.R., Schiffer, C.A., Larson, R.A. & Bloomfield, C.D. Pretreatment cytogenetic abnormalities are predictive of induction success, cumulative incidence of relapse, and overall survival in adult patients with de novo acute myeloid leukemia: results from Cancer and Leukemia Group B (CALGB 8461): Presented in part at the 43rd annual meeting of the American Society of Hematology, Orlando, FL, December 10, 2001, and published in abstract form.59. *Blood* **100**, 4325-4336 (2002).
52. Slovak, M.L., Kopecky, K.J., Cassileth, P.A., Harrington, D.H., Theil, K.S., Mohamed, A., Paietta, E., Willman, C.L., Head, D.R., Rowe, J.M., Forman, S.J. & Appelbaum, F.R. Karyotypic analysis predicts outcome of preremission and postremission therapy in adult acute myeloid leukemia: a Southwest Oncology Group/Eastern Cooperative Oncology Group study. *Blood* **96**, 4075-4083 (2000).
53. Griffin, J. & Lowenberg, B. Clonogenic cells in acute myeloblastic leukemia. *Blood* **68**, 1185-1195 (1986).
54. Bonnet, D. & Dick, J.E. Human acute myeloid leukemia is organized as a hierarchy that originates from a primitive hematopoietic cell. *Nat Med* **3**, 730-737 (1997).
55. McCulloch, E. Stem cells in normal and leukemic hemopoiesis (Henry Stratton Lecture, 1982). *Blood* **62**, 1-13 (1983).
56. Clarke, M.F., Dick, J.E., Dirks, P.B., Eaves, C.J., Jamieson, C.H.M., Jones, D.L., Visvader, J., Weissman, I.L. & Wahl, G.M. Cancer Stem Cells—Perspectives on Current Status and Future Directions: AACR Workshop on Cancer Stem Cells. *Cancer Research* **66**, 9339-9344 (2006).
57. Lapidot, T., Sirard, C., Vormoor, J., Murdoch, B., Hoang, T., Caceres-Cortes, J., Minden, M., Paterson, B., Caligiuri, M.A. & Dick, J.E. A cell initiating human acute myeloid leukaemia after transplantation into SCID mice. *Nature* **367**, 645-648 (1994).
58. Taussig, D.C., Miraki-Moud, F., Anjos-Afonso, F., Pearce, D.J., Allen, K., Ridler, C., Lillington, D., Oakervee, H., Cavenagh, J., Agrawal, S.G., Lister, T.A., Gribben, J.G. & Bonnet, D. Anti-CD38 antibody–mediated clearance of human repopulating cells masks the heterogeneity of leukemia-initiating cells. *Blood* **112**, 568-575 (2008).
59. Eppert, K., Takenaka, K., Lechman, E.R., Waldron, L., Nilsson, B., van Galen, P., Metzeler, K.H., Poeppl, A., Ling, V., Beyene, J., Canty, A.J., Danska, J.S., Bohlander, S.K., Buske, C., Minden, M.D., Golub, T.R., Jurisica, I., Ebert, B.L. & Dick, J.E. Stem cell gene expression programs influence clinical outcome in human leukemia. *Nat Med* **17**, 1086-1093 (2011).
60. Miyamoto, T., Weissman, I.L. & Akashi, K. AML1/ETO-expressing nonleukemic stem cells in acute myelogenous leukemia with 8;21 chromosomal translocation. *Proceedings of the National Academy of Sciences* **97**, 7521-7526 (2000).
61. Krivtsov, A.V., Feng, Z. & Armstrong, S.A. Transformation from Committed Progenitor to Leukemia Stem Cells. *Annals of the New York Academy of Sciences* **1176**, 144-149 (2009).
62. Majeti, R., Chao, M.P., Alizadeh, A.A., Pang, W.W., Jaiswal, S., Gibbs Jr, K.D., van Rooijen, N. & Weissman, I.L. CD47 Is an Adverse Prognostic Factor and Therapeutic Antibody Target on Human Acute Myeloid Leukemia Stem Cells. *Cell* **138**, 286-299 (2009).
63. Berardi, A.C., Meffre, E., Pflumio, F., Katz, A., Vainchenker, W., Schiff, C. & Coulombel, L. Individual CD34+CD38lowCD19−CD10− Progenitor Cells From Human Cord Blood Generate B Lymphocytes and Granulocytes. *Blood* **89**, 3554-3564 (1997).
64. Mori, Y., Iwasaki, H., Kohno, K., Yoshimoto, G., Kikushige, Y., Okeda, A., Uike, N., Niiro, H., Takenaka, K., Nagafuji, K., Miyamoto, T., Harada, M., Takatsu, K. & Akashi, K. Identification of the human eosinophil lineage-committed progenitor: revision of

phenotypic definition of the human common myeloid progenitor. *The Journal of Experimental Medicine* **206**, 183-193 (2009).
65. La Motte-Mohs, R.N., Herer, E. & Zúñiga-Pflücker, J.C. Induction of T-cell development from human cord blood hematopoietic stem cells by Delta-like 1 in vitro. *Blood* **105**, 1431-1439 (2005).
66. Six, E.M., Benjelloun, F., Garrigue, A., Bonhomme, D., Morillon, E., Rouiller, J., Cacavelli, L., Blondeau, J., Beldjord, K., Hacein-Bey-Abina, S., Cavazzana-Calvo, M. & André-Schmutz, I. Cytokines and culture medium have a major impact on human in vitro T-cell differentiation. *Blood Cells, Molecules, and Diseases* **47**, 72-78 (2011).
67. Galy, A., Travis, M., Cen, D. & Chen, B. Human T, B, natural killer, and dendritic cells arise from a common bone marrow progenitor cell subset. *Immunity* **3**, 459-473 (1995).
68. Hao, Q.-L., Zhu, J., Price, M.A., Payne, K.J., Barsky, L.W. & Crooks, G.M. Identification of a novel, human multilymphoid progenitor in cord blood. *Blood* **97**, 3683-3690 (2001).
69. Chen, N., He, Y., Su, Y., Li, X., Huang, Q., Wang, H., Zhang, X., Tai, R. & Fan, C. The cytotoxicity of cadmium-based quantum dots. *Biomaterials* **33**, 1238-1244 (2012).
70. Derfus, A.M., Chan, W.C.W. & Bhatia, S.N. Probing the Cytotoxicity of Semiconductor Quantum Dots. *Nano Letters* **4**, 11-18 (2003).
71. Lovrić, J., Cho, S.J., Winnik, F.M. & Maysinger, D. Unmodified Cadmium Telluride Quantum Dots Induce Reactive Oxygen Species Formation Leading to Multiple Organelle Damage and Cell Death. *Chemistry & Biology* **12**, 1227-1234 (2005).
72. Notta, F., Doulatov, S., Laurenti, E., Poeppl, A., Jurisica, I. & Dick, J.E. Isolation of Single Human Hematopoietic Stem Cells Capable of Long-Term Multilineage Engraftment. *Science* **333**, 218-221 (2011).
73. Nishihara, M., Wada, Y., Ogami, K., Ebihara, Y., Ishii, T., Tsuji, K., Ueno, H., Asano, S., Nakahata, T. & Maekawa, T. A combination of stem cell factor and granulocyte colony-stimulating factor enhances the growth of human progenitor B cells supported by murine stromal cell line MS-5. *European Journal of Immunology* **28**, 855-864 (1998).
74. Yoshikawa, Y., Ikebuchi, K., Ohkawara, J.-i., Hirayama, F., Yamaguchi, M., Sato, N., Mori, J.K., Kasai, M. & Sekiguchi, S. A Clonal Culture Assay for Human Cord Blood Lymphohematopoietic Progenitors. *Human Immunology* **60**, 75-82 (1999).
75. Technologies, S.C. L-Calc Software. Vol. 2013 (2005).
76. Schmitt, T.M. & Zúñiga-Pflücker, J.C. Induction of T Cell Development from Hematopoietic Progenitor Cells by Delta-like-1 In Vitro. *Immunity* **17**, 749-756 (2002).
77. Blom, B. & Spits, H. Development Of Human Lymphoid Cells. *Annual Review of Immunology* **24**, 287-320 (2006).
78. Armstrong, F., de la Grange, P.B., Gerby, B., Rouyez, M.-C., Calvo, J., Fontenay, M., Boissel, N., Dombret, H., Baruchel, A., Landman-Parker, J., Roméo, P.-H., Ballerini, P. & Pflumio, F. NOTCH is a key regulator of human T-cell acute leukemia initiating cell activity. *Blood* **113**, 1730-1740 (2009).
79. Mohtashami, M., Shah, D.K., Nakase, H., Kianizad, K., Petrie, H.T. & Zúñiga-Pflücker, J.C. Direct Comparison of Dll1- and Dll4-Mediated Notch Activation Levels Shows Differential Lymphomyeloid Lineage Commitment Outcomes. *The Journal of Immunology* **185**, 867-876 (2010).
80. Canque, B., Camus, S., Dalloul, A., Kahn, E., Yagello, M., Dezutter-Dambuyant, C., Schmitt, D., Schmitt, C. & Gluckman, J.C. Characterization of dendritic cell differentiation pathways from cord blood CD34+CD7+CD45RA+hematopoietic progenitor cells. *Blood* **96**, 3748-3756 (2000).
81. Sutherland DR, M.J., Davidson J, Baker MA, Keating A, Mellors A. Differential sensitivity of CD34 epitopes to cleavage by Pasteurella haemolytica glycoprotease: implications for purification of CD34-positive progenitor cells. *Experimental Hematology* **20**, 590-599 (1992).

82. Chang, H.H., Hemberg, M., Barahona, M., Ingber, D.E. & Huang, S. Transcriptome-wide noise controls lineage choice in mammalian progenitor cells. *Nature* **453**, 544-547 (2008).
83. Fairbairn, L.J., Cowling, G.J., Reipert, B.M. & Dexter, T.M. Suppression of apoptosis allows differentiation and development of a multipotent hemopoietic cell line in the absence of added growth factors. *Cell* **74**, 823-832 (1993).
84. Rieger, M.A., Hoppe, P.S., Smejkal, B.M., Eitelhuber, A.C. & Schroeder, T. Hematopoietic Cytokines Can Instruct Lineage Choice. *Science* **325**, 217-218 (2009).
85. Mossadegh-Keller, N., Sarrazin, S., Kandalla, P.K., Espinosa, L., Stanley, E.R., Nutt, S.L., Moore, J. & Sieweke, M.H. M-CSF instructs myeloid lineage fate in single haematopoietic stem cells. *Nature* **497**, 239-243 (2013).
86. Kouro, T., Yokota, T., Welner, R. & Kincade, P.W. In Vitro Differentiation and Measurement Of B Cell Progenitor Activity in Culture. *Current Protocols in Immunology*, 22F.22.21-22F22.22.12 (2005).
87. Chen, X., Esplin, B.L., Garrett, K.P., Welner, R.S., Webb, C.F. & Kincade, P.W. Retinoids Accelerate B Lineage Lymphoid Differentiation. *The Journal of Immunology* **180**, 138-145 (2008).
88. Breitman, T., Collins, S. & Keene, B. Terminal differentiation of human promyelocytic leukemic cells in primary culture in response to retinoic acid. *Blood* **57**, 1000-1004 (1981).
89. Huang, M., Ye, Y., Chen, S., Chai, J., Lu, J., Zhoa, L., Gu, L. & Wang, Z. Use of all-trans retinoic acid in the treatment of acute promyelocytic leukemia. *Blood* **72**, 567-572 (1988).
90. Maillard, I., Fang, T. & Pear, W.S. Regulation of lymphoid development, differentiation and function by the notch pathway. *Annual Review of Immunology* **23**, 945-974 (2005).
91. Toru, N. Lymphohematopoietic development from embryonic stem cells in vitro. *Seminars in Immunology* **7**, 197-203 (1995).
92. Radtke, F., Wilson, A., Stark, G., Bauer, M., van Meerwijk, J., MacDonald, H.R. & Aguet, M. Deficient T Cell Fate Specification in Mice with an Induced Inactivation of Notch1. *Immunity* **10**, 547-558 (1999).
93. Hozumi, K., Negishi, N., Suzuki, D., Abe, N., Sotomaru, Y., Tamaoki, N., Mailhos, C., Ish-Horowicz, D., Habu, S. & Owen, M.J. Delta-like 1 is necessary for the generation of marginal zone B cells but not T cells in vivo. *Nat Immunol* **5**, 638-644 (2004).
94. Hozumi, K., Mailhos, C., Negishi, N., Hirano, K.-i., Yahata, T., Ando, K., Zuklys, S., Holländer, G.A., Shima, D.T. & Habu, S. Delta-like 4 is indispensable in thymic environment specific for T cell development. *The Journal of Experimental Medicine* **205**, 2507-2513 (2008).
95. Reid, D.C.D.L. THE DENDRITIC CELL LINEAGE IN HAEMOPOIESIS. *British Journal of Haematology* **96**, 217-223 (1997).
96. Wu, L. & Liu, Y.-J. Development of Dendritic-Cell Lineages. *Immunity* **26**, 741-750 (2007).
97. Hoebeke, I., De Smedt, M., Stolz, F., Pike-Overzet, K., Staal, F.J.T., Plum, J. & Leclercq, G. T-, B- and NK-lymphoid, but not myeloid cells arise from human CD34+CD38-CD7+ common lymphoid progenitors expressing lymphoid-specific genes. *Leukemia* **21**, 311-319 (2006).
98. Eilken, H.M., Nishikawa, S.-I. & Schroeder, T. Continuous single-cell imaging of blood generation from haemogenic endothelium. *Nature* **457**, 896-900 (2009).
99. Hulspas, R., Dombkowski, D., Preffer, F., Douglas, D., Kildew-Shah, B. & Gilbert, J. Flow cytometry and the stability of phycoerythrin-tandem dye conjugates. *Cytometry Part A* **75A**, 966-972 (2009).
100. Shultz, L.D., Lyons, B.L., Burzenski, L.M., Gott, B., Chen, X., Chaleff, S., Kotb, M., Gillies, S.D., King, M., Mangada, J., Greiner, D.L. & Handgretinger, R. Human Lymphoid and Myeloid Cell Development in NOD/LtSz-scid IL2Rγnull Mice Engrafted with Mobilized Human Hemopoietic Stem Cells. *The Journal of Immunology* **174**, 6477-6489 (2005).
101. Pearson, T., Schultz, L.D., Miller, D., King, M., Laning, J., Fodor, W., Cuthbert, A., Burzenski, L., Gott, B., Lyons, B., Foreman, O., Rossini, A.A. & Greiner, D.L. Non-obese

diabetic–recombination activating gene-1 (NOD–Rag 1 null) interleukin (IL)-2 receptor common gamma chain (IL 2 rγnull) null mice: a radioresistant model for human lymphohaematopoietic engraftment. *Clinical and Experimental Immunology* **154**, 270-284 (2008).

102. Billerbeck, E., Barry, W.T., Mu, K., Dorner, M., Rice, C.M. & Ploss, A. Development of human CD4+FoxP3+ regulatory T cells in human stem cell factor–, granulocyte-macrophage colony-stimulating factor–, and interleukin-3–expressing NOD-SCID IL2Rγnull humanized mice. *Blood* **117**, 3076-3086 (2011).
103. Kyoizumi, S., Baum, C., Kaneshima, H., McCune, J., Yee, E. & Namikawa, R. Implantation and maintenance of functional human bone marrow in SCID-hu mice. *Blood* **79**, 1704-1711 (1992).
104. Lam, P., Yang, W., Amemiya, Y., Kahn, H., Yee, A., Holloway, C. & Seth, A. A human bone NOD/SCID mouse model to distinguish metastatic potential in primary breast cancers. *Cancer Biology & Therapy* **8**, 1010-1017 (2009).
105. Nemeth, J.A., Harb, J.F., Barroso, U., He, Z., Grignon, D.J. & Cher, M.L. Severe Combined Immunodeficient-hu Model of Human Prostate Cancer Metastasis to Human Bone. *Cancer Research* **59**, 1987-1993 (1999).
106. Muguruma, Y., Matsushita, H., Yahata, T., Yumino, S., Tanaka, Y., Miyachi, H., Ogawa, Y., Kawada, H., Ito, M. & Ando, K. Establishment of a xenograft model of human myelodysplastic syndromes. *Haematologica* **96**, 543-551 (2011).
107. Muguruma, Y., Yahata, T., Miyatake, H., Sato, T., Uno, T., Itoh, J., Kato, S., Ito, M., Hotta, T. & Ando, K. Reconstitution of the functional human hematopoietic microenvironment derived from human mesenchymal stem cells in the murine bone marrow compartment. *Blood* **107**, 1878-1887 (2006).
108. Horejsi, V. & Vlcek, C. Novel structurally distinct family of leucocyte surface glycoproteins including CD9, CD37, CD53 and CD63. *FEBS Letters* **288**, 1-4 (1991).
109. Rasmussen, A., Blomhoff, H., Stokke, T., Horejsi, V. & Smeland, E. Cross-linking of CD53 promotes activation of resting human B lymphocytes. *The Journal of Immunology* **153**, 4997-5007 (1994).
110. Mannion, B., Berditchevski, F., Kraeft, S., Chen, L. & Hemler, M. Transmembrane-4 superfamily proteins CD81 (TAPA-1), CD82, CD63, and CD53 specifically associated with integrin alpha 4 beta 1 (CD49d/CD29). *The Journal of Immunology* **157**, 2039-2047 (1996).
111. Matsunaga, T., Takemoto, N., Sato, T., Takimoto, R., Tanaka, I., Fujimi, A., Akiyama, T., Kuroda, H., Kawano, Y., Kobune, M., Kato, J., Hirayama, Y., Sakamaki, S., Kohda, K., Miyake, K. & Niitsu, Y. Interaction between leukemic-cell VLA-4 and stromal fibronectin is a decisive factor for minimal residual disease of acute myelogenous leukemia. *Nat Med* **9**, 1158-1165 (2003).
112. Veillette, A. SLAM-Family Receptors: Immune Regulators with or without SAP-Family Adaptors. *Cold Spring Harb Perspect Biol.* **2**(2010).
113. Veillette, A. & Latour, S. The SLAM family of immune-cell receptors. *Current Opinion in Immunology* **15**, 277-285 (2003).
114. Plum, J., De Smedt, M., Leclercq, G., Verhasselt, B. & Vandekerckhove, B. Interleukin-7 is a critical growth factor in early human T-cell development. *Blood* **88**, 4239-4245 (1996).
115. Radtke, F., Wilson, A., Mancini, S.J.C. & MacDonald, H.R. Notch regulation of lymphocyte development and function. *Nat Immunol* **5**, 247-253 (2004).
116. Sintes, J., Romero, X., Marin, P., Terhorst, C. & Engel, P. Differential expression of CD150 (SLAM) family receptors by human hematopoietic stem and progenitor cells. *Experimental Hematology* **36**, 1199-1204 (2008).
117. Rosen, S.D. Ligands for L-Selectin: Homing, Inflammation, and Beyond. *Annual Review of Immunology* **22**, 129-156 (2004).

118. Bendall, S.C., Simonds, E.F., Qiu, P., Amir, E.-a.D., Krutzik, P.O., Finck, R., Bruggner, R.V., Melamed, R., Trejo, A., Ornatsky, O.I., Balderas, R.S., Plevritis, S.K., Sachs, K., Pe'er, D., Tanner, S.D. & Nolan, G.P. Single-Cell Mass Cytometry of Differential Immune and Drug Responses Across a Human Hematopoietic Continuum. *Science* **332**, 687-696 (2011).
119. Weksberg, D.C., Chambers, S.M., Boles, N.C. & Goodell, M.A. CD150− side population cells represent a functionally distinct population of long-term hematopoietic stem cells. *Blood* **111**, 2444-2451 (2008).
120. Nodland, S.E., Berkowska, M.A., Bajer, A.A., Shah, N., de Ridder, D., van Dongen, J.J.M., LeBien, T.W. & van Zelm, M.C. IL-7R expression and IL-7 signaling confer a distinct phenotype on developing human B-lineage cells. *Blood* **118**, 2116-2127 (2011).
121. Balciunaite, G., Ceredig, R., Fehling, H.-J., Zúñiga-Pflücker, J.-C. & Rolink, A.G. The role of Notch and IL-7 signaling in early thymocyte proliferation and differentiation. *European Journal of Immunology* **35**, 1292-1300 (2005).
122. Dykstra, B., Olthof, S., Schreuder, J., Ritsema, M. & de Haan, G. Clonal analysis reveals multiple functional defects of aged murine hematopoietic stem cells. *The Journal of Experimental Medicine* **208**, 2691-2703 (2011).
123. Dykstra, B., Kent, D., Bowie, M., McCaffrey, L., Hamilton, M., Lyons, K., Lee, S.-J., Brinkman, R. & Eaves, C. Long-Term Propagation of Distinct Hematopoietic Differentiation Programs In Vivo. *Cell Stem Cell* **1**, 218-229 (2007).
124. Kuranda, K., Vargaftig, J., de la Rochere, P., Dosquet, C., Charron, D., Bardin, F., Tonnelle, C., Bonnet, D. & Goodhardt, M. Age-related changes in human hematopoietic stem/progenitor cells. *Aging Cell* **10**, 542-546 (2011).
125. Han, S., Yang, K., Ozen, Z., Peng, W., Marinova, E., Kelsoe, G. & Zheng, B. Enhanced Differentiation of Splenic Plasma Cells but Diminished Long-Lived High-Affinity Bone Marrow Plasma Cells in Aged Mice. *The Journal of Immunology* **170**, 1267-1273 (2003).
126. Dorshkind, K., Montecino-Rodriguez, E. & Signer, R.A.J. The ageing immune system: is it ever too old to become young again? *Nat Rev Immunol* **9**, 57-62 (2009).
127. Mocchegiani, E. & Malavolta, M. NK and NKT cell functions in immunosenescence. *Aging Cell* **3**, 177-184 (2004).
128. Uyemura, K., Castle, S.C. & Makinodan, T. The frail elderly: role of dendritic cells in the susceptibility of infection. *Mechanisms of Ageing and Development* **123**, 955-962 (2002).
129. Van Zant, G. & Liang, Y. Concise Review: Hematopoietic Stem Cell Aging, Life Span, and Transplantation. *Stem Cells Translational Medicine* **1**, 651-657 (2012).
130. Franceschi, C., Capri, M., Monti, D., Giunta, S., Olivieri, F., Sevini, F., Panourgia, M.P., Invidia, L., Celani, L., Scurti, M., Cevenini, E., Castellani, G.C. & Salvioli, S. Inflammaging and anti-inflammaging: A systemic perspective on aging and longevity emerged from studies in humans. *Mechanisms of Ageing and Development* **128**, 92-105 (2007).
131. Lansdorp, P.M., Dragowska, W. & Mayani, H. Ontogeny-related changes in proliferative potential of human hematopoietic cells. *Journal of Experimental Medicine* **178**, 787-791 (1993).
132. Abdulrazzak, H., Moschidou, D., Jones, G. & Guillot, P.V. Biological characteristics of stem cells from foetal, cord blood and extraembryonic tissues. *Journal of The Royal Society Interface* **7**, S689-S706 (2010).
133. Broxmeyer, H.E., Douglas, G.W., Hangoc, G., Cooper, S., Bard, J., English, D., Arny, M., Thomas, L. & Boyse, E.A. Human umbilical cord blood as a potential source of transplantable hematopoietic stem/progenitor cells. *Proceedings of the National Academy of Sciences* **86**, 3828-3832 (1989).
134. Broxmeyer, H.E., Hangoc, G., Cooper, S., Ribeiro, R.C., Graves, V., Yoder, M., Wagner, J., Vadhan-Raj, S., Benninger, L. & Rubinstein, P. Growth characteristics and expansion of human umbilical cord blood and estimation of its potential for transplantation in adults. *Proceedings of the National Academy of Sciences* **89**, 4109-4113 (1992).

135. Carow, C.E., Hangoc, G., Cooper, S.H., Williams, D.E. & Broxmeyer, H.E. Mast cell growth factor (c-kit ligand) supports the growth of human multipotential progenitor cells with a high replating potential. *Blood* **78**, 2216-2221 (1991).
136. Carow, C.E., Hangoc, G. & Broxmeyer, H.E. Human multipotential progenitor cells (CFU-GEMM) have extensive replating capacity for secondary CFU-GEMM: An effect enhanced by cord blood plasma. *Blood* **81**, 942-949 (1993).
137. McGuckin, C.P., Forraz, N., Allouard, Q. & Pettengell, R. Umbilical cord blood stem cells can expand hematopoietic and neuroglial progenitors in vitro. *Experimental Cell Research* **295**, 350-359 (2004).
138. Ewing, B., Hillier, L., Wendl, M.C. & Green, P. Base-Calling of Automated Sequencer Traces UsingPhred. I. Accuracy Assessment. *Genome Research* **8**, 175-185 (1998).
139. Note, I.T. Quality Scores For Next-Generation Sequencing. Vol. 2013 (2011).
140. ClonTech. SMARTer™ PCR

cDNA Synthesis Kit

User Manual. Vol. 2013 (2012).
141. Ozsolak, F. & Milos, P.M. RNA sequencing: advances, challenges and opportunities. *Nat Rev Genet* **12**, 87-98 (2011).
142. Ramskold, D., Luo, S., Wang, Y.-C., Li, R., Deng, Q., Faridani, O.R., Daniels, G.A., Khrebtukova, I., Loring, J.F., Laurent, L.C., Schroth, G.P. & Sandberg, R. Full-length mRNA-Seq from single-cell levels of RNA and individual circulating tumor cells. *Nat Biotech* **30**, 777-782 (2012).
143. Goetz, J.J. & Trimarchi, J.M. Transcriptome sequencing of single cells with Smart-Seq. *Nat Biotech* **30**, 763-765 (2012).
144. L., D. Blood Groups and Red Cell Antigens (National Center for Biotechnology Information (US), 2005).
145. Goardon, N., Lambert, J.A., Rodriguez, P., Nissaire, P., Herblot, S., Thibault, P., Dumenil, D., Strouboulis, J., Romeo, P.-H. & Hoang, T. ETO2 coordinates cellular proliferation and differentiation during erythropoiesis. *EMBO J* **25**, 357-366 (2006).
146. Labbaye, C., Quaranta, M.T., Pagliuca, A., Militi, S., Licht, J.D., Testa, U. & Peschle, C. PLZF induces megakaryocytic development, activates Tpo receptor expression and interacts with GATA1 protein. *Oncogene* **21**, 6669-6679 (2002).
147. Qiagen. RNeasy ® Plus Mini Handbook (2010).
148. Lunter, G. & Goodson, M. Stampy: A statistical algorithm for sensitive and fast mapping of Illumina sequence reads. *Genome Research* **21**, 936-939 (2011).
149. Trapnell, C., Pachter, L. & Salzberg, S.L. TopHat: discovering splice junctions with RNA-Seq. *Bioinformatics* **25**, 1105-1111 (2009).
150. Lu, R., Neff, N.F., Quake, S.R. & Weissman, I.L. Tracking single hematopoietic stem cells in vivo using high-throughput sequencing in conjunction with viral genetic barcoding. *Nat Biotech* **29**, 928-933 (2011).